2 & Copies

NASA CR-66601
DAC-58131

DEFINITION OF A RESISTOJET CONTROL SYSTEM FOR THE MANNED ORBITAL RESEARCH LABORATORY FINAL REPORT

VOLUME II
RESISTOJET CONTROL SYSTEM ANALYSIS

MAY 1968

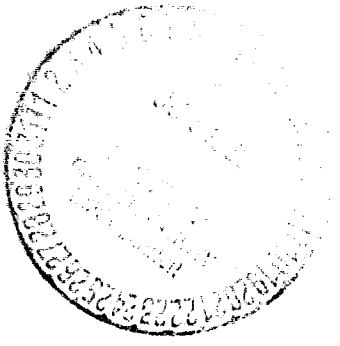

Prepared under Contract No. NAS 1-6702
by Douglas Aircraft Company
Missile and Space Systems Division
Huntington Beach, California
for
NATIONAL AERONAUTICS AND SPACE ADMINISTRATION

NASA CR-66601
DAC-58131

DEFINITION OF A RESISTOJET CONTROL SYSTEM FOR THE MANNED ORBITAL RESEARCH LABORATORY FINAL REPORT

VOLUME II
RESISTOJET CONTROL SYSTEM ANALYSIS

MAY 1968

BY A. PISCIOTTA, JR., E.N. EUSANIO, et al

Prepared under Contract No. NAS 1-6702
by Douglas Aircraft Company
Missile and Space Systems Division
Huntington Beach, California
for
NATIONAL AERONAUTICS AND SPACE ADMINISTRATION

PREFACE

This report is submitted to the National Aeronautics and Space Administration's Langley Research Center (NASA-LRC), Langley AFB, Virginia. It has been prepared under Contract No. NAS1-6702 and describes the results of a detailed assessment of the use of a resistojet control system for the MORL.

The study results are documented in five volumes:

DAC-58130	I	Summary
DAC-58131	II	Resistojet Control System Analysis
DAC-58132	III	Biowaste Utilization
DAC-58133	IV	Ground and Flight Test Plan
DAC-58134	V	Resistojet Design and Development

Volume I is a summary report in which the significant results are presented. Volume II contains a detailed definition of the selected resistojet control system, the recommended orbit injection system, the supporting system analyses and integration, and comparative evaluation data. Volume III presents the biowaste utilization analysis. Volume IV details the ground and flight test program for a resistojet control system. Volume V presents the results of the resistojet design and development program. Life test data will be provided in a separately bound addendum to Volume V at the conclusion of the life test.

Requests for further information concerning this report will be welcomed by the following Douglas representative:

- Mr. T. J. Gordon, Director, Advance Space and Launch Systems
  Huntington Beach, California
  Telephone: 714-897-0311, Extension 2994

FOREWORD

Units, abbreviations, and prefixes used in this report correspond to the International System of Units (SI) as prescribed by the Eleventh General Conference on Weights and Measures and presented in NASA Report SP-7012. The basic units for length, mass, and time are meter, kilogram, and second, respectively. Throughout the report, the English equivalent (foot, pound, and second) are presented for convenience.

The SI units, abbreviations, and prefixes most frequently used in this report are summarized below:

Basic Units

Length	meter	m
Mass	kilogram	kg
Time	sec	s
Electric current	ampere	A
Temperature	degree Kelvin	^{o}K

Supplementary Units

Plane angle	radian	rad

Derived Units

Area	square meter	m^2	
Volume	cubic meter	m^3	
Frequency	hertz	Hz	(s^{-1})
Density	kilogram per cubic meter	kg/m^3	
Velocity	meter per second	m/s	
Angular velocity	radian per second	rad/s	
Acceleration	meter per second squared	m/s^2	
Angular acceleration	radian per second squared	rad/s^2	
Force	newton	N	$(kg\text{-}m/s^2)$
Pressure	newton per sq meter	N/m^2	
Kinematic viscosity	sq meter per second	m^2/s	
Dynamic viscosity	newton-second per sq meter	$N\text{-}s/m^2$	

Work, energy, quantity of heat	joule	J	(N-m)
Power	watt	W	(J/s)
Electric charge	coulomb	C	(A-s)
Voltage, potential difference, electromotive force	volt	V	(W/A)
Electric field strength	volt per meter	V/m	
Electric resistance	ohm	Ω	(V/A)
Electric capacitance	farad	F	(A-s/V)
Magnetic flux	weber	Wb	(V-s)
Inductance	henry	H	(V-s/A)
Magnetic flux density	tesla	T	(Wb/m^2)
Magnetic field strength	ampere per meter	A/m	
Magnetomotive force	ampere	A	

Prefixes

Factor by which unit is multiplied	Prefix	Symbol
10^6	mega	M
10^3	kilo	k
10^{-2}	centi	c
10^{-3}	milli	m
10^{-6}	micro	μ

CONTENTS

FIGURES

TABLES

DEFINITION OF A RESISTOJET CONTROL SYSTEM FOR THE MANNED ORBITAL RESEARCH LABORATORY

FINAL REPORT

VOLUME II – RESISTOJET CONTROL SYSTEM ANALYSIS

By A. Pisciotta, Jr., E. N. Eusanio, et al.

INTRODUCTION AND SUMMARY

Continuing studies conducted by NASA and its associated contractors have resulted in the design, development, and test of many candidate subsystems for future space exploration and experimentation. The Manned Orbital Research Laboratory (MORL) (fig. 1) studies conducted by Douglas for NASA during the past 4 years produced several potential candidate subsystem concepts (ref. 1). As a result of these studies, the MORL Resistojet Control System Study (NAS1-6702) was funded in November 1966. The study, which identifies a fully integrated resistojet control system for the MORL, is presented in this report.

The study, as shown in fig. 2, consisted of four major phases:

(1) Phase I, System Analysis and Integration--A detailed analysis to define a resistojet control system for the MORL.

(2) Phase II, Resistojet Development--A detailed design, fabrication, and performance test effort leading to 0.044-N (10-mlbf) resistojet thrustors employing an evacuated concentric-tube concept. This phase of the study was conducted by The Marquardt Corporation under subcontract to Douglas.

(3) Phase III, Ground and Flight Test Plan--A detailed program-planning activity to define a resistojet control system module with primary emphasis on the qualification test plan prerequisite to flight test experiments.

(4) Phase IV, Life Test--A test program to verify the endurance capability of the selected resistojet thrustor design under typical operating conditions. This phase was conducted by The Marquardt Corporation.

Phase I included a review and evaluation of the mission's operational profile from the time of initial launch and injection into orbit to the cycle of regularly scheduled events required to sustain the 5-year mission. In this evaluation, the requirements for a MORL reaction control system were examined and the feasibility was assessed of modifying the profile so that the low-thrust capability of the resistojet thrustors could be used more effectively.

Several orbit-injection systems were parametrically evaluated for integration with a resistojet control system: storable and cryogenic bipropellant, monopropellant, and solid-propellant systems. Also evaluated was the concept of using thrustors in conjunction with a spiral transfer from an initial

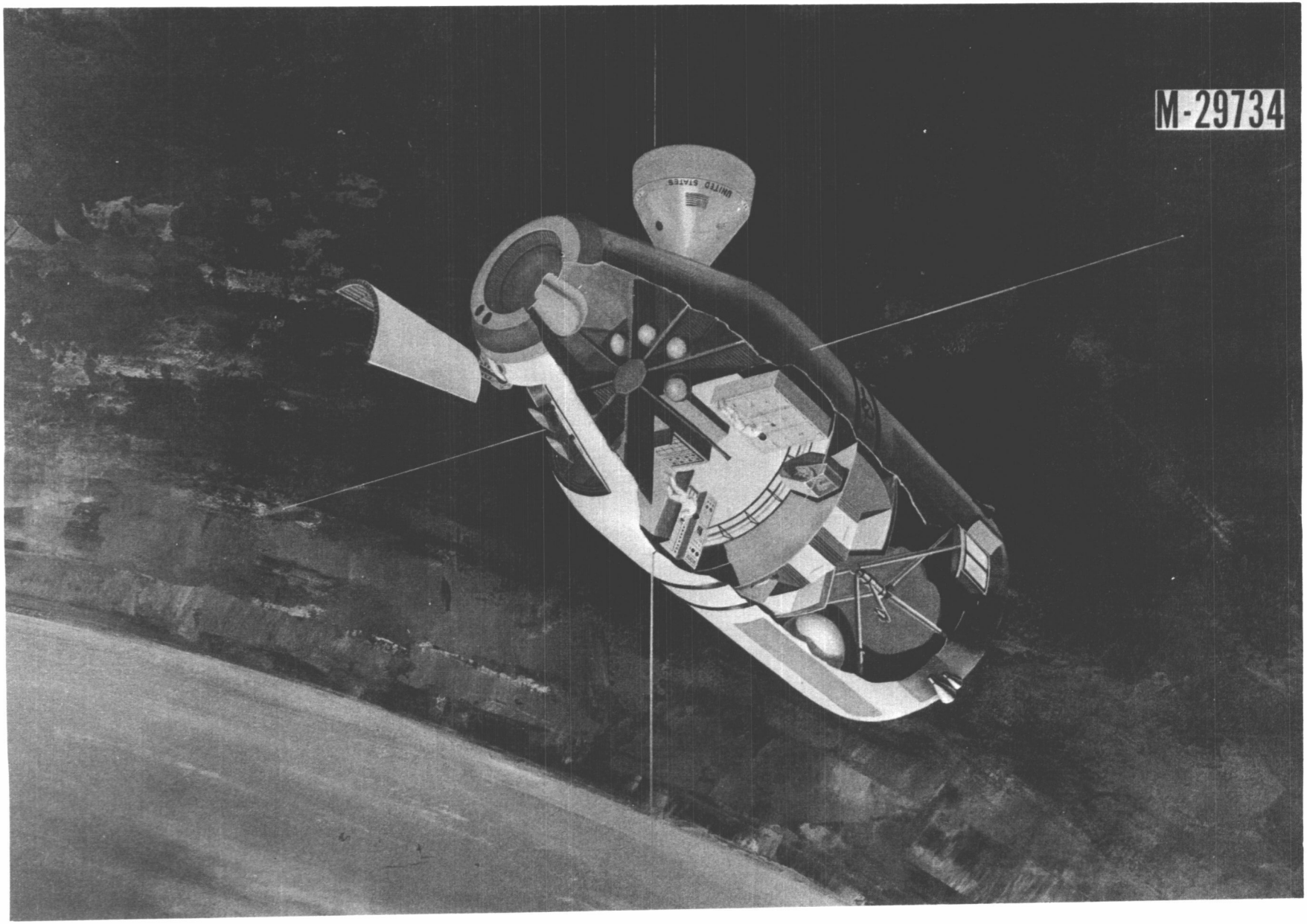

Figure 1. Artist's Conception of MORL

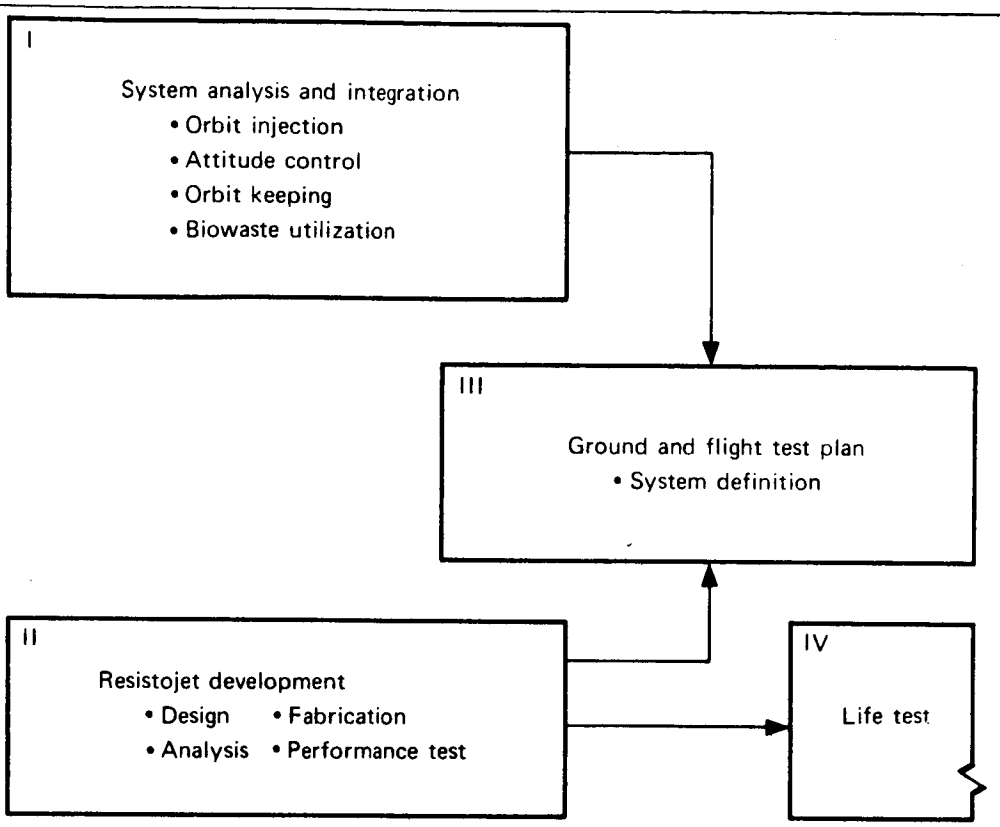

Figure 2. Study Plan – MORL Resistojet Control System

low-altitude orbit to the final 304-km (164-nmi) circular orbit. Hydrogen (H_2) and ammonia (NH_3) resistojet systems were analyzed. The resultant payload capability with resistojet thrustors is comparable to that obtained with conventional thrustor systems. However, the time required to achieve final orbit with maximum payload varies from 4.5 days for H_2 to 7.5 days for NH_3.

The use of the S-IVB to provide the injection velocity to final orbit was also evaluated. Two S-IVB systems were evaluated through use of an apogee-injection maneuver: the auxiliary propulsion system (APS) developed for Saturn V application and the J-2S mainstage engine. It was established that four APS kits can provide the apogee circularization impulse without necessitating major modification to the S-IVB; however, there would be a severe degradation in payload capability. The J-2S engine has the capability of igniting and sustaining combustion with gaseous or mixed-phase propellant while operating in an idle (low-thrust) mode. At ignition, the thrust level of the idle mode is 4448 N (1000 lbf), building up to 26 700 N (6000 lbf) steady state in approximately 40 sec. The J-2S engine can provide the total impulse required for orbit circularization by using only the residual propellant and vapor remaining in the tank after completion of the primary burn.

As a result of the orbit-injection systems analyses, the launch trajectory was redefined to take advantage of the payload gained by launching to the lowest perigee permitted by Eastern Test Range (ETR) tracking considerations. It was recommended that the S-IVB with the J-2S be used for orbit

injection. This system is described in detail in Selected System Description, and the factors influencing its selection are discussed in System Analyses and Integration.

The disturbances which affected the control requirements were analyzed and classified into two categories: orbital disturbances and scheduled disturbances. Such orbital disturbances as gravity gradient and aerodynamic drag are relatively low in magnitude and are most effectively controlled by the use of control-moment gyro (CMG)/resistojet system. Such scheduled disturbances as docking impact and centrifuge operation require relatively high control torques which can be provided most effectively by a conventional thrustor.

Parametric analysis and preliminary system integration of thrustor systems using NH_3, cryogenic H_2, and CO_2 biowaste led to a preliminary definition of three alternate systems for control of orbital disturbances. Subsequent comparison and evaluation resulted in the selection of the NH_3 system.

The NH_3 resistojet system best satisfies most of the criteria. It yields a lower launch weight and lower power requirement, and it has a greater growth potential than the cryogenic H_2 system. In addition, the NH_3 system is simpler and more reliable. The launch facilities and prelaunch operations are greatly simplified as no cryogenic system is required, thus no chill-down operations are necessary, and there is no effect on the NH_3 system from a prolonged hold during countdown. The cryogenic H_2 system and the CO_2 biowaste system present higher development risks than the NH_3 system. Although the H_2 and NH_3 resistojets have the same development status, the cryogenic tankage design and the cryogenic propellant resupply system were considered to require concentrated developmental effort.

Even though the NH_3 resistojet system has been selected for use on the MORL baseline, the CO_2 biowaste resistojet remains an attractive candidate. However, basic materials research is necessary before a high-performance thrustor for use with the oxidizing CO_2 biowaste propellants can be developed.

Six reaction control systems (RCS's) were initially considered to provide attitude control during the scheduled disturbances affecting the MORL. Three of these are referred to as heated-gas systems and include (1) a stored gaseous nitrogen (GN_2) RCS, (2) a cryogenic H_2 RCS, and (3) an NH_3 system. The other three systems are conventional chemical propulsion concepts and include (1) an O_2/H_2 cryogenic bipropellant RCS, (2) a nitrogen tetroxide/monomethylhydrazine (N_2O_4/MMH) storable bipropellant RCS, and (3) a hydrazine (N_2H_4) monopropellant system.

Although the heated-gas systems take advantage of the waste heat available from the isotope Brayton power system, they were eliminated from further consideration because of weight, complexity, or limited thrust capability. The N_2H_4 monopropellant system was selected because of its relative simplicity, greater reliability, and lower development cost in comparison with either the storable or cryogenic bipropellants.

The objective of the resistojet development phase was to demonstrate the soundness of the resistojet performance predictions used in the system analysis. The study dictated the use of small electrical rockets with specific impulse and life times which had not yet been achieved.

A 0.044-N (10-mlbf) resistojet, designed to operate on either H_2 or NH_3, was developed to meet the high performance goals set by the study. On the basis of earlier studies of specific impulse, minimum values of 720 sec for H_2 and 350 sec for NH_3 were set. The effort was directed toward flight-type hardware.

Two new significant features of the resultant design are the extensive use of rhenium (Re) for the small high-temperature elements and the use of the vacuum-jacket concept. These permitted the attainment of the relatively high performance at the 0.044-N (10-mlbf) thrust level.

Pure Re was found to be superior to all other materials for resistojets of high specific impulse. Its relatively unknown technology and high costs have heretofore deterred its use. Many of its high-temperature properties are second only to tungsten (W), but unlike W, it remains ductile after being heated above the recrystallization temperature. Therefore, it is readily weldable to produce a strong joint.

The geometry conceived for the resistojet heater element is described as an evacuated concentric tube. An evacuated jacket is interposed between the heating elements and the outer heat-transfer passages in the pressure case. This jacket reduces radial heat flow by removing the continuum gas-conductive term; the regime is thus made free molecular where heat flow is proportional to pressure. Thin radiation shields are used to further reduce the radiant-heat transport. Shields and high-performance thermal insulation are used on the outside of the case.

SELECTED SYSTEM DESCRIPTION

This section describes the integrated propulsion/reaction control system (P/RCS) selected for the baseline mission (ref. 2). The P/RCS includes the NH_3 resistojet/CMG system that is used for long-term stabilization and control and the N_2H_4 monopropellant RCS used for high-disturbance control. Interfacing systems that enter into the optimization of design operating points or influence the selection of candidate subsystems are also defined in sufficient depth to ensure compatibility between systems. These systems include the J-2S engine on the S-IVB used for orbit injection of the laboratory and the logistics resupply vehicle.

The systems defined in this document have the following functional requirements for the MORL mission:

(1) Orbit circularization and attitude-control moments during the orbit-injection phase.

(2) Attitude control during scheduled disturbances caused by rendezvous and docking, logistics-vehicle stowage, and centrifuge operation.

(3) Attitude control and orbit keeping during orbital disturbances caused by aerodynamic drag, aerodynamic torques, and gravity-gradient torques.

The selected systems are summarized in table 1. Orbit injection is accomplished by apogee circularization using the J-2S engine on the S-IVB. Use of the J-2S engine for orbit injection simplifies the MORL propulsion requirements and provides a maximum payload capability. Attitude control and orbit keeping are accomplished by a CMG/resistojet system and an N_2H_4 monopropellant system. The inboard profile of the MORL vehicle shown in fig. 3 indicates the location of the NH_3 resistojet thrustor modules and the N_2H_4 thrustor modules.

Orbit Injection System

The MORL is launched by the Saturn IB shown in fig. 4. This vehicle consists of an S-IB first stage, and S-IVB second stage, and an instrument unit (IU) in which the guidance system is located. The S-IB, an improved first stage of the Saturn I, has eight 890 000-N (200 000-lbf) H-1 engines.

The S-IVB, shown in fig. 5, uses a 1 020 000-N (230 000-lbf) thrust J-2S mainstage engine. Four 156 000-N (35 000-lbf) TE-29-1B solid retrorockets are on the aft interstage of the S-IVB to decelerate the S-IB first stage at separation; thus, the aft interstage of the S-IVB remains with the first stage. Pitch and yaw attitude are controlled during powered flight by gimbaling the

Table 1

SELECTED SYSTEMS

Function	System	Primary Advantages
Orbit injection	J-2S engine	• Has highest payload capability • Allows the S-IVB to be placed in orbit
Attitude control and orbit keeping	CMG/NH_3 resistojet system Four resistojet modules Six thrustors/module 0.044 N [10 mlbf] each Four CMG's Two double-gimbal (pitch and yaw) 2430 N-m-sec (1790 ft-lbf-sec) each Two single-gimbal (roll) 2210 N-m-sec (1625 ft-lbf-sec) each	• Has lower launch weight, power, and volume than H_2 resistojet system • Is already developed, whereas CO_2 resistojet is conceptual design • Has lower launch weight than high-thrust system (chemical engines) • Eliminates noise, vibration, and CMG unloading transients of high-thrust systems • Has less-complex resupply than LH_2 resistojet or high-thrust systems • Minimizes environment contamination • Has a cold-flow operating mode
Scheduled-disturbance control (docking impact and centrifuge operation)	N_2H_4 monopropellant system Four engine modules Three engines/module 44.5-N [10 lbf] each	• Has superior thrust capability to heated-gas systems • Is less complex and has higher reliability than bipropellant system • Has less-complex resupply than bipropellant system

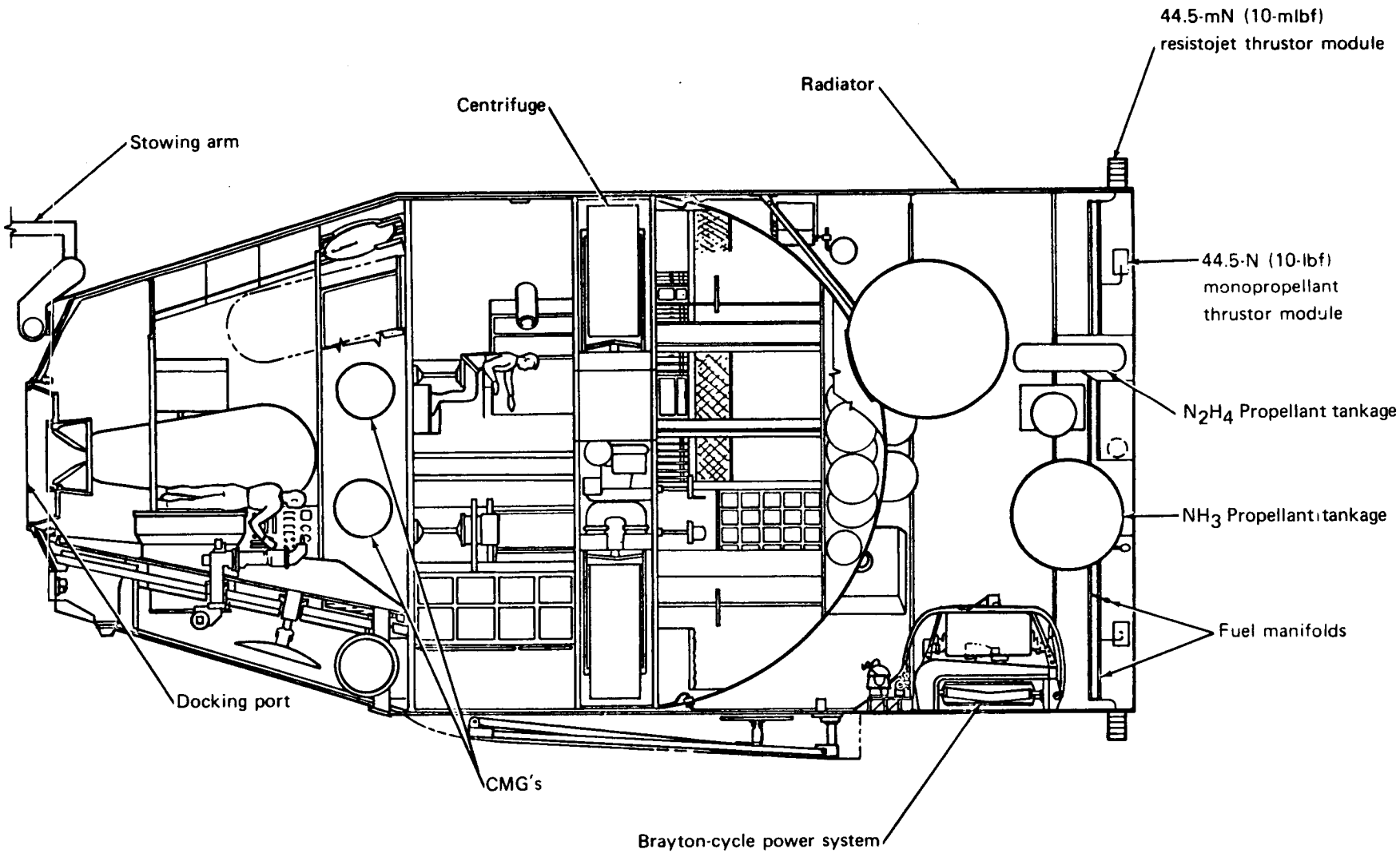

Figure 3. MORL Inboard Profile

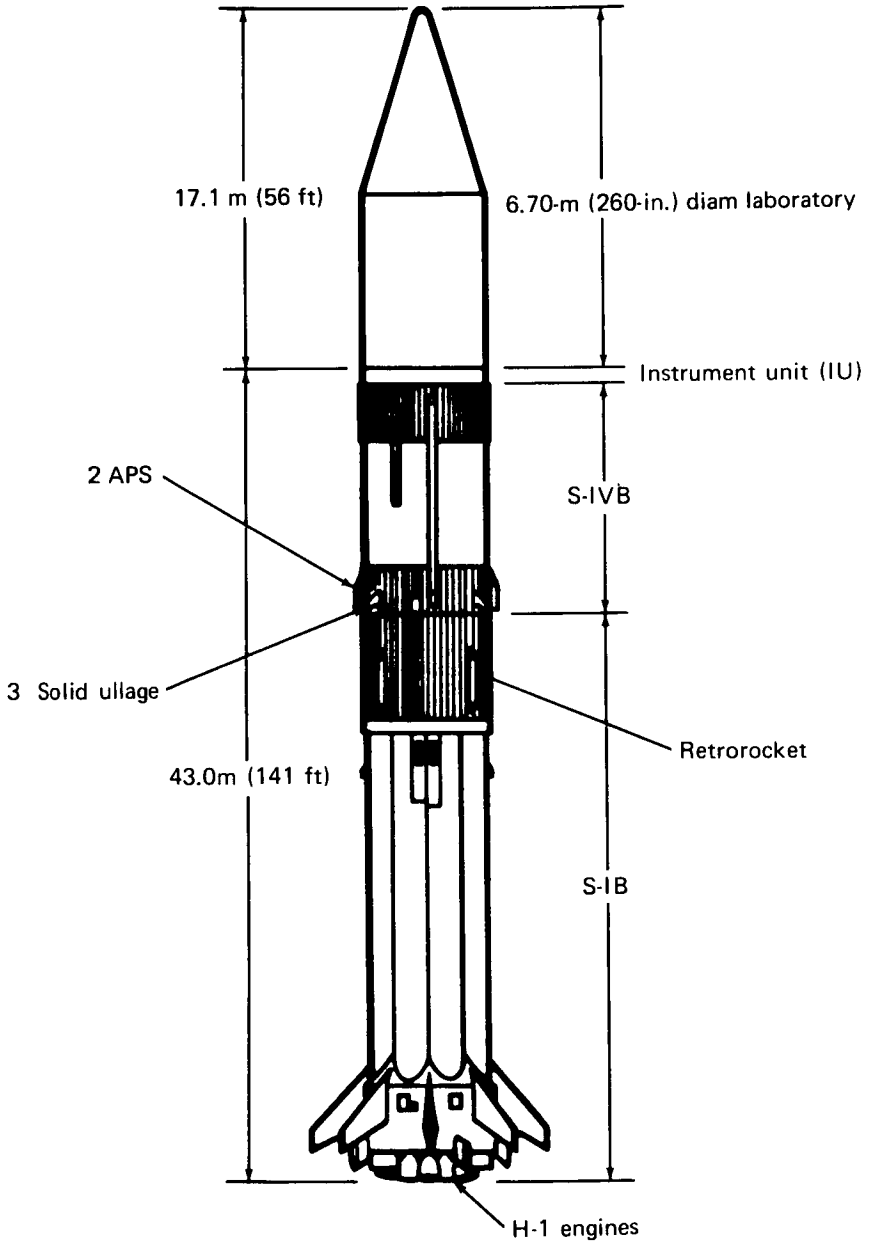

Figure 4. MORL Launch Configuration

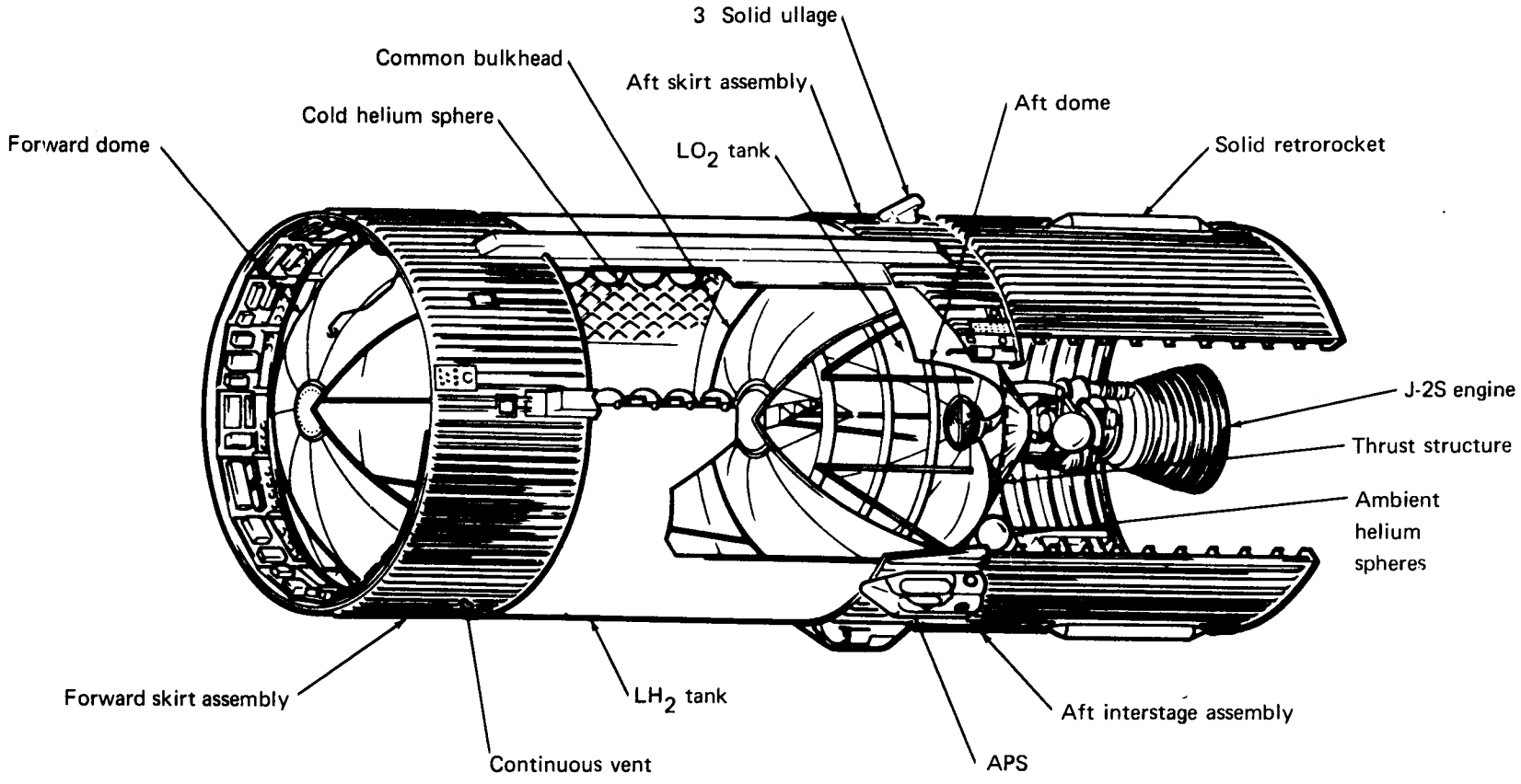

Figure 5. The S-IVB (Structural Cutaway)

J-2S engine. Roll is controlled by 668-N (150-lbf) thrustors located in the auxiliary propulsion system (APS) modules. Three-axis (roll, pitch, and yaw) attitude control during unpowered flight is provided entirely by the APS. Apogee circularization is achieved by the restart of the J-2S engine operating in the idle mode at a maximum thrust level of 26 800 N (6000 lbf).

Launch and injection sequence. – Fig. 6 shows the sequence of the launch and apogee circularization injection for an ETR launch into a 304-km (164-nmi) altitude and 0.875 rad (50°) inclination orbit. The boost phase, indicated by (1) in the figure, is provided by the engines of S-IB stage at a total thrust of 7.12×10^6 N (1.6 Mlbf). The duration of the boost phase is 150 sec.

At an altitude of 55.5 km (30 nmi), the booster separates from the payload and S-IVB, and the J-2S mainstage engine ignites as shown at (2) in fig. 6. To maximize payload in orbit, the J-2S engine is programmed for a step variation in thrust level during engine operation (fig. 7). This is accomplished by operating the J-2S engine at a higher oxidizer/fuel mixture ratio initially, thus providing a high thrust level when flight-path angles are high and gravity losses are greatest. This high initial thrust level is advantageous in maximizing the payload weight in orbit, even though there is a decrease in delivered specific impulse. After 300 sec of operation, the flight-path angle is reduced so that the high thrust level is no longer advantageous. At this point, a programmed reduction in mixture ratio will cause the thrust level to drop and the performance to increase.

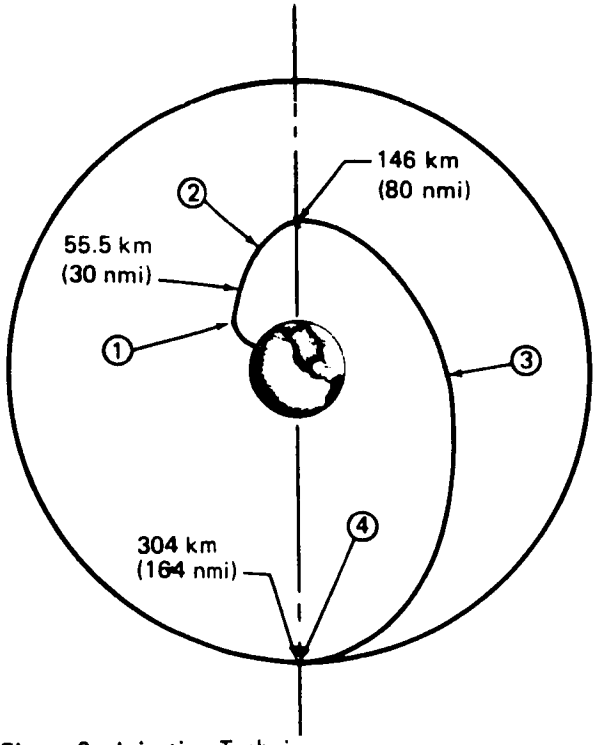

① S-IB F = 7.12×10^6 N (1.6×10^6 lbf)
② S-IVB F_{avg} = 912 250 N (205 000 lbf)
③ Coast
④ Apogee circularization
S-IVB restart (idle mode)
F = 4450 to 26 700 N (1000 to 6000 lbf)

Figure 6. Injection Technique

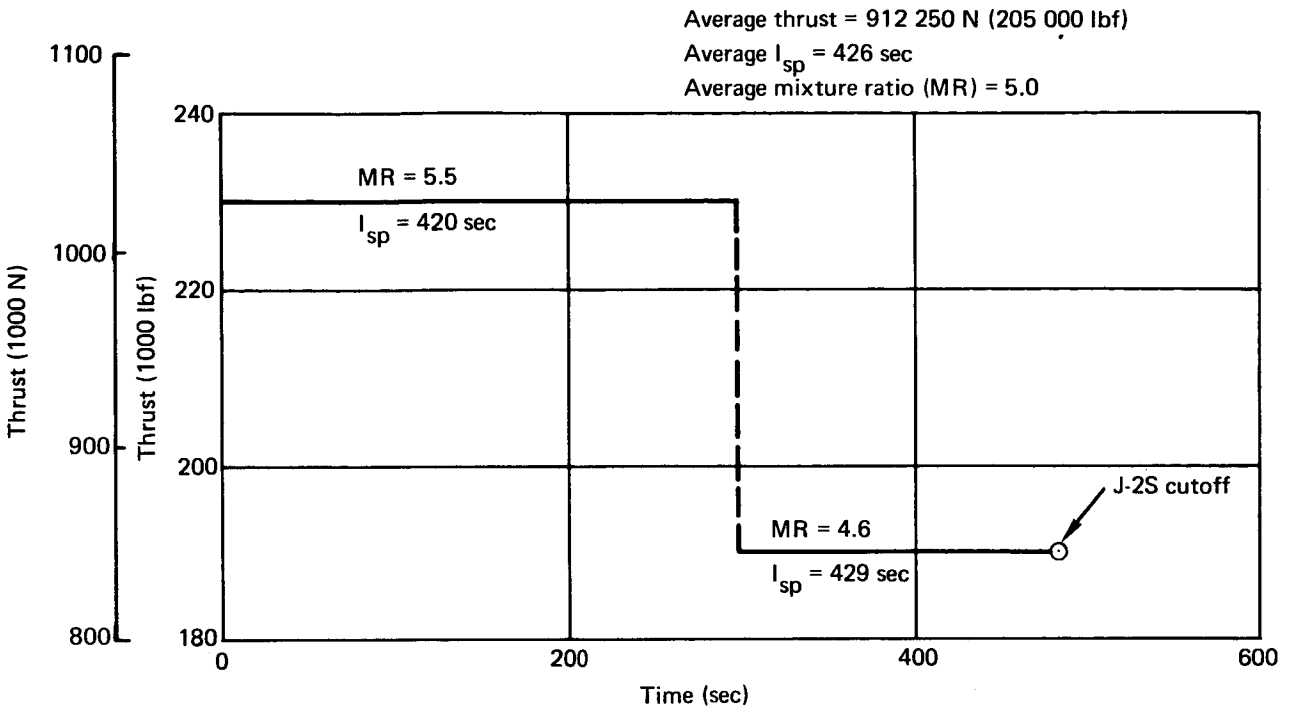

Figure 7. Programmed Thrust Level Step Variation

At the end of the initial J-2S engine operation, the vehicle is in a 146- x 304-km (80- x 164-nmi) elliptical orbit. After a coast period of approximately 45 min, as shown at (3) in fig. 6, the J-2S engine is restarted in the idle mode, (4), to provide a velocity increment of 44.2 m/sec (146 fps) that circularizes the orbit at the 304-km (164-nmi) apogee.

This impulse must be applied to the 30 900-kg (68 100-lbm) combined weight of the S-IVB and MORL vehicle. A total burn time of 69 sec is required for the apogee circularization in idle-mode operation. A total propellant weight of 590 kg (1300 lbm) is required to perform this maneuver. This is well below the 965 kg (2123 lbm) of residual propellants available on the S-IVB, which are not normally usable with the standard J-2 engine. Consequently, the orbit transfer is accomplished with no additional propellant requirement.

J-2S engine system. — Simpler operation and greater mission flexibility are the principal objectives of a technology effort by NASA now being conducted to improve the S-IVB mainstage J-2 engine. This improved engine, designated J-2S, incorporates a number of improved features: (1) operation in an idle mode, (2) solid-propellant gas generator, (3) recontoured nozzle, and (4) thrust chamber tapoff. Although all of these features are not essential to the MORL mission, they have been proposed as a single package for a developed J-2S engine. Thus, an improved J-2 engine with a single desired feature such as idle-mode operation was not considered in this study.

A schematic of the J-2S engine, which shows its significant improved features, is presented in fig. 8. A detailed description of the J-2S engine may be found in ref. 4. The characteristics of the engine in idle-mode operation are given in table 2. The engine can operate with liquid, vapor, or mixed-phase propellant flow. Propellant flow is accomplished by tank-feed pressure. Both the thrust level and the performance of the J-2S in the idle mode are functions of the quality of the propellant flow. The thrust level is initially 4450 N (1000 lbf) when ignition is initiated in zero-g and all vapor flows to the J-2S. As the liquids are settled under the influence of vehicle acceleration, the flow begins to shift to all liquid and the thrust level builds up to about 26 700 N (6000 lbf) (fig. 9).

The engine performance is slightly higher during the vapor flow portion, because there is a nearer optimum mixture ratio than in the all-liquid case. Thus, the initial specific impulse of 290-sec decays to 225 sec when the 26 700 N (6000 lbf) level is reached. A mixture ratio of 0.5 is maintained after all liquid flow is established to maintain a low chamber temperature.

Attitude control during idle-mode operation is accomplished through the use of the on-board APS for roll control and by means of gimbaling the J-2S for pitch and yaw control. The APS thrust level is too low to control pitch and yaw when the 26 700 N (6000 lbf) idle mode is in operation. The IU, currently a part of the Saturn launch vehicle, provides the impulse control during idle-mode burn. This is accomplished by integrating the ΔV supplied during idle-mode operation.

The most significant effect that the J-2S has on the S-IVB is that it permits the deletion of hardware. Several functions previously performed by a number of other subsystems are now accomplished by the J-2S. A 132-kg (292-lbm) weight saving is thus realized, and this results in an increase in payload capability for the Saturn IB. The weight reduction mainly results from replacing the H_2 bottle blowdown, turbine prespin system with a solid-propellant gas generator and from replacing the O_2/H_2 gas generator with a thrust-chamber bleed system. The fact that the J-2S can operate on mixed-phase flow means that the ullage motor and chilldown systems can be deleted for a weight savings of 353 kg (778 lbm). The J-2S engine in idle mode can run to LO_2 depletion. The deletion of some miscellaneous stage hardware results in a total S-IVB weight decrease of 495 kg (1091 lbm). The payload capability for the Saturn IB launch vehicle in a 364-km (164-nmi) circular orbit is therefore increased from 1690-kg (37 370-lbm) to 17 400 kg (38 461 lbm). Fig. 10 shows a comparison of Saturn IB direct-injection capability and J-2S apogee circularization.

Attitude-Control and Orbit-Keeping System

The attitude-control and orbit-keeping system is required to orient and stabilize the MORL and to provide orbit-altitude maintenance during all phases of the mission. During the experimental phase of the mission, an attitude-hold accuracy of $\pm 8.7 \times 10^{-3}$ rad ($\pm 0.5^{\circ}$) and a rate limit of

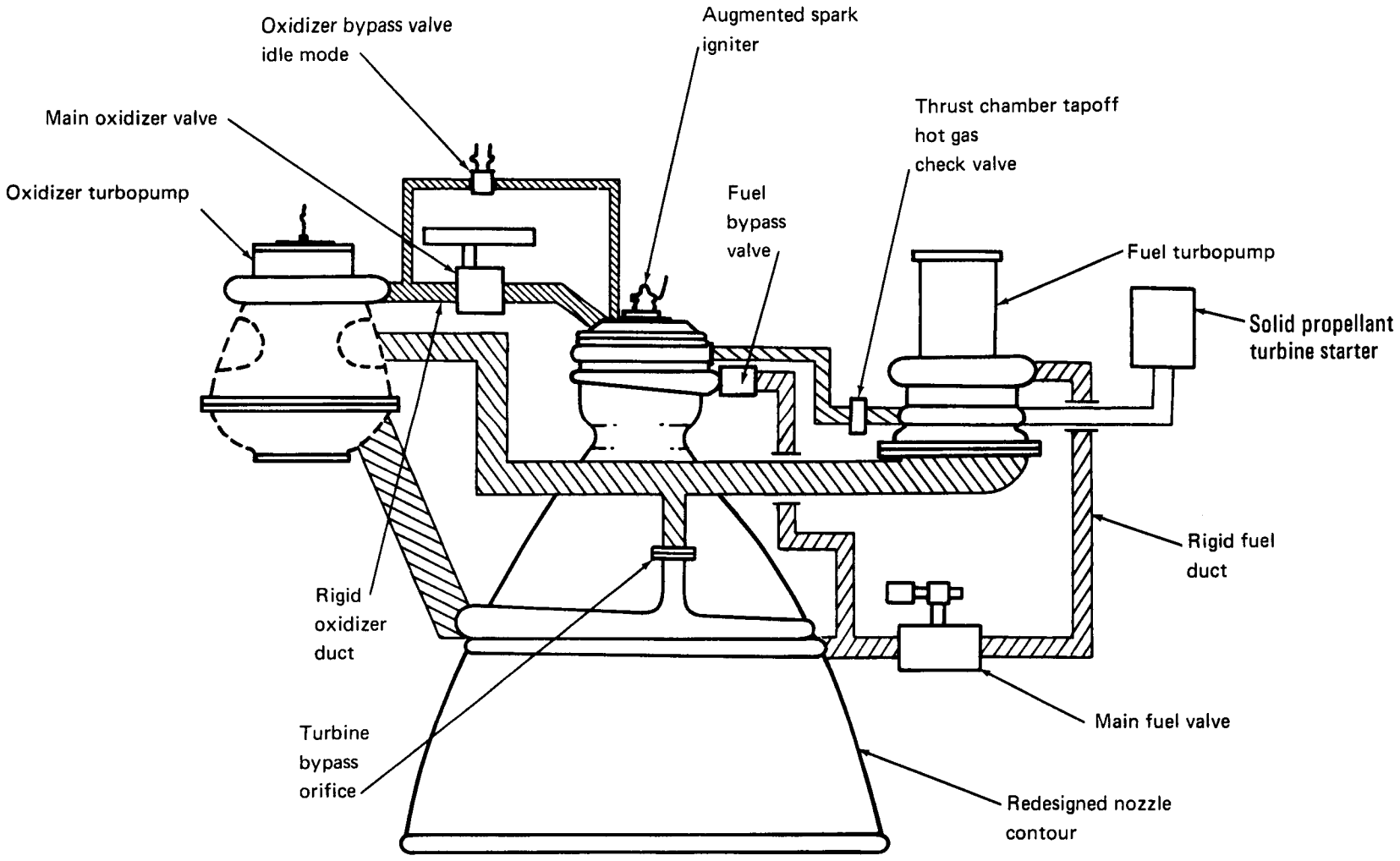

Figure 8. J-2S Engine

TABLE 2

J-2S IDLE-MODE OPERATION

Item	Characteristic
Thrust	4450 to 26 700 N (1000 to 6000 lbf)
I_{sp} (delivered)	244 sec
Burn time	69 sec
Propellant required	586 kg (1295 lbm)
Propellant condition	O_2/H_2 in two-phase flow
Status	Qualification testing required
Systems eliminated	Ullage motors Chilldown system LO_2 depletion circuit

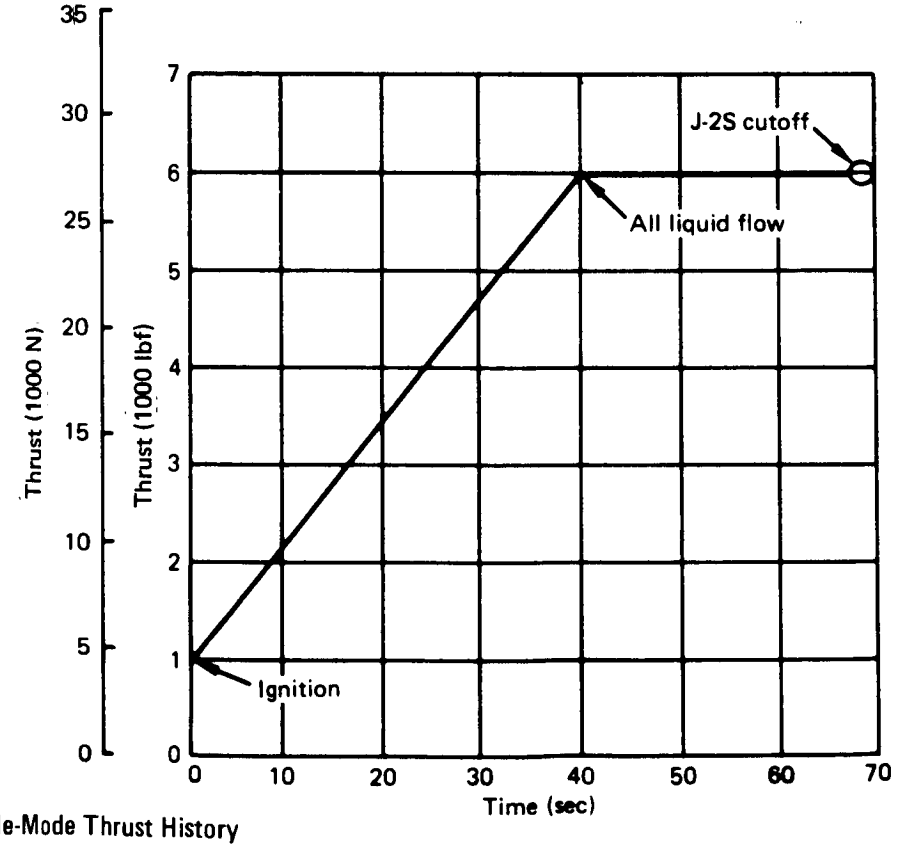

Figure 9. J-2S Idle-Mode Thrust History

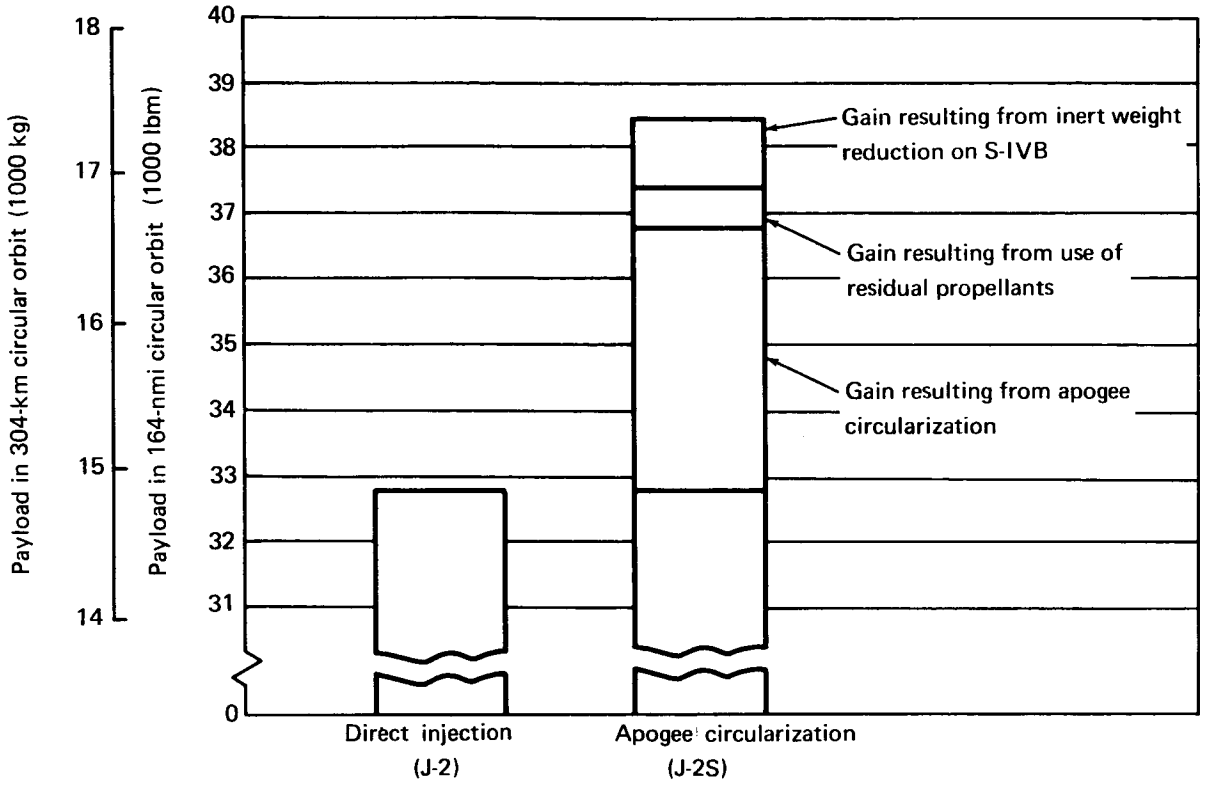

Figure 10. Payload Capability – J-2S

0.0005 rad/sec (0.03°/sec) are required for routine Earth-oriented experiments. For precision Earth-oriented and inertial-oriented experiments, an attitude hold accuracy of $\pm 1.74 \times 10^{-3}$ rad ($\pm 0.1°$) with a rate limit of 1.74×10^{-4} rad/sec (0.01°/sec) is required. No precise attitude hold accuracy is specified during the nonexperimental phase of the mission. However, based on specific mission activities, attitude hold accuracies have been established.

Two primary orientations (fig. 11) are utilized during the MORL mission. The belly-down orientation is selected for long-term stabilization, since it is easily mechanized and results in minimum aerodynamic drag. Earth-centered experiments are best performed in this orientation. The longitudinal roll or X-axis is aligned in the direction of the orbital velocity vector. The yaw or Z-axis is aligned along the local vertical. The pitch or Y-axis is aligned perpendicular to the orbit plane. In the inertial orientation, the vehicle attitude is maintained essentially fixed with reference to inertial space. This orientation is required for those experiments that have fixed pointing requirements such as those needed for celestial observations.

During the mission, the vehicle is subjected to disturbance forces that may be classified into two categories. Orbital disturbances are relatively low in magnitude and result from aerodynamic drag and torques, gravity-gradient torques, and small internal forces such as rotating machinery and crew motion. The effects of these disturbances are controlled by the CMG's, with the resistojet thrustors providing desaturation and orbit keeping. The

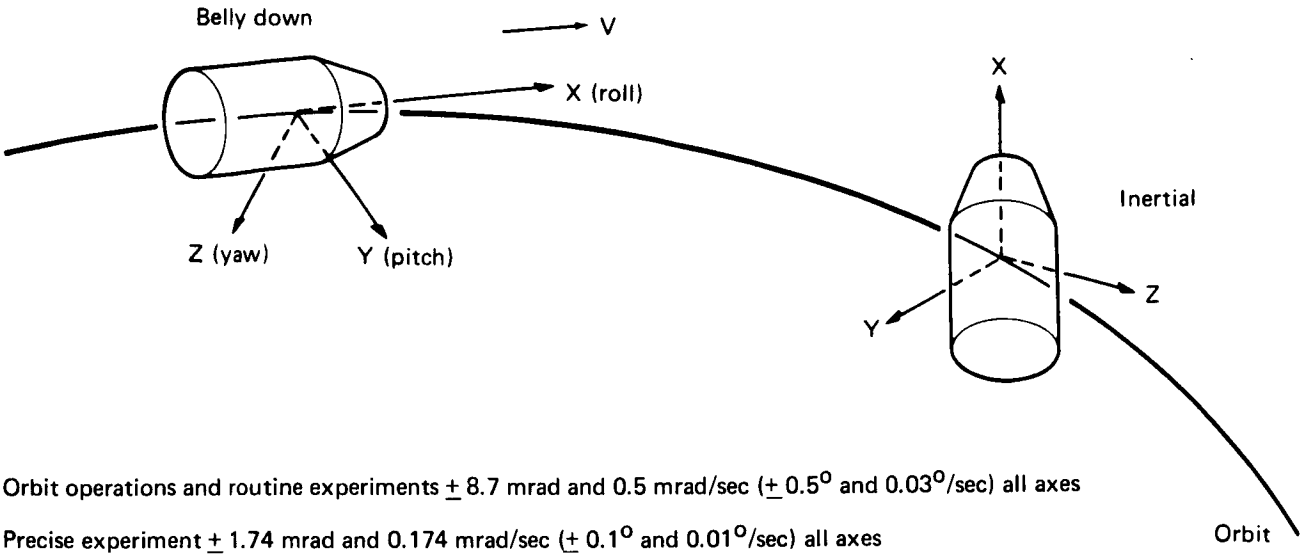

Figure 11. MORL Orientations

second category is the scheduled disturbances which occur during the non-experimental phase of the mission and are defined as those which occur at a predetermined time and frequency and which require a relatively high control torque. These disturbances are controlled by the N_2H_4 monopropellant system. The resistojet and monopropellant system installations are shown in fig. 12.

CMG/resistojet control system. – The CMG package and resistojet thrustor module locations are shown in fig. 12. The CMG package consists of two double-gimbal CMG's (DG CMG) and two single-gimbal CMG's (SG CMG), as described in detail in Douglas Report SM-48817. The DG CMG provides control moments for pitch and yaw, and the SG CMG provides control moments for roll. Momentum storage capabilities of each gyro are 2210 N-m-sec (1625 ft-lbf-sec) for the DG CMG and 2430 N-m-sec (1790 ft-lbf-sec) for the SG CMG. Torque output capability is 34 N-m (25 ft-lbf) per gimbal. The pitch and yaw sizing will accommodate the maximum cyclical disturbance torques with sufficient momentum reserve to perform maneuvers. The roll sizing will simultaneously accommodate the maximum gravity-gradient and aerodynamic-disturbance torques and the disturbance generated by 1-g centrifuge operation.

The resistojet control system (fig. 13) consists of four resistojet thrustor modules located at $\pi/2$ rad (90°) intervals around the aft periphery of the MORL. Each of the four modules contains 0.044-N (10-mlbf) NH_3 resistojet

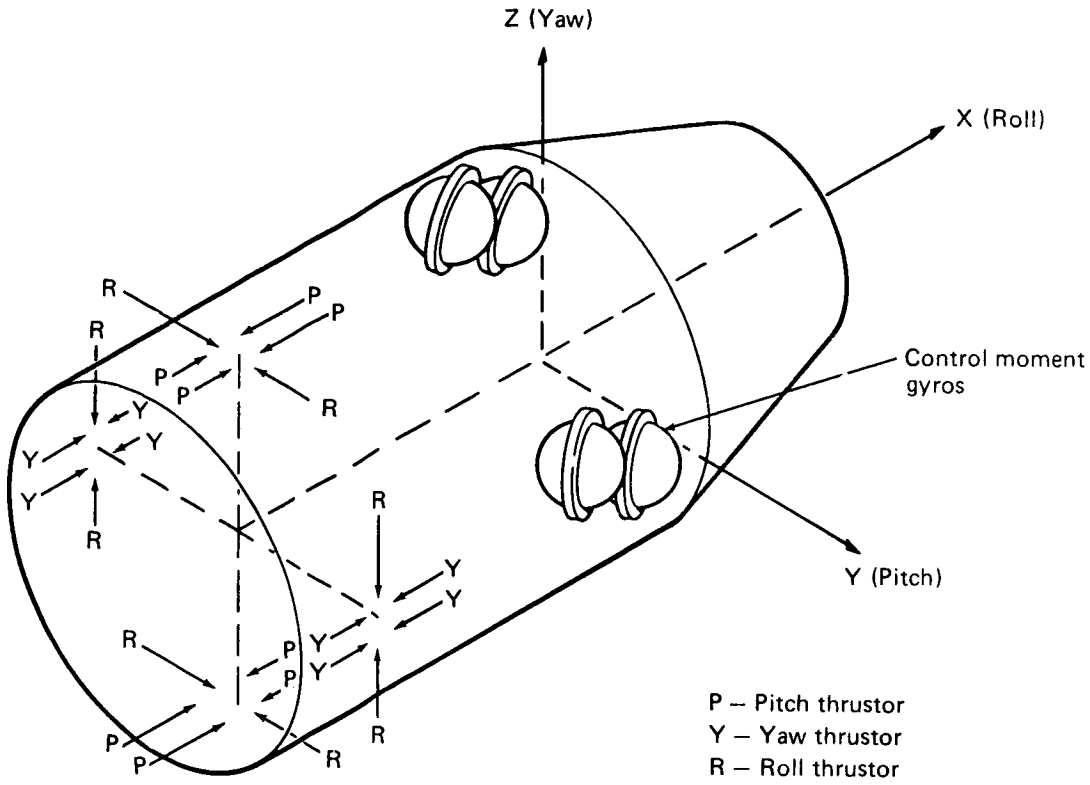

Figure 12. CMG/Resistojet Thrustor Locations

thrustors that are oriented as shown by the thrust vectors in fig. 12. The selection of identical thrust levels for the pitch, roll, and yaw orientations results in identical thrustors and thrustor modules.

Thrust levels and thrust schedules were derived for the thrustor modules on the basis of requirements for orbit keeping and CMG-desaturation total impulse. Compatibility of constant total thrust and minimum CMG size was investigated, and it was determined that constant to near-constant thrust schedules resulted in minimum CMG size, where CMG's were sized only to control gravity-gradient and aerodynamic-disturbance torques. The thrust schedules utilized to desaturate the CMG's and to provide orbit keeping for both the inertial and the belly-down orientation is shown in fig. 14. During the belly-down orientation, only aft-facing thrustors are fired for the pitch and yaw functions. This allows the orbit keeping or drag make-up impulse to be provided without the expenditure of additional propellant.

The resistojet thrust schedule for both the inertial orientation and the belly-down orientation is shown in fig. 15. A total of 4 hours/day are spent in the inertial orientation, with 0.5 hour spent in maneuvering, and the remaining time in the belly-down orientation. This schedule represents a total impulse requirement of 8300 N-sec (1870 lbf-sec)/day, resulting in a daily propellant consumption of approximately 2.31 kg (5.1 lbm). Constant thrust throughout the orbit allows for a constant power demand from the MORL electrical system.

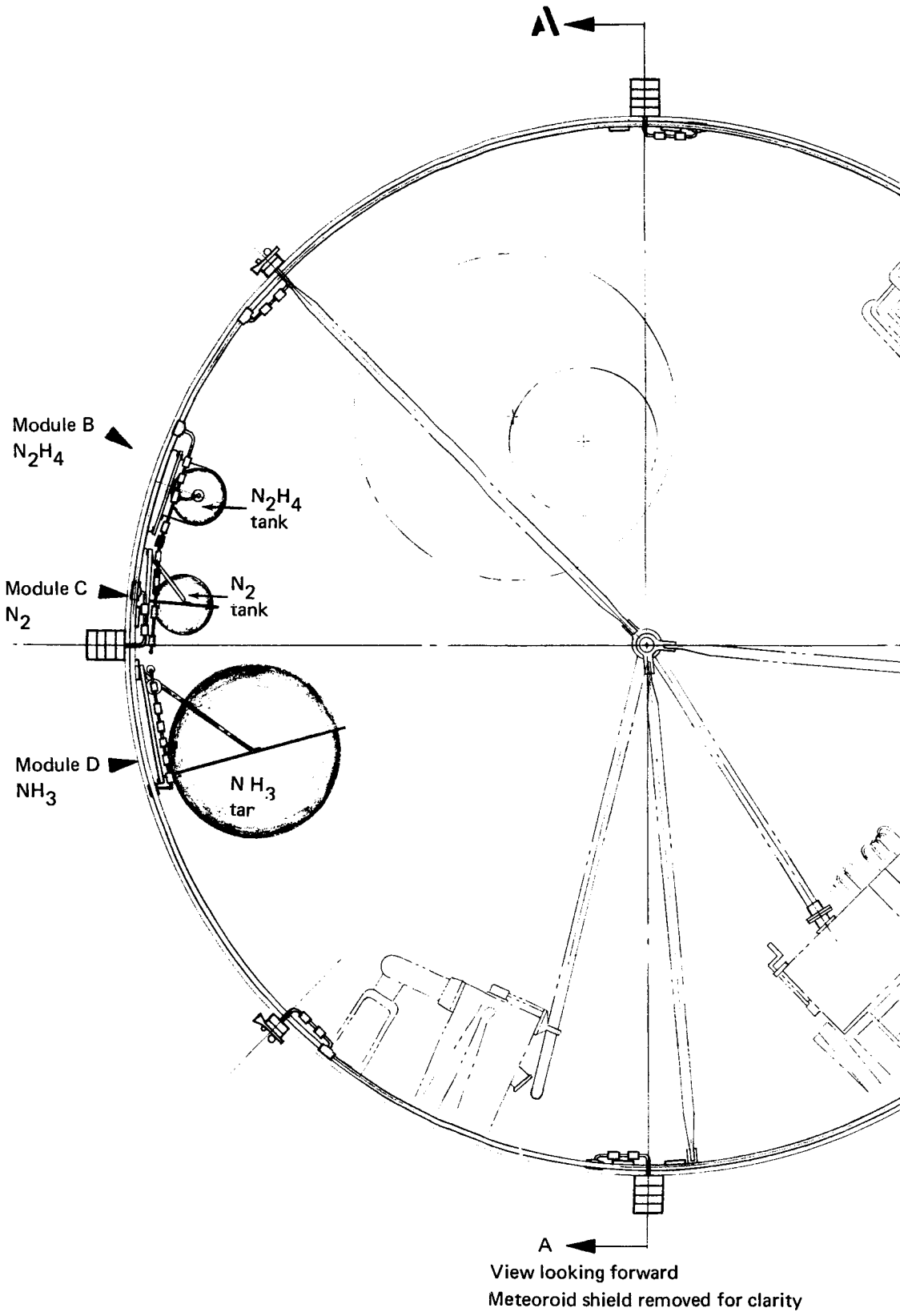

Figure 13. MORL Resistojet System

FOLDOUT FRAME 1

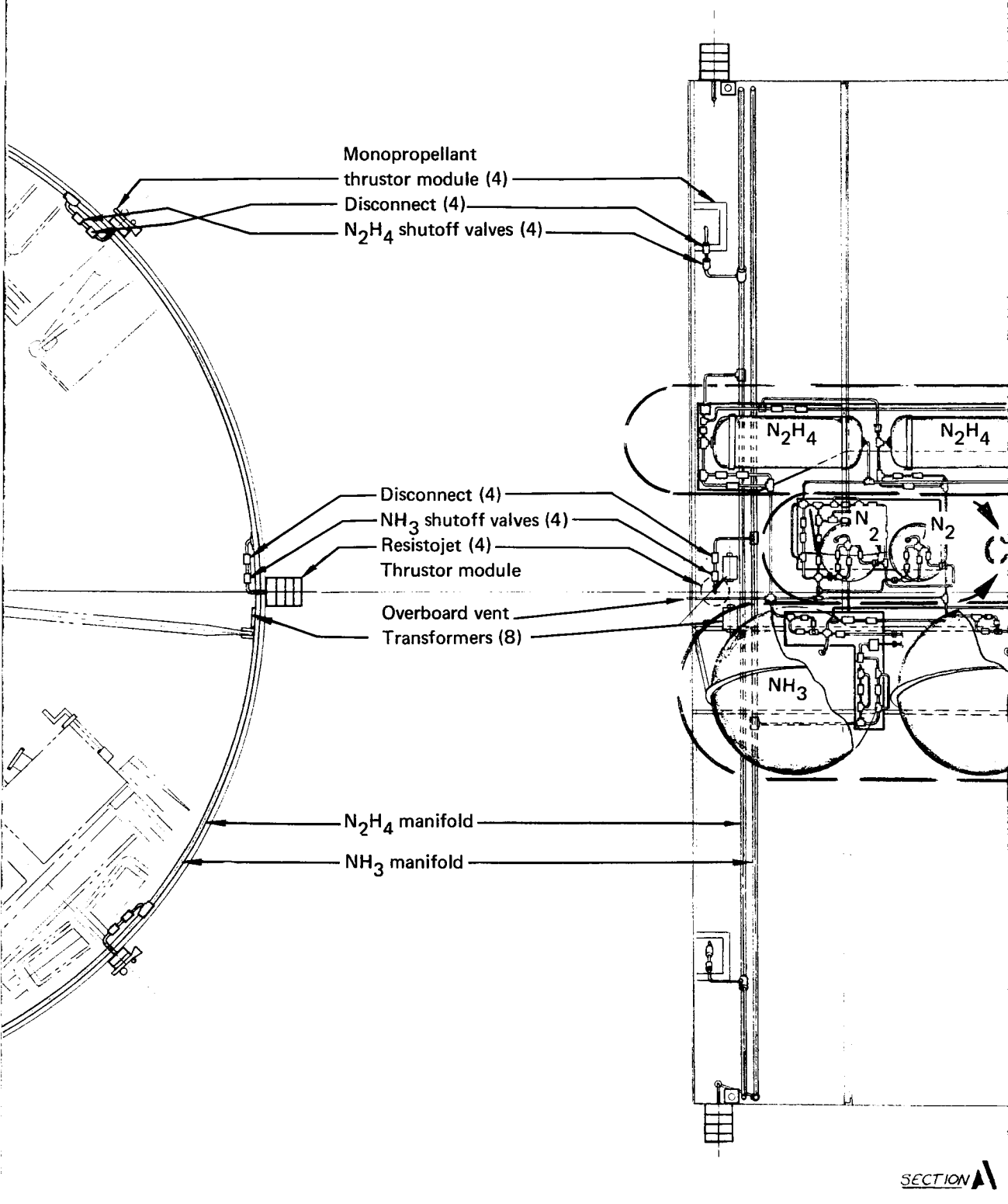

SECTION A

FOLDOUT FRAME 2

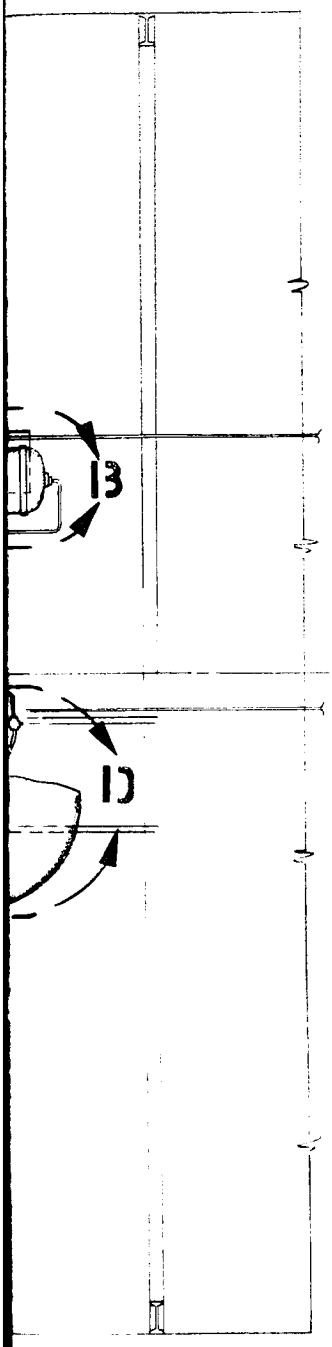

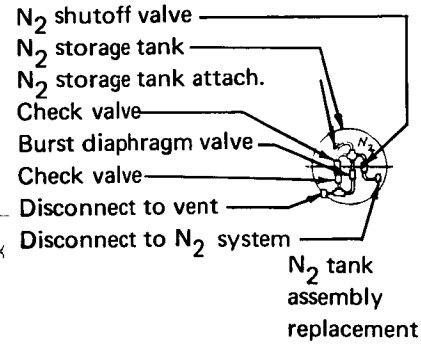

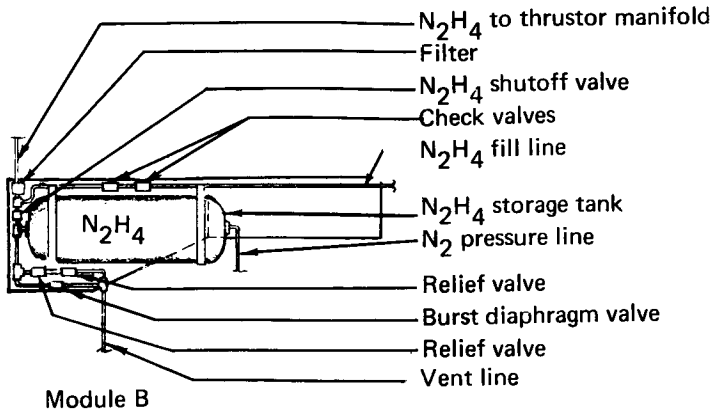

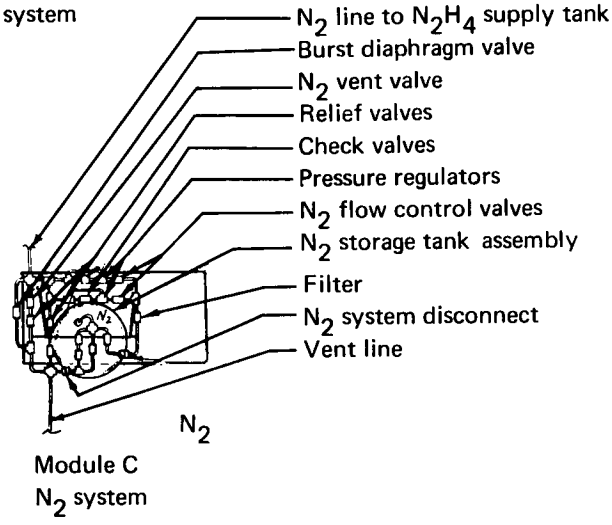

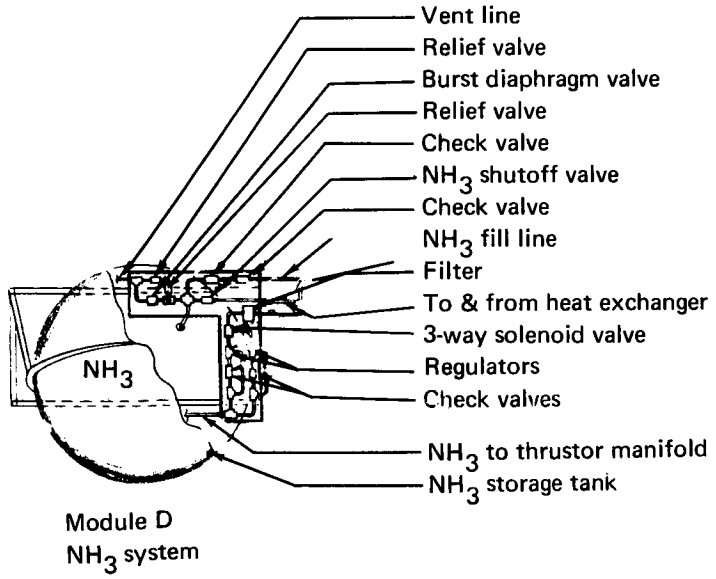

FOLDOUT FRAME 3

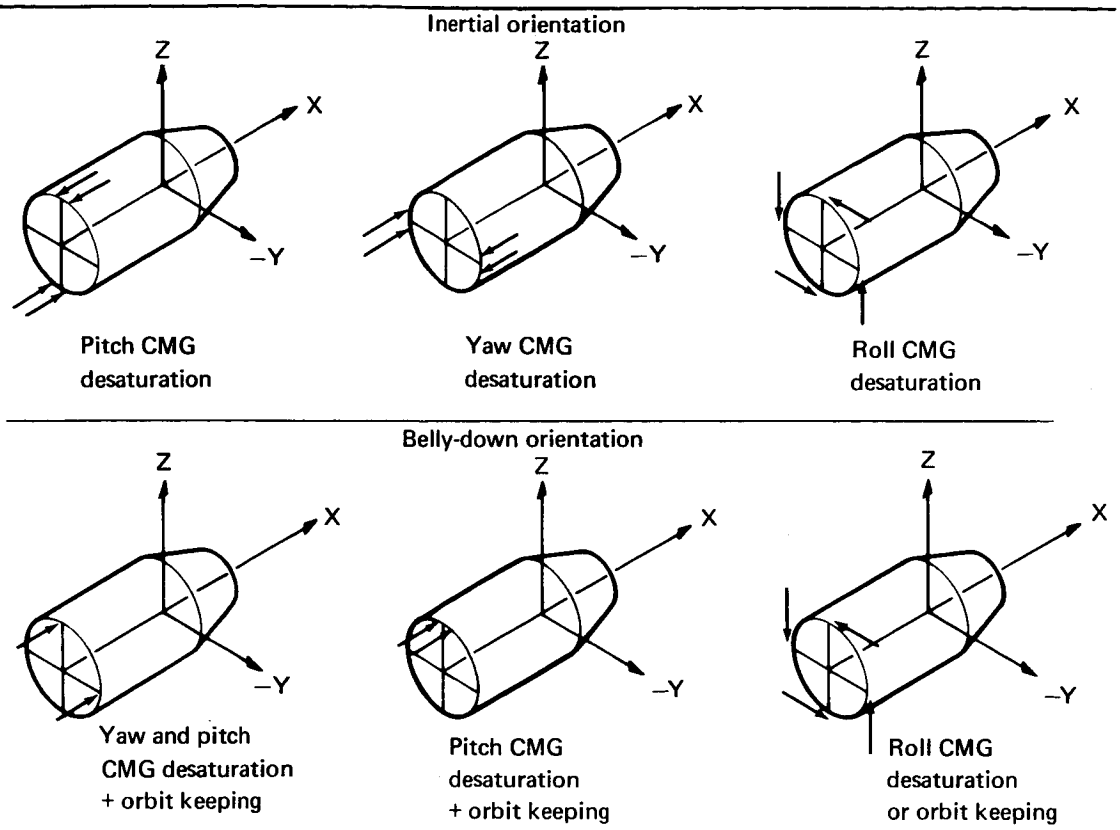

Figure 14. Thrust Logic

Resistojet thrustor module: The resistojet thrustor module, shown in fig. 16, is located outside the vehicle, approximately 25.4 cm (10 in.) from the end station. The modules can be replaced from the inside by means of turning four Dzus fasteners, disconnecting the fuel and electrical connections, and withdrawing the module from its service position. The module is installed by means of inserting it into its hole until the four Dzus fasteners position themselves into their holds. Once the four fasteners are turned, the thrustor module is automatically aligned and locked into the final service position. When the fuel line and electrical connections are made, the module is ready for operation.

Each of the four thrustor modules is identical and interchangeable, and contains six resistojets in three layers of matched pairs. Each layer has a pair of thrustors in parallel but mounted in the support structure to thrust in opposite directions. A common central structure, in the shape of a cross of equal webs $\pi/2$ rad (90°) apart, supports the thrustor pairs. The fuel manifold is located in the center of the support structure. The solenoid-operated shutoff valves are attached to the fuel manifold, with a short fuel line to the resistojet thrustor assembly.

The thrustor assemblies are fastened to the support structure by four screws that are $\pi/2$ rad (90°) apart. Four adjusting screws between the four mounting screws align the thrustor assemblies.

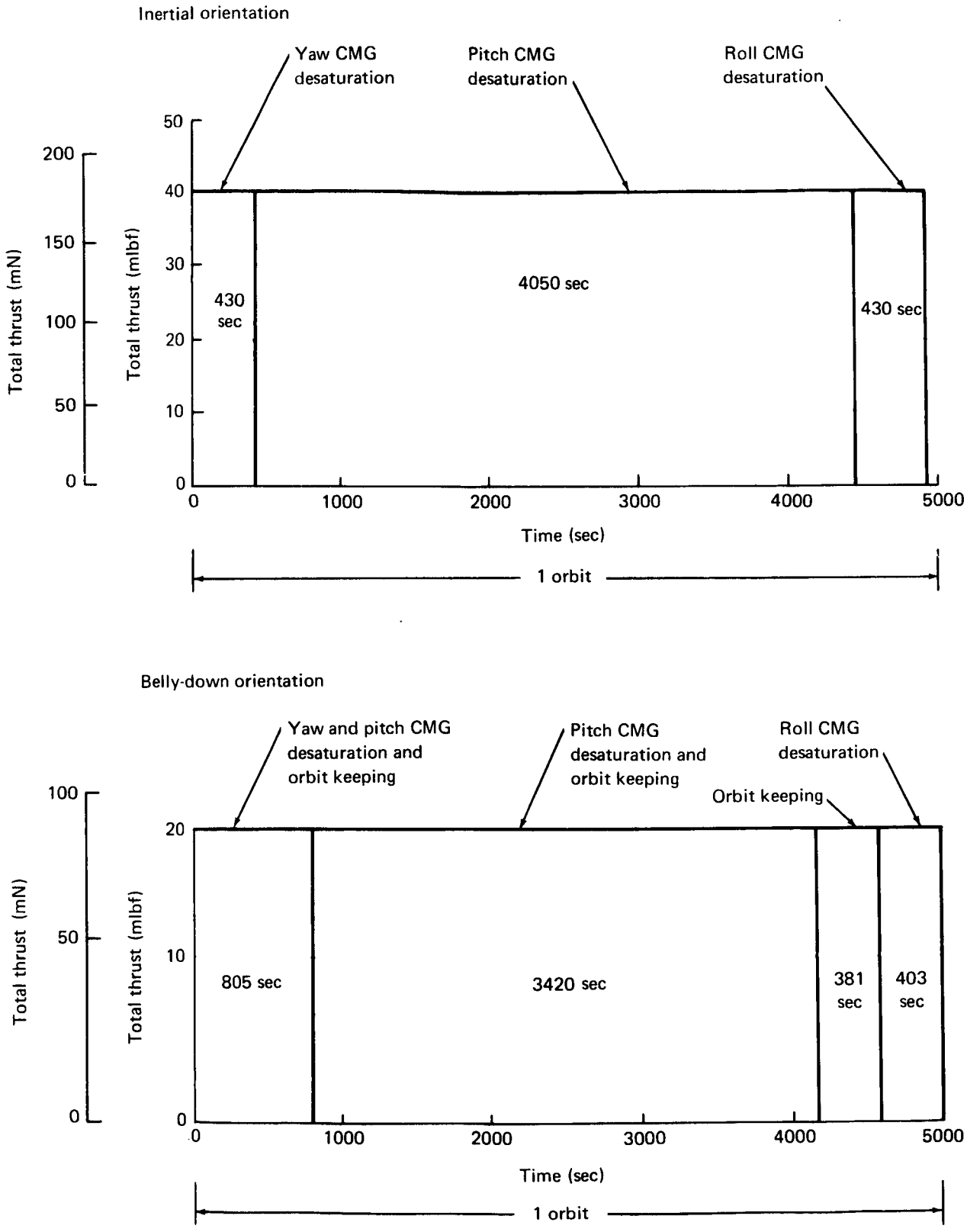

Figure 15. Thrust Schedules

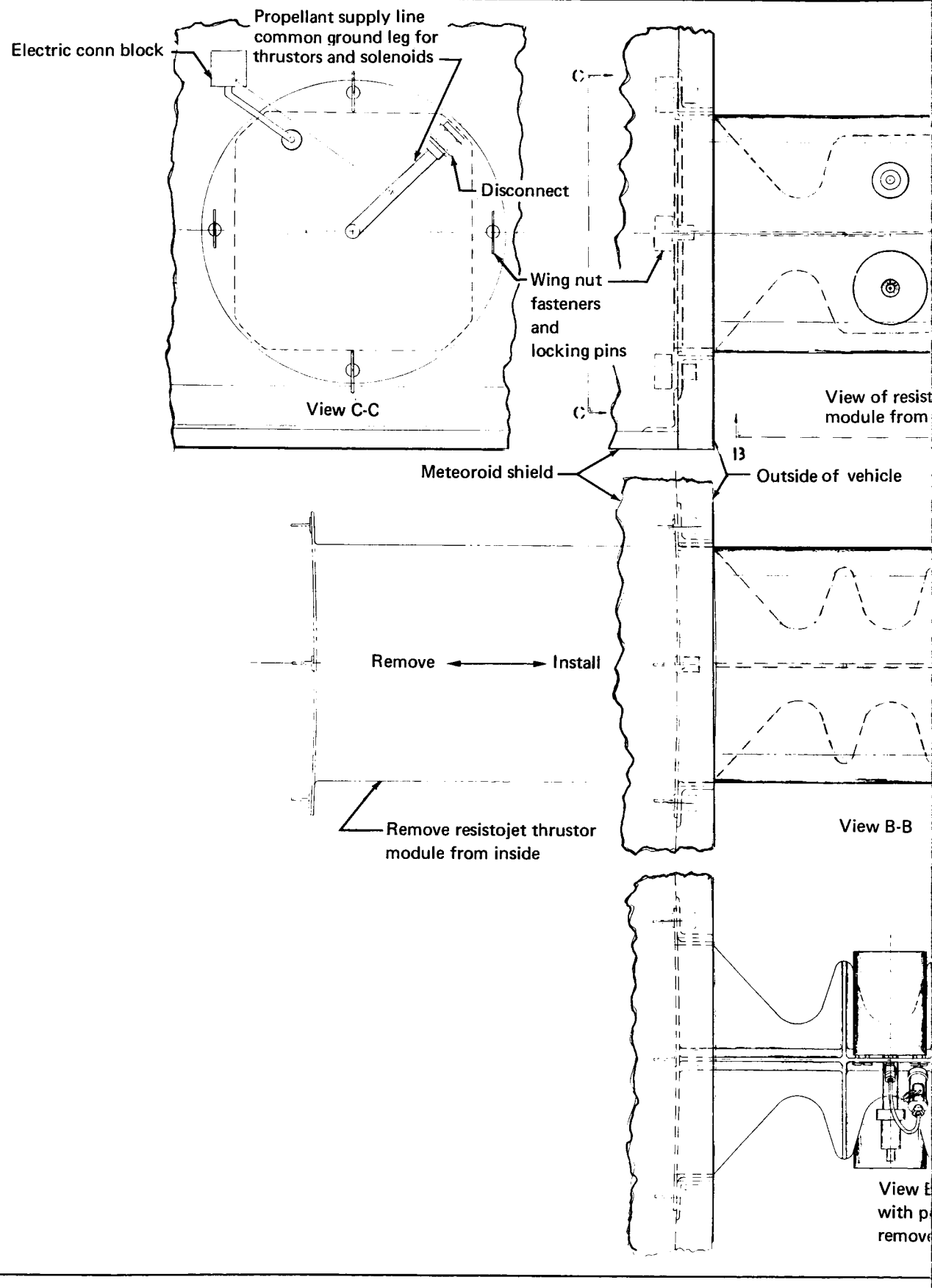

FOLDOUT FRAME

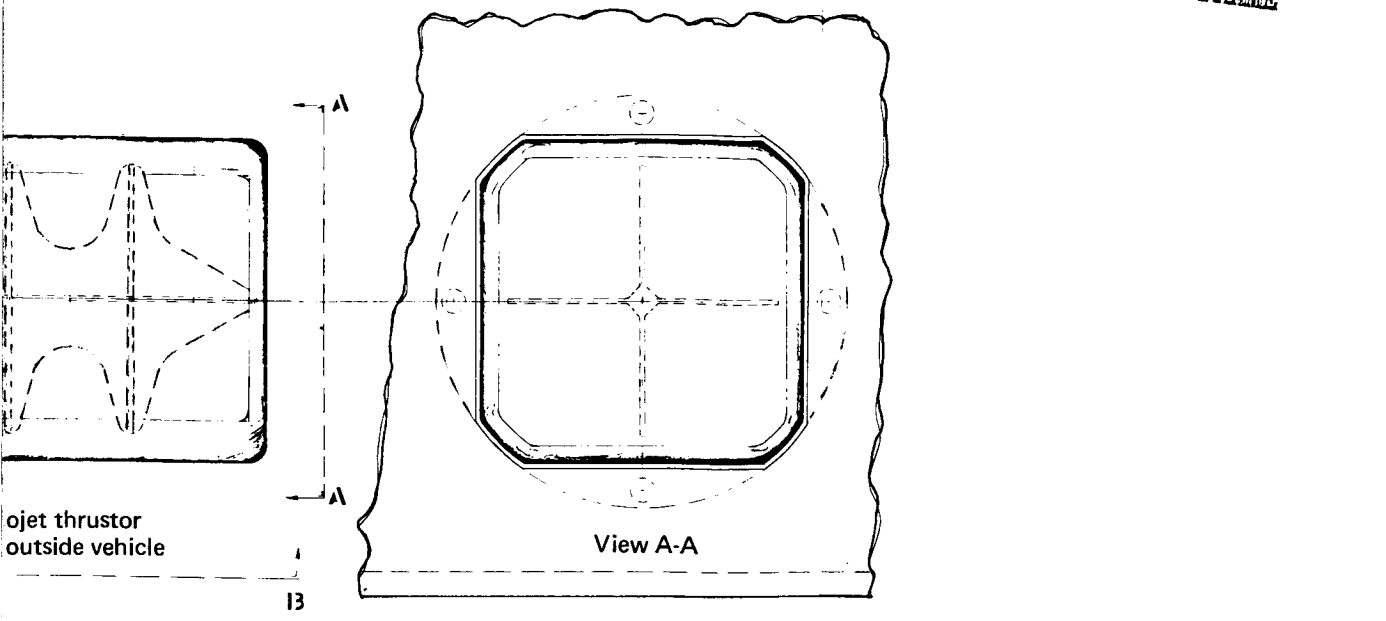

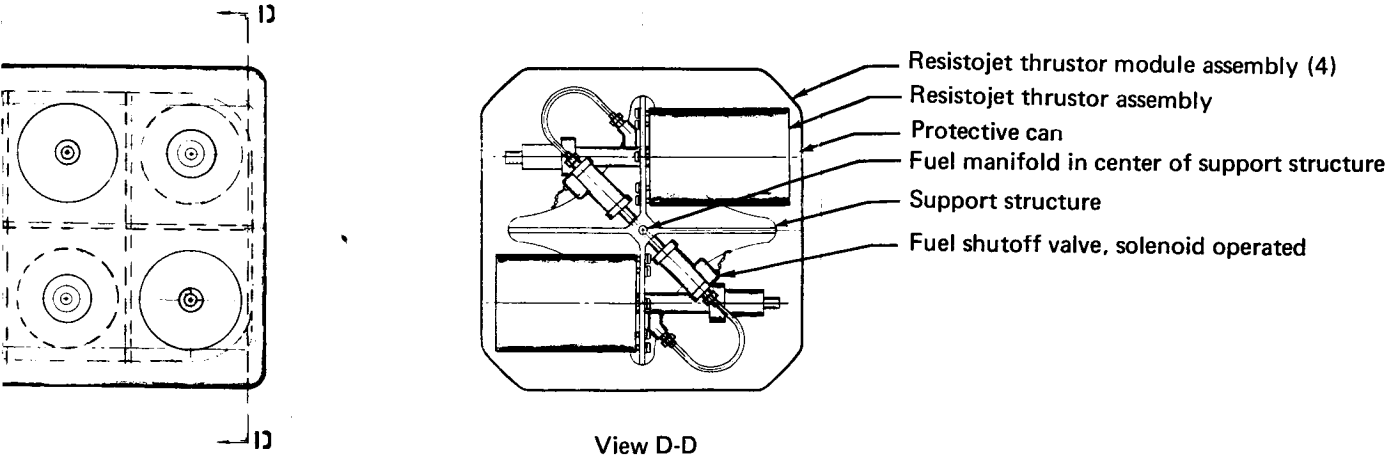

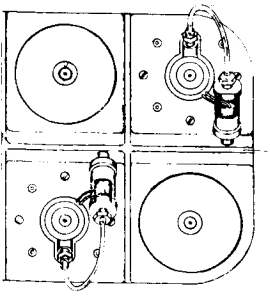

Figure 16. Resistojet Thrustor Module

FOLDOUT FRAME 2

1

FOLDOUT FRAME

The evacuated concentric-tubular design for the 0.044-N (10-mlbf) NH_3 resistojet thrustor is shown schematically in fig. 17. The two primary inputs to the thrustor are the electric power and the propellant flow, which are supplied simultaneously. The electrical path is through the outer pressure case, the case end, the nozzle, and the inner heating element. A strut connector electrically joins the inner and outer heating elements and permits a gas passage between them. The current passes along the outer heating element and the inner pressure case, completing the circuit at the power source. The ohmic heating takes place primarily in the inner heating element (80%) and the outer heating element (15%). A small percentage is developed in the pressure cases. The gas flow is introduced into the annulus between the inner and outer pressure cases and flows down the passage, through the transition area, and back between the inner and outer heating element, where a significant amount of gas heating occurs. The flow passes through the strut connector and down the center heating element, where it approaches the wall temperature before it is expanded through the nozzle. Heat loss is minimized and electrical efficiency is maximized by use of the vacuum jacket, the regenerative passage between the inner and outer pressure case, and the thermal insulation. The thermal- and gas-pressure loads are minimized by a bellows expansion compensator at the rear of the resistojet.

The detailed design of the thrustor, which has been successfully fabricated and performance tested at Marquardt, is shown in fig. 18. The performance of the thrustor is given in table 3. The inner and outer heating elements and the regeneratively cooled case passages are the only surfaces

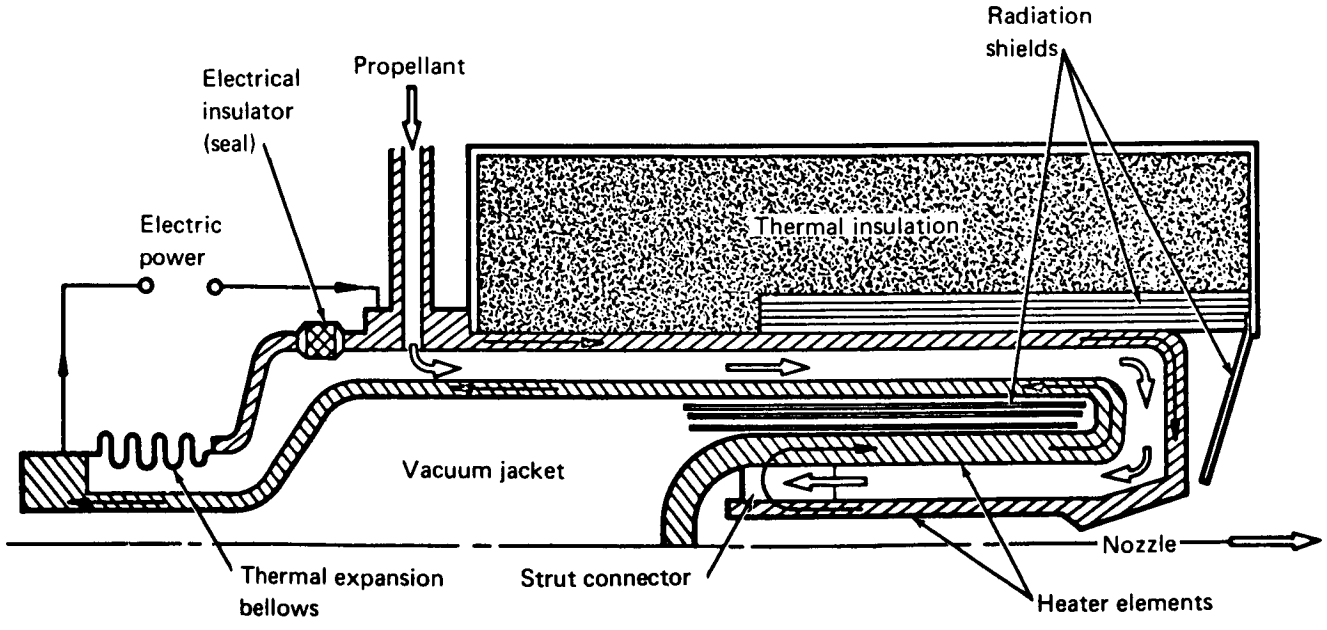

Note: Radial scale exaggerated

Figure 17. Evacuated Resistojet Concept

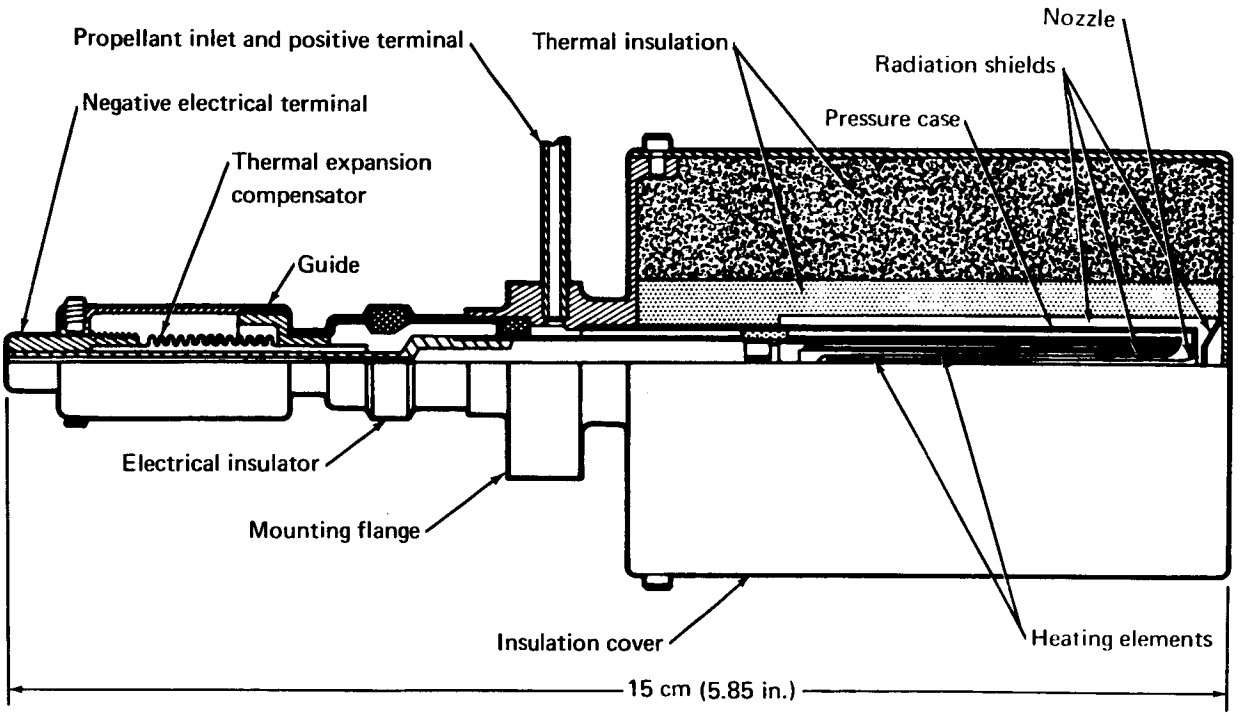

Figure 18. Model II Resistojet Thrustor

exposed to the gas. The intermediate elements are extremely thin radiation shields located in an area which is vented to space vacuum to eliminate conductive heat losses through the gas. No mechanical seals are used. The only seals required are at the propellant line connection, which is located a sufficiently remote distance from the hot case and where the electrical lead comes out of the concentric propellant connector (ceramic-to-metal seal), which is also located at a remote distance from the thrustor case and is cooled by the inlet propellant. Electrical insulators are used in the case at the outer annulus to prevent misalignment.

To avoid thermal stresses caused by dissimilar metals at these high temperatures, the thrustor is made almost exclusively of rhenium (Re). The Re heating elements are fabricated by vapor-deposition technique and are readily weldable. A metal bellows is used to alleviate induced axial stresses from thermal expansion. The design permits operation of the inner element at essentially negligible longitudinal stress at operating temperature. The radiation shield assembly is made of 0.076-mm (0.0003-in.) thick tantalum foil. The thrustor is surrounded by a layer of Dyna-Quartz insulation which serves to reduce the outer surface temperature to less than 1255°K (2260°R). The Dyna-Quartz is surrounded by a layer of Min-K-2000 thermal insulation, which keeps the stainless-steel case wall at or below 422°K (760°R).

TABLE 3

NH_3 RESISTOJET THRUSTOR PERFORMANCE

Element	Performance
Chamber pressure	2.41×10^5 N/m^2 (35 psia)
Thrust	4.45×10^{-2} N (10 mlbf)
Expansion ratio	35:1
Thrust coefficient	1.42
Chamber temperature	2420°K (4356°R)
I_{sp} (delivered)	364 sec
Required thrustor power	149 watts
Heater efficiency	81%
Power efficiency	87%
Propellant tank pressure	2.24×10^6 N/m^2 (325 psia)
Propellant tank temperature	325°K (585°R)
Throat diameter	0.41 mm (0.016 in.)
Mass flow rate--per thrustor	1.2×10^{-2} g/sec (2.75×10^{-5} lbm/sec)
Total flow rate--max	4.9×10^{-2} g/sec (11×10^{-5} lbm/sec)
Total flow rate--min	2.4×10^{-2} g/sec (5.5×10^{-5} lb/sec)

Tank and feed system: The NH_3 storage and feed system is shown in fig. 19. The NH_3 is stored in spherical tanks of 6-Al-4V titanium. Tank pressure is equal to the vapor pressure of the NH_3, nominally 2.13×10^6 N/m^2 (310 psia) at the ambient temperature in the aft interstage compartment. The propellant tank contains no positive expulsion system, since the NH_3 is expelled by its own vapor pressure. There is a relief and vent system to prevent overpressurization of the tank.

The NH_3 flows from the tank through a shutoff valve which can be used to isolate the tank from the remainder of the feed system. Downstream of the valve, the NH_3 flows through a heat exchanger where it picks up heat from the Brayton-cycle waste-heat radiator loop. This ensures that the flow will be vaporized before entering the pressure regulator.

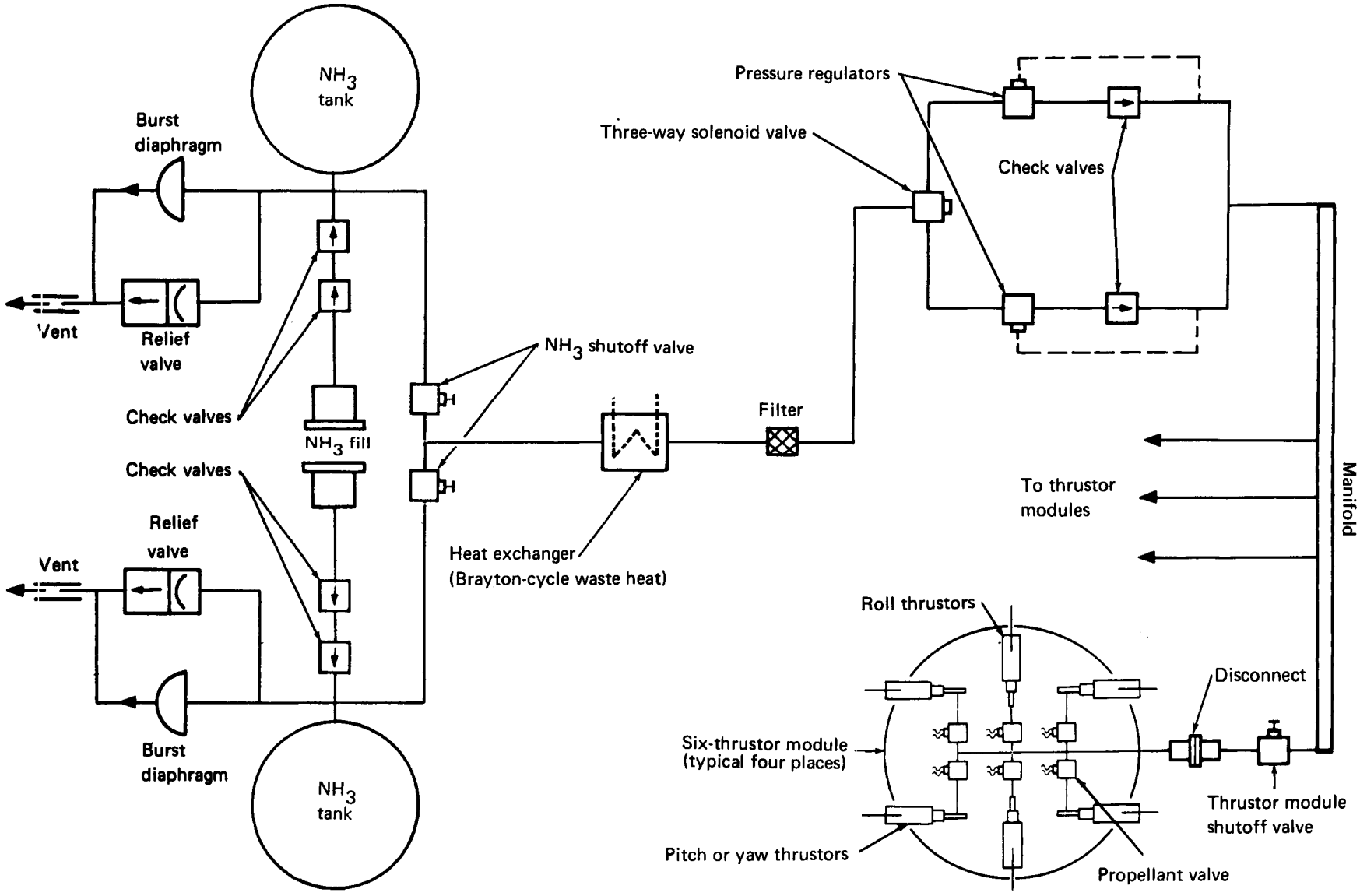

Figure 19. NH_3 Resistojet System

The heat exchanger is a 3.18-mm (1/8-in.) ID tube, 1.22-m (4-ft) in length, which is brazed to the inert-fluorochemical (FC-75) loop radiator tube. The output temperature of the NH_3 is identical to the FC-75, 400°K (720°R), as a result of the much greater flow of the radiator fluid. The FC-75 temperature is unaffected for the same reason.

The NH_3 flows from the heat exchanger to a three-way solenoid valve through a redundant pressure-regulator system. It then flows to an accumulator and finally to a manifold around the MORL which supplies the four thrustor modules. The redundant regulator system maintains the downstream pressure at 2.41×10^5 N/m^2 (35 psia). A valve and disconnect at each thrustor module allows thrustor removal and replacement, if necessary.

Electrical control module: The NH_3 resistojet uses an eight-transformer electric power-control system, two 163-watt transformers per thrustor module. The electrical schematic diagram for the selected power system is shown in fig. 20. Electrical power is supplied from two 400-Hz, single-phase, 200-volt square-wave inverters, one of which supplies the entire system, while the other is on standby. Inverter power comes from the 260 Vdc link bus, and the control power comes from the nonessential 28-Vdc bus. Voltage regulation requirement of the NH_3 resistojet is 1/2% at 4.8 volts. The stepdown transformers are utilized to reduce the 200-volt inverter voltage to the proper level. With 1/4% regulation in the inverter and careful design of the distribution system, 1/2% resistojet voltage regulator is achievable at the load.

Fig. 21 shows the resistojet-power wiring diagram for one of the four thrustor modules. This system consists of five subassemblies:

(1) Primary patch panel and breaker.

(2) Power-control connector.

(3) Stepdown transformer.

(4) Resistojet solenoid switches.

(5) Resistojet heater elements.

The primary patch panel and breaker subassembly are located centrally on the vehicle at the resistojet power bus and the inverters. Other subassemblies will be located in each thrustor module.

The control system operates as follows: If a signal is applied through the power-control connector, a solenoid valve will be opened that allows propellant to flow in one of the resistojets. This solenoid also closes two electrical contacts which energize the primary of the applicable transformer and connect the secondary winding to the correct heater element.

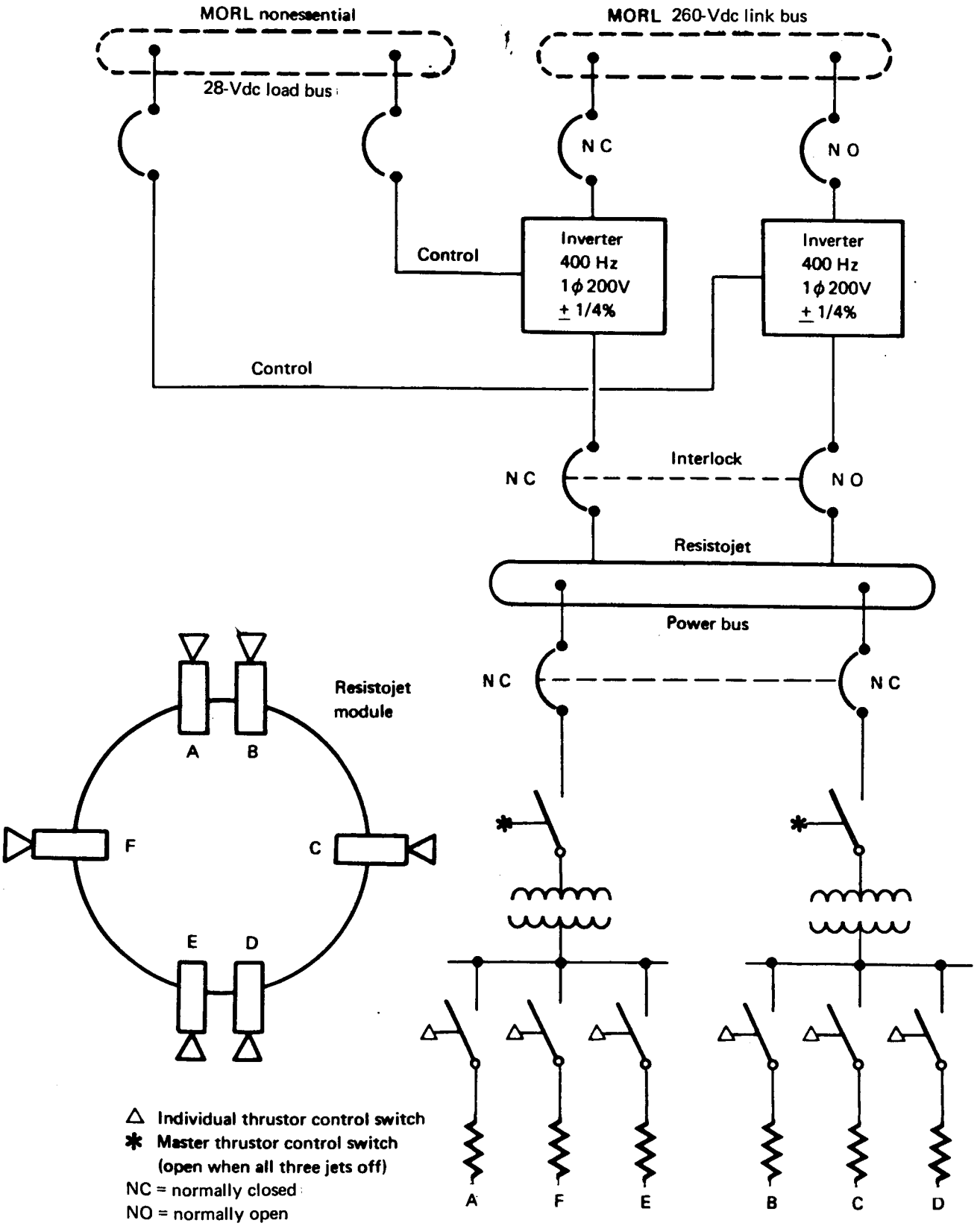

Figure 20. Resistojet Power System Schematic Diagram

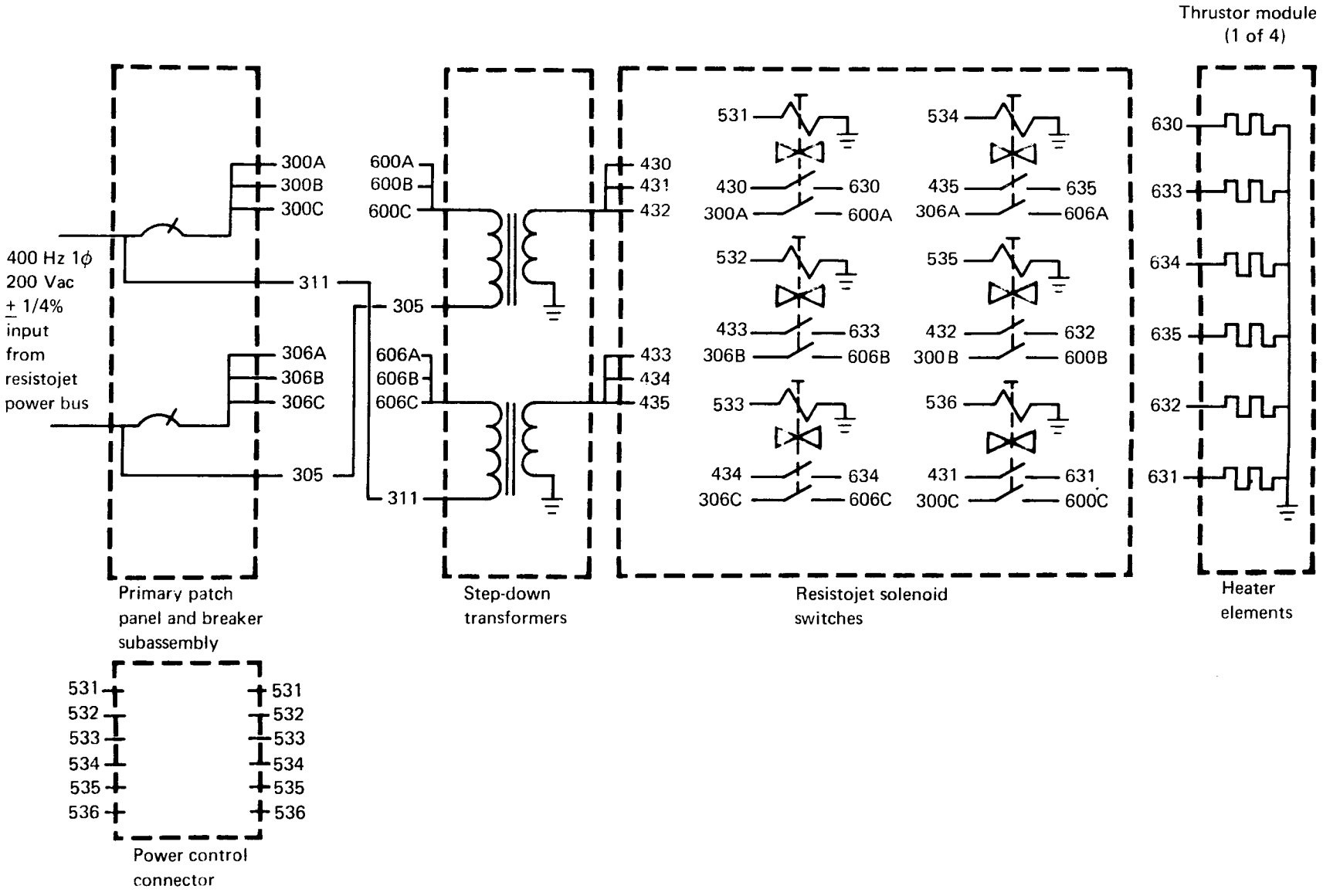

Figure 21. Resistojet Power System Wiring Diagram

Each transformer will dissipate 6.75 watts in the loaded condition. With no load on the secondary of the transformer, the unit would still dissipate 3.6 watts in core losses. To eliminate this unnecessary no-load loss, the system is designed to turn off the primary of the transformer if there is no secondary load. One electrical contactor on the solenoid valve in each resistojet may be eliminated if the primaries of all transformers are left energized; this might be desirable if the heat resulting from the loss to the no-load transformer could be beneficially used.

The transformers have 4-mil grain-oriented silicon steel C-cores and exhibit a magnetic flux density of 1.2 T (12 000 gauss). Wire size of 750 circular mils/amp was selected to ensure the proper current density for maximum efficiency.

At present, the failure-rate design goal for transformers of this type is 0.001%/1000 hours before failure (MORL mission time is 43 700 hours). While the goal has not been proved through test, it has been adopted for such aerospace projects as MOL and Spartan. It is therefore expected that this is a reasonable rate for the MORL vehicle.

The schematic shown has no provision for a talk-back signal from the individual resistojet solenoid valves. If a talk-back is designed, a third electrical contactor should be added. This contact would energize a lamp on a display panel when the solenoid is opened.

Scheduled-disturbance control system. — The scheduled-disturbance control system is a N_2H_4 monopropellant thrustor system, which provides control through use of four thrustor modules mounted at $\pi/2$ rad (90°) intervals around the aft periphery of the MORL, as shown in fig. 22. Each module contains three 44.5-N (10-lbf) thrust N_2H_4 engines (fig. 23); one roll and two pitch or yaw. Meteoroid shield protection is provided for the propellant-valve end of the thrustors, and the nozzles are exposed to facilitate heat radiation. The modules are replaced in same manner as are the resistojet thrustor modules. The performance of the selected system is summarized in table 4. The system provides the high thrust necessary to control the MORL vehicle during the periods of scheduled high disturbances such as logistics-vehicle docking and 9-g centrifuge operation, and also provides backup attitude-control capability.

The docking disturbance based on typical Gemini data is illustrated in fig. 24 in which the logistics vehicle approaches the MORL at a relative velocity of 0.305 m/sec (1.0 ft/sec), a lateral offset of 15.2-cm (0.5-ft), and a vehicle centerline misalignment of 0.087 rad (5°). The combination of these errors results in a 0.0044 rad/sec (0.25°/sec) tumble rate. The thrustors of the scheduled-disturbance control system null the tumble rate in 17 sec, and the resultant attitude error is 0.044 rad (2.5°).

The centrifuge aboard the MORL provides 1-g acceleration for occupants undergoing normal crew conditioning and 9-g acceleration for re-entry simulation. The CMG's are sized to store the angular momentum generated by 1-g operation. The disturbances resulting from the 9-g acceleration are

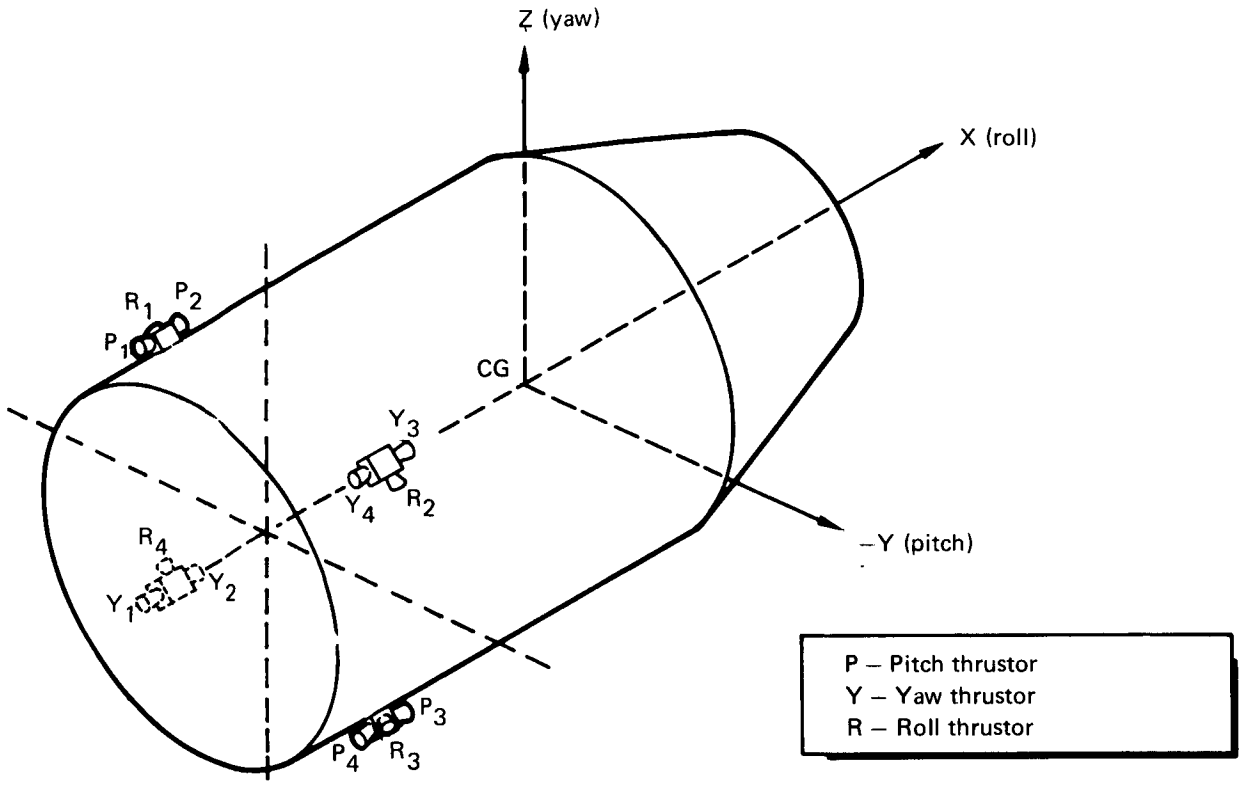

Figure 22. Monopropellant Thrustor Locations

damped by the monopropellant engine system. The re-entry simulation (9-g acceleration) alternately accelerates and decelerates the occupants at realistic onset rates to produce an approximation of the g-forces experienced during re-entry. The acceleration profile is shown in fig. 25 for a worst case (minimum range) Apollo re-entry from a 370-km (200-nmi) orbit. Each centrifuge run lasts about 20 min. including a 1-g hold for 15 min. after the re-entry run, to more closely simulate an actual re-entry. The peak angular momentum and disturbance to torque generated by a 9-g re-entry simulation is 11 970 N-m-sec (8800 ft-lbf-sec) and 81.6 N-m (60 ft-lbf), respectively.

During uncontrolled centrifuge operation, there is a momentum exchange between centrifuge and spacecraft which results in the attitude errors shown in fig. 26. The 9-g centrifuge operation aboard the MORL produces a maximum roll rate of 0.0122 rad/sec (0.7°/sec). At the end of the operation, the roll-attitude error would be 1.18 rad (68°). Pitch- and yaw-attitude errors are considerably smaller [approximately 0.174 rad (10°)] since 9-g run extends over only a small portion of the total precession period. Control of this disturbance can be provided with a 299-N-m (220-ft-lbf) roll moment. The scheduled-disturbance control system provides this through use of two 44.5-N (10-lbf) thrust roll engines fired in a couple. The pitch and yaw corrections are achieved by the 44.5-N thrust engines firing in those axes.

FOLDOUT FRAME

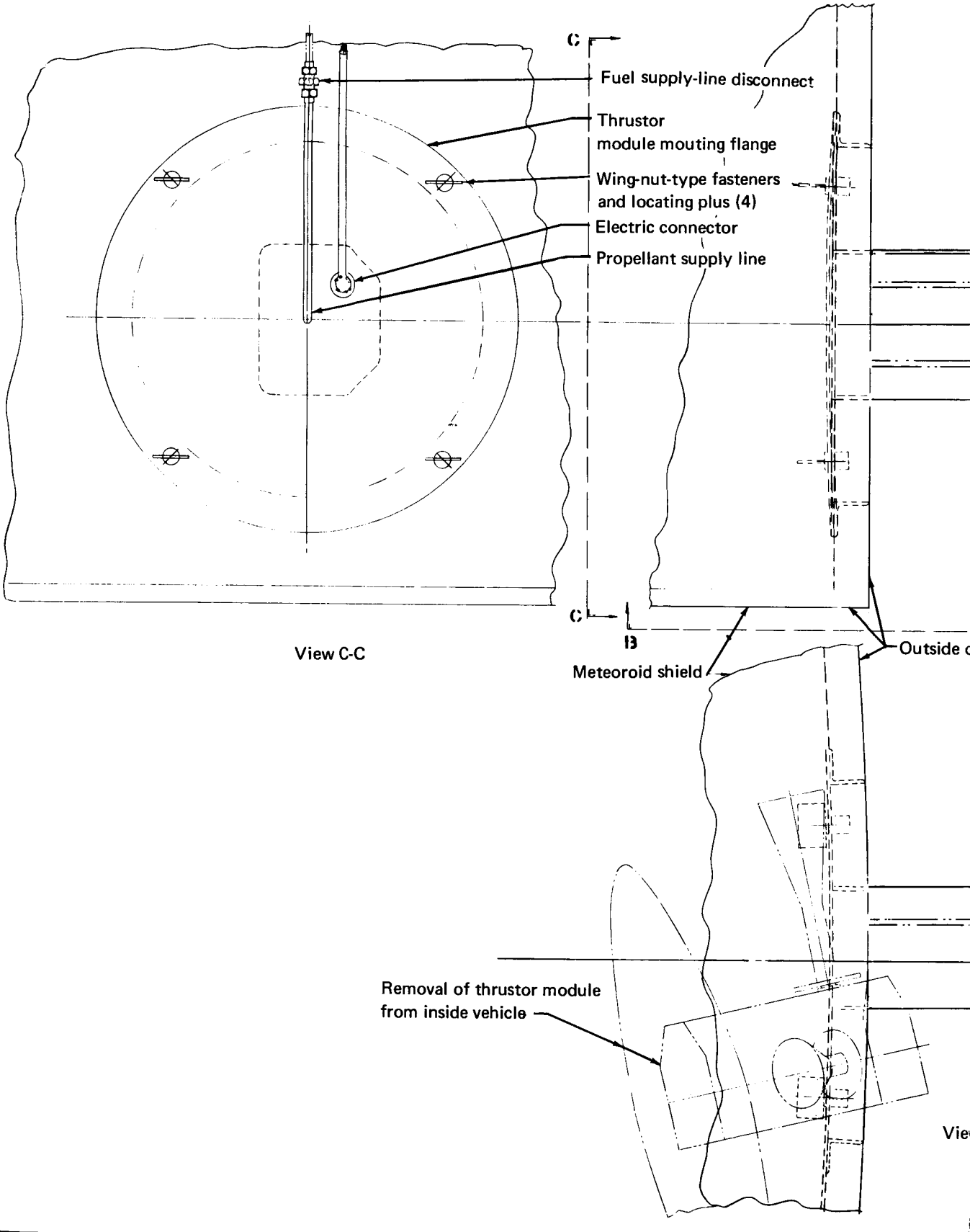

View C-C

FOLDOUT FRAME

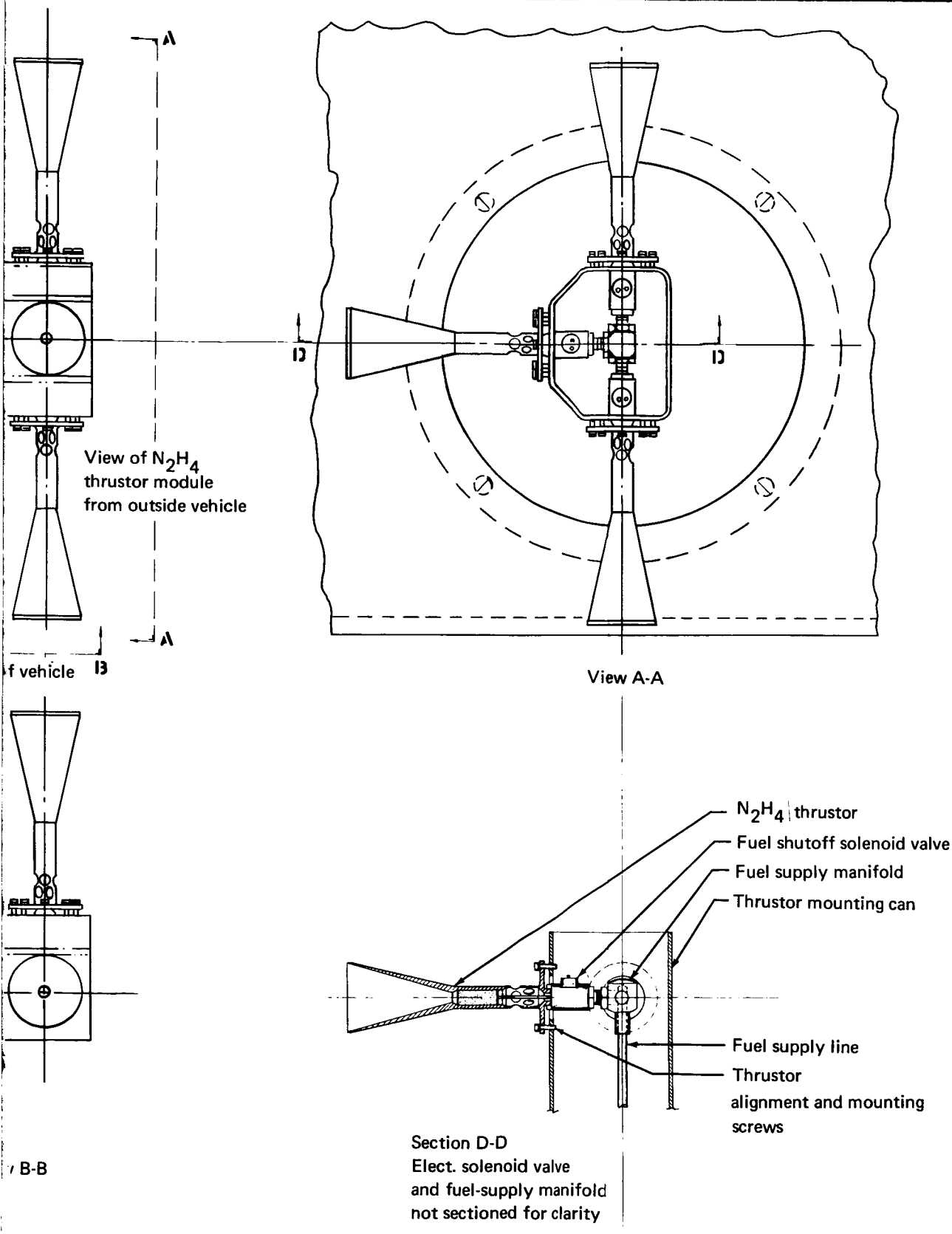

Figure 23. Monopropellant Thrustor Module

TABLE 4

MONOPROPELLANT PERFORMANCE SUMMARY

Element	Performance
Propellant	N_2H_4
Thrust per engine	44.5 N (10 lbf)
Number of engines	12
Total impulse per 90 days	1.3×10^5 N-sec (23 150 lbf-sec)
I_{sp} (mission average)	188 sec
I_{sp} (steady-state delivered)	235 sec
Propellant weight per 90 days	55.6 kg (123 lbm)
Chamber pressure	6.89×10^5 N/m^2 (100 psia)
Expansion ratio	50:1
Chamber temperature	1250°K (2260°R)
Propellant tank pressure	1.72×10^6 N/m^2 (250 psia)
Propellant tank temperature	325°K (585°R)
Bellows expulsion efficiency	98%
N_2 bottle initial pressure	2.06×10^7 N/m^2 (3000 psia)

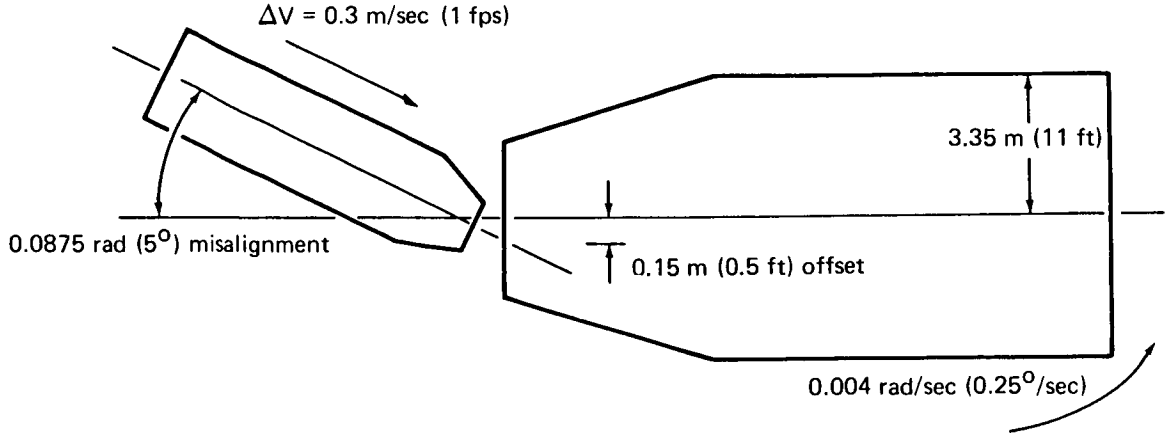

Figure 24. Docking Disturbance

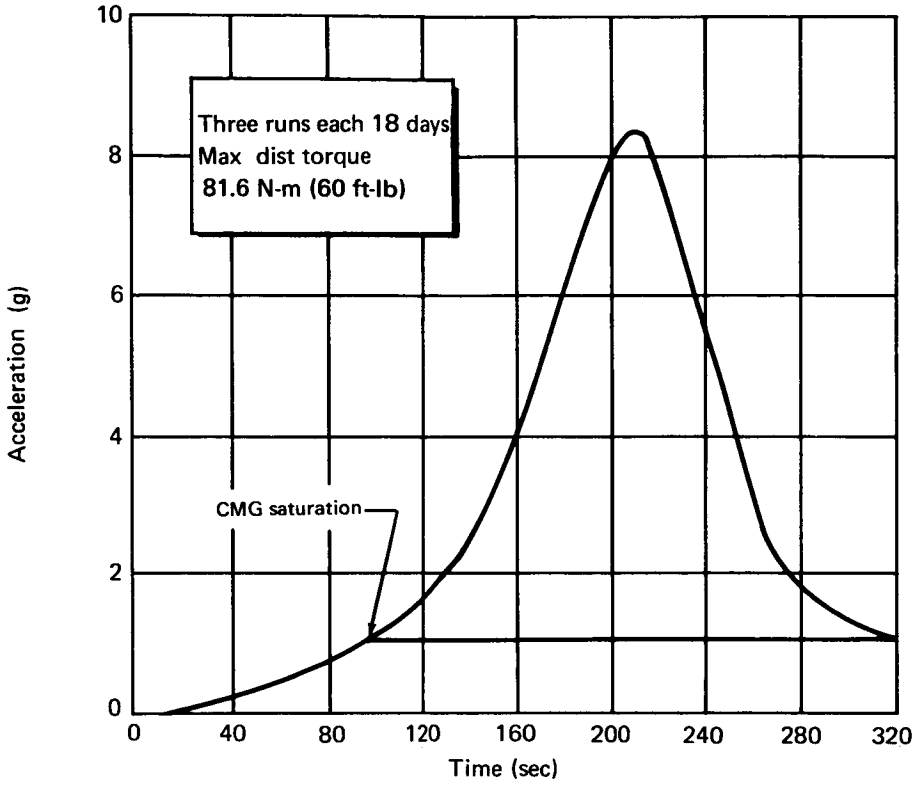

Figure 25. Centrifuge Simulated Re-entry Profile

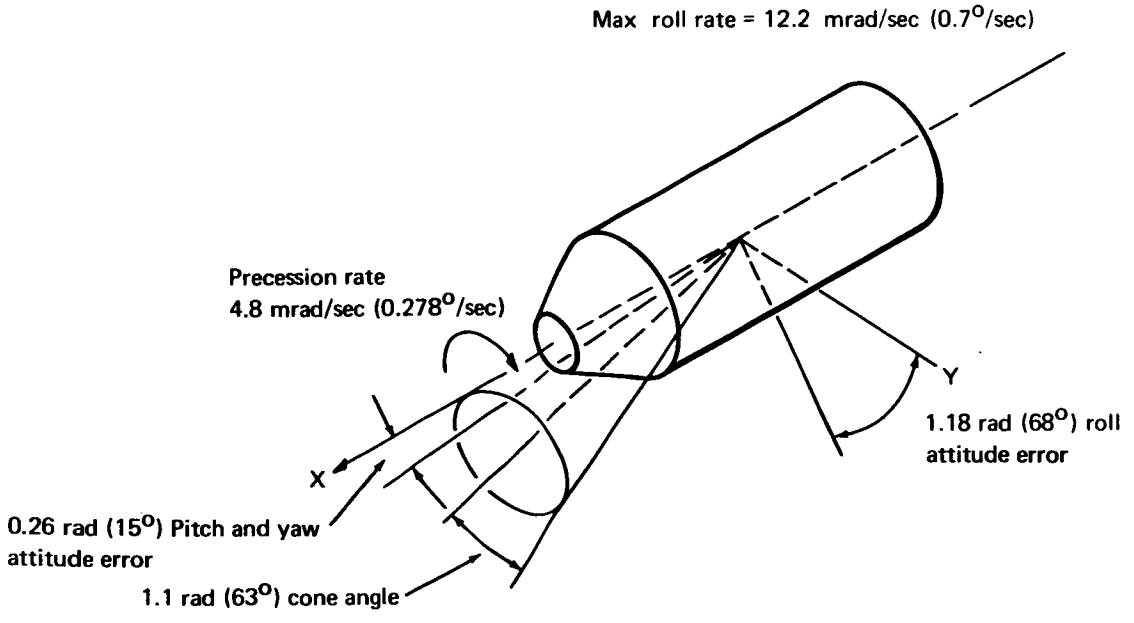

Figure 26. Centrifuge Disturbance Effects

The scheduled-disturbance control system also acts as an emergency backup attitude control system for periods when the CMG's may be inoperative for either scheduled or unscheduled maintenance. For this end, 8900 N-sec (2000 lbf-sec) of limit-cycle operation is provided. Table 5 presents the impulse requirements for the scheduled-disturbance control system to provide the control as described above. These requirements are derived elsewhere in this volume.

Logistics-vehicle stowage creates an additional scheduled disturbance, which must be considered. After a logistics vehicle docks with the MORL and the crew and supplies have transferred to the MORL, the vehicle is manipulated to a radial storage position on the conical forward section of the laboratory. The stowage cycle (fig. 27) consists of rotating the logistics module π rad (180°) about one of the stowing arms, rotating the module and the stowing arm 1.27 rad (73°) to bring the module in line with one of the five stowage ports, and translating the module along the stowage to bring it to the stowed position.

The magnitude and duration of the stowing disturbances are functions of the moments and force applied to accomplish rotations and translation. The typical stowage cycle can be accomplished by applying a constant 67-N-m (50-ft-lbf) moment, to complete the cycle in minimum time. This would result in the attitude errors shown in fig. 27 if no control torques were applied. The moment required to stabilize the vehicle within ±0.087 rad (±0.5°) is 268 N-m (200 ft-lbf), which can be provided by two of the monopropellant 44.5-N (10-lbf) thrustors. However, proper regulation of the stowage cycle will allow the CMG's to provide control actuation without use

TABLE 5

SCHEDULED-DISTURBANCE CONTROL SYSTEM REQUIREMENT

Operation	Impulse--per 90 days, N-sec (lbf-sec)	Pulse width (sec)
Limit cycle	8 900 (2 000)	0.08
Docking	2 000 (450)	11.0
Centrifuge	92 100 (20 700)	0.25
Total	103 000 (23 150)	

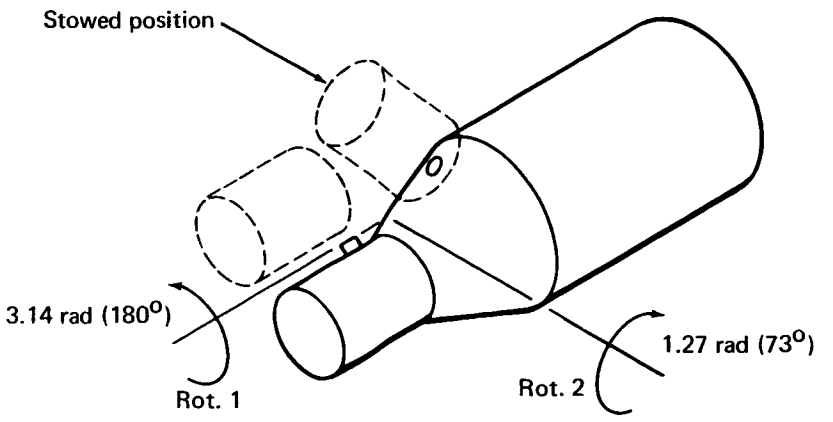

Effect on spacecraft

Stowing schedule	Accelerate-decelerate		Accelerate-coast-decelerate
Attitude errors	Pitch	0.012 rad (7°)	—
	Yaw	0.014 rad (8°)	—
	Roll	0.714 rad (41°)	—
Time to stow	4 min		5 min

Figure 27. Stowage Disturbance

of the monopropellant thrustors. This cycle consists of the application of a 68-N-m (50-ft-lbf) moment until 1360 N-m-sec (1000 ft-lbf-sec) of angular momentum about pitch and/or 3400-N-m-sec (2500 ft-lbf-sec) about roll have been generated. The logistics vehicle then rotates at a constant rate maintaining constant angular momentum. At an appropriate stowing angle, a 68-N-m decelerating moment is applied to stop the rotation, thus removing the angular momentum. Stowing time is increased to 5 min, compared to 4 min for the constant-moment procedure. The result of this latter procedure is that the allowable attitude error ±8.7 rad (±0.5°) is not exceeded, and consequently, no requirements are imposed on the scheduled-disturbance control system.

N_2H_4 monopropellant thrustor: The monopropellant thrustor utilizes N_2H_4 propellant, which exothermally decomposes while passing over a catalyst bed to provide the thrust energy. The monopropellant thrustor provides a steady-state specific impulse of about 235 sec, with a gas temperature of 1255°K (2260°R). Thus, ordinary materials (heat-resisting stainless steels) are employed for thrust chamber construction. There are no high-temperature material problems as there are with the refractory metals or ablative materials used in high-temperature bipropellant systems. Consequently, long engine life is possible with N_2H_4 thrustors.

Fig. 28 shows a schematic of the monopropellant thrustor and gives thrustor dimensions for the 44.5-N (10-lbf) thrust level. A radiation heat barrier is located between the catalyst bed and the propellant valves. This heat barrier is installed to prevent heat soakback from the hot catalyst bed to the propellant valve after engine shutdown, thus preventing a high temperature rise which would vaporize propellant in the propellant valve. Test data indicate that a valve operation at 298°K (535°R) can be limited to a temperature rise of approximately 333°K (600°R) after engine shutdown with this radiative heat barrier.

The thrustors operate at a chamber pressure of 6.89×10^5 N/m^2 (100 psia) and have an expansion ratio of 50:1. The thrustor performance (shown in table 4) is a function not only of pulse width but also of thrustor off time. These effects are shown in fig 29. For long off times, some of the residual thermal energy of the catalyst bed will be radiated to the space environment with subsequent reduction in the pulsing performance. These performances were integrated with the duty cycles defined for the various scheduled-disturbance operations. Results of this analysis are presented in table 6. The monopropellant system exhibits a performance of 188 sec of specific impulse for the overall requirements. This somewhat reduced performance results because many of the operations require duty cycles with significant thrustor off times between firings. The use of an electrical heater blanket surrounding the catalyst bed can significantly improve the overall performance. A total of 55.8 kg (123 lbm) of N_2H_4 is required to meet the high thrust requirements for a 90-day period.

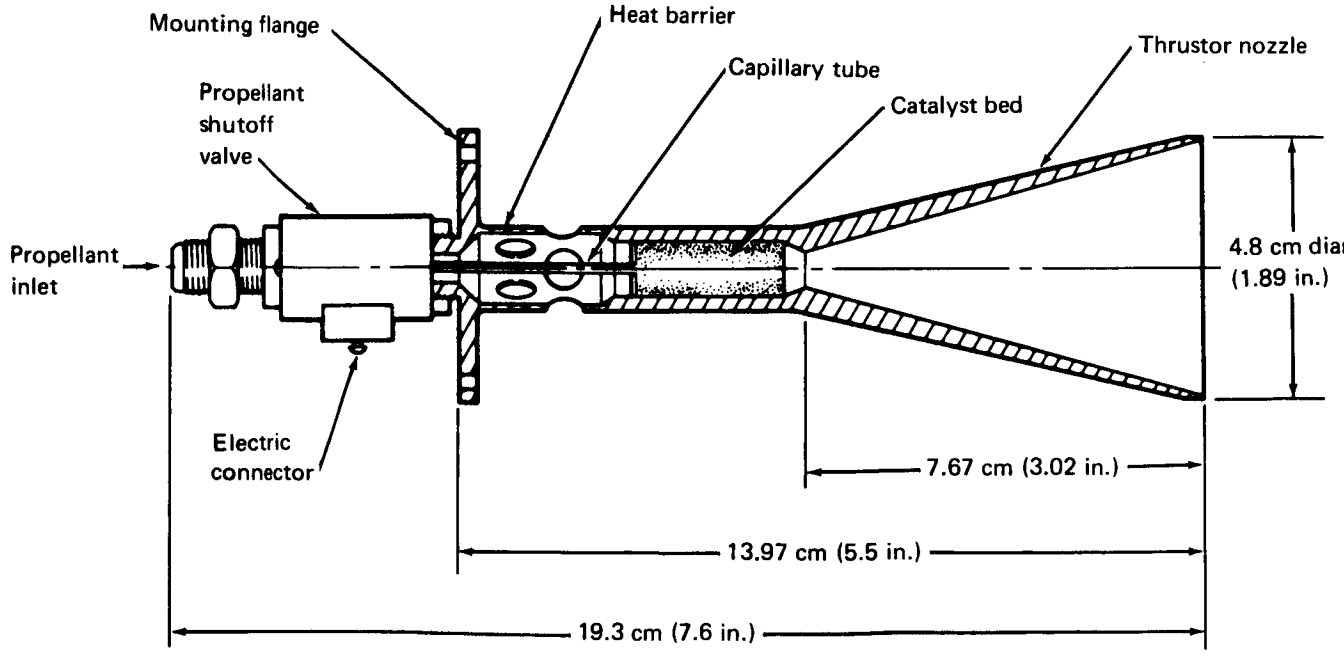

Figure 28. Monopropellant N_2H_4 Thrustor

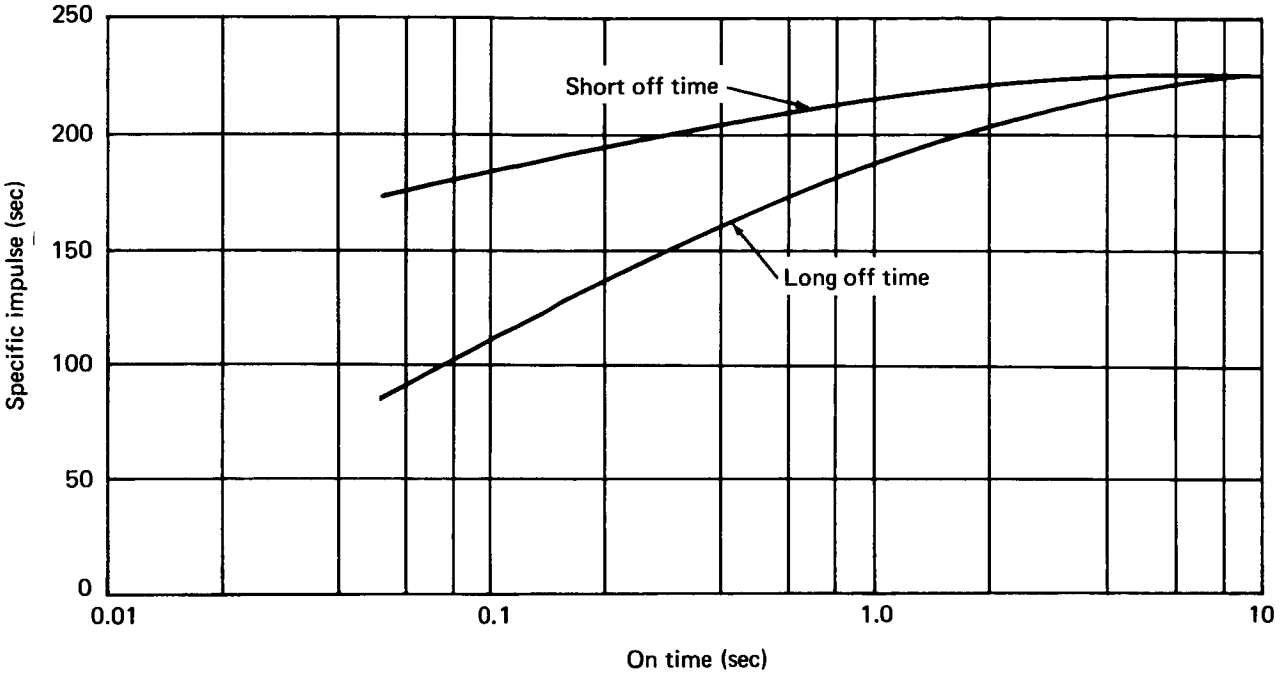

Figure 29. Monopropellant Pulsing Performance

Monopropellant tank and feed system: Propellant is stored in the aft interstage of the MORL vehicle at the ambient temperature of 325°K (586°R) and a tank pressure of 1.72×10^6 N/m^2 (250 psia) (fig. 30). The N_2H_4 is expelled by a positive-expulsion system with a metal bellows which is compatible

TABLE 6

HIGH-THRUST SYSTEM PERFORMANCE

Operation	Impulse per 90-days N-sec (lbf-sec)	Pulse width (sec)	Specific Impulse (sec) monopropellant	90-day propellant weight, kg (lb)
Limit cycle	8 900 (2 000)	0.08	120	7.70 (17)
Docking	2 000 (450)	11.0	230	0.91 (2)
Centrifuge	92 000 (20 7000)	0.25	200	47.1 (104)
Total	103 000 (23 150)	---	188	55.7 (123)

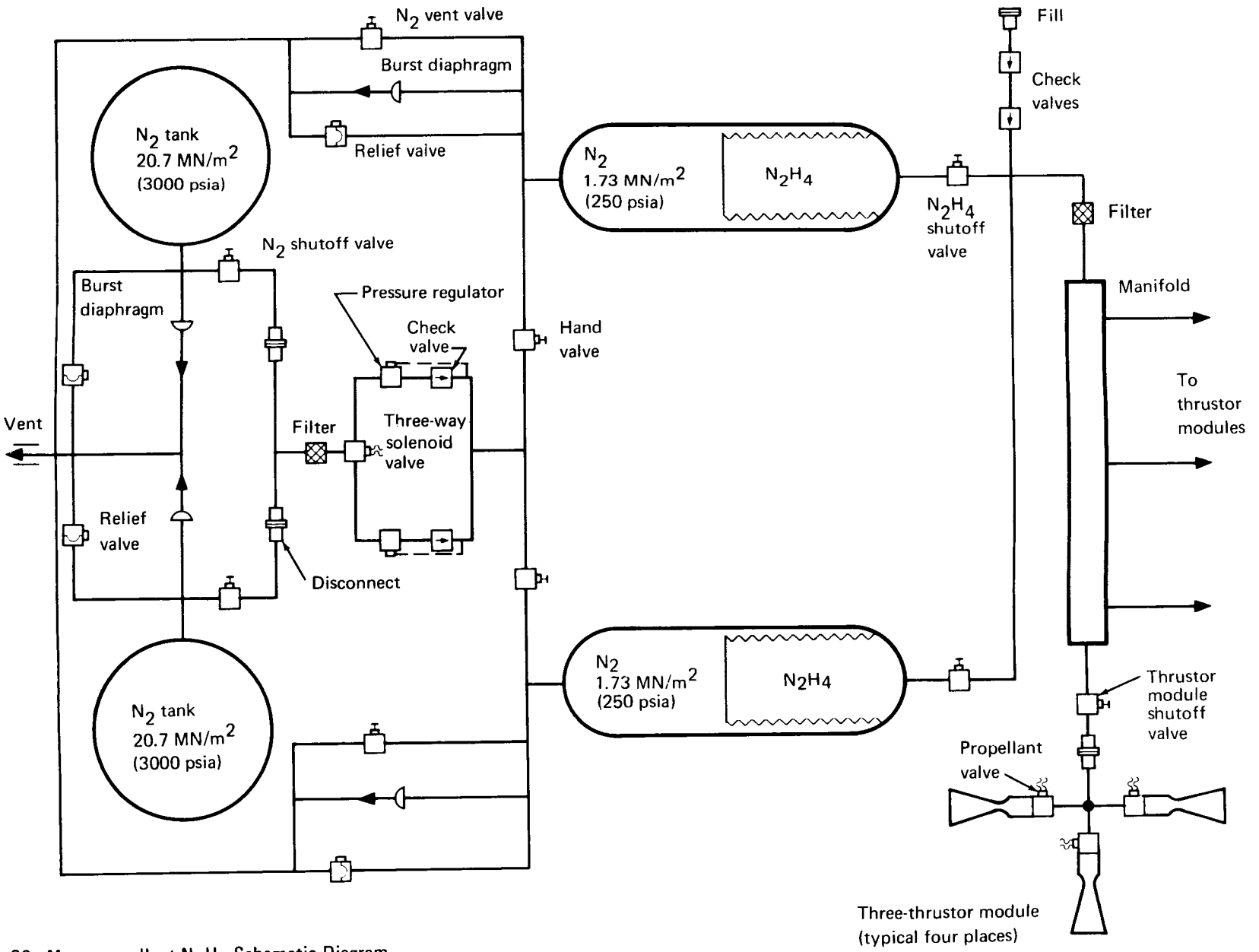

Figure 30. Monopropellant N_2H_4 Schematic Diagram

with N_2H_4 over the 5-year mission and may be recycled to allow for propellant resupply from the logistics vehicle. The propellant tanks are fabricated from AM-350 stainless steel. The tanks are 34.3 cm (13.5 in.) in diameter to accommodate a nominal 30.5-cm (12-in.) diam bellows.

Pressurization of the propellant tank is provided by a 2.07×10^7-N/m^2 (3000-psia) N_2 bottle of 6 Al-4V-Ti alloy. A total of 4.5 kg (10.0 lbm) of nitrogen is required for the monopropellant system. Table 7 summarizes the characteristics of the metal bellows, propellant tank, and N_2 bottle.

TABLE 7

HIGH-THRUST SYSTEM PROPELLANT TANKAGE

Description	Characteristic
Propellant Weight, kg (lbm)	
Loaded	92.5 (204)
Usable	90.6 (200)
Bellows	
Diameter, cm (in.)	31.7 (12.5)
Length, cm (in.)	128.1 (50.5)
Weight, kg (lbm)	23.1 (51)
Propellant Tank	
Material	AM–350 stainless steel
Pressure, N/m^2 (psia)	1 720 000 (250)
Diameter, cm (in.)	34.2 (13.5)
Gage, mm (in.)	0.51 (0.020)
Weight, kg (lbm)	11.3 (25)
Pressurant Bottle	
Pressurant	Nitrogen
Pressure, N/m^2 (psia)	20 7000 000
Material	6 Al–4V–Ti alloy
Diameter, cm (in.)	34.6 (13.6)
Gage, mm (in.)	2.25 (0.088)
Nitrogen weight, kg (lbm)	4.58 (10.1)
Bottle weight, kg (lbm)	4.07 (9)

The N_2 bottle is allowed to blow down to a minimum of 2.07×10^6 N/m^2 (300 psia) at the end of the expulsion cycle. A relief system is provided for both the high- and low-pressure systems. The low-pressure relief system includes a solenoid valve which enables the pressurant to be vented during propellant refill. The gas relief systems are manifolded to a common vent line through the aft meteoroid shield.

From the storage tank, N_2H_4 is fed under pressure through redundant solenoid valves and filters to a manifold around the MORL vehicle perimeter and then to the thrustor modules. A valve and disconnect are provided at each thrustor module to allow thrustor module removal and replacement, if required. If a tank fails, removal of the N_2H_4 tank for replacement can be accomplished after closing the shutoff valve and venting the N_2 gas pressure. Removal of the N_2 gas bottle for replacement can be accomplished by closing the shutoff valve and disconnecting the vent line on the relief side of the high-pressure relief system.

Logistics resupply. — The logistics vehicle consists of a modified Apollo command module (CM) and a special service pack used in conjunction with a multimission module. This entire complex is mounted atop of a Saturn IB launch vehicle (fig. 31). A nominal launch weight of 14 900 kg (33 000 lbm) is assumed, including full cargo and crew.

During the 5-year MORL mission, the logistics vehicle will supply propellants to the MORL at 90-day intervals. Both the NH_3 resistojet system and the N_2H_4 high-thrust system will be resupplied by transfer of the propellants from the logistics vehicle tanks to the MORL propellant tankage.

The NH_3 resistojet system requires 209 kg (462 lbm) of NH_3 to be resupplied every 90 days. A schematic of the logistics NH_3 transfer system is shown in fig. 32. The NH_3 is stored in a 92.5-cm (36.5-in.) spherical tank with a positive expulsion bladder for zero-g transfer. The transfer of the NH_3 is accomplished by an N_2 pressurization system. The N_2 bottle stores 19.9 kg (44 lbm) of N_2 at 2.07×10^7 N/m^2 (3000 psia). A total of 5.89 kg (13 lbm) of NH_3 remains trapped in the system after the transfer process. The total launch weight chargeable to the NH_3 logistics system is 296.69 kg (653 lbm). The detailed weight breakdown is given in table 8.

A flow schematic of the monopropellant transfer system is shown in fig. 33. The N_2H_4 aboard the logistics vehicle is stored in a spherical tank with a positive expulsion bladder. Transfer is effected by an N_2 pressurization system. The tank pressure is maintained at 3.45×105 N/m^2 (50 psia) during the transfer process. This requires venting of the pressurant gas in the MORL tanks during the propellant transfer process. Flow control of the liquid propellant is accomplished by a cavitating venturi. After termination of the transfer process, the MORL tank is repressurized to its operating pressure of 1.72×10^6 N/m^2 (250 psia). N_2 is resupplied by means of replacing the expended gas bottle with a full one. This is preferable to gas transfer, since both an isentropic transfer process and a pneumatic pumping scheme are excessively heavy. For example, analysis indicates that about 145 kg (32 lbm) is required to transfer 3.62 kg (8 lbm) of N_2. This results

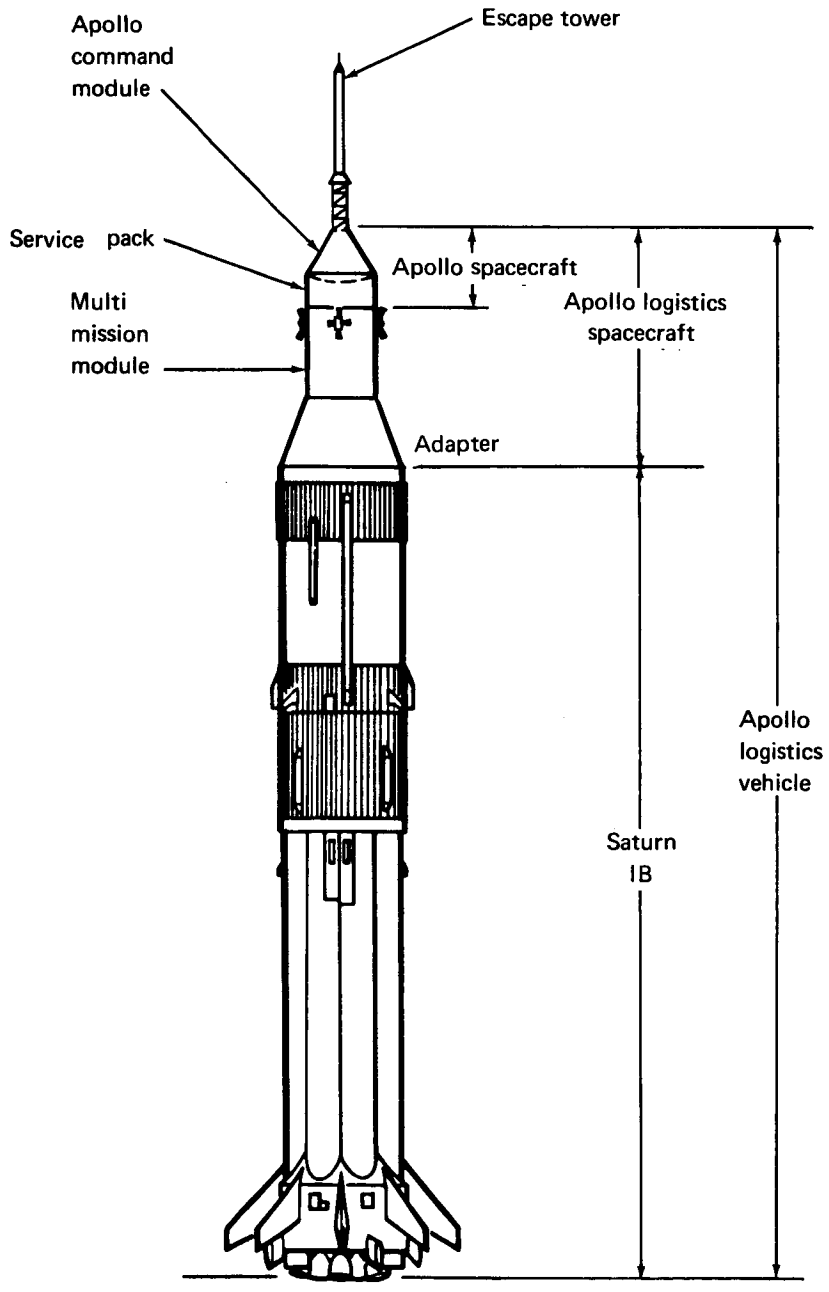

Figure 31. Apollo Logistics Vehicle

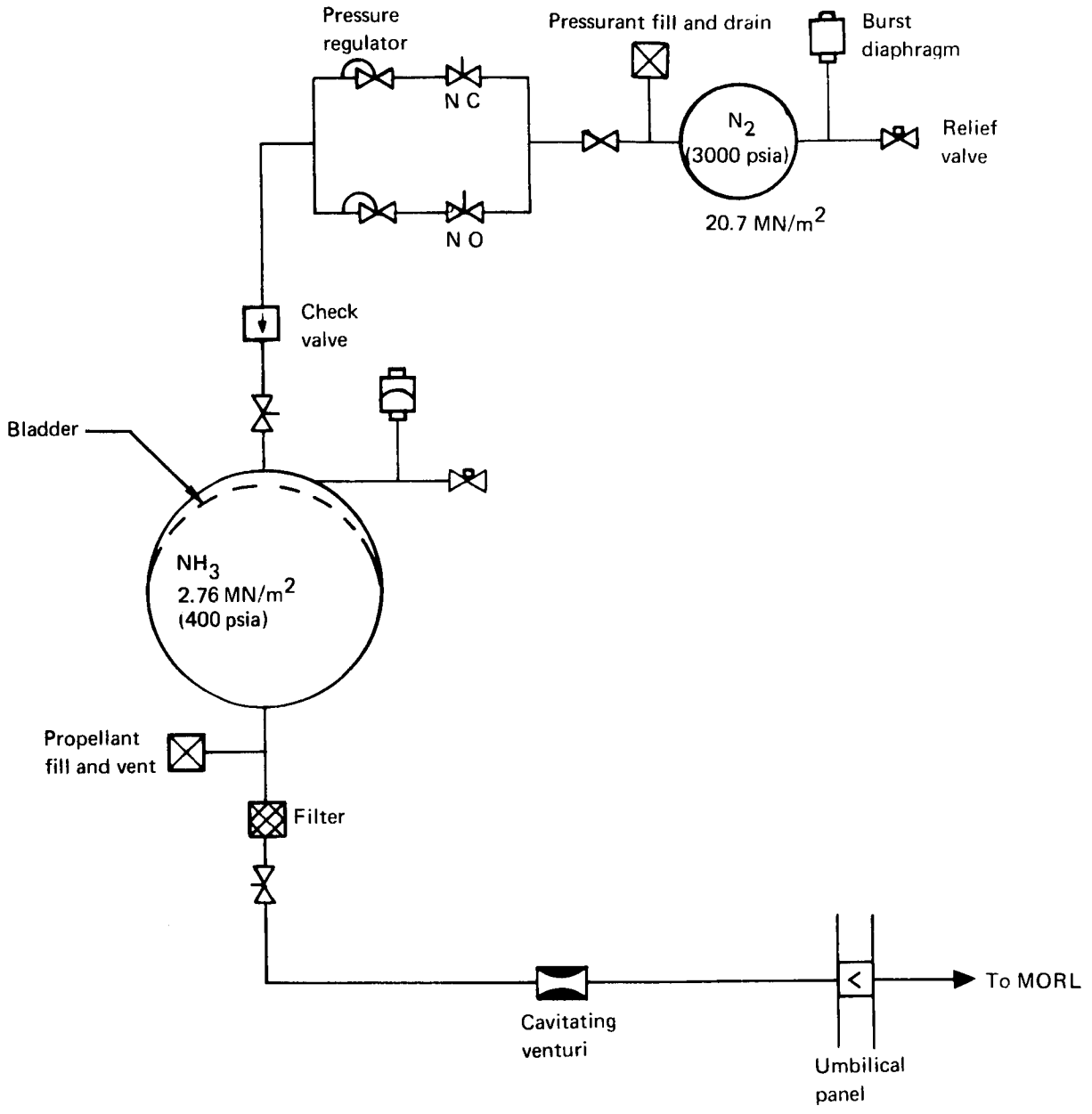

Figure 32. NH_3 Resupply System

TABLE 8

NH_3 RESUPPLY SYSTEM WEIGHT SUMMARY

Item	Weight, kg (lbm)
Propellant	
Usable	209.0 (462)
Trapped	5.9 (13)
Loaded	214.9 (475)
N_2	19.9 (44)
Propellant tank	27.2 (60)
Lines and valves	9.5 (21)
Pressurant bottle	27.0 (59)
Total weight at launch	298.5 (659)

from the temperature drop during an isentropic transfer. A weight summary of the logistics resupply system for the monopropellants is shown in table 9.

Weight summary. — Weight of the attitude-control and orbit-keeping system is summarized in table 10. The total system launch weight includes the CMG system, the N_2H_4 monopropellant thrustor system, the NH_3 resistojet thrustor system, and the resistojet power-control system. In addition to these weights, a weight penalty for consumption of electric power is charged to the system to arrive at the total chargeable launch weight.

The total CMG system weight is 284 kg (628 lbm), and it requires 151 watts of electric power. The weight penalty for power consumption has been established in previous studies at 136 kg/kW (300 lbm/kW); hence, the weight assessment for power consumption assigned to the CMG system is 20.4 kg (45 lbm).

The NH_3 resistojet system operates at maximum power for 4 hours/day while the MORL is in the inertial orientation. During the remaining 20 hours, the MORL is in the belly-down orientation, and the resistojet system power requirement is reduced to 50% of maximum. The extra power can be stored in batteries at an efficiency of 50%, that is, one half of the excess power can actually be stored. Thus, the average power requirement per day is 79% of the maximum. For the NH_3 resistojet system, the maximum power required is 636 watts, which yields an average daily value of 502 watts. The weight penalty for power consumption for the NH_3 resistojet system is 69 kg (151 lbm).

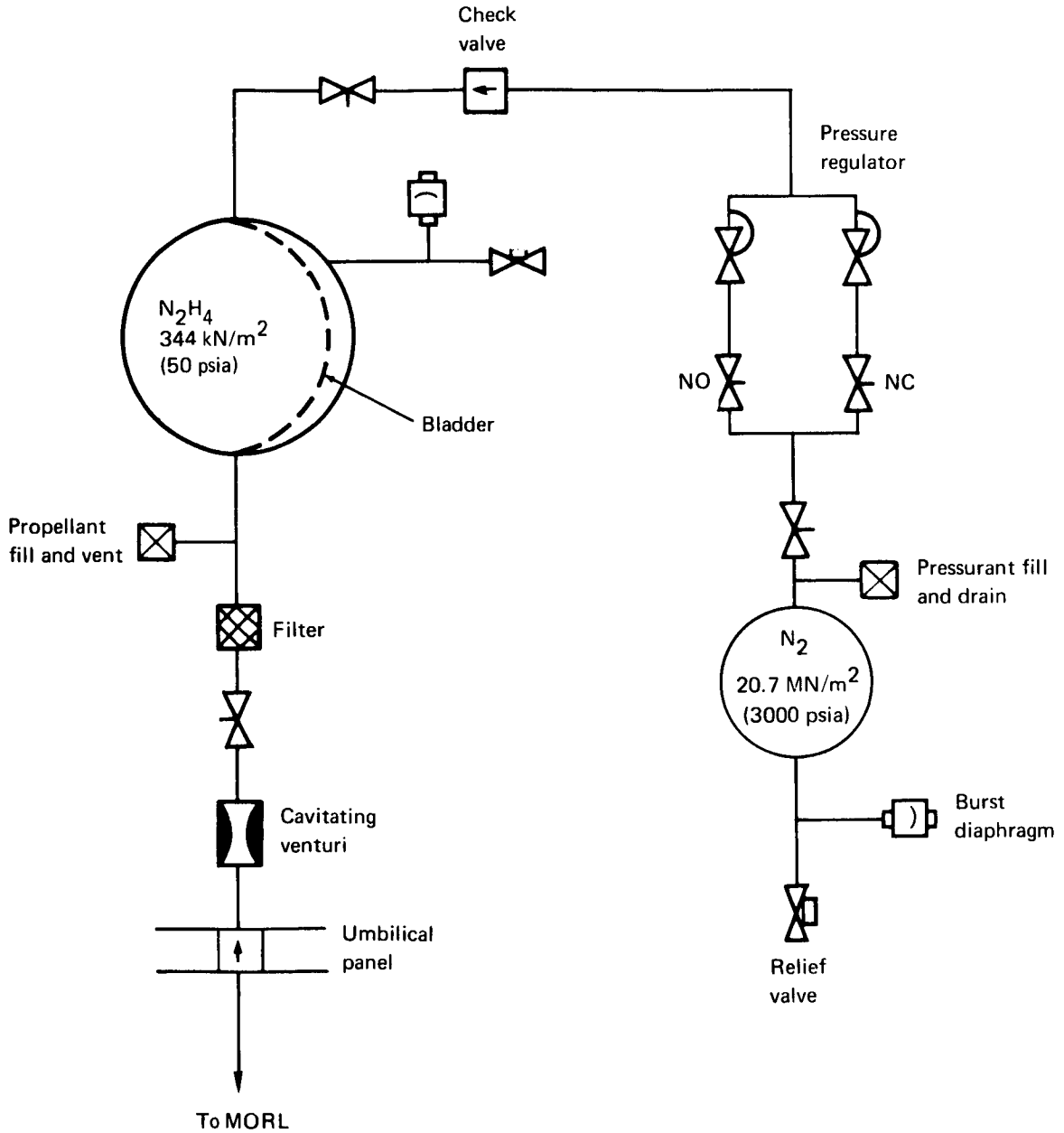

Figure 33. N_2H_4 Resupply System

TABLE 9

WEIGHT SUMMARY: LOGISTICS RESUPPLY OF HIGH-THRUST SYSTEM

Item	Weight, kg (lbm)
Propellants resupplied--N_2H_4; N_2	
90-day propellant weight[a]	60.2 (133)
System dry weight[b]	22.2 (49)
Weight chargeable to logistics launch	82.4 (182)

[a]Includes pressurant resupplied to MORL.

[b]Includes pressurant gas required for propellant transfer and trapped propellants.

The propellant weights listed for the N_2H_4 monopropellant system include allowances for both ullage and outage, as well as sufficient pressurization gas to allow the N_2 tank to blow down to a minimum pressure of 2.07×10^6-N/m^2 (300 psia) at the end of 147 days of orbital operation. The NH_3 resistojet propellant weights include an allowance for a 5% ullage with the tank fully loaded.

The total propulsion chargeable launch weight aboard the logistics vehicle includes all the hardware and pressurization gas weight required to store and transfer the resupply propellant, an allowance for trapped propellants, and the propellant weight to be transferred.

Table 11 presents a detailed dry-weight breakdown of the attitude-control and orbit-keeping system.

TABLE 10

WEIGHT SUMMARY: ATTITUDE-CONTROL AND ORBIT-KEEPING SYSTEM

Description	Weight, kg (lbm)		
MORL			
CMG system		284.0	(628)
Propulsion dry weight			
NH_3 resistojet	78.8 (174)		
N_2H_4 monopropellant	68.8 (152)		
Total	147.6 (326)		
Propellant weight			
NH_3	48.0 (106)		
N_2H_4	17.2 (38)		
Pressurization gas (N_2)	4.8 (10)		
Total	70.0 (154)		
Total propulsion system launch weight		217.6	(480)
Weight assessment for electrical power		68.4	[a](151)
Total chargeable launch weight		570.0	[a](1259)
Orbital wet weight			
NH_3	352.0 (779)		
N_2H_4 and N_2	93.0 (204)		
Total propellant	445.0 (983)		
Total dry weight	432.0 (954)		
Total system		877.0	[b](1937)
Logistics vehicle			
Total propulsion dry weight	80.7 (178)		
NH_3	215.0 (475)		
N_2H_4	57.6 (127)		
N_2	24.9 (55)		
Total chargeable launch weight per 90 days		378.0	(835)

[a]Based on weight penalty of 136 kg/kW (300 lbm/kW).

[b]Does not include assessments for electric power consumption.

TABLE 11

DETAILED DRY-WEIGHT SUMMARY: ATTITUDE-CONTROL AND ORBIT-KEEPING SYSTEM

Description	Weight, kg (lbm)			
Resistojet thrustor system				
Thrustor modules (4)	13.6	(30)		
Valves	2.3	(5)		
Pressure regulators	3.2	(7)		
Display module	2.3	(5)		
Power control module	16.3	(36)		
Propellant tank	29.4	(65)		
Heat exchanger	1.4	(3)		
Mounting brackets, lines and miscellaneous	10.5	(23)		
Total resistojet system dry weight	79.0	(174)		
Scheduled disturbance control system				
Thrustor modules (4)				
12 thrustors at 44.5-N (10-lbf) thrust	13.6	(30)		
Mounting structure	2.3	(5)		
Total	15.9	(35)		
Tankage system				
Tank and mounting brackets	11.3	(25)		
Bellows	23.1	(51)		
Quantity gage system	3.6	(8)		
Total	38.0	(84)		
Feed system				
Valves	2.7	(6)		
Lines and fittings	4.1	(9)		
Umbilical panel	0.9	(2)		
Total	7.7	(17)		
Pressurization system				
Nitrogen bottle	4.1	(9)		
Valves	0.9	(2)		
Total	5.0	(11)		
Display module	2.3	(5)		
Total monopropellant system dry weight		69.0		(152)
Total dry weight		148.0		(326)

SYSTEM ANALYSES AND INTEGRATION

This section summarizes the parametric analyses and tradeoff studies performed during both the preliminary analysis and system-integration phases of the study. In some cases, the values of the various parameters are preliminary choices held constant during the preliminary analysis in order to derive significant relationships. During the integration phase of the study, these values were then modified to be consistent with overall system considerations.

Orbit Injection

Several orbit-injection systems were evaluated to determine the one best suited for integration with a resistojet control system. These included storable and cryogenic bipropellant, monopropellant, and solid-propellant systems. An evaluation was made of 0.67-N to 1.1-N (150-mlbf to 250-mlbf) resistojet thrustors used in a spiral transfer from an initial low-altitude orbit to the final 304-km (164-nmi) circular orbit. The use of the S-IVB to provide the injection velocity to final orbit was also investigated. The launch vehicle used with the MORL is the Saturn IB booster. In this study, the weight and performance parameters were based on the Saturn Vehicle 207. Weight data for this vehicle are presented in table 12. Payload capability of this vehicle was generated assuming that the payload fairing is jettisoned 10 sec after ignition of the second stage (S-IVB). A programmed mixture ratio (PMR) step occurs at the end of the first 295 sec of S-IVB burn. Initially, the mixture ratio is set at 5.5:1, yielding a vacuum specific impulse of 420 sec and a thrust level of 1025 kN (230 klbf). At 295 sec of second-stage burn, the mixture ratio is changed to 4.6:1, which yields a vacuum specific impulse of 429 sec and a thrust level of 845 kN (190 klbf). This PMR step during second-stage burning is used to improve the launch-vehicle performance.

Fig. 34 shows the Saturn IB payload capabilities as a function of circular orbit altitude [for an ETR launch into a 0.87-rad (50°) inclination]based on the vehicle parameters defined in the previous paragraph. The launch azimuth corresponding to this inclination is 0.77 rad (44.5°) measured from North. The effect of perigee injection altitude on payload for a 0.87-rad (50°) inclined orbit is shown in fig. 35 [the apogee altitude is maintained constant at the mission altitude of 304 km (164 nmi)]. An altitude constraint of 148 km (80 nmi), shown in figs. 34 and 35, was dictated by the NASA Marshall Space Flight Center (MSFC). The major consideration that resulted in fixing this constraint was the ground-tracking requirements, namely, the radar elevation angles for Cape Kennedy and Bermuda.

TABLE 12

SATURN VEHICLE 207 WEIGHT BREAKDOWN

Item	Weight	
	kg	(lbm)
S-IB drystage	39 000	(85 800)
S-IB residuals	4 480	(9 866)
Outboard engine cutoff (OECO) thrust decay propellant	256	(563)
Interstage	3 000	(6 600)
S-IVB aft frame	11	(25)
Ullage propellant	83	(183)
Ullage system hardware	2	(4)
S-IB separation weight	46 832	(103 041)
S-IB propellant		
Main stage	402 000	(883 902)
Frost	454	(1 000)
Service items[a]	258	(568)
Inboard engine cutoff (IECO) thrust decay propellant	979	(2 154)
OECO thrust decay propellant	710	(1 560)
	404 401	(889 184)
S-IVB propellant	104 000	(228 500)
S-IVB drystage	10 430	(22 954)
Residuals	965	(2 123)
Flight performance reserve (FPR) and mixture ratio reserve (MRR)	682	(1 500)
Instrument unit (IU)	1 885	(4 150)
S-IVB separation weight	13 962	(30 727)
Ullage rocket cases	99	(217)
Payload fairing	218	(480)

[a]Service items--oil, lubricants, etc.

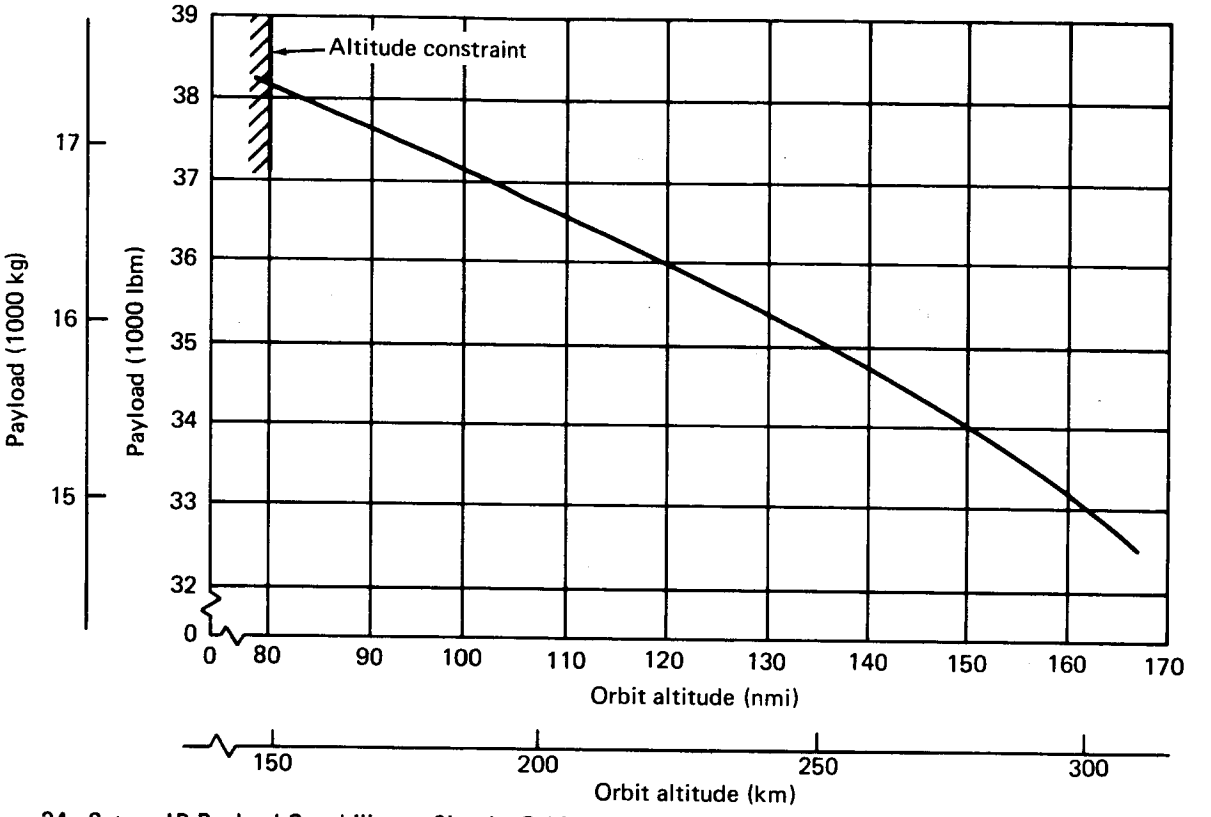

Figure 34. Saturn IB Payload Capability to Circular Orbit

Fig. 34 indicates the direct-ascent payload capability of the Saturn IB to the 304-km (164 nmi) orbit is 14 900 kg (32 750 lbm). Large increases in payload can be obtained by going to lower orbit altitudes. For example, 17 300 kg (38 150 lbm) of payload can be delivered to an 148-km (80-nmi) circular orbit. If an orbit transfer from the 148-km (80-nmi) orbit to the required 304-km (164-nmi) mission orbit can be made with only a small propellant expenditure, a large portion of the 2450-kg (5400-lbm) payload differential can be realized as discretionary payload. An evaluation and subsequent comparison of the various injection systems resulted in the selection of the J-2S engine operating in the idle mode as the best system for the orbit injection maneuver. Two of the most important factors in this selection were its superior payload capability to orbit and the possibilities provided by retention of the S-IVB in orbit.

Resistojet systems. – Spiral trajectories using a resistojet propulsion system are feasible to transfer either from low-altitude-circular or low-perigee-elliptical orbits to the required 304-km (164-nmi) circular orbit. An initial elliptical orbit can be circularized by means of applying a constant-magnitude thrust normal to the radius vector. However, no significant advantage is realized over an initial low-altitude-circular orbit mode; therefore, only the low-altitude-circular orbit was investigated in detail.

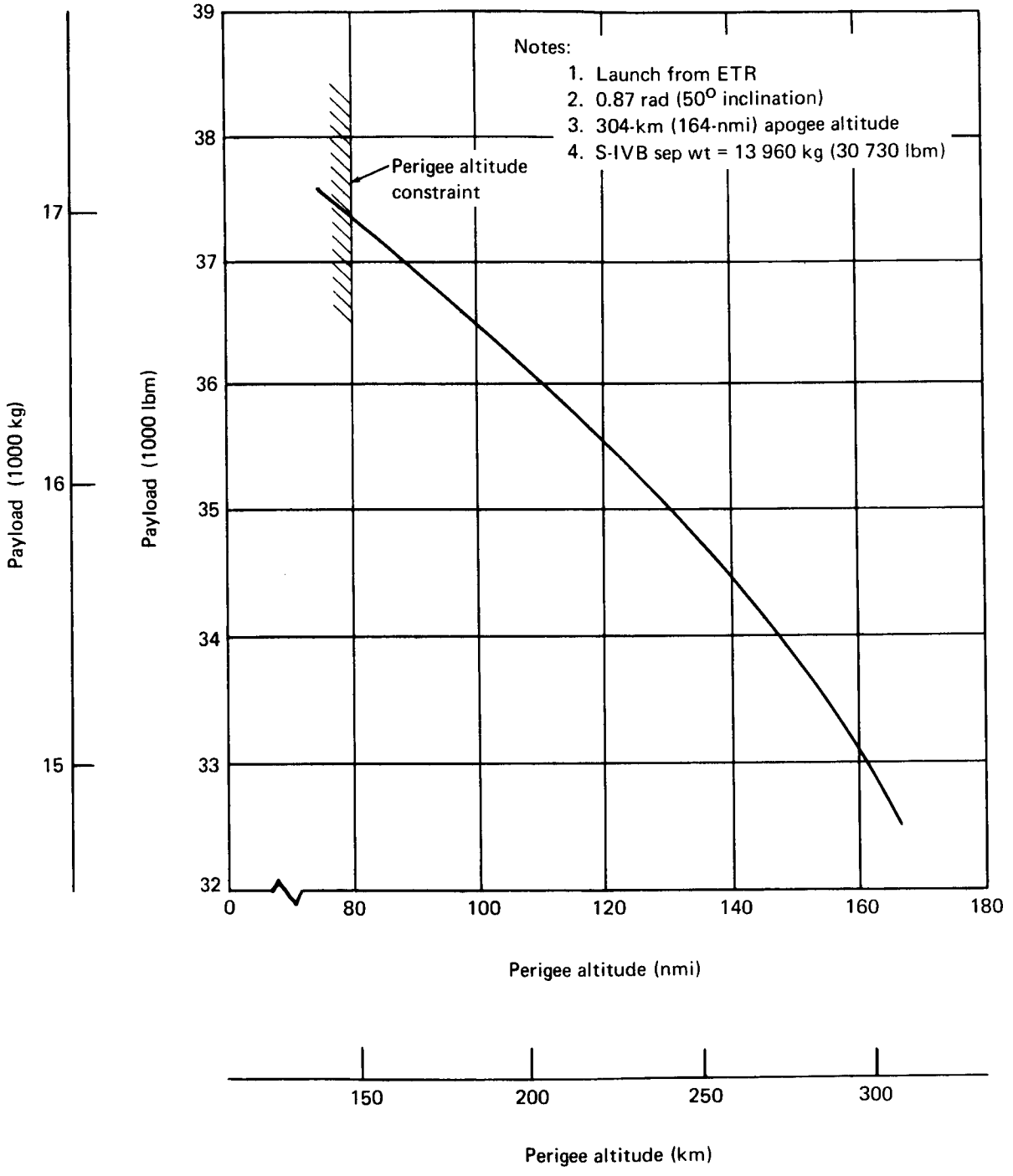

Figure 35. Saturn IB/MORL Elliptical Orbit Payload

A sketch of the spiral trajectory is presented in fig. 36. The MORL is placed in low-altitude orbit by the S-IB launch vehicle. The resistojet engines are then used to provide thrust to transfer to the mission orbit. The parameters investigated were the time required to perform the transfer, the magnitude of thrust vector, and the effect of thrust misalignment, initial altitude, and atmospheric density.

The time required to perform the transfer is shown as a function of initial altitude and thrust level in fig. 37. For any given thrust level, a minimum altitude capability exists for an acceptable thrust-to-drag ratio. The constant-thrust curves asymptotically approach the orbit altitude at which the thrust-to-drag ratio equals one. For this study, the minimum thrust-to-drag ratio was chosen to 2:1 to allow for variations in atmospheric density and other factors.

This constraint line is plotted in fig. 37, and the intersection of this curve with the family of constant-thrust curves represents those points at which maximum payload can be achieved for a given thrust level. Although a higher thrust level is desirable to permit lower initial orbits and minimize spiral time to final orbit, a degradation in thrustor performance occurs at the higher thrust levels because of the power limitation on the MORL. Fig. 38 shows the degradation in specific impulse for the H_2 and NH_3 propellants as the injection thrust level is increased with the maximum available MORL power level of 6.68 kWe.

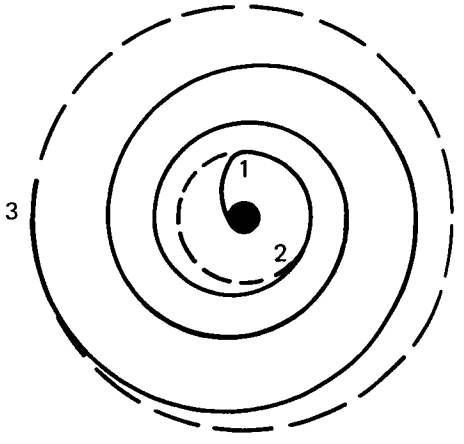

1. Launch into low-altitude circular orbit
2. Spiral transfer trajectory thrust provided by resistojet engines
3. Final 304-km (164-nmi) circular orbit

Optimization parameters

Initial orbit altitude	Power limitation
Thrustor performance	Thrust-to-drag limitation

Figure 36. Spiral Trajectory

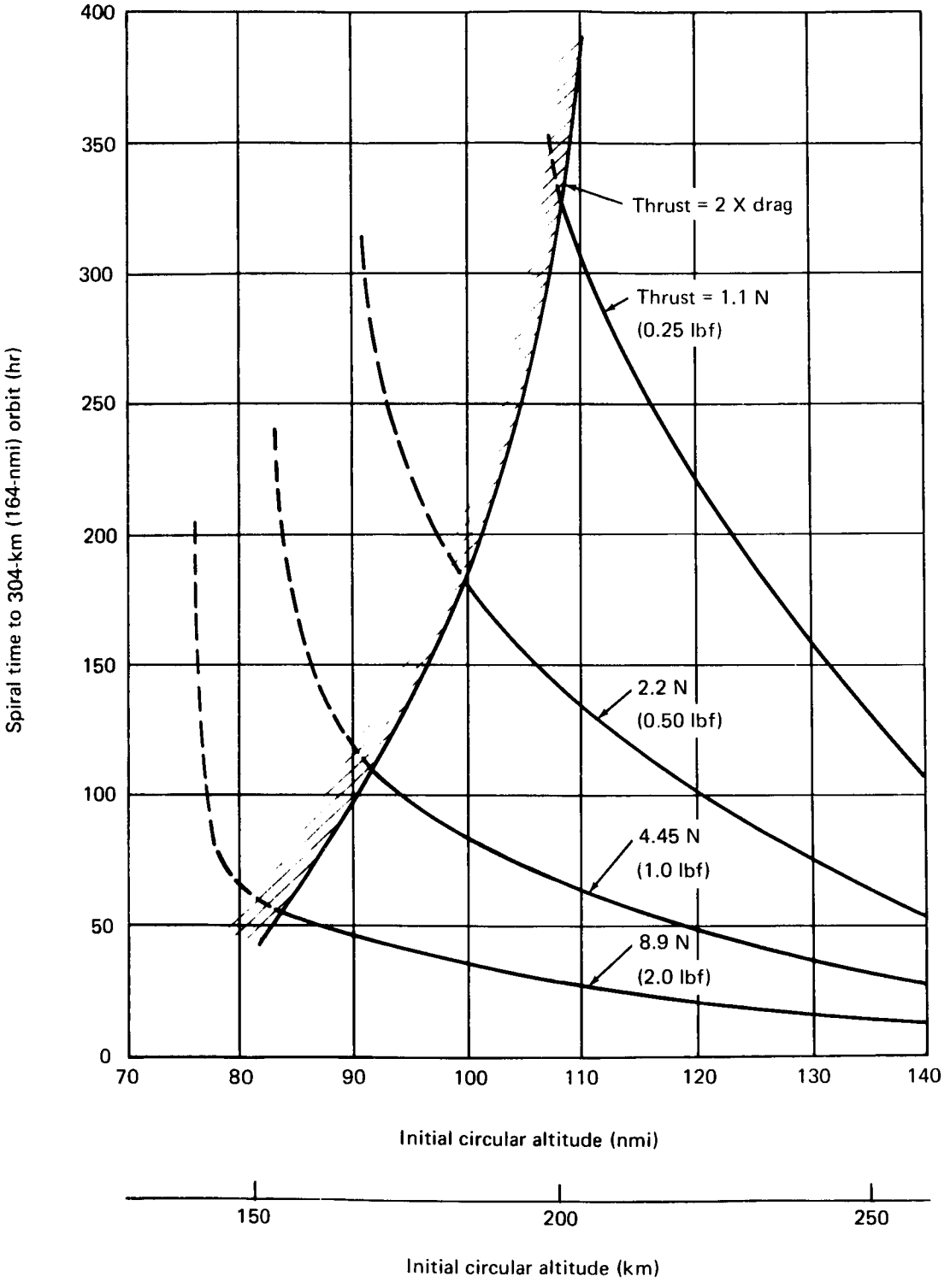

Figure 37. Time to Final Orbit (Spiral Trajectory)

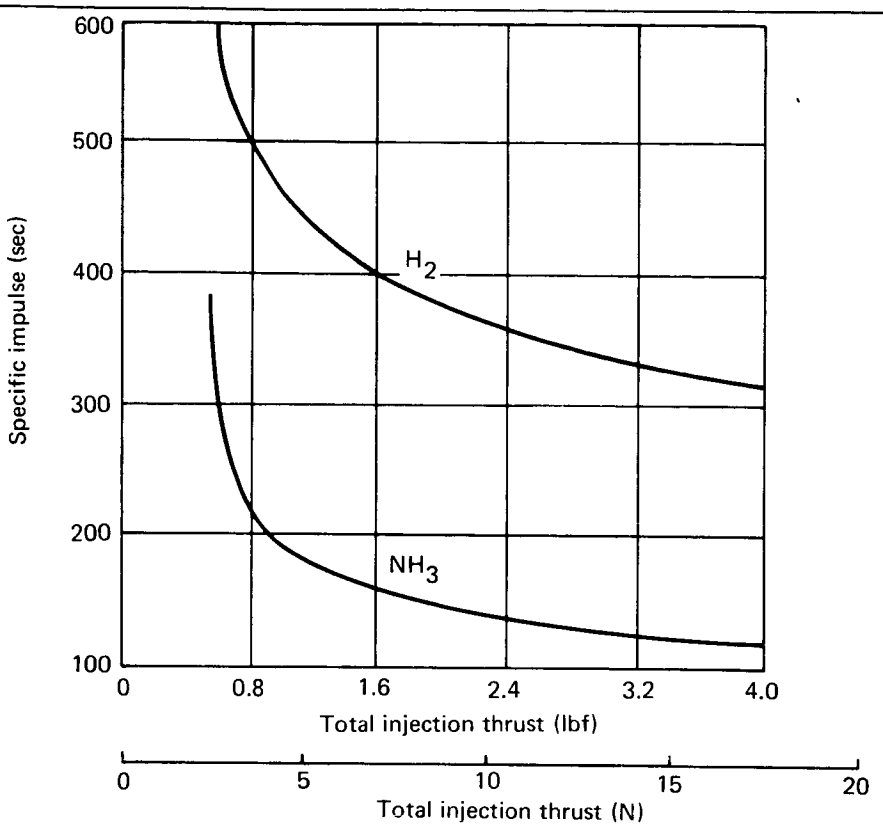

Figure 38. Resistojet Performance – Electric Power = 6.68 kWe

Because the maximum payload in final orbit depends upon both the performance of the injection thrustor and the required velocity increment for injection, a tradeoff is necessary to establish the optimum thrust-level selection.

The results of thrust-level optimization for maximum weight in final orbit is shown in figs. 39 for H_2 and 40 for NH_3. For the available power (6.68 kWe), maximum payload is obtained at a thrust level of approximately 4 N (0.9 lbf) for H_2 and approximately 2 N (0.45 lbf) for NH_3. The rapid decrease in payload shown for the NH_3 system at thrust levels below 2 N is the result of reaching the maximum temperature limit imposed on the resistojet thrustor. Further decrease in thrust level does not result in higher thrustor performance but merely decreases payload capability because of the need to launch to a higher initial orbit. The thrust levels were selected slightly to the right of the optimum point shown on the curve. For H_2 the selected thrust level is 4.45 N (1.0 lbf), resulting in a spiral time of 4.7 days. For NH_3, the thrust is 2.67 N (0.60 lbf), with a spiral time of 7.4 days.

The atmospheric density model used in the analysis is representative of the 1972 low solar flux period. Using a high solar activity atmosphere, representative of the 1978 to 1980 time period, the spiral transfer time was determined as a function initial orbit altitude assuming a 4.45-N (1.0-lbf) thrust level. A comparison between this high atmospheric density case and

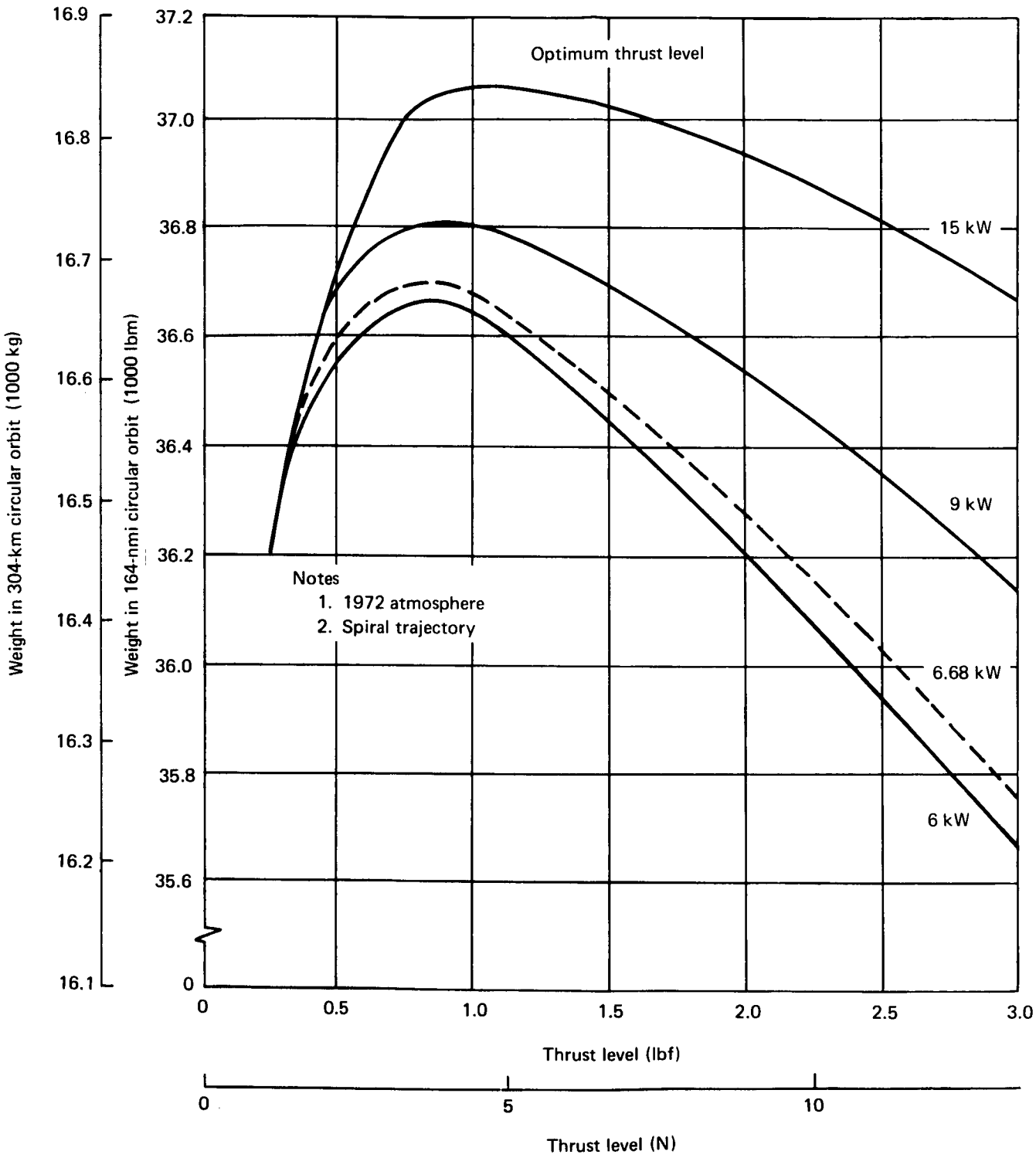

Figure 39. Effect of H_2 Resistojet Thrust Level on Payload

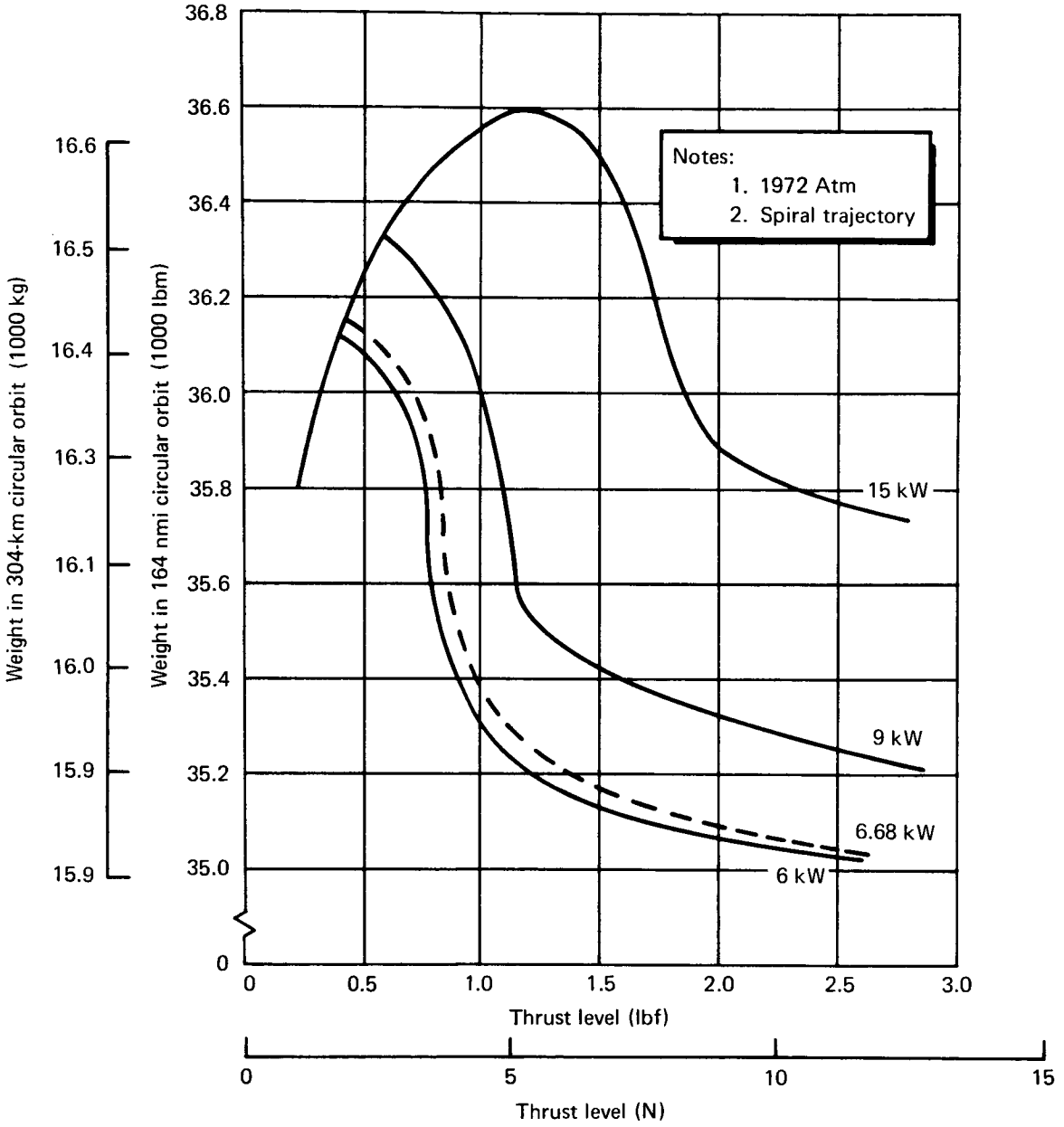

Figure 40. Effect of NH_3 Resistojet Thrust Level on Payload

nominal case is illustrated in fig. 41. Differences in transfer times due to the density variation are less than 5% for initial altitudes greater than 167 km (90 nmi) (the altitude at which thrust equals twice the nominal drag level).

The effect of thrust misalignment (pointing error) during the transfer was also found to be small for realistic errors. For a 4.45-N (1-lbf) thrust level, a constant pointing error of 17.4 mrad (1°) in the orbit plane was found to produce negligible changes; an error of 87 mrad (5°) increased the transfer time by less than 1%. Therefore, it is concluded that transfer time is not significantly affected by either parameter.

Attitude control during orbit injection: This section defines the resistojet systems used for attitude control during orbit injection and the associated control logic appropriate for a resistojet injection system. The location of the orbit injection system is shown in fig. 42. The four rear-facing thrustors provide orbit-injection impulse and pitch and yaw control moments by shutting down one thrustor of a pair. Therefore, pitch and yaw control moments are obtained as a by-product of the orbit-injection thrust and require no propellant in excess of that required for orbit injection. Roll control moments are provided by the 0.044-N (10-mlbf) thrustors used for orbit keeping and CMG desaturation during orbit operation. Assuming a 3.35-m (11-ft) moment arm, the control moment capability of the system is:

M_ϕ (roll) = 0.6 N-m (0.44 ft-lbf)

M_θ (pitch) = 3.7 N-m (2.75 ft-lbf)

M (yaw) = 3.7 N-m (2.75 ft-lbf)

The angular accelerations provided by the above moments are:

$\ddot{\phi}$ (roll) = 4.4×10^{-6} rad/sec^2 (2.53×10^{-4} deg/sec^2)

$\ddot{\theta}$ (pitch) = 1.37×10^{-5} rad/sec^2 (7.9×10^{-4} deg/sec^2)

$\ddot{\Psi}$ (yaw) = 1.62×10^{-5} rad/sec^2 (9.3×10^{-4} deg/sec^2)

where the moments of inertia are: roll = 1.36×10^5 kg-m^2 (100 000 slug-ft^2), pitch = 2.72×10^5 kg-m^2 (200 000 slug-ft^2), and yaw - 2.31×10^5 kg-m^2 (170 000 slug-ft^2).

Uncertainties associated with the orbit-injection thrustors and the resulting disturbances are shown in table 13. The uncertainties are assumed to be independent random variables with a normal distribution and zero mean. Thrust eccentricity is almost entirely due to an uncertainty in the center-of-gravity location.

The yaw-attitude control system proposed for orbit injection is shown in fig. 43. Identical systems are provided for pitch and roll control. Simple control logic is employed. Control moments are applied whenever the error signal $K_{\dot{\Psi}}\dot{\Psi} + \Psi$ exceeds δ and are removed when the error signal magnitude is less than δ. Turn on and turn off occur at slightly different levels because

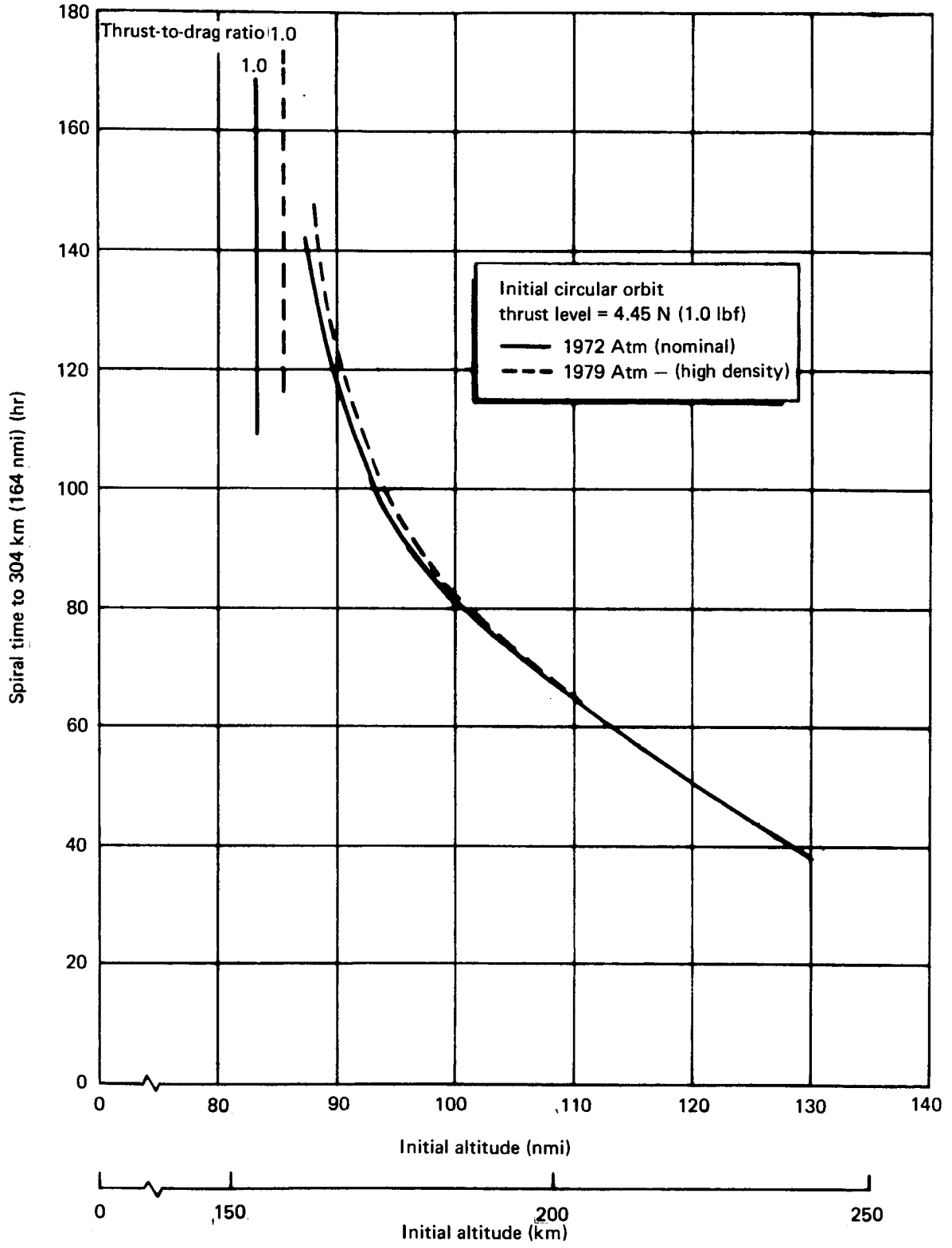

Figure 41. Effect of Atmospheric Density on Spiral Transfer Time

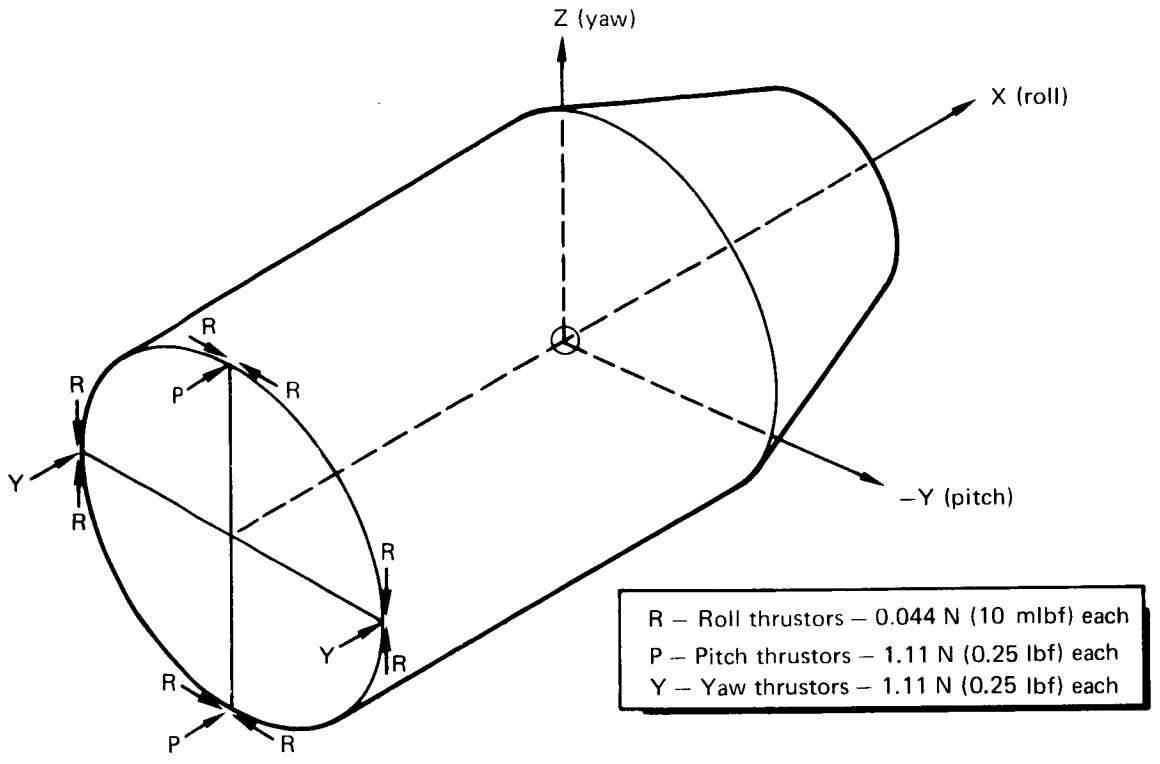

Figure 42. Resistojet P/RCS Orbit-Injection System Thrustor Configuration

of hysteresis in the switching amplifier. For several reasons, this system was selected in preference to one capable of operating in a minimum impulse mode. Pitch and yaw control moments are obtained as a by-product or orbit-injection thrust and require no propellant in excess of that required for orbit injection. A minimum impulse mode for pitch and yaw control is considered unnecessary. Propellant consumed by the roll control system is determined primarily by the distrubance torques produced by orbit-injection thrustor misalignment. A minimum impulse mode would not reduce roll propellant consumption during disturbance operation. During orbit operations certain functions might be performed by the resistojet P/RCS. However, none of these functions establish a definite requirement for the minimum impulse mode.

A deadzone (δ) of $\pm 8.7 \times 10^{-3}$ rad ($\pm 0.5^{o}$) was selected for all three axes. The most desirable feature of a small deadzone is the minimization of gravity-gradient torques which for the δ selected are negligible. Aerodynamic torques are not a problem since the vehicle is neutrally stable.

Typical duty cycles for the resistojet P/RCS are defined by the limit cycles of figs. 44 and 45. RCS parameters selected to derive the limit cycles were:

$$K\dot{\Psi} = 4 \text{ rad/sec}$$

$$\delta = 8.7 \times 10^{-3} \text{ rad } (0.5^{o})$$

$$\ell = 3.35 \text{ m } (11 \text{ ft})$$

Thrust levels and moments of inertia were previously established.

TABLE 13

ORBIT-INJECTION THRUSTOR UNCERTAINTIES AND ASSOCIATED DISTURBANCES

Uncertainties	Magnitude (3δ)	Disturbance (rad/sec)	Disturbance (°/sec)
Thrust misalignment	2.61×10^{-2} rad (1.5°)	R--1.01×10^{-6}	(5.8×10^{-5})
		P--9.75×10^{-7}	(5.6×10^{-5})
		Y--1.15×10^{-6}	(6.6×10^{-5})
Thrust variation	5%	R--0	
		P--9.05×10^{-7}	(5.2×10^{-5})
		Y--1.06×10^{-7}	(6.1×10^{-5})
Thrust eccentricity	0.152 m (0.5 ft)	R--0	
		P--1.25×10^{-6}	(7.2×10^{-5})
		Y--1.48×10^{-6}	(8.5×10^{-5})
Total disturbance	---	R--1.01×10^{-6}	(5.8×10^{-5})
		P--1.65×10^{-6}	(9.5×10^{-5})
		Y--1.95×10^{-6}	(11.2×10^{-5})

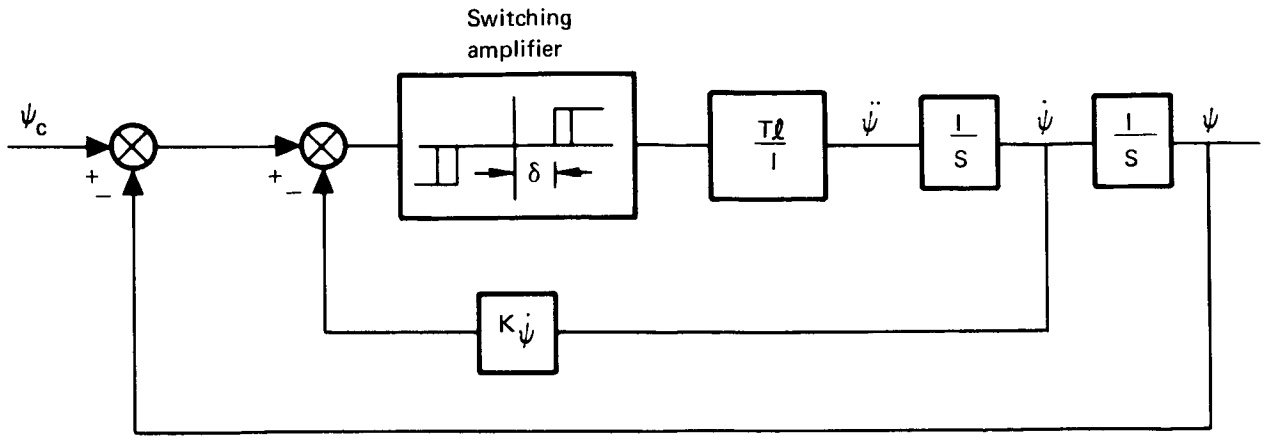

ψ_c – Yaw command – rad
T – Control thrust – N
ℓ – Moment arm – m
I – Yaw moment-of-inertia – kg-m^2
$\ddot{\psi}$ – Yaw angular acceleration – rad/sec^2
$\dot{\psi}$ – Yaw angular rate – rad/sec
ψ – Yaw attitude – rad
$K\dot{\psi}$ – Rate gyro gain – rad/rad/sec
δ – Attitude deadzone – rad
S – Laplace variable – sec^{-1}

Figure 43. Yaw-Attitude Control System

Fig. 44 shows two roll limit cycles. One is in the presence of the disturbances listed in table 13. Gravity-gradient torques and gyroscopic cross-coupling torques were found to be negligible for the belly-down orientation used for orbit injection. The other limit cycle shown is for no disturbance. Duty cycles for each case are shown in the figure. The disturbance limit cycle should be used for further system definition. Impulse requirement for that particular case is 133 N-sec/hr (30 lbf-sec/hr).

Yaw limit cycles for no disturbance and the disturbances of table 13 are shown on fig. 45 along with duty cycles for each case. As mentioned previously, control moments are obtained by shutting down one yaw thrustor. Therefore, an impulse requirement for yaw does not exist. Pitch limit cycles will be considered identical to yaw for purposes of further system definition.

System definitions (H_2 and NH_3 resistojet): The total electric power available for the resistojet thrustors during orbit injection is 7.79 kWe, of which 0.926 kWe is required for the four 0.045-N (10-mlbf) roll thrustors. Considering line losses, 6.7 kWe is available for the four injection thrustors (1.67 kWe/injection thrustor). The optimum total thrust level for this available power is about 4.5 N (1 lbf) for a high-thrust resistojet system utilizing hydrogen as the propellant. This corresponds to four 1.12-N (0.25-lbf) injection thrustors. Allowing for a 100% variation in aerodynamic drag,

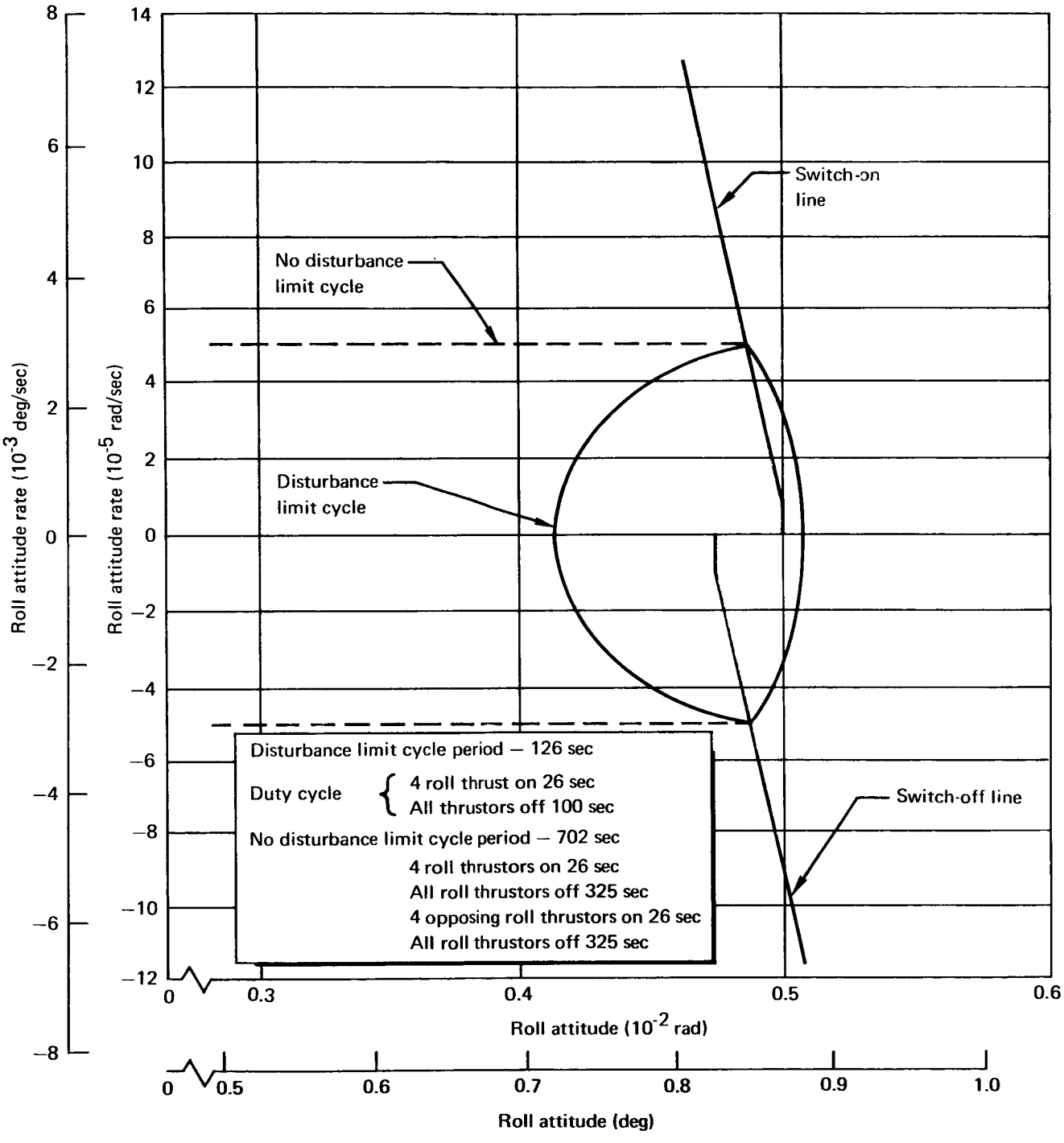

Figure 44. Roll Limit Cycles

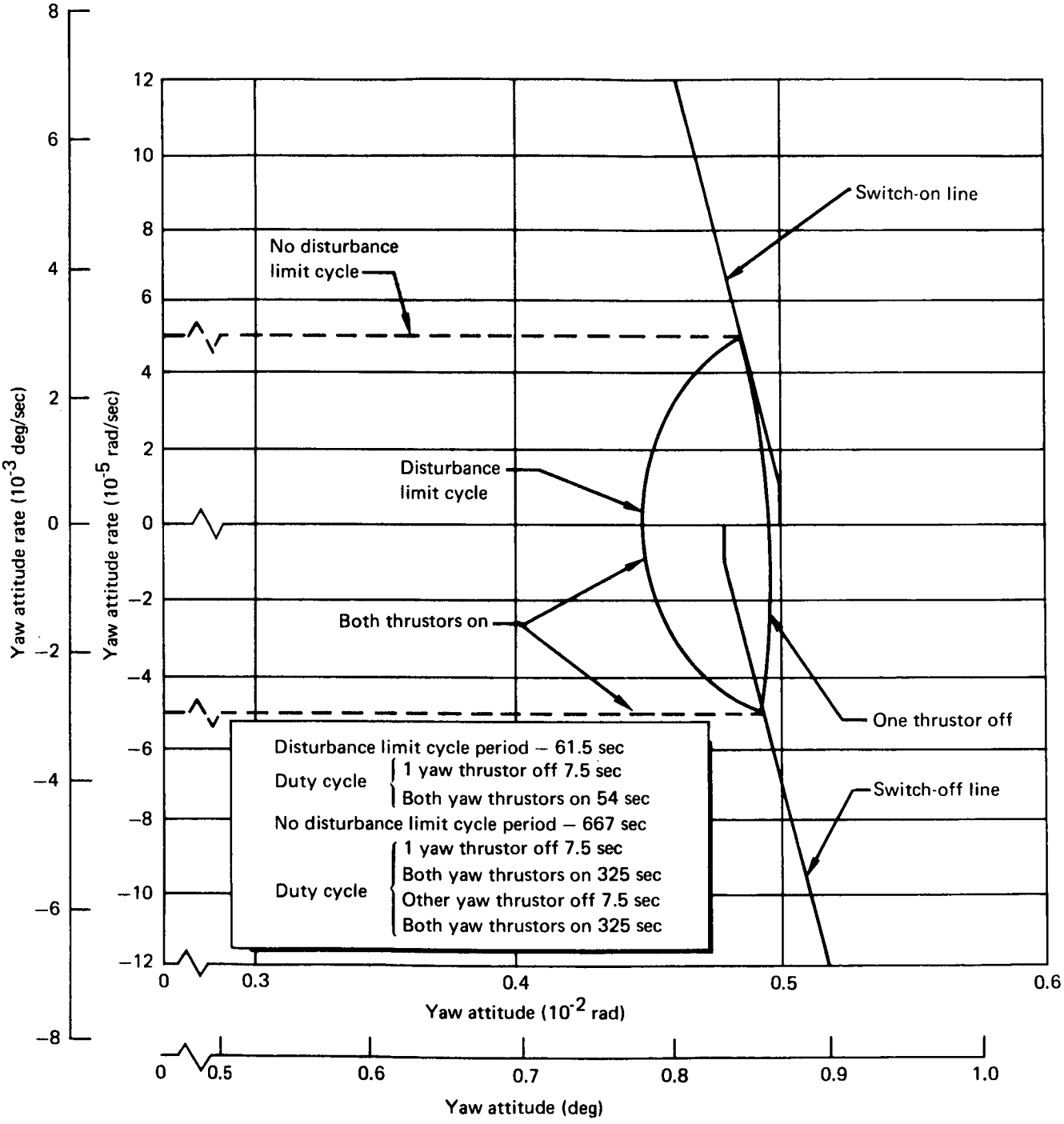

Figure 45. Yaw Limit Cycles

the minimum initial circular orbit is 168 km (91 nmi). From this attitude, 114 hours (4. 7 days) is required to spiral the MORL vehicle to the mission altitude. The performance of a hydrogen resistojet operating at these defined conditions (1. 12-N thrustor at 1. 67 kWe) is 447 sec delivered specific impulse. The total impulse required is 1. 81 x 10^6 N-sec (406 000 lbf-sec) or a propellant requirement of 414 kg (910 lbm).

The orbit-injection thrustors also may be used as a backup attitude control system. During this time, only 500 watts would be available to each of the 1. 12-N (0. 25-lbf) thrustors. Fig. 46 shows the thrustor performance as a function of power available. Performance during the nominal orbit-injection mode is 447 sec delivered specific impulse; this is reduced to 325 sec during the backup mode because less power is available.

The H_2 tank required for the 0. 044-N (10 mlbf) resistojet control system is sized for 147 days of resistojet operation. However, it is normally off-loaded at MORL launch and consequently may be used to hold 144 kg (316 lbm) of the 414-kg (910-lbm) spiral trajectory requirements. A separate H_2 tank is required to hold the additional 270 kg (594 lbm) of H_2 required for orbit injection. Tank conditions are assumed to be 27. 8°K for a vapor pressure of 5. 5 x 10^5 N/m^2 (80 psia). A 10% ullage factor is included to damp out thermal transients during the MORL boost. Other pertinent design information regarding this additional H_2 tank required for the MORL spiral trajectory is summarized in table 14.

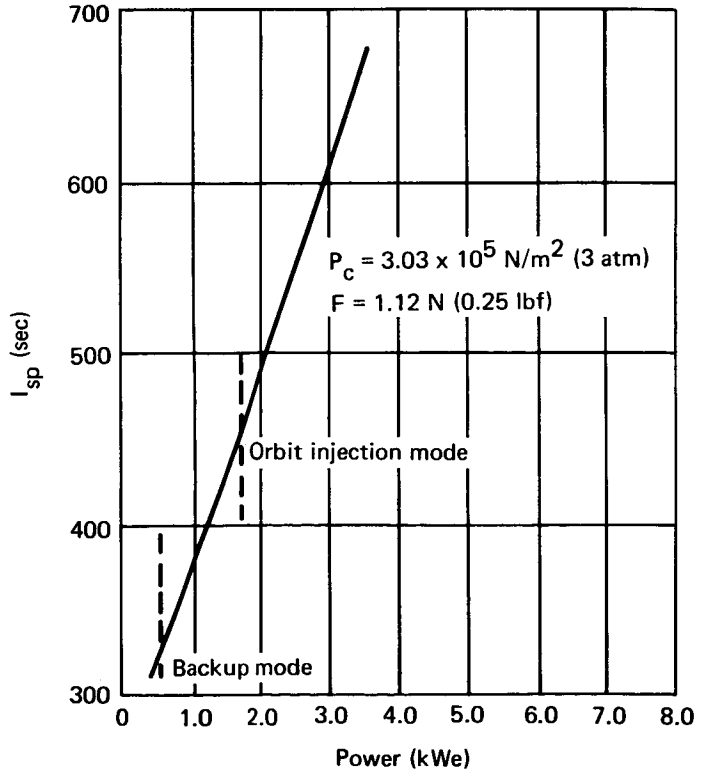

Figure 46. H_2 Resistojet Performance

TABLE 14

MORL RESISTOJET ORBIT-INJECTION TANKS

Description	H_2 Tank	NH_3 Tank
Tank material	2014-T6 Al	6 Al-4V-Ti
Tank conditions	27.8°K, 5.5×10^5 N/m^2 (50°R, 80 psia)	325°K, 2.24×10^6 N/m^2 (585°R, 325 psia)
Ullage	10%	10%
Propellant loaded	308 kg (679 lbm)	214 kg (472 lbm)
Propellant usable	270 kg (594 lbm)	208 kg (458 lbm)
Tank diameter	2.22 m (87.5 in.)	0.93 m (37 in.)
Gage	0.124 cm (0.049 in.)	0.114 cm (0.045 in.)
Dry weight	59 kg (130 lbm)	15.9 kg (35 lbm)

The NH_3 system consists of four 0.67-N (0.15-lbm) thrustors with an available electric power of 1.67 kWe/thrustor for orbit injection. Fig. 47 shows the performance of this selected thrustor as a function of the available electrical power. A specific impulse of 347 sec is obtained for the NH_3 thrustors during orbit injection, and 145 sec during the backup mode.

Allowing 100% variation in orbital drag, the minimum initial altitude is 180 km (97.5 nmi). The Saturn IB capability to the 180-km (97.5-nmi) circular orbit is 16 900 kg (37 200 lbm). The four 0.67-N (0.15-lbf) NH_3 resistojet thrustors will spiral the MORL to the 304-km (164-nmi) circular mission orbit. The total impulse required to spiral to the mission orbit is 1.7×10^6 N-sec (383 000 lbm-sec), or a propellant requirement of 504 kg (1110 lbm).

The 0.044-N (10-mlbf) NH_3 system has storage capabilities for 343 kg (755 lbm) of usable NH_3. However, only 47 kg (103 lbm) of usable NH_3 will be loaded on this tank at MORL launch. Consequently, 296 kg (652 lbm) of the orbit-injection NH_3 may be stored in this off-loaded tank. An additional tank is required to store the remaining 208 kg. The NH_3 is stored at the ambient temperature of 325°K (585°R) which will provide a nominal tank pressure of 2.24×10^6 N/m^2 (325 psia). In order to allow for thermal transients during boost, a 10% ullage factor is utilized and an overpressure allowance to 2.4×10^6 N/m^2 (400 psia) is included. Table 14 presents a summary of the pertinent design features of the NH_3 tank.

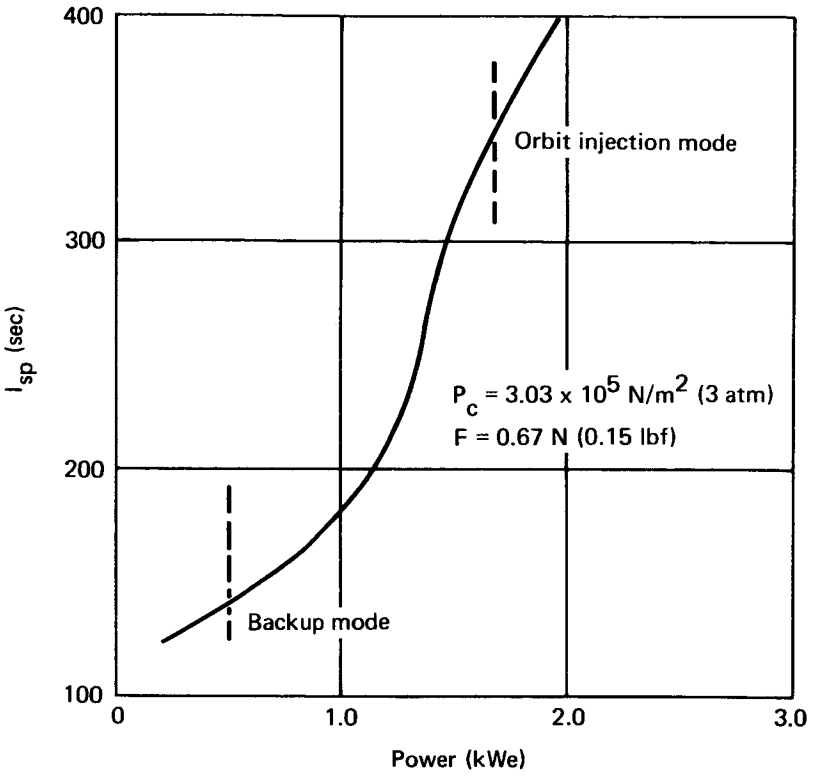

Figure 47. NH_3 Resistojet Performance

A summary of the spiral-trajectory concept is shown in table 15. The H_2 and the NH_3 orbit-injection thrustors are in addition to the resistojet thrustors used for attitude control and orbit keeping during the mission. The optimum H_2 system operates at a specific impulse of 447 sec and requires 4.7 days to reach the mission orbit. A reference payload (weight capability to orbit minus the chargeable dry weight) of 16 500 kg (36 435 lbm) is injected into mission orbit. The optimum NH_3 system operates at a specific impulse of 347 sec and requires 7.4 days to attain the mission orbit. Its reference payload capability is 16 370 kg (36 018 lbm).

High-thrust orbit-injection systems. — High-thrust propulsion systems aboard the MORL spacecraft and systems aboard the S-IVB stage of the Saturn IB launch vehicle were investigated for orbit injection using an apogee circularization technique. Fig. 48 is a sketch of the mission profile for an apogee circularization mode. The Saturn IB booster places the MORL in an initial 148 x 304-km (80 x 164-nmi) elliptical orbit. During the 45-min coast phase, the MORL traverses the orbit from perigee to apogee. At apogee, the orbit is circularized using the high-thrust orbit-injection system. If an S-IVB system is used, the MORL does not separate from the S-IVB, but rather, the S-IVB is injected into the final orbit along with the MORL.

The first mission phase is a coast to apogee of the transfer orbit, during which the orbit-injection system must provide control moments for attitude control. At apogee, the system provides the velocity increment for orbit

TABLE 15

RESISTOJET ORBIT-INJECTION SYSTEM SUMMARY

Item	H_2 Concept	NH_3 Concept
Initial orbital altitude	168 km (91 nmi)	180 km (97.5 nmi)
Weight injected into initial orbit	17 060 kg (37 560 lbm)	16 900 kg (37 200 lbm)
Total impulse required	1.81×10^6 N-sec (406 000 lbf-sec)	1.7×10^6 N-sec (383 000 lbf-sec)
Total transfer time	4.7 days	7.4 days
Injection thrust level	4.45 N, four at 1.11 N (1.0 lbf, four at 0.25)	2.67 N, four at 0.67 N (0.6 lbf, four at 0.15)
Power requirements		
Roll thrustors	1.1 kWe	1.1 kWe
Per injection thrustor	1.67 kWe	1.67 kWe
I_{sp}	447 sec	347 sec
Propellant weight required	414 kg (910 lbm)	504 kg (1110 lbm)
Chargeable weight[a]		
Wet	512 kg (1125 lbm)	(1159 lbm)
Dry	98 kg (215 lbm)	22 kg (49 lbm)
Reference payload (weight capability to orbit minus chargeable dry weight)	16 500 kg (36 435 lbm)	16 370 kg (36 018 lbm)

[a]Includes unusable propellant weights.

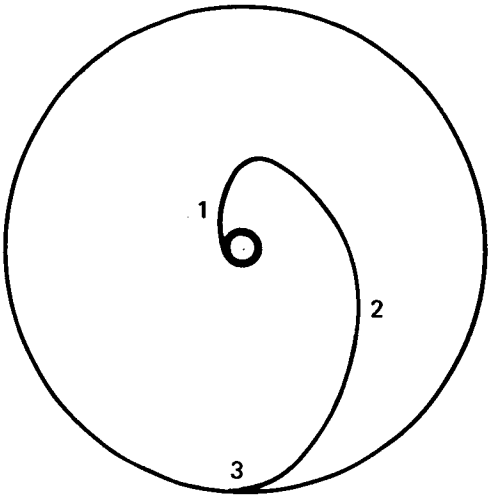

1. Launch into an 148 x 304-km (80 x 164-nmi) elliptical orbit
2. Coast
3. Injection into the 304-km (164-nmi) circular orbit at apogee.

Figure 48. Apogee Circularization

injection and attitude control during injection. The evaluation of thrust requirements for orbit injection and high-distrubance orbit operation yielded thrust levels of 222 N (50 lbf) for pitch and yaw engines and 44. 5 N (10 lbf) for roll engines. Evaluation of total impulse requirements showed that orbit injection and orbit operations high-thrust functions could be performed by a single system. Therefore, the selection of thrust levels to perform the combined functions was a compromise between orbit-injection requirements, scheduled-disturbance requirements, and the need for thrust levels which provide good limit cycle efficiency. Table 16 lists the various disturbances, their magnitude, minimum thrust level for their control, selected thrust levels, and impulse for their control. The reason for differences in minimum and selected thrust levels will be discussed later.

Fig. 49 shows the velocity requirements for orbit injection as a function of total thrust level. An orbit-injection thrust of at least 2700 N (600 lbf) to obtain an impulsive ΔV would be desirable. However, such a thrust level results in inefficient operation during performance of other functions. The narrow pulse width associated with high thrust degrades specific impulse when the thrustors provide only control moments. An orbit-injection thrust level of 890 N (200 lbf) was selected as a compromise for meeting all requirements with a resulting ΔV penalty of 2. 13 m/sec (7 fps).

The thrustor locations are shown in fig. 50. There are four modules aligned with the pitch and yaw axis, each housing two pitch or two yaw thrustors and a roll thrustor.

TABLE 16

THRUST LEVEL SELECTION FOR DISTURBANCE CONTROL

Disturbance	Magnitude	Minimum thrust for baseline requirements (per thrustor)	Selected thrust levels[a] (per thrustor)	Impulse requirement (per 90 days)
9-g centrifuge operation	81.5 N-m (60 ft-lb) maximum about roll axis	Roll: 44.5 N (10 lbf) Pitch: none Yaw: none	Roll: 44.5 N (10 lbf)	Roll: 9.2×10^4 N-sec (20 700 lbf-sec) Pitch: 0 Yaw: 0
Stowing logistics vehicle	67.8 N-m (50 ft-lb) maximum all axes	Roll: 35.6 N (8 lbf) Pitch: none Yaw: none	Event to be scheduled to eliminate propulsion requirement	Roll: 1.29×10^4 N-sec (2890 lbf-sec) Pitch: 1.28×10^4 N-sec (2870 lbf-sec) Yaw: 1.28×10^4 N-sec (2870 lbf-sec)
Docking	67.8 N-m (50 ft-lb) body rate pitch or yaw	Roll: none Pitch: 187 N (42 lbf) Yaw: 187 N (42 lbf)	Pitch: 44.5 N (10 lbf) Yaw: 44.5 N (10 lbf)	Roll: 0 Pitch: 1×10^3 N-sec (225 lbf-sec) Yaw: 1×10^3 N-sec (225 lbf-sec)
Total				Roll: 10.5×10^4 N-sec (23 590 lbf-sec) Pitch: 1.38×10^4 N-sec (3095 lbf-sec) Yaw: 1.38×10^4 N-sec (3095 lbf-sec) 13.26×10^4 N-sec (39 780 lbf-sec)

[a] Thrust levels based on 3.35-m (11-ft) moment arm and two thrustors providing couple pivot.

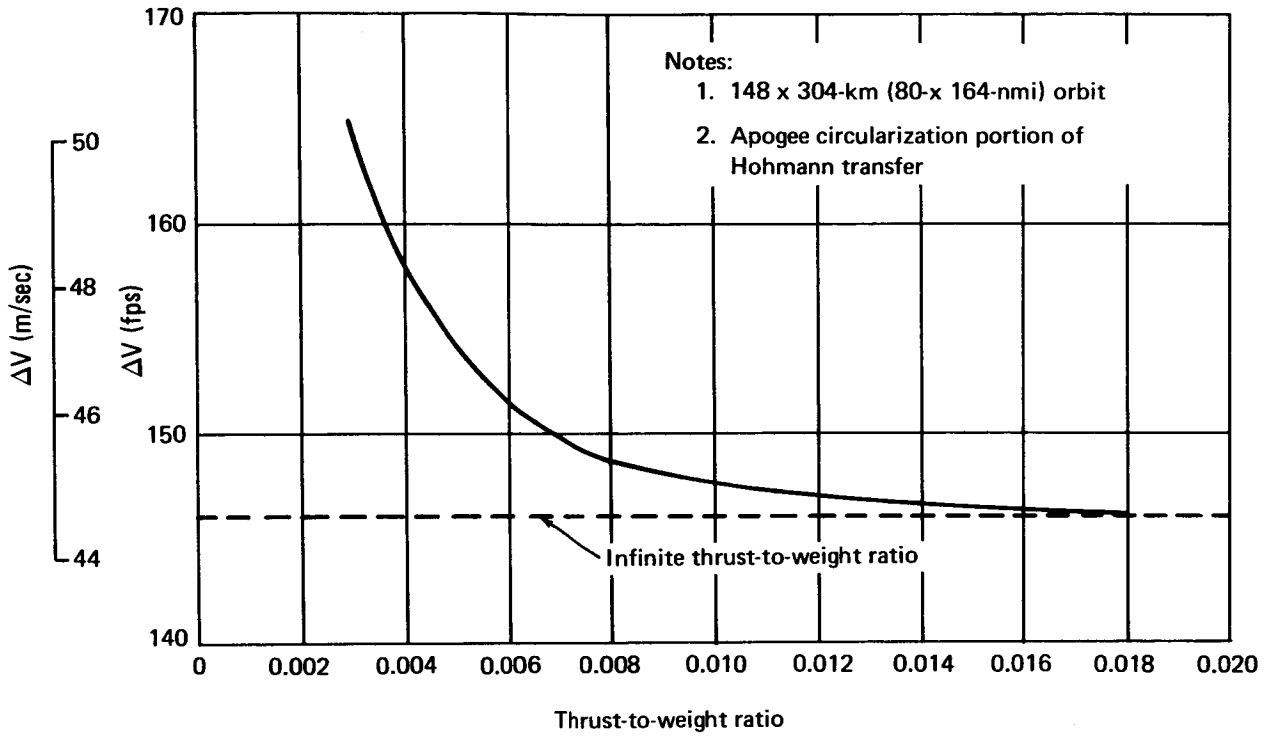

Figure 49. Circularization Velocity Requirements

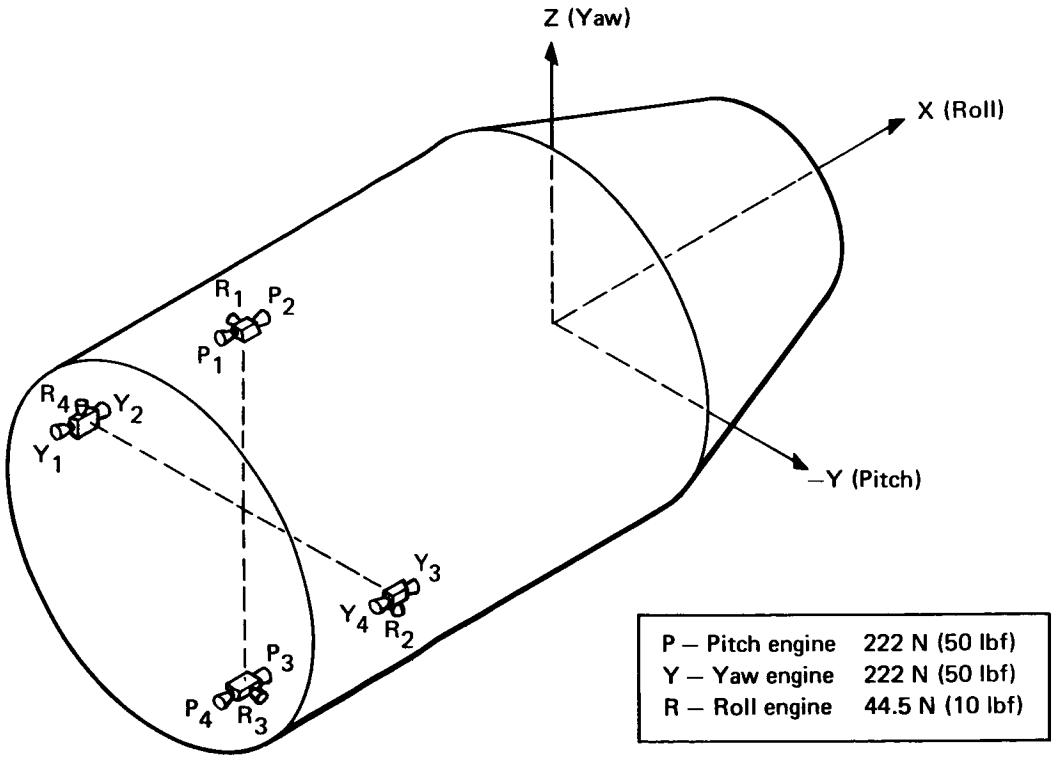

Figure 50. Thrustor Configuration

All attitude-control moments are obtained by turning on opposing thrustors to provide a couple, except pitch and yaw control during apogee circularization. During circularization, all four rear-facing thrustors are operating.

Storable bipropellant system. – The candidate storable bipropellant system consists of radiation-cooled thrustors using the hypergolic propellants nitrogen tetroxide (N_2O_4) and monomethylhydrazine (MMH) at a nominal mixture ratio of 1.6:1. The thrustors operate at thrust levels of 44.5 N (10 lbf) and 222 N (50 lbf) and a chamber pressure of 6.89×10^5 N/m^2 (100 psia) with an expansion ratio of 40:1.

A design and performance summary of these thrustors is shown in table 17. The minimum-impulse-bit capability of 0.44 N-sec (0.10 lbf-sec) for the roll thrustors and 2.22 N-sec (0.50 lbf-sec) for the pitch and yaw thrustors is within that required by the defined MORL profile. Fig. 51 shows the steady-state delivered specific impulse as a function of thrust level. Poor performance associated with the lower thrust levels results from the kinetic losses associated with the shorter residence times of the combustion species in shorter nozzles, with a subsequent shift toward frozen-flow performance.

TABLE 17

STORABLE BIPROPELLANT SYSTEM PERFORMANCE

Description	Design or Performance
Propellants	N_2O_4/MMH
Mixture ratio	1.6:1
Tank conditions	
Pressure	1.73×10^6 N/m^2 (250 psia)
Temperature	266° to 324°K
Chamber pressure	6.9×10^5 N/m^2 (100 psia)
Area ratio	40:1
I_{sp}	
44.5-N (10-lbf) thrustor	290 sec
222-N (50-lbf) thrustor	295 sec
Minimum impulse bit	
44.5-N (10-lbf) thrustor)	0.44 N-sec (0.10 lbf-sec)
222-N (50-lbf) thrustor	2.22 N-sec (0.50 lbf-sec)
Ignition	Hypergolic

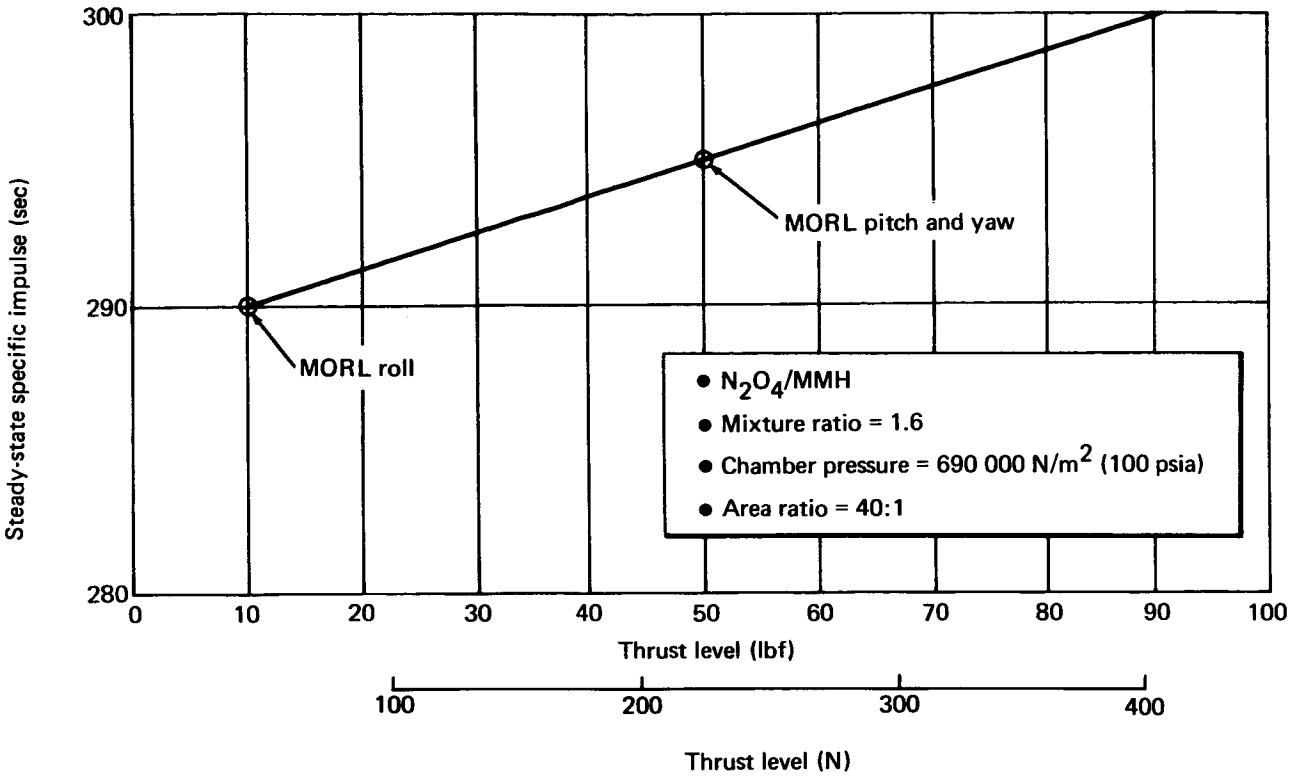

Figure 51. Delivered I_{sp} versus Thrust Level

Fig. 52 shows performance as a function of pulse width. The single-element injector performs better in a pulsed mode because it has less dribble volume than a multi-element injector. However, the multi-element injector will give better steady-state performance because it provides better propellant mixing in the combustion chamber with resulting higher combustion efficiencies.

Three thrustor design concepts are considered as representative of current bipropellant thrustors:

(1) The beryllium thrustor (Rocketdyne).

(2) The radiation thrustor (Marquardt).

(3) The C-1 radiamic thrustor (Thiokol).

Each of these thrustor concepts uses N_2O_4 as the oxidizer and MMH as the fuel at a mixture ratio of 1.6:1. Each concept utilizes a different cooling technique. These thrustors are considered typical of the currently available bipropellant thrustors within the thrust range of interest for the MORL. All of these concepts have demonstrated capabilities through extensive test programs and, in some cases, have demonstrated capabilities on actual space missions.

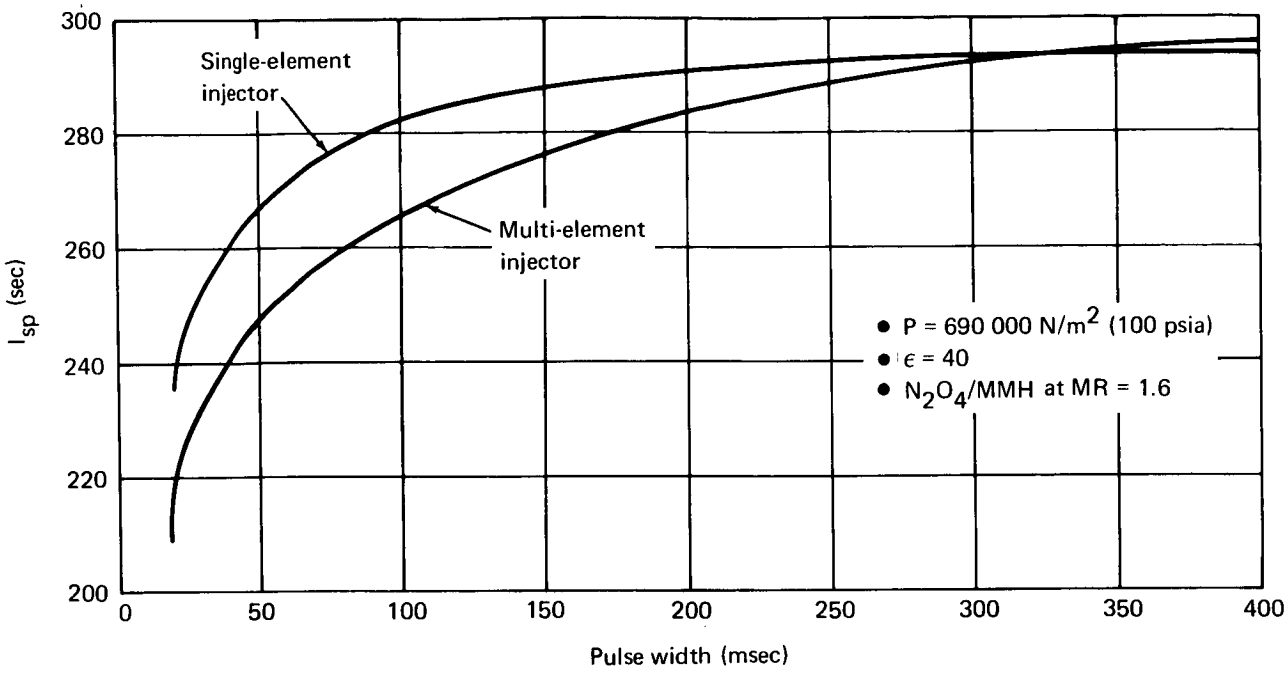

Figure 52. Bipropellant Pulsing Performance

The beryllium thrustor (Rocketdyne) is shown in fig. 53. Thrustor dimensions are given for a 44.5-N (10-lbf) thrust level. The properties that make beryllium attractive for thrust chamber construction are low density, high heat capacity, high thermal conductivity, and a relatively high melting point. This lateral-heat-transfer concept utilizes the high thermal conductivity of the beryllium to transfer heat from the hot throat area toward the combustion chamber. The combustion chamber is film cooled by injecting approximately 44% of the fuel into the boundary layer next to the combustion chamber wall. This process does not significantly affect the overall performance because the MMH acts as good monopropellant. The boundary-layer film provides a low-temperature zone along the inner surface of the combustion chamber, which serves as a heat sink for the higher flux regions of the thrust chamber such as the throat region. This configuration is self-sustaining, that is, it does not rely on radiant heat transfer to the environment, permitting application in buried installations. This cooling concept permits the production of thrustors whose operation is insensitive to duty cycle variation. Fabrication techniques are well established for beryllium, a nonrefractory metal. The injector consists of an eight-element orifice unlike doublet with 16 boundary layer cooling (BLC) orifices. At a chamber pressure of 6.9×10^5 N/m^2 (100 psia) and an expansion ratio of 40:1, a steady-state specific impulse of 295 sec is realized. Lifetimes of from 10 000 to 20 000 sec are attainable with this thrustor. Combustion chamber temperatures never exceed 1325°K (2390°R) during either steady-state or pulsed operation.

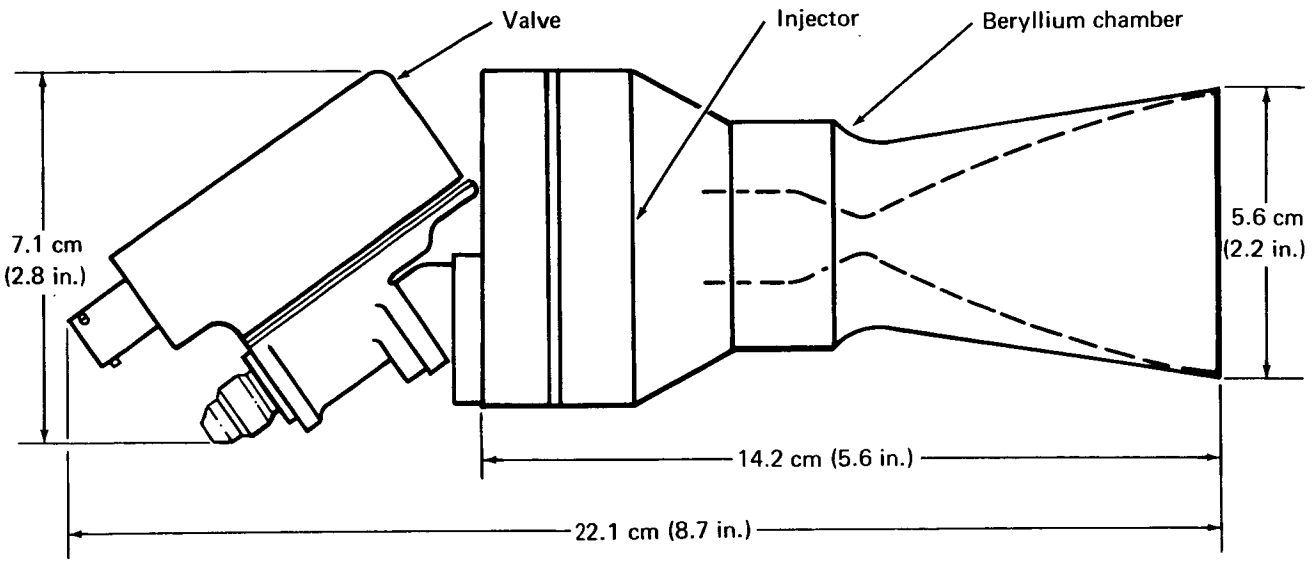

N_2O_4/MMH at MR = 1.6
Radiation/film cooled
Thrust = 44.8 N (10 lbf)
$P_c = 6.9 \times 10^5$ N/m^2 (100 psia)
$\epsilon = 40$

Figure 53. Rocketdyne Thrustor

The radiation thrustor (Marquardt) is shown in fig. 54. This thrustor is fabricated from molybdenum to an area ratio of 6.8:1, at which point a lightweight stainless-steel ribbed nozzle extension expands to an area ratio of 40:1. Use of the L-605 cobalt-base alloy for construction of the nozzle extension allows for weight reduction where gas temperatures and pressures are less severe than in the combustion chamber. The thrust chamber and nozzle are coated with molybdenum disilicide, which provides oxidation protection from the exhaust gases. The life of the chamber is dependent upon the coating loss rate which, in turn, is dependent upon the wall temperature and the duty cycle. At a mixture ratio of 1.6:1, the chamber temperature is 1330°K (2400°R) for a chamber pressure of 6.7×10^5 N/m^2 (97 psia). At these defined conditions, the thrustor will deliver 293 sec steady-state impulse. This thrustor has a demonstrated life in excess of 12 000 sec for duty cycles much more severe than those of the MORL requirements. The thrustor injector head assembly consists of an eight-on-eight doublet, eight BLC orifices, and a preigniter. The BLC's direct fuel streams onto the wall of the combustion chamber to produce a fuel film layer between the burning gases in the chamber and the wall of the chamber. This fuel film reduces the temperature of the chamber wall about 810°K (1460°R) by the vaporization of the fuel and by providing added heat transfer resistance between the bulk gas and the wall. The preigniter chamber is a tubular chamber extending from the face of the injector heat assembly and contains a single doublet. It is designed to ignite a small quantity of the propellant prior to ignition of the

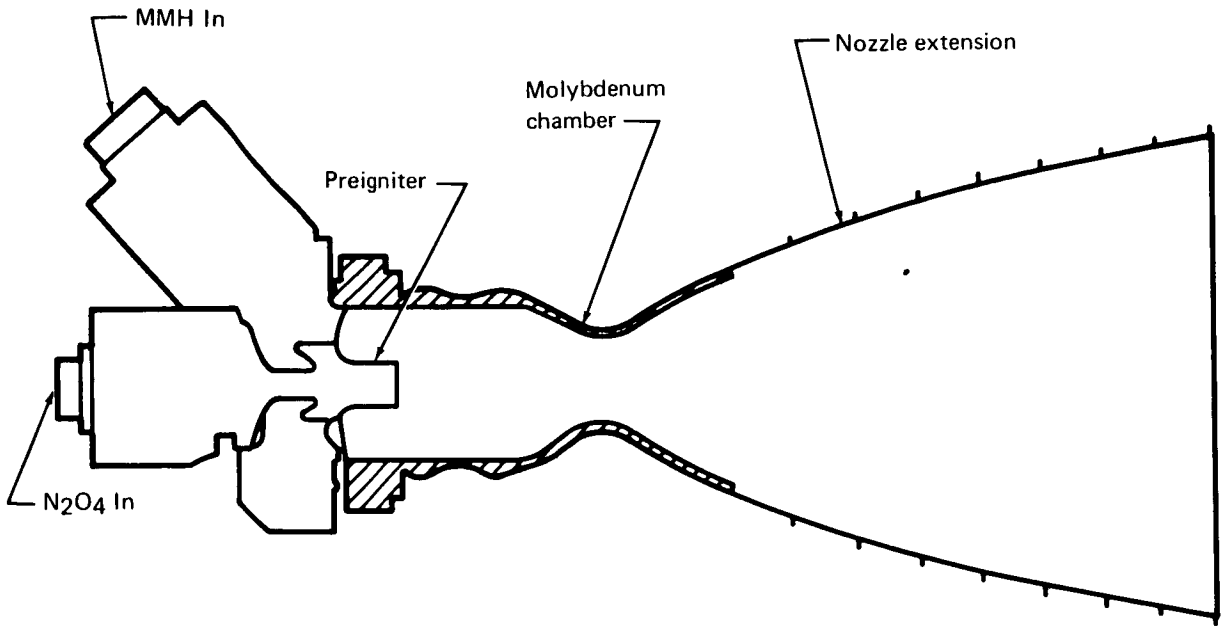

Figure 54. Marquardt Thrustor

main combustion chamber. Initial ignition of the preigniter chamber pre-pressurizes the main combustion chamber, thereby minimizing ignition delays of the main propellant stream and suppressing ignition pressure spikes. The propellant valves have a maximum soakback temperature of 353°K (635°R) due to limitations imposed by the oxidizer vapor pressure. This requirement is met by a standoff tube which reduces heat soakback to the propellant valves following thrustor shutdown. The valves are designed so that the fuel valve will open prior to the oxidizer valve. This produces a fuel lead which, along with the preigniter, provides a smooth ignition.

The C-1 radiamic thrustor (Thiokol) is shown in fig. 55. The significant features of this thrustor are a full-diameter vortex injector, a low-mass radiation liner separated from a double-cooling jacket (regeneration circuit), a minimum heat storage throat insert, and a radiation-cooled nozzle. The full-diameter vortex injector induces secondary recirculation in the combustion chamber to provide an increased combustion efficiency. This injector also provides a swirling liquid layer at the chamber wall which provides a film cooling. The vortex injector concept also reduces the vacuum ignition pressure spikes. A chamber radiation liner of tantalum-tungsten is utilized in conjunction with a two-pass cooling jacket. The inside portion of the radiation liner is coated with preoxidized hafnium to prevent deterioration from the combustion gases. Tantalum-tungsten was chosen as the liner material to reduce the embrittlement problem associated with the pressure

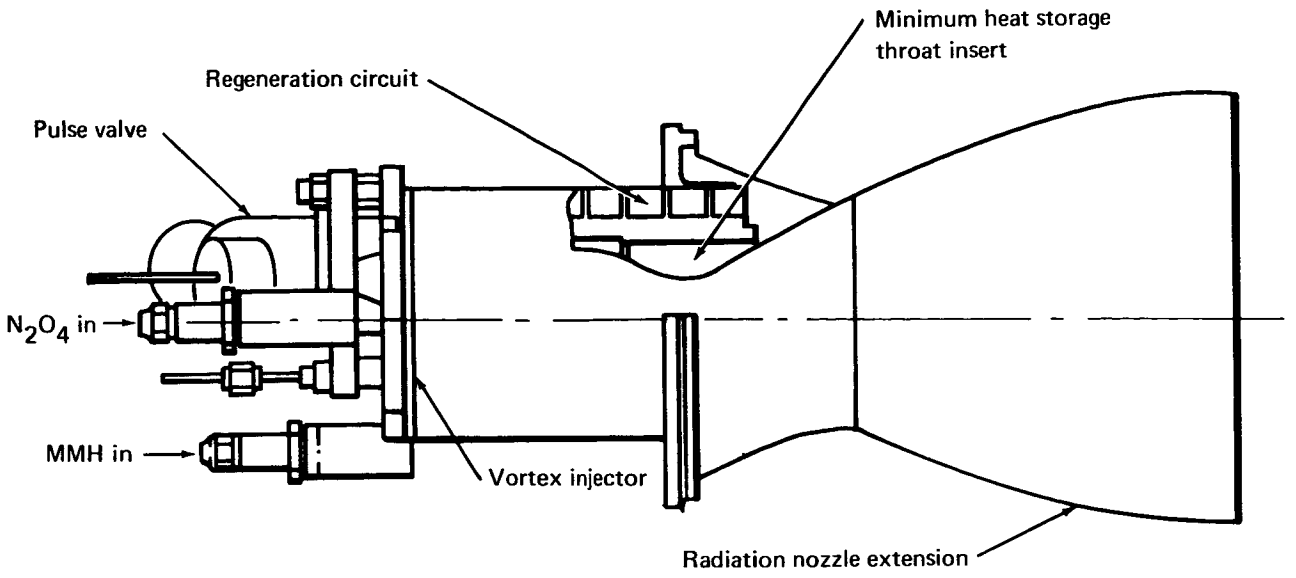

Figure 55. C-1 Radiamic Thrustor Thiokol

spike effects of starting the thrustor at low temperatures. This cooling concept will maintain the outside wall temperature of the combustion chamber at less than 590°K (1060°R). The C-1 thrustor utilizes a foamed-molybdenum throat insert with a low heat storage capacity. This concept conducts heat into the coolant jacket during thrustor operation and prevents a high bulk temperature rise at the throat after thrustor shutdown. The radiation-cooled nozzle is constructed of columbium to an area ratio of 40:1 and of titanium to an area ratio of 60:1. A silicide coating is utilized to reduce the oxidizing effects of the combustion gases. The C-1 thrustor operating at a mixture ratio of 1.6:1 and a chamber pressure of 6.9×10^5 N/m^2 (100 psia) will provide a steady-state specific impulse of 297 sec. It has successfully performed the Apollo Service Module duty cycle, and more than 10 000 sec has been accumulated on one of Thiokol's test thrustors. Current thrust levels of the C-1 thrustor are 380 N and 445 N (85 and 100 lbf). Either a linked bipropellant or a quad-redundant valve may be utilized.

The storable propellants and associated pressurant gas are stored in the aft section of the MORL vehicle at the ambient temperature of 325°K (585°R) An N_2 bottle (6 Al-4V-Ti alloy) at 2.07×10^7 N/m^2 (3000 psia) is utilized to pressurize the propellant tanks to a pressure of 1.73×10^6 N/m^2 (250 psia). Metal bellows are utilized for positive expulsion and to provide recycling capabilities for propellant resupply. The storable propellant tanks are fabricated from AM-350 double-aged stainless steel and are compatible with the designated propellants.

The bipropellant tanks must hold a total of 283 kg (622 lbm) of propellant at MORL launch. Two sets of tanks will meet these requirements and provide system redundancy during the MORL mission. Because of the selected 1.6 mixture ratio, the tanks have the same volume. These equal volume tanks are 0.305 m (12 in.) in diameter and 1.1 m (3.6 ft) in length. They are constructed of minimum gage 0.051 cm (0.020 in.) stainless steel and weigh 4.55 kg (10 lbm) per tank excluding bosses, flanges, fittings, and positive expulsion bellows. Fig. 56 shows a schematic of the bipropellant system.

Monopropellant system. – The candidate monopropellant system utilizes N_2H_4 which exothermally decomposes while passing over a catalyst bed to provide the thrust energy. This thrustor provides a steady-state specific impulse of about 235 sec with a gas temperature of 1255°K (2260°R). Thus, ordinary materials (stainless steel or Haynes No. 25 alloy) are used for thrust chamber construction. There are no high-temperature material problems and, consequently, long engine life is possible with N_2H_4 thrustors.

The thrustor design details are shown in fig. 28. The dimensions shown are for a 44.5-N (10-lbf) thrust level. A radiation heat barrier is located between the catalyst bed and the propellant valve. This heat barrier is installed to prevent heat soakback from the hot catalyst bed to propellant in the propellant valve after engine shutdown, thus preventing a temperature rise which would vaporize propellant in the propellant valve. Test data indicate that a valve operating at 297°K (525°R) can be limited to a temperature rise of approximately 330°K (595°R) after engine shutdown with this radiative heat barrier.

An adverse effect associated with this heat barrier is the large dribble volume. (Dribble volume is defined as that volume which is located between the propellant valve seat and the thrustor chamber injector.) Because of the large dribble volume, the monopropellant thrustor has long thrust buildup and thrust decay times which result in reduced pulsing performance. The pulsed performance of the N_2H_4 monopropellant thrustor is also a function of the initial catalyst bed temperature. The specific impulse at 0.1 to 10 sec pulse widths is reduced because of the residual heat energy left in the thrustor after shutdown of flow. This energy can be picked up by the next pulse or left to dissipate to the environment. The specific impulse at short pulse widths is also reduced because of cold-bed effects that result in an incomplete decomposition of all the injected propellant. The first pulse performance for very short pulses can fall below the theoretical value for N_2H_4 at 288°K (518°R) as a result of some liquid propellant passing through the thrustor without vaporizing. Each pulse leaves some heat energy in the catalyst bed; this residual heat energy is made available to the following pulse until the steady-state conditions are attained. Because of these catalyst bed temperature effects, the pulse-to-pulse reproducibility is about ±15% compared to about ±20% for a bipropellant system. The bipropellant reproducibility is limited by off-mixture ratio effects and effects associated with fuel or oxidizer lead during thrustor start and stop. These effects do not apply to a monopropellant N_2H_4 thrustor.

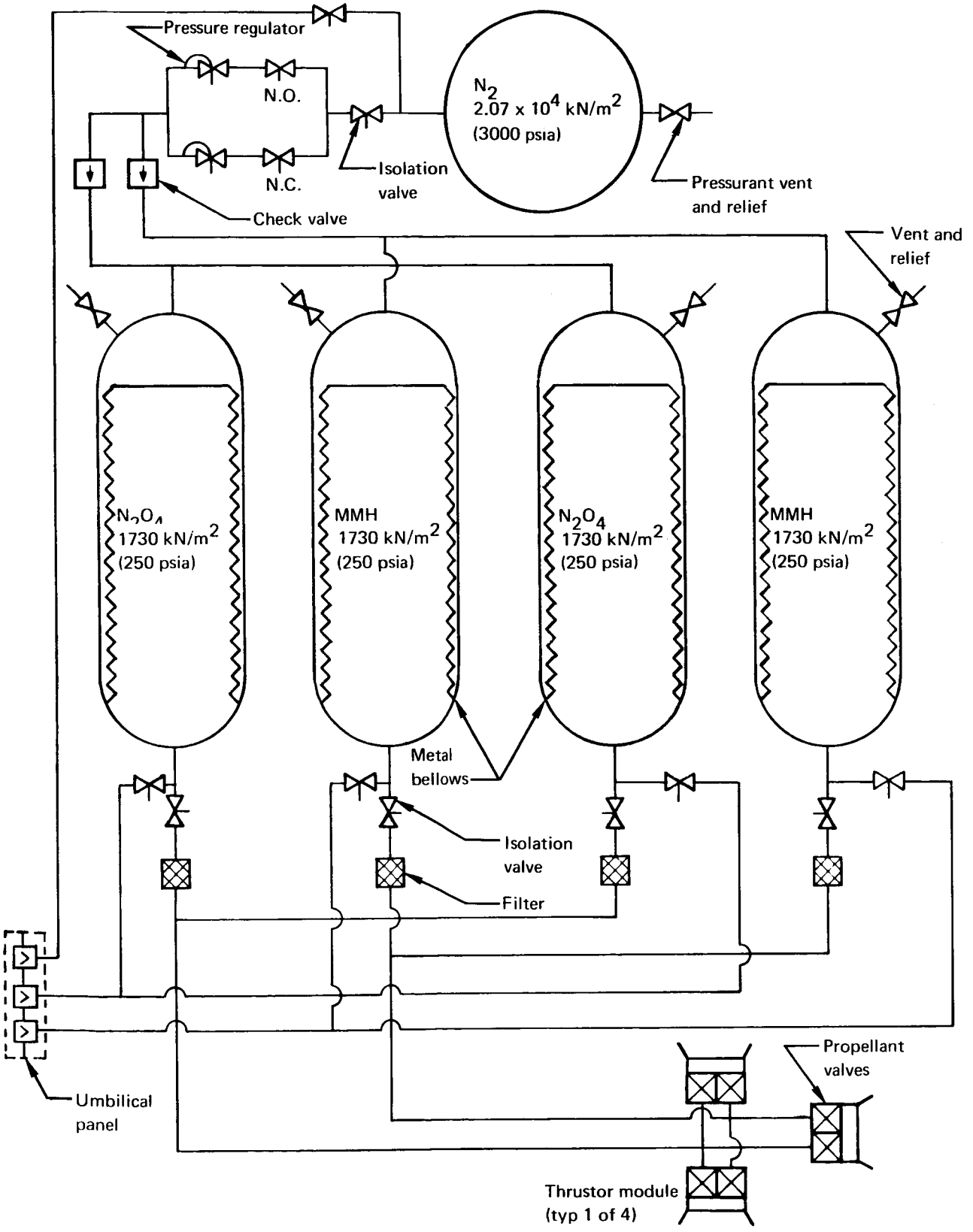

Figure 56. Bipropellant Schematic Diagram

Shell 405 spontaneous catalyst is used in the reaction chamber to decompose the N_2H_4 into NH_3, N_2, and H_2. This catalyst is composed of 32% iridium impregnated on the surfaces of Al-1404 supports. Most of the thrustor reaction bed is composed of 14 to 18 mesh size catalysts with the upper portion of the reaction bed composed of a small layer of 20 to 30 mesh size catalysts. This finer grade catalyst stabilizes the thrustor operation by maintaining the flame front in a relatively fixed position in the top of the bed. An injector head assembly ensures proper distribution of propellant to the catalyst bed to optimize the response time of the thrustor. High-velocity straight-shot injector holes are used to wash out any catalyst fines that migrate upstream of the injector. Deterioration of the catalyst bed in a vacuum environment will not be significant because the catalyst consists of metal oxides with low vapor pressures. During the first 5 min of steady operation, the aluminum in the catalyst bed will undergo a phase shift to alumina. This will reduce the area loading of the catalyst bed from 150 cm^2/gm to 70 cm^2/gm, which is well above the 40 cm^2/gm lower limit. After this initial phase shift, the area loading should remain relatively constant for the duration of the MORL mission.

A performance summary of the monopropellant system is shown in table 18. The monopropellant tank and feed system was derived utilizing a design philosophy similar to that used for the bipropellant system. Fig. 57 shows a schematic of the monopropellant system. Five equal-volume tanks are utilized to provide the orbit-injection requirements. Each tank will hold approximately 82 days of high-thrust propellant and will be resupplied as required during the MORL mission. Each tank is 30.5 cm (12.0 in.) in diameter and has a length of 122 cm (48 in.).

TABLE 18

MONOPROPELLANT SYSTEM PERFORMANCE

Item	Description
Propellant	N_2H_4
Thrustor inlet pressure	12.4×10^5 N/m^2 (180 psia)
Thrustor inlet temperature	Liquid range
Chamber pressure	6.9×10^5 N/m^2 (100 psia)
Area ratio	50:1
I_{sp} (avg)	235 sec
Minimum impulse bit	
Hot pulse (700 to 1810°K)	0.81 N-sec (0.18 lbf-sec)
Cold pulse (298°K)	0.448 N-sec (0.10 lbf-sec)
Ignition	Catalyst

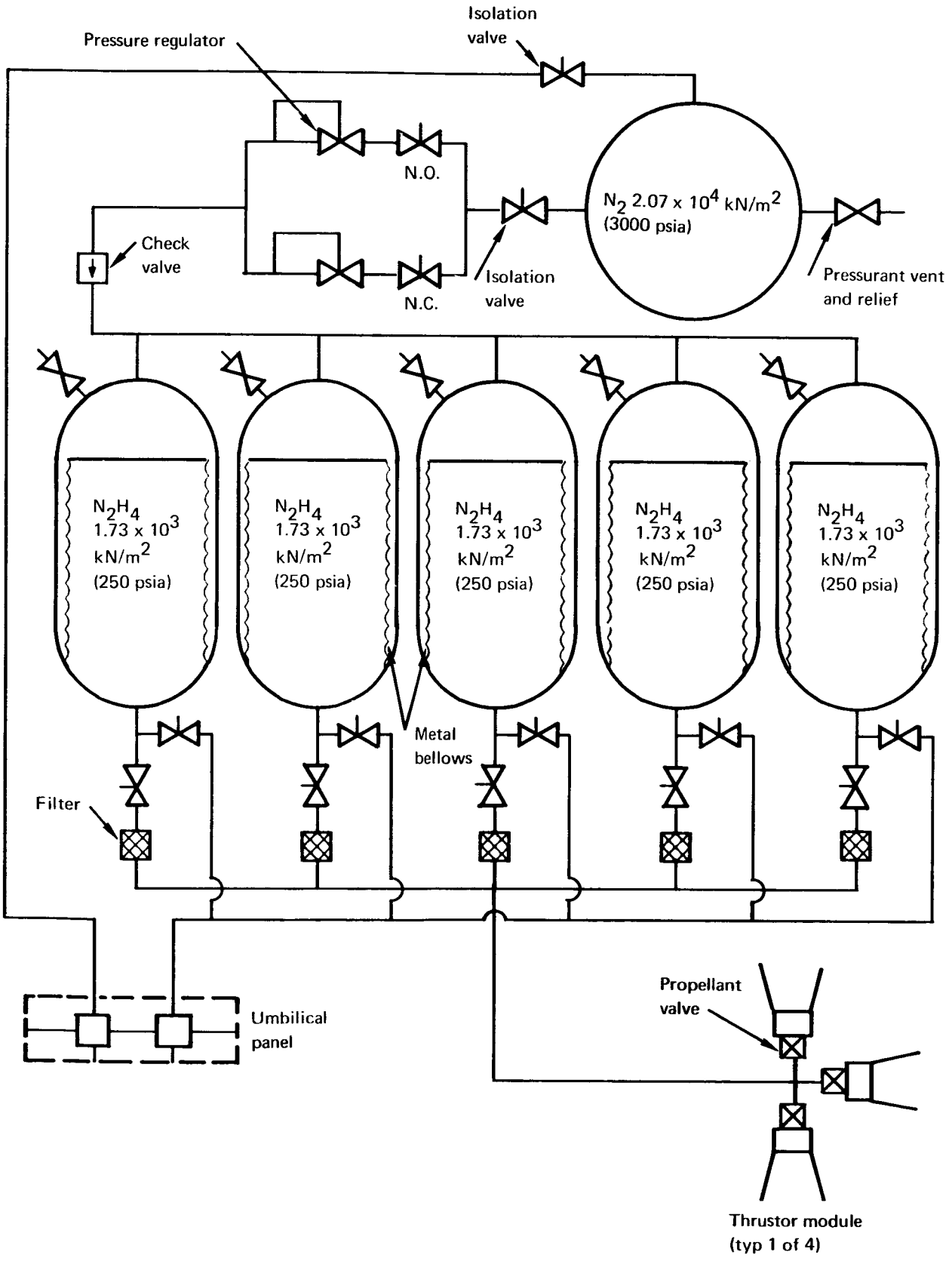

Figure 57. Monopropellant Schematic Diagram

Table 19 summarizes the characteristics of the monopropellant and bipropellant tank and feed systems. Defined characteristics for both the propellant tanks and the N_2 pressurization bottle are shown. Chargeable dry and wet weights at MORL launch are shown for the defined systems. These preliminary system weights do not include tank mounts, flanges, fittings, or associated feed system valve and line weights.

Cryogenic bipropellant system. – The candidate O_2/H_2 thrustors operate at a chamber pressure of 345 kN/m^2 (50 psia) and have an expansion ratio of 40:1. The 44.5-N (10-lbf) roll thrustors have a minimum-impulse-bit capability of 4.45 N-sec (1.0 lbf-sec), and the 224-N (50-lbf) thrustors have a 17.8 N-sec (4.0 lbf-sec) minimum-impulse-bit capability. Both thrustors deliver a specific impulse of 318 sec, since performance is relatively insensitive to thrust level at the 1.0 mixture ratio. A performance summary of the candidate O_2/H_2 thrustors is shown in table 20.

The system uses a low mixture ratio to keep the chamber temperature down to about 1090°K (1960°R), allowing both the combustor and nozzle to be fabricated of electrodeposited nickel for extended operational life without special cooling techniques. Each thrustor assembly consists of a mechanically linked bipropellant valve, injector mixer, pilot catalyst ignition bed, combustor, and a converging-diverging nozzle. Since only a small portion of the total flow (2 to 5%) passes through the catalyst bed, good pulse repeatability is maintained. The balance of the flow enters the combustor downstream of the pilot bed and is ignited by the hot gases. The initial temperature of the bed is maintained near operating temperatures by an electric heater.

Fig. 58 shows a system schematic of the O_2/H_2 system. The system consists of a propellant conditioner and an accumulator for both the O_2 and the H_2 propellants. The propellant conditioner delivers gaseous oxygen (GO_2) and gaseous hydrogen (GH_2) to the thrustors at a specified pressure and temperature. This enables the thrustors to operate at a relatively constant mixture ratio and flowrate, resulting in predictable and repeatable operation. The two primary control variables are accumulator pressure and temperature. For the MORL system the accumulators store GO_2 and GH_2 at 4.13×10^5 N/m^2 (60 psia) and a temperature of 111°K (200°R). The propellant conditioner consists of two O_2/H_2 gas generators and heat exchangers, one each for O_2 conditioning and H_2 conditioning. The gas generators are fed O_2 and H_2 from the accumulators at a mixture ratio of about 1.33:1. This provides an exhaust gas at a temperature of about 1390°K (2500°R) to be utilized for propellant conditioning. A pilot ignition bed is not required for the gas generator since response times are not as critical for this system as for the thrustors system. Consequently, all the gas generator propellant flows over the catalyst bed contained within the gas generator case. The exhaust from the gas generator is passed to the heat exchanger, which consists of a helical tube carrying the propellant placed within an annular shell through which the gas generator exhaust products pass. The gas generator operates only when the thrustors are firing and propellant is flowing. If the temperature of the propellant in the accumulator falls below some lower limit, the gas generator valves are signalled to open. An electric heating element located in the accumulator provides temperature control when the thrustors are inoperative and no propellant is flowing. The accumulators are constructed of aluminum and serve as pneumatic capacitors as well as propellant manifolds.

TABLE 19

STORABLE PROPELLANT TANK AND FEED SYSTEM

Item	Bipropellant system	Monopropellant system
Propellants	N_2O_4/MMH	N_2H_4
Mixture ratio	1.6:1	---
Propellant tank concept	4 tanks (2 fuel, 2 oxidizer)	5 tanks
Expulsion	Metal bellows	Metal bellows
Tank material	AM-350 double-aged stainless steel	AM-350 double-aged stainless steel
Tank conditions		
Pressure	1.73×10^6 N/m^2 (250 psia)	1.73×10^6 N/m^2 (250 psia)
Temperature	325°K (586°R)	325°K (586°R)
Propellant tank diameter	30.5 cm (12 in.)	30.5 cm (12 in.)
Propellant tank length	110 cm (43.2 in.)	122 cm (48 in.)
Propellant tank gage	0.051 cm (0.020 in.)	0.051 cm (0.020 in.)
Pressurization system (N_2)		
Pressure	2.17×10^6 N/m^2 (3000 psia)	2.17×10^6 N/m^2 (3000 psia)
Temperature	325°K (586°R)	325°K (586°R)
Pressurant bottle material	6 Al-4V-Ti	6 Al-4V-Ti
Pressurant bottle diameter	41.4 cm (16.3 in.)	44.7 cm (17.6 in.)
Pressurant bottle gage	0.29 cm (0.113 in.)	0.33 cm (0.128 in.)
Propellant tank weight	18 kg (40 lbm)	24 kg (52 lbm)
Pressurant bottle weight	6.7 kg (15 lbm)	10 kg (22 lbm)
Total dry weight	25 kg (55 lbm)	34 kg (74 lbm)
Propellant weight [a]	282 kg (622 lbm)	355 kg (784 lbm)
N_2 gas weight	8.2 kg (18 lbm)	12 kg (25 lbm)
Total wet weight	315 kg (695 lbm)	400 kg (883 lbm)

[a]Includes orbit injection plus 20 days of mission high-thrust requirements.

TABLE 20

O_2/H_2 SYSTEM PERFORMANCE

Item	Description
Propellants	O_2/H_2
Mixture ratio	1.0:1
Feed pressure	4.13×10^5 N/m^2 (60 psia)
Chamber pressure	3.44×10^5 N/m^2 (50 psia)
Area ratio	40:1
I_{sp}	318 sec
Minimum impulse bit	
44.5-N (10-lbf) thrustors	4.45 N-sec (1.0 lbf-sec)
224-N (50-lbf) thrustors	17.8 N-sec (4.0 lbf-sec)
Ignition	Catalyst

Pressure control from the MORL tankage system is maintained by a pressure regulator on the H_2 line and a pressure follower on the O_2 line (fig. 59). The regulator senses the pressure in the H_2 accumulator and operates to maintain that pressure at some fixed level. The follower senses the pressure differential between the O_2 and H_2 accumulator and operates so that the O_2 accumulator pressure will follow that of the H_2 accumulator. This concept keeps the variations in accumulator pressure in close phase, thus limiting the potential mixture ratio variation and enhancing system stability. The follower is used with the O_2 because of its significantly greater density variation.

The cryogenic tank and feed system must supply 253 kg (557 lbm) of propellant for orbit injection and have storage capabilities for 72 kg (159 lbm) of propellant for the 147-day mission high-thrust requirements. O_2 is stored in the subcritical state for orbit injection and would require venting and positive expulsion if it were utilized for providing the 147-day high-thrust requirements. Consequently, a separate tank is used to provide this capability. The 147-day O_2 tank stores O_2 in a supercritical state at 2.17×10^7 N/m^2 (3000 psia) and at the ambient temperature of 325°K (585°R). Because of the supercritical storage, no thermodynamic control of this tank is required. Table 21 summarizes the characteristics of the O_2 tanks. The H_2 requirements are met by resizing the resistojet H_2 tank. This tank stores H_2 in a cryogenic state at 27.8°K and 4.9×10^5 N/m^2 (80 psia). The

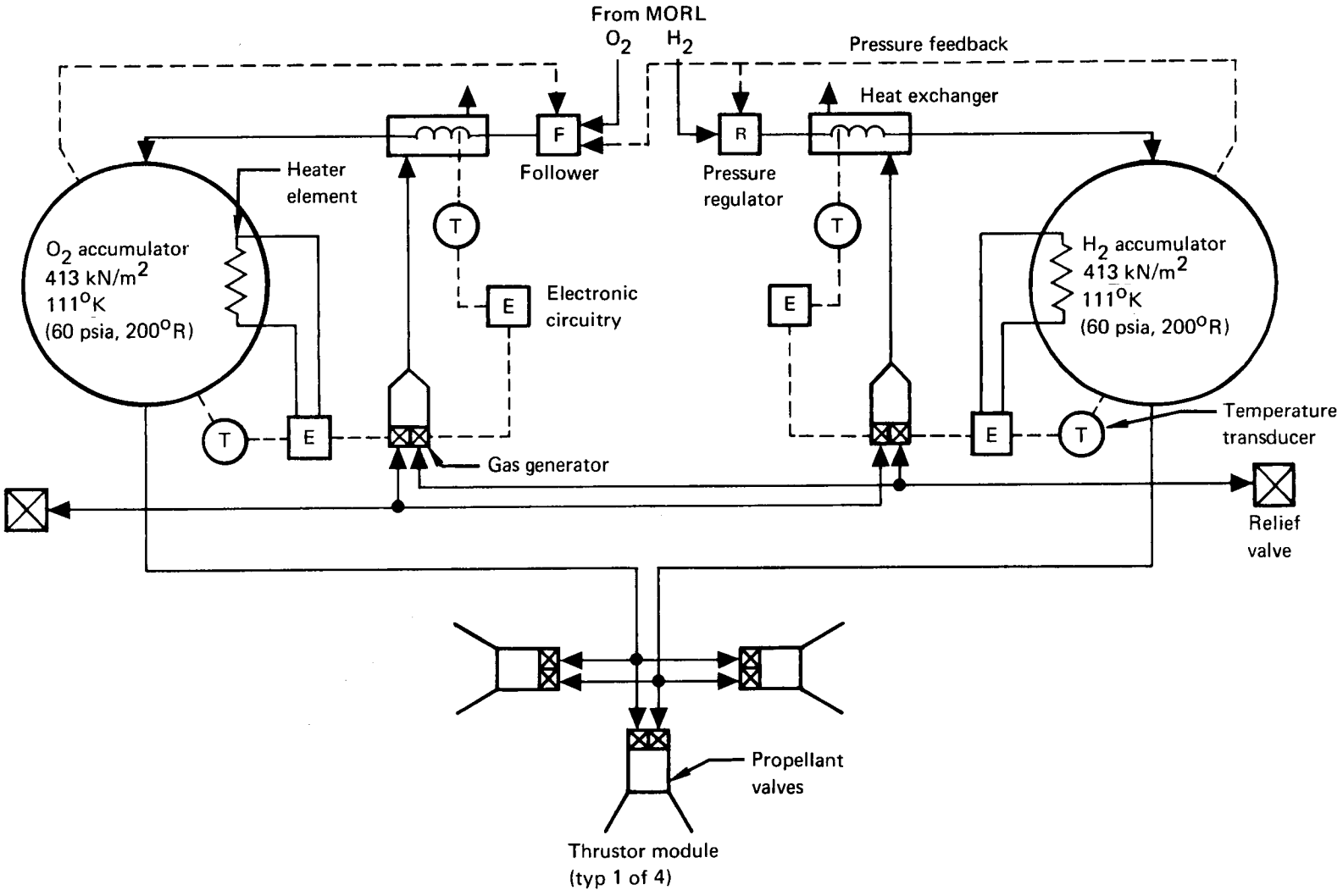

Figure 58. O_2/H_2 Flow Schematic

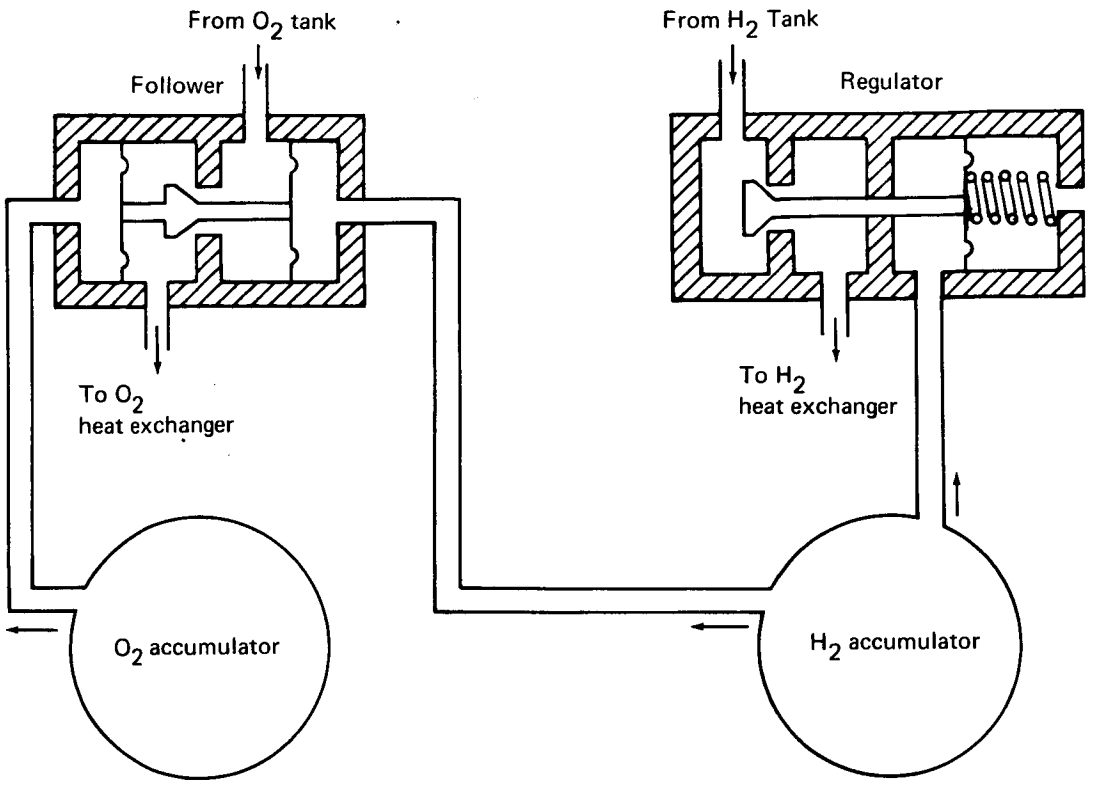

Figure 59. Pressure Control System

resized tank fulfills the baseline resistojet requirements plus 147 days of high-thrust requirements. Since the resistojet H_2 tank is off loaded at MORL launch, the resized H_2 tank can meet the orbit-injection requirements. Table 22 summarizes the characteristics of this resized H_2 tank and compares them with the resistojet H_2 tank.

Solid-propellant motor system. – For system simplicity, a solid-propellant-motor orbit-injection system was considered for the MORL. The solid-propellant orbit-injection system, shown in fig. 60, consists of four 11.12-N (250-lbf) (average) thrust motors firing simultaneously. Attitude control is provided by a liquid-engine control system (fig. 60) with 222.5-N (50-lbf) thrust pitch and yaw engines and 44.5-N (10-lbf) thrust roll engines. This attitude control system is capable of providing pitch and yaw restoring moments of 1355 N-m (1000 ft-lb) and roll restoring moments of 677 N-m (500 ft-lb). Thrust vector control (TVC) methods, such as gimballed nozzles and secondary injection, were considered and rejected. Rejection of these techniques was based primarily on the determination that (1) TVC solids have poor mass ratios and (2) TVC solids would require extensive modification and increase the complexity of the control network logic.

The solid-propellant orbit-injection total thrust was limited to approximately 4450 N (1000 lbf) by selection of the attitude control system. Preliminary evaluation of solid-propellant engine configurations shows that a

TABLE 21

CRYOGENIC TANK AND FEED SYSTEM—O_2 TANK

Item	Description
Orbit injection	
Scheme	One spherical tank
Tank material	2014-T6 Al
Tank conditions	
Temperature	111°K (200°R)
Pressure	4.9×10^5 N/m^2 (80 psia)
Wall thickness	0.051 cm (0.020 in.)
Tank diameter	63 cm (24.8 in.)
Tank weight	1.8 kg (4 lbm)
Propellant loaded	129 kg (285 lbm)
Propellant usable	126 kg (279 lbm)
147-day tank	
Scheme	One spherical tank
Tank material	6 Al-4V-Ti
Tank conditions	
Temperature	325°K (585°R)
Pressure	2.17×10^7 N/m^2 (3000 psia)
Wall thickness	0.452 cm (0.178 in.)
Tank diameter	65.2 cm (25.7 in.)
Tank weight	27 kg (59 lbm)
Propellant loaded	37 kg (83 lbm)
Propellant usable	36 kg (80 lbm)

TABLE 22

CRYOGENIC TANK AND FEED SYSTEM—H_2 TANK

Item	MORL resistojet	Resized tank
Scheme	One spherical tank	One spherical tank
Tank material	2014-T6 Al	2014-T6 Al
Tank conditions		
Temperature	27.8°K (50°R)	27.8°K (50°R)
Pressure	4.9×10^5 N/m^2 (80 psia)	4.9×10^5 N/m^2 (80 psia)
Wall thickness	0.145 cm (0.057 in.)	0.15 cm (0.059 in.)
Tank diameter	1.86 m (73.5 in.)	1.95 m (77 in.)
Tank weight	44.5 kg (98 lbm)	54.5 kg (120 lbm)
Propellant loaded	187 kg (412 lbm)	229 kg (505 lbm)
Propellant usable	167 kg (367 lbm)	203 kg (447 lbm)

four-motor system should be selected. This judgment was based on an evaluation which showed that significant weight reductions could not be obtained with 8- or 16-motor systems, and that solid-propellant motor characteristics did not easily lend themselves to 8- and 16-motor system designs.

The four-motor system, at an average thrust level of 1112 N (250 lbf) was established. At this average thrust level, extremely long burn times 188 012 N-sec (42 250 lb-sec) are required (approximately 170 sec) to provide the required total impulse for each motor. To satisfy these orbit-injection requirements, an end-burning grain design was selected. The design is shown in fig. 61, and the thrust time curve is shown in fig. 62. The associated performance and pertinent characteristics are listed in table 23.

A polycarbutene propellant, designated LPC 543-A, was selected after an overall evaluation of propellant properties and proposed usage. The high performance, low burning rate, and simple casting characteristics influenced this selection. The polybutadine cup and insulation (Lockheed formulation LPE-2) are tapered to prevent over-temperature of the case (at the nozzle end). This insulation will boil off during firings and contribute impulse, although this was not considered in the design. The nozzle design and the ignition technique through the nozzle seal are shown in fig. 61. The selected solid-propellant and attitude-control engine arrangement are shown in fig. 60.

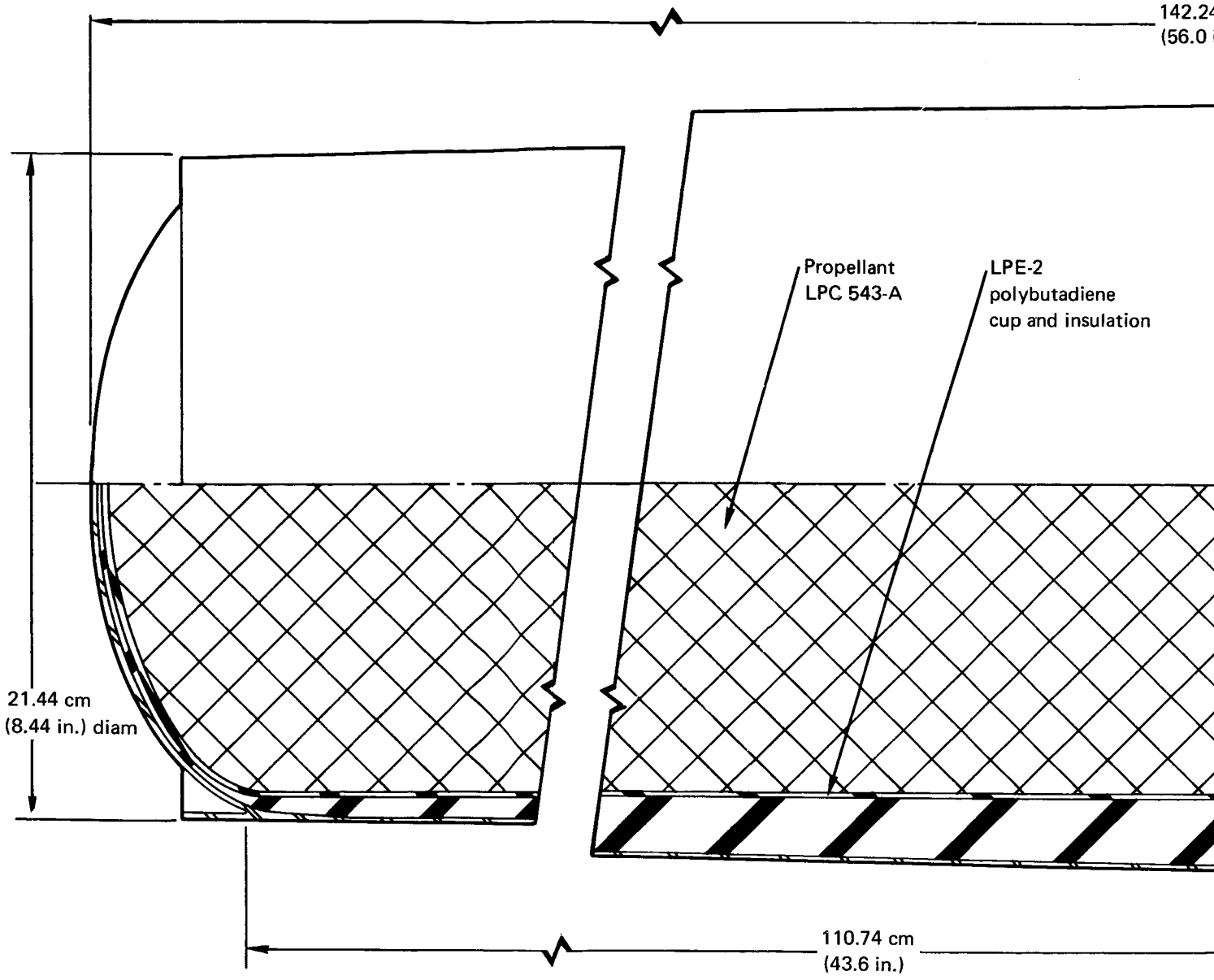

Figure 61. Solid-Propellant Orbit-Injection Motor

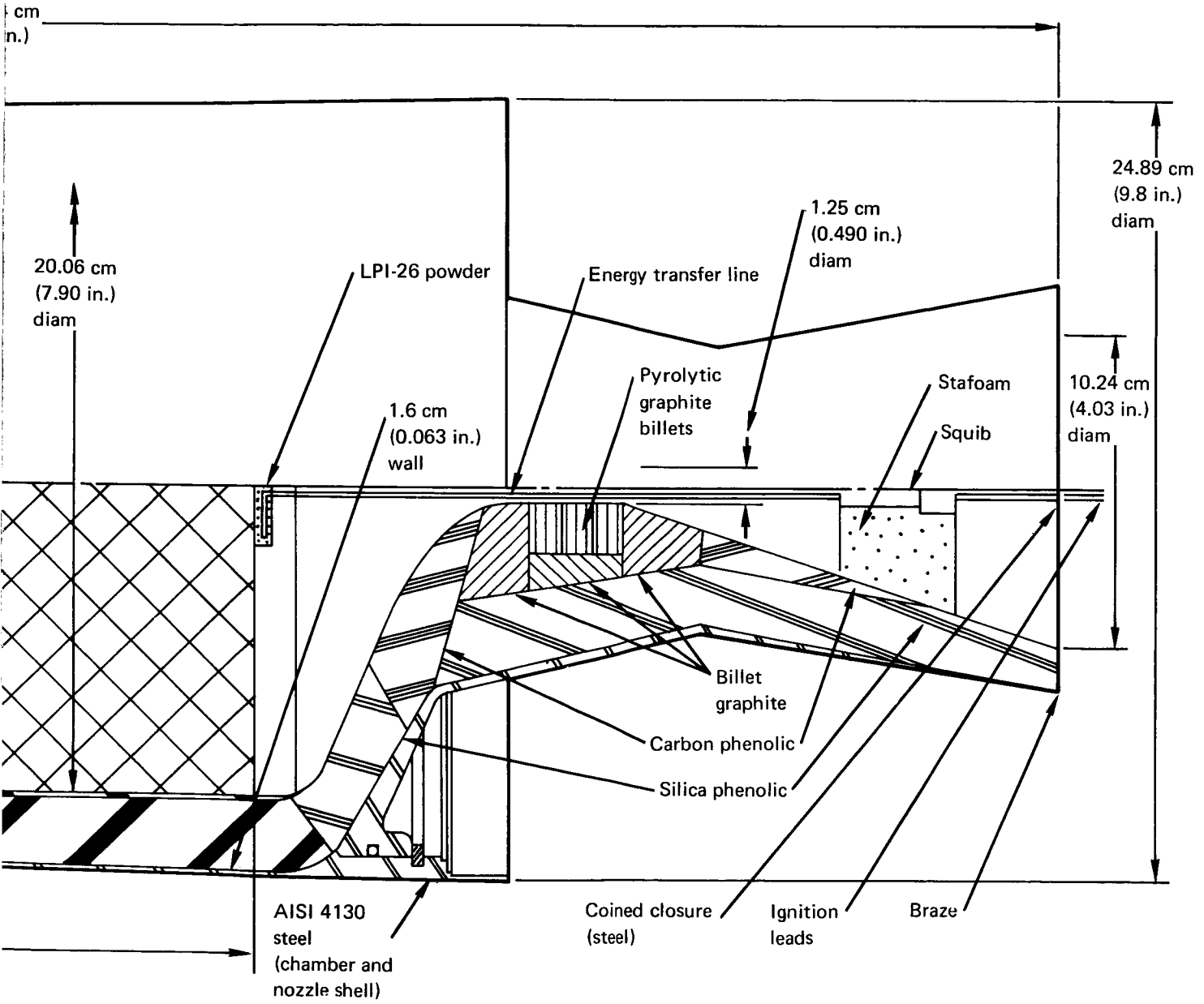
cm
n.)
24.89 cm
(9.8 in.)
diam
20.06 cm
(7.90 in.)
diam
LPI-26 powder
Energy transfer line
1.25 cm
(0.490 in.)
diam
Pyrolytic
graphite
billets
Stafoam
Squib
10.24 cm
(4.03 in.)
diam
1.6 cm
(0.063 in.)
wall
Billet
graphite
Carbon phenolic
Silica phenolic
AISI 4130
steel
(chamber and
nozzle shell)
Coined closure
(steel)
Ignition
leads
Braze

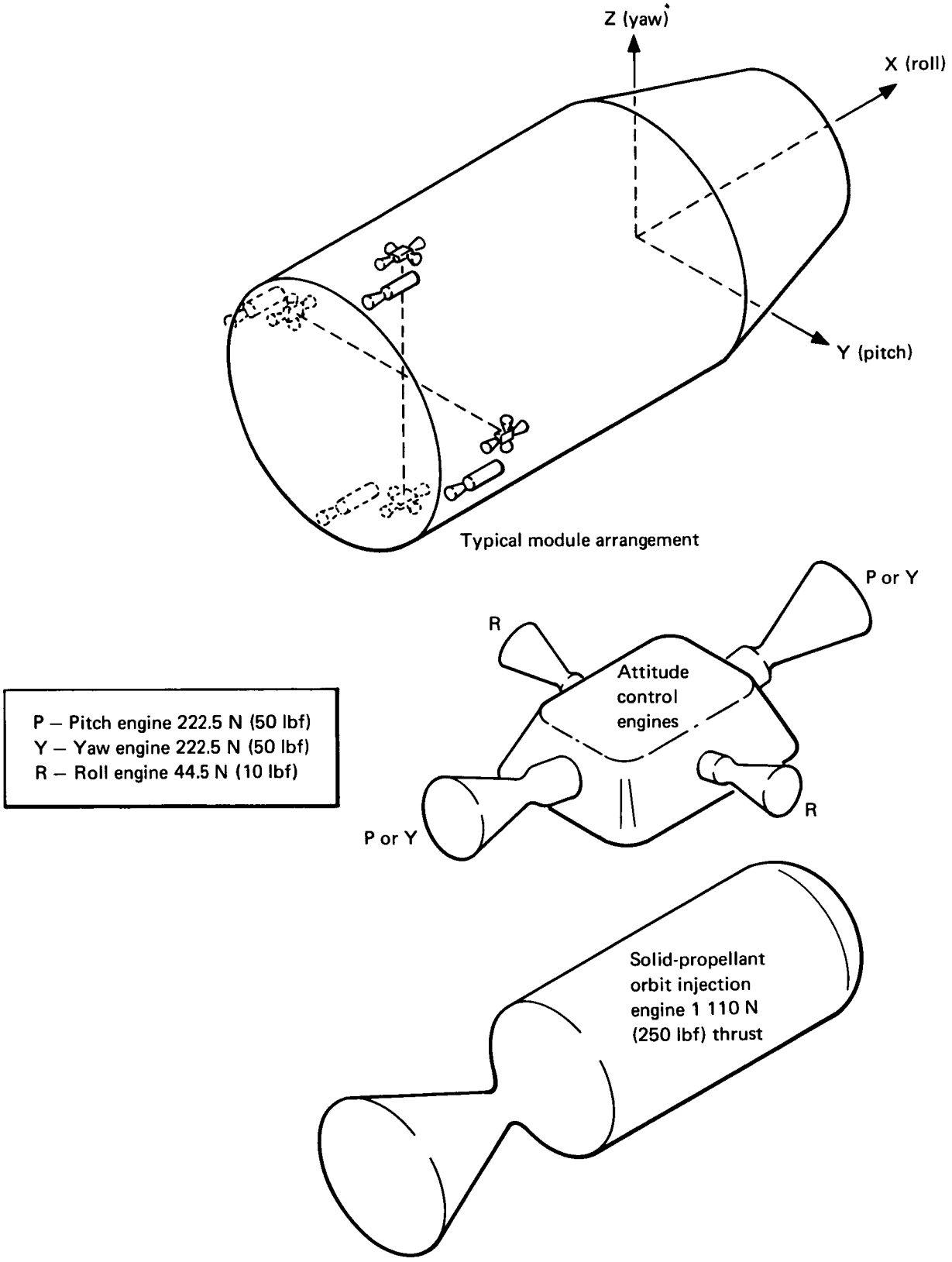

Figure 60. Solid-Propellant Orbit-Injection System

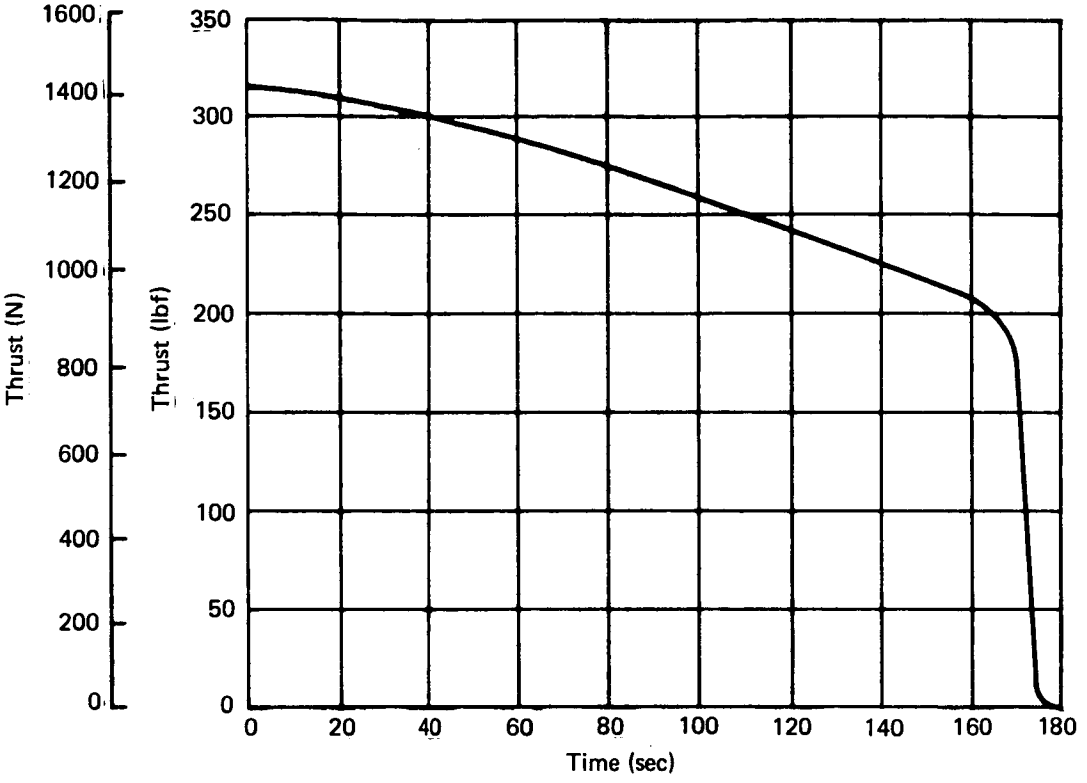

Figure 62. Solid-Propellant Orbit Injection Motor Thrust History

The solid-propellant motor weight summary is shown in table 24, along with applicable attitude-control-system engine weight.

Auxiliary propulsion system (S-IVB). – There are two APS modules designs for the S-IVB: one for the Saturn IB launch vehicle, the other for the Saturn V launch vehicle. The APS for the Saturn V was the one investigated because it has a thrustor for ullage control which is oriented in the direction of the desired orbit-injection impulse.

The Saturn V APS module is shown in fig. 63. Two of these are mounted on the S-IVB aft skirt. Four modules may be used without major modification to the stage. Each module contains one 320-N (72-lbf) and three 667-N (150-lbf) ablative bipropellant thrustors using the hypergolic propellants N_2O_4 and MMH. Each APS module contains a fuel tank, oxidizer tank, helium pressurization system, and a positive-expulsion propellant-feed system for zero-g operation. The loaded mixture ratio is 1.65, where 54 kg (119.4 lbm) of MMH and 87.4 kg (192.6 lbm) of N_2O_4 are loaded on each APS module.

The 667-N (150-lbf) thrustor (fig. 64) is capable of pulsing operation and operates at a chamber pressure of 689 000 N/m^2 (100 psia) and a mixture ratio of 1.67. The nozzle has an expansion ratio of 33.9:1. The injector consists of 12-on-12 doublets with fuel on the outside and oxidizer on the inside. The chamber temperature is 2110°K (3800°R) and the maximum

TABLE 23

SOLID-PROPELLANT ORBIT-INJECTION MOTOR CHARACTERISTICS

Item	Performance
Performance [294°K(530°R) and vacuum]	
Web time	166 sec
Average pressure during web time	5175 x 10^3 N/m^2 (750 psia)
Average thrust during web time	1112.5 N (250 lbf)
Impulse during web time	184 675 N-sec (41 500 lbf-sec)
Total impulse	188 012 N-sec (42 250 lbf-sec)
Average I_{sp} during web time	290 sec
Average thrust coefficient during web time	1.883
Discharge coefficient	0.96
Miscellaneous	
Overall length	142.24 cm (56.0 in.)
Case outer diameter	24.89 cm (9.8 in.)
Initial nozzle throat area	1.23 cm^2 (0.189 $in.^2$)
Initial nozzle throat diameter	1.25 cm (0.490 in.)
Nozzle exit diameter	0.48 cm (4.03 in.)
Initial nozzle expansion ratio	67.5
Average nozzle expansion ratio	50.0
Volumetric loading	82.5%
Grain web thickness	111.76 cm (44.0 in.)
Case material	AISI 4130
Case ultimate strength	1 242 000 N/m^2 (180 000 psia)
Case ultimate pressure	13 800 N/m^2 (2000 psia)
Case wall thickness	1.6 cm (0.063 in.)

TABLE 24

SOLID-PROPELLANT ORBIT-INJECTION SYSTEM WEIGHT SUMMARY

Item	Weight
Solid-propellant motor	
Case	13.5 kg (29.7 lbm)
Insulation	9.7 kg (21.3 lbm)
Nozzle	6.4 kg (14.0 lbm)
Total inerts	29.5 kg (65.0 lbm)
Propellant	66.7 kg (146.5 lbm)
Total loaded motor	96 kg (211.5 lbm)
(Mass ratio = 0.70)	
Total weight of four solid-rocket motors	383 kg (846.0 lbm)
Liquid-engine control system (LECS)	
Liquid engines (four required)	2.73 kg (6.0 lbm) total
Propellant	16.4 kg (36.0 lbm)
Tank and feed system (estimated)	2.27 kg (5.0 lbm)
Attributable total LECS weight	21.3 kg (47.0 lbm)
Total solid-propellant injection system weight	405 kg (893.0 lbm)

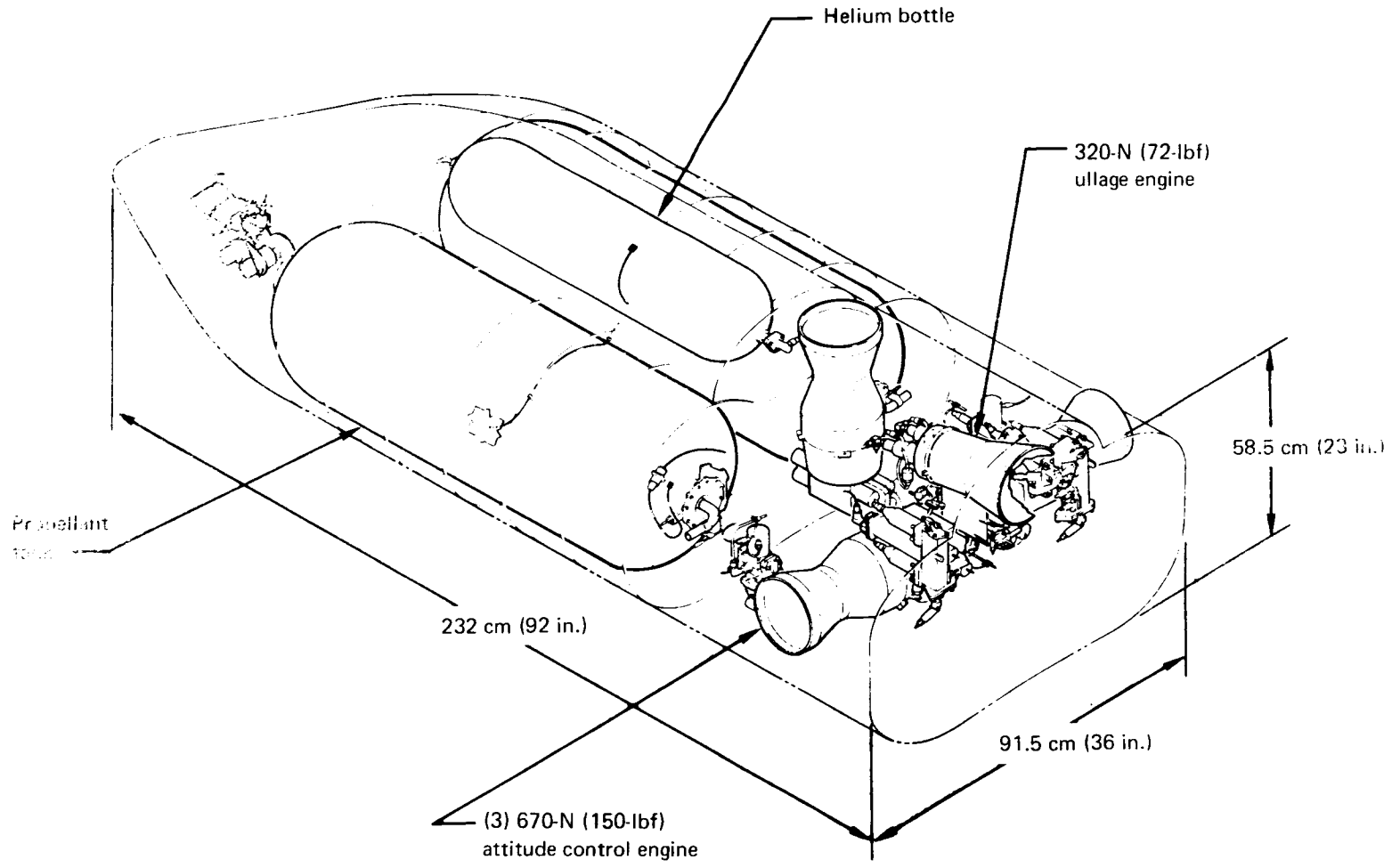

Figure 63. Saturn V Auxiliary Propulsion System (Cutaway)

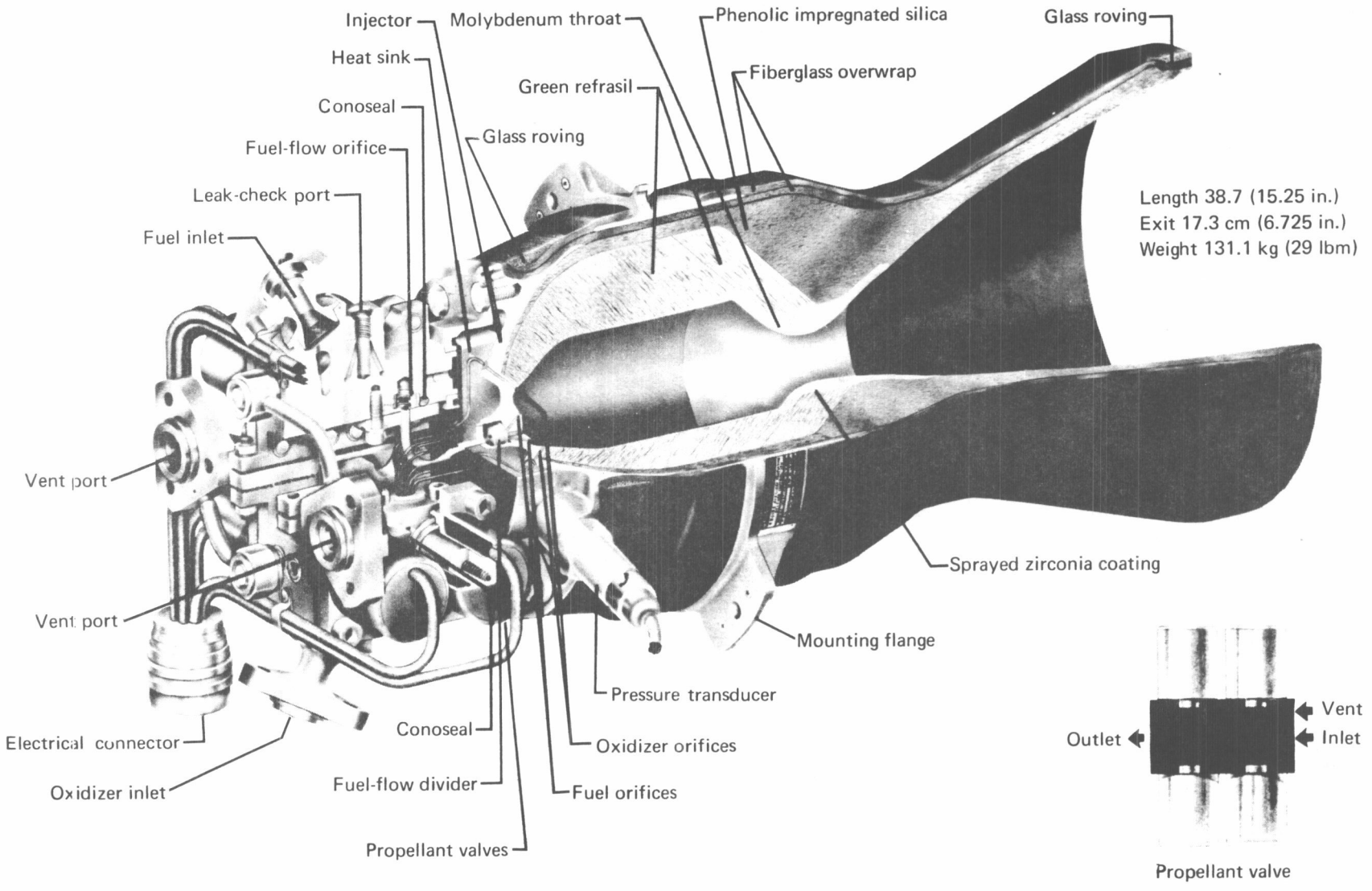

Figure 64. S-IVB 667-N (150-lbf) Attitude Control Engine

temperature of the refrasil is 445°K (800°R). The valve package consists of eight solenoid valves arranged in two quad-series-parallel banks, one for fuel and one for oxidizer. This series-parallel valve arrangement precludes an operational failure due to any single valve malfunction. The thrustor is designed for an operational life of 300 sec using an operational pulse-duty-cycle mode. However, testing has demonstrated a pulse-mode capability of over 20-min accumulated burn time. This thrustor has a minimum-impulse-bit capability of 33.4 N-sec (7.5 lbf-sec) with an electrical pulse width of approximately 65 msec. Operation at a pulse frequency of up to 10 pulse/sec (pps) is possible.

The 320-N (72-lbf) ullage thrustor (fig. 65) is an ablatively cooled modified Gemini thrustor. It operates at a chamber pressure of 689 000 N/m^2 (100 psia) and a mixture ratio of 1.27. This reduced mixture ratio is necessary so that temperature limits will not be exceeded. Because of the reduced mixture ratio, this thrustor has a minimum vacuum steady-state specific impulse of only 255 sec. Propellant flow is controlled by two fast-action solenoid valves mounted behind the injector. The injector is surrounded by a fuel-cooling ring with 16 orifices directed toward the combustor wall, while propellant mixing is accomplished by 16 pairs of fuel-on-oxidizer doublets. Impingement of the fuel and oxidizer takes place at a splash plate that is integral with the injector body. Chamber cooling is accomplished by the combination of a combustor-wall boundary layer of pure fuel and the ablative action of the silica-laminate portion of the wall itself. Because of limitations on the ablative material, this thrustor has an operational life limit of 600 sec. The nozzle has a 40:1 expansion ratio with the exit plane scarfed at 0.174 rad (10°).

The propellant tanks consist of a titanium cylindrical shell with hemispherical ends. Each tank has a capacity of approximately 0.067 cu m (4080 cu in.), being 99 cm (39 in.) long and 44.5 cm (17.5 in.) in diameter. The shell assemblies have a maximum operating pressure rating of 2×10^6 N/m^2 (290 psia) and a burst rating of approximately 5.5×10^6 N/m^2 (800 psia). A 0.15-mm (6-mil) Teflon bladder provides the system with positive expulsion capabilities. The tank has a propellant expulsion range of 0 to 0.017 cu m (0 to 0.6 cu ft) per min and an expulsion efficiency of 98%, with a 1.4×10^4 N/m^2 (2 psia) differential pressure across the bladder. The high-pressure helium tank stores 15 200 cc (925 cu in.) of helium at a maximum working pressure of 2.2×10^7 N/m (3200 psia). The tank is made of 6 Al-4V-Ti and is 79 cm (31 in.) long by 17.7 cm (7 in.) in diameter. Proof-test pressure is 3.3×10^7 N/m^2 (4800 psia). A helium pressure regulator is set to regulate propellant-tank pressure to $1.38 \times 10^6 \pm 2 \times 10^4$ N/m^2 (200 ±3 psia) plus the ambient reference pressure with a helium-bottle pressure range of 2.4×10^6 to 2.2×10^7 N/m^2 (350 to 3200 psia). The propellant-control module consists of two solenoid valves (one for fill and one for recirculation), a filter, and two check valves. Two propellant-control modules are used for each APS assembly, one for fuel and one for oxidizer. The 25-micron filter is located to prevent contaminants which may be entrained in the propellants from reaching the APS engine.

Analysis indicates that at least four APS units would be required to provide an orbit-injection capability. These units would be mounted at 1.57 rad (90°) intervals about the aft skirt of the S-IVB. Each of these

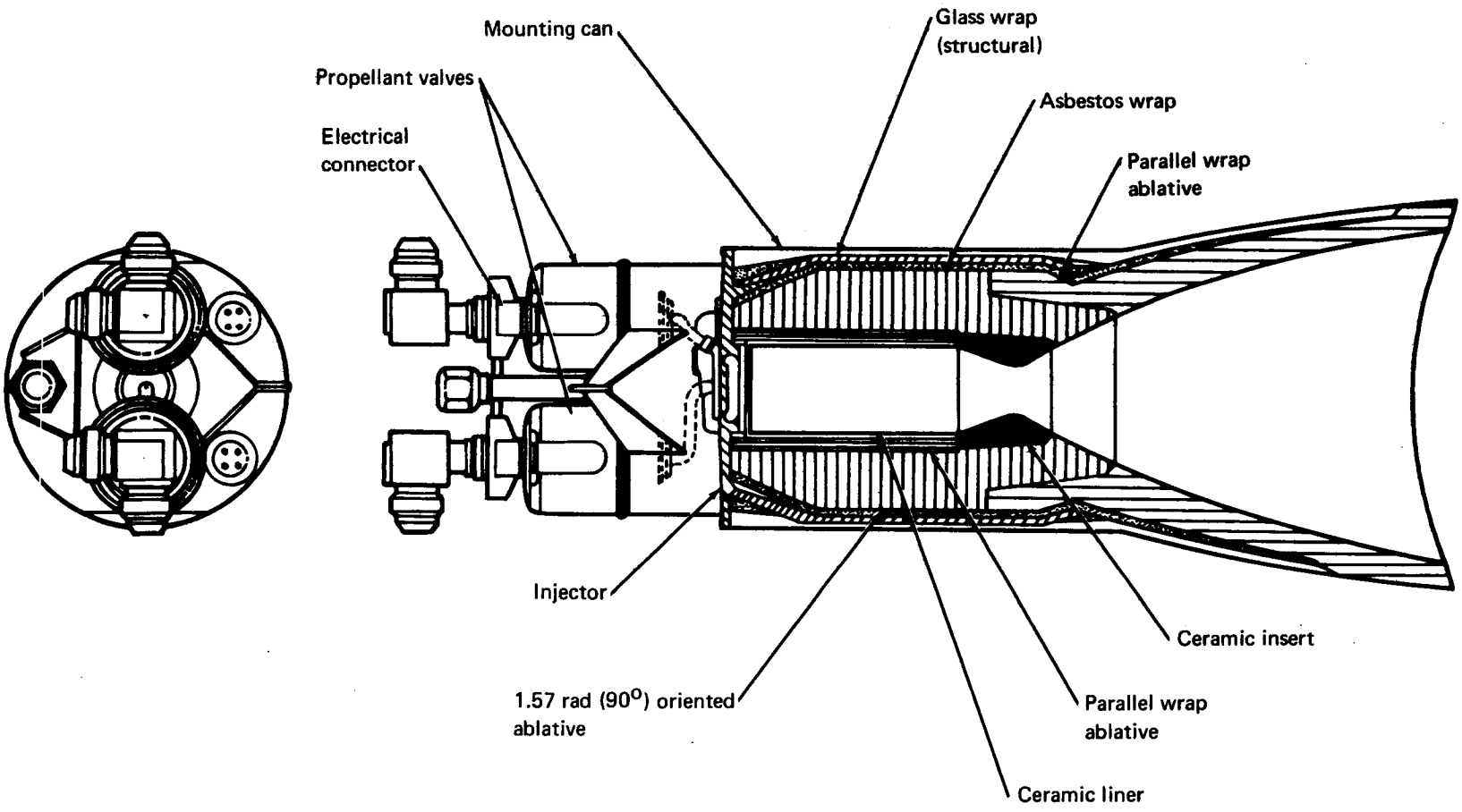

Figure 65. Saturn V 320-N (70-lbf) Ullage Engine

Saturn V APS units has a wet weight of 371 kg (818 lbm) and a dry weight of 229 kg (506 lbm) for a total propellant weight of 141 kg (312 lbm) per module. It is assumed that the attitude-control requirements can be met by 353 kg (122 lbm) of propellant as established by the Saturn IB requirements. This leaves a total of 537 kg (1187 lbm) of APS propellant for the orbit-injection impulse. Apogee circularization is considered for the APS orbit-injection concept. Utilizing this mode, the Saturn IB launch vehicle would place the MORL into an initial elliptical orbit with apogee at 364 km (164 nmi). After J-2 engine burnout, the S-IVB and MORL would coast to apogee. When apogee is reached, the APS ullage thrustors would fire to circularize the orbit at the 304-km (164-nmi) mission altitude. An initial 148 x 304-km (80 x 164-nmi) ellipse was analyzed, and it was determined that a total burn time of 1085 sec was required of the 320-N (72-lbf) ablative thrustors. As the operational life of these thrustors is 600 sec, it would not be possible to use an initial 148 x 304-km (80 x 164-nmi) ellipse. The initial perigee must be adjusted to be consistent with the 600-sec burn time limit, and the attendant payload loss must be accepted. For the 250 N-sec/kg (255 lb-sec/lbm) of steady-state specific impulse of the 320-N (72-lbf) ullage thrustors and the operational life limit of 600 sec, it is established that only 25.6 m/sec (84 fps) of velocity increment is available for apogee circularization of the S-IVB and MORL vehicle. Consequently, only 307 kg (678 lbm) of the available 540 kg (1187 lbm) of injection propellant could be utilized. Thus, 55.2 kg (122 lbm) of propellant would be utilized at a mixture ratio of 1.67 for attitude control, and 307 kg (678 lbm) of propellant at a mixture ratio of 1.27 would be utilized for the apogee circularization impulse. The initial orbit is established as a 220-km (119-nmi) perigee, with apogee at 304-km (164-nmi). The Saturn IB launch vehicle will launch a 16 400-kg (36 080-lbm) payload into this 220 x 304-km (119 x 164-nmi) ellipse. However, allowance must be made for the increased weight of the four Saturn V APS units. Two wet Saturn IB APS units weigh 438 kg (966 lbm), and four wet Saturn V APS units utilized for this injection concept weigh 1285 kg (2824 lbm). Consequently, this APS injection system must be charged a total of 844 kg (1858 lbm). On the basis of these results, a reference payload in orbit of 15 500 kg (34 222 lbm) is established.

Because of life limitations imposed on the 320-N (72-lbm) ullage thrustor with the resulting payload loss, it is desirable to consider an upgraded APS unit. Such a unit, utilizing Thiokol C-1 thrustors for the aft-facing ullage thrustors, is currently being considered for advanced Saturn V missions requiring more than one restart of the J-2 engine. These thrustors would be required to provide 91-sec burn for propellant slosh control during each J-2 shutdown and 330-sec ullage settling prior to each J-2 start (except the first J-2 firing following staging from the S-IB, where the solids on the aft skirt of the S-IVB provide the initial ullage settling). This concept would be used for missions requiring more than one restart of the J-2 engine, such as a synchronous-orbit mission. The Thiokol C-1 radiamic concept was discussed in detail earlier. The thrustor scheduled to replace the APS ullage thrustor is a 445-N (100-lbf) radiative regeneratively cooled thrustor that burns the on-board propellants N_2O_4 and MMH at a mixture ratio of 1.6. Because of this more favorable mixture ratio, a steady-state specific impulse of 297 sec is realized.

An initial 148 x 304-km (80 x 164-nmi) elliptical orbit would establish a payload of 16 900 kg (37 370 lbm) and a dry S-IVB weight of 13 900 kg (30 727 lbm). Using four APS units for a total thrust of 1780 N (400 lbf), a thrust-to-weight ratio of 5.88×10^{-3} results. Mission analysis gives a total velocity increment of 46.4 m/sec (152 fps) for the apogee circularization at the 304-km (164-nmi) mission altitude. A propellant weight of 489 kg (1080 lbm) is required to meet the apogee circularization requirements. A total burn time of 805 sec is required for this apogee circularization, which is well within the C-1 thrustor life. Allowing for a total of 55.2 kg (122 lbm) of attitude control propellant, a chargeable APS weight of 1000 kg (2205 lbm) is established. Consequently, the C-1 concept would provide a reference payload of 15 960 kg (35 224 lbm) to mission orbit.

Helium heater. – The O_2/H_2 burner (helium heater) is the primary repressurization system for the S-IVB J-2S engine (fig. 66). The helium heater system consists of an O_2/H_2 burner which heats helium stored in nine titanium helium spheres located in the H_2 tank. The helium heater begins to burn when the continuous vent valves are closed and operates for about 4.5 min, during which time it heats the helium stored in the H_2 tank which is then expanded for tank repressurization. The operating characteristics of the O_2/H_2 burner (helium heater) during this burn are shown in fig. 67. A nominal chamber pressure of 4.15×10^2 N/m^2 (6 psia) and a nominal thrust level of 72 N (16 lbf) is established. The overall performance of the O_2/H_2 burner is about 300 sec of specific impulse. The system is currently limited to a single start due to burnout of the ignition system; however, a new swing-out igniter is being developed. Although current life is limited to about 5 to 6 min of operation, a development program is in progress to extend the operational life of the O_2/H_2 burner to 4.5 hours.

Orbital injection must be performed using a spiral trajectory because of the low thrust level of the helium heater and the weight of the combined S-IVB and MORL vehicle. An analysis for an initial 148-km (80-nmi) circular orbit revealed that the helium heater would have to burn for approximately 12 hours, which is well beyond the projected life of 4.5 hours. Consequently, an orbit mechanic analysis was performed. The results of this analysis are shown in fig. 68. Thrust levels of both 72 N and 108 N (16 and 24 lbf) are shown. The 72-N thrust level corresponds to operation of the helium heater only, whereas the 108-N thrust level corresponds to operation of both the helium heater and the positive-propulsive venting of the H_2 tank. The positive-propulsive-venting mode was not considered in detail because of the small amount of residual propellant in the H_2 tank at S-IVB burnout for the MORL launch trajectory. The 4.5-hour operating life of the helium heater establishes a minimum initial circular-orbit altitude of 241 km (130 nmi). This initial altitude then establishes a reference payload for the MORL of 16 080 kg (35 360 lbm). The propellant required for this spiral transfer is about 391 kg (860 lbm) based on the 4.5-hour burn time and I_{sp} of 300 sec. This is well below the residual propellant at S-IVB burnout of 965 kg (2123 lbm). Consequently, preliminary analysis indicates that it is feasible to inject the S-IVB and MORL by the helium heater if the operational life of the helium heater is extended to 4.5 hours. However, this could only be accomplished at the expense of large payload weight loss due to the high initial altitude (241 km) of this scheme and the consequent direct-injection losses associated with launches into circular orbits of high altitudes.

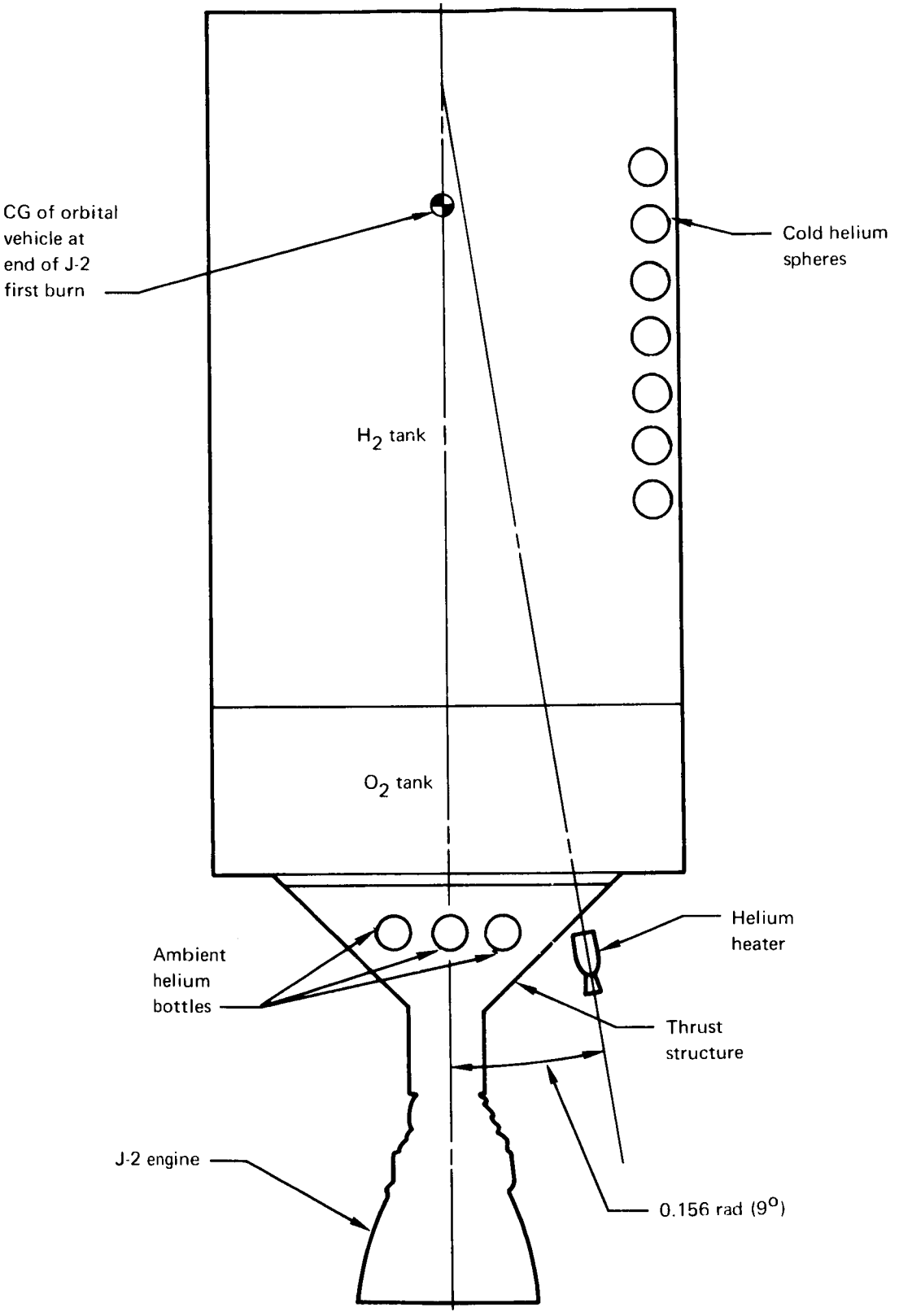

Figure 66. Helium Heater on S-IVB

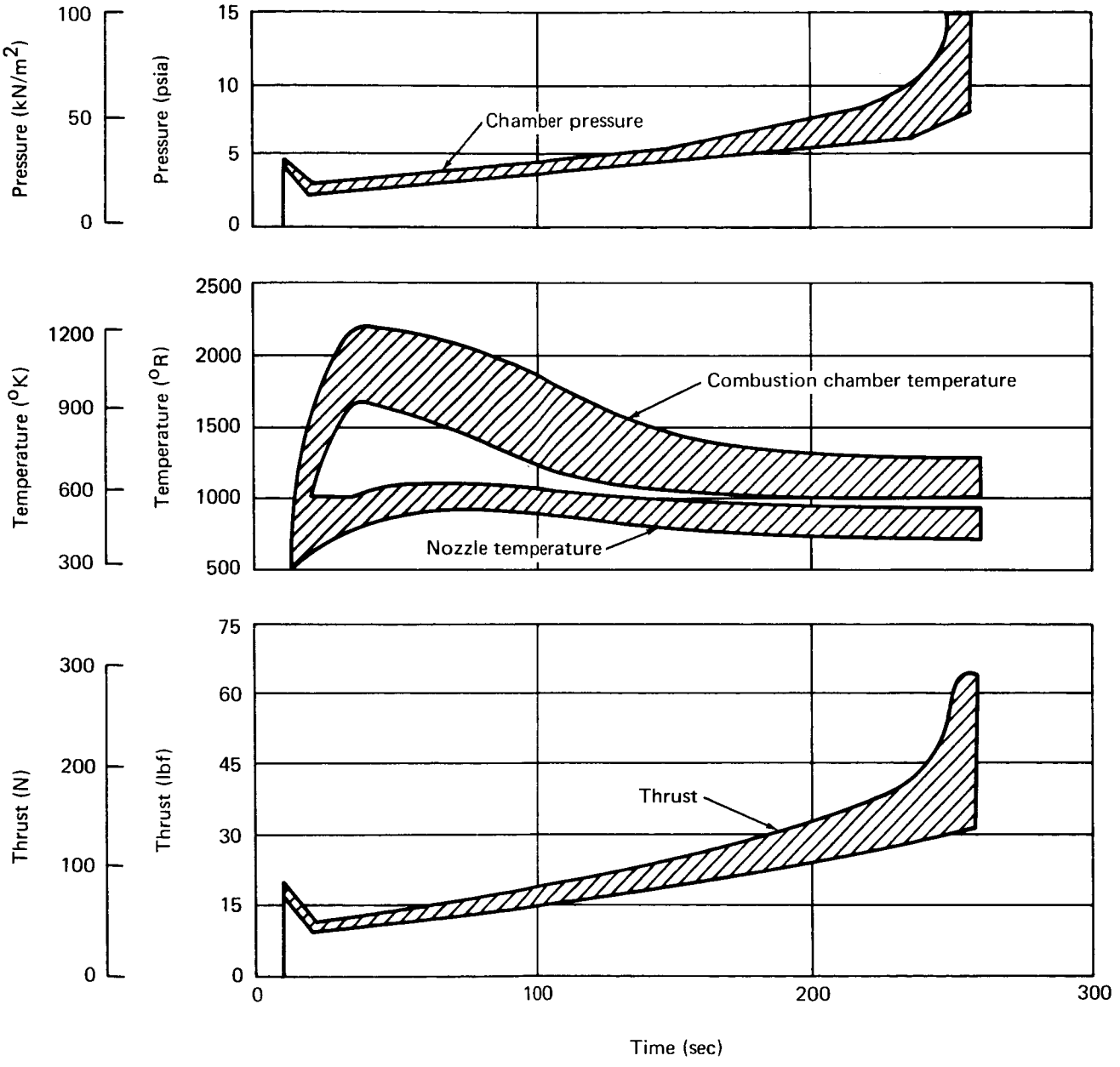

Figure 67. Helium Heater Operating Characteristics

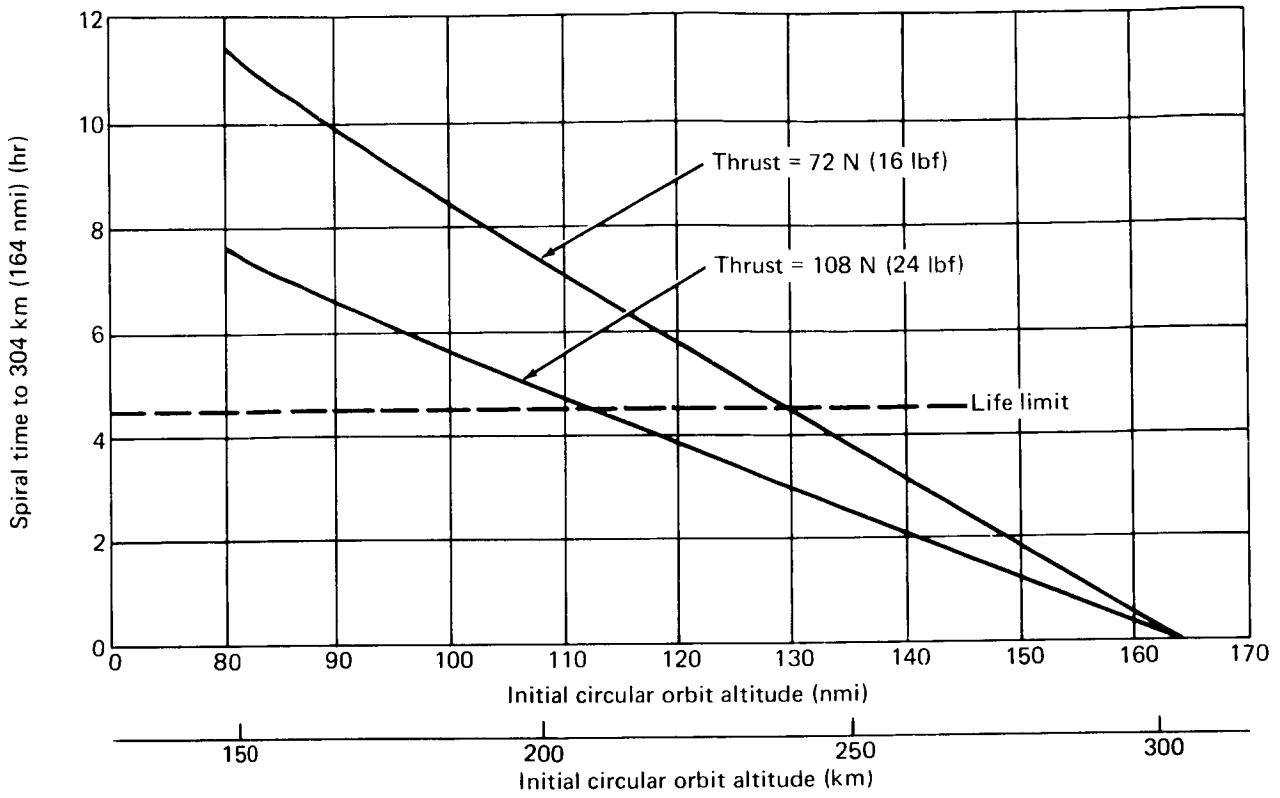

Figure 68. Helium Heater – Time Required to Reach 304-kM (164-nmi) Orbit

J-2S engine system. – The J-2S engine is a specific engine configuration evolved from Rocketdyne's experimental J-2 development program. Prime exphasis is on simplifying the engine. The following significant features distinguish the J-2S engine from the conventional J-2. (See fig. 8.)

(1) Idle-mode operation--The engine can operate on tank head pressure only, without the use of turbopumps, and it can use gas, liquid, or mixed-phase combinations of both oxidizer and fuel. Applications for the idle-mode concept are propellant system chilldown, propellant slosh control, propellant settling, and minor stage velocity increments.

(2) Solid-propellant gas generator (SPGG)--The SPGG replaces the pressurized H_2 spin bottle required to initiate turbopump operation for engine start. Up to three SPGG's may be installed on the engine, enabling up to three starts. Time limitations between engine starts and spin-bottle conditioning prior to launch are eliminated.

(3) Thrust-chamber fuel-jacket bypass--By means of diverting part of the fuel flow directly to the injector during engine start, the thrust-chamber chilldown process has been eliminated without the danger of turbopump stall caused by high-thrust-chamber jacket back pressure.

(4) Thrust chamber tapoff turbine drive--A hot gas tapoff of combustion products from the thrust chamber has eliminated the gas generator as a source of turbopump power. Associated valves, lines, and miscellaneous hardware have been eliminated.

(5) LO_2 depletion cutoff--The J-2S can run to LO_2 depletion, thereby eliminating the requirement for stage LO_2 depletion circuitry. The LO_2 tank-propellant reserve level can be lowered because approximately 114 kg (250 lbm) of previously unusable LO_2 below the low-level sensor is now available.

(6) New contour thrust chamber--Through redesign of the engine thrust-chamber nozzle the J-2S will be capable of sea-level full-thrust operation with no flow separation.

Of these features, the idle mode is the one which permits the J-2S to perform orbit injection. Although all of these features are not essential for the MORL mission, a single desired feature, such as idle-mode operation, could not be considered to reduce total development expenditures.

On the standard J-2, all of the LH_2 discharged from the pump flows through the thrust-chamber regenerative cooling jacket. On the J-2S, however, 85% of the LH_2 coming out of the pump can bypass the cooling jacket and be fed directly into the thrust chamber where it is burned with LO_2. Bypassing the cooling circuit reduces the pressure drop between tank and injector, allowing operation on tank head pressure. In the idle mode, the pumps windmill and the propellants enter the thrust chamber rather than returning to their tanks as in the standard chilldown mode. In the thrust chamber, they are burned to produce a low-idle thrust of about 26 700 N (6000 lbf). This thrust is sufficient for main-propellant-tank ullage control, attitude control in pitch and yaw, and minor maneuvers of the S-IVB. Operation in the idle mode for 40 to 50 sec conditions the system for subsequent mainstage operation and thus eliminates the thrust chamber chilldown and stage recirculation requirements.

Propellant flow in the idle mode is accomplished by tank feed pressure. H_2 tank pressure is at its vent setting of 2.3×10^5 N/m^2 (34 psia) and the oxidizer tank pressure is increased from its repressurization value of 2.6×10^5 N/m^2 (38 psia) to about 2.8×10^5 N/m^2 (41 psia). During idle-mode operation, the O_2 tank pressure may drop as low as 1.38×10^5 N/m^2 (20 psia).

Mixture ratio control is accomplished by utilizing the O_2 bypass valve to reduce the flow of O_2 to the injector. This is the same valve utilized for the propellant utilization system and would return some of the O_2 to the inlet of the O_2 pump and thus reduce the engine mixture ratio.

The Saturn IB launch vehicle will launch the MORL into an 148 x 304-km (80 x 164-nmi) elliptical orbit at 0.87 rad (50°) inclination. The combined S-IVB/MORL will coast from the 148-km (80-nmi) perigee to the 304-km (164-nmi) apogee. During the coasting period, the attitude control requirements are provided by the APS thrustors of the S-IVB. When the 304-km (164-nmi) apogee is reached, the J-2S will fire in its idle mode to provide the apogee-circularization impulse requirements. During the injection period when the J-2S is operating in its 26 700-N (6000-lbf) thrust idle mode, the APS thrustors provide roll control and the pitch and yaw functions are met by gimballing the J-2S engine.

A velocity increment of 44.5 m/sec (146 fps) must be provided by the J-2S in idle mode in order to circularize the orbit at the 304-km (164-nmi) apogee. This impulse must be applied to the 30 900-kg (68 100-lbm) combined weight of the S-IVB and MORL. Utilizing the defined performance of the J-2S in idle-mode operation, it is found that a total propellant weight of about 290 kg (1300 lbm) is required to perform this maneuver. This is well below the 1000 kg (2123 lbm) of residual propellants available on the S-IVB. Both the S-IVB and the MORL would be injected into the mission orbit.

An increased payload capability results from three effects: (1) utilization of on-board propulsion systems, (2) utilization of residual propellants on board the S-IVB, and (3) deletion of S-IVB hardware. These three effects combine to provide a reference payload capability of 17 400 kg (38 460 lbm) for the J-2S concept.

Candidate system evaluation and comparison. – Preliminary evaluation of the candidate high-thrust concepts on board MORL indicates that all three concepts could fulfill the MORL requirements for both orbit injection and the mission scheduled disturbances. Table 25 summarizes the characteristics of each of the candidate thrustor systems. A performance summary of the systems is shown in table 26. Performance for the mission high-thrust requirements is somewhat degraded for the monopropellant concept due to the loss in performance at the lower duty cycles. Propellant weight requirements are directly related to the established mission performance. Comparable weight capabilities in orbit are exhibited by each of the candidate concepts.

A comparison of the operational characteristics of the candidates is shown in table 27. Due to low operating temperatures, both the monopropellant and cryogenic biporpellant thrustors are constructed from common materials, whereas the high-temperature storable bipropellant thrustors must be constructed from more expensive refractory metals. The cryogenic bipropellant system will utilize the offloaded resistojet hydrogen tank at MORL launch, but requires a complicated system for propellant preconditioning. Both the storable bipropellant and monopropellant systems require pressurization and positive expulsion systems. These systems are not required for the cryogenic bipropellant system because it utilizes vapor feed.

TABLE 25

CANDIDATE THRUSTOR SYSTEM CHARACTERISTICS

Description	Storable bipropellant		Monopropellant		Cryogenic propellant	
Propellant	N_2O_4/MMH		N_2H_4		O_2/H_2	
Mixture ratio	1.6:1		--		1.0:1	
Chamber pressure	689 kN/m^2 (100 psia)		689 kN/m^2 (100 psia)		345 kN/m^2 (50 psia)	
Area ratio	40:1		50:1		40:1	
Tank conditions						
Pressure	1720 kN/m^2 (250 psia)		1720 kN/m^2 (250 psia)		551 kN/m^2 (80 psia)	
Temperature	325°K (588°R)		325°K (585°R)		28°K (H_2), (50°R) 111°K (O_2) (200°R)	
	Pitch and yaw	Roll	Pitch and yaw	Roll	Pitch and yaw	Roll
Thrust level	222.5 N (50 lbf)	44.5 N (10 lbf)	222.5 N	44.5N	222.5 N	44.5 N
Minimum impulse bit	2.22 N-sec (0.50 lbf-sec)	0.445 N-sec (0.10 lbf-sec)	0.80 N-sec (0.18 lbf-sec)	0.44 N-sec (0.10 lbf-sec)	17.8 N-sec (4.0 lbf-sec)	4.45 N-sec (1.0 lbf-sec)
I_{sp} (steady state)	295 sec	290 sec	235 sec	235 sec	318 sec	318 sec
Dry weight (per thrustor)	1.14 kg 2.5 lbm)	0.68 kg (1.5 lbm)	1.11 kg (2.45 lbm)	0.41 kg (0.90 lbm)	2.95 kg (6.5 lbm)	2.04 kg (4.5 lbm)

TABLE 26

CANDIDATE SYSTEMS PERFORMANCE AND WEIGHT SUMMARY

Description	Storable bipropellant	Monopropellant	Cryogenic bipropellant
I_{sp} (sec)			
Orbit injection	295.0	235.0	318.0
Mission high thrust	280.0	215.0	302.0
Propellant weight, kg (lbm)			
Orbit injection	272.0 (600)	342.0 (754)	2 531.0 (557)
90 days	47.6 (105)	61.7 (136)	44.0 (97)
147 days	77.5 (171)	101.0 (223)	72.2 (159)
Dry weight, kg (lbm)			
Thrustor modules	11.8 (26)	10.9 (24)	33.51 (74)
Tank and feed system	25.0 (55)	33.5 (74)	83.0[a] (183)
Chargeable P/RCS weight, kg (lbm)			
Dry[c]	36.6 (81)	44.4 (98)	72.2[b] (159)
Wet[d]	327.0 (721)	411.0 (907)	325.0 (721)
Reference payload (Weight capability to orbit minus chargeable wet weight)	16 600 (36 649)	16 520 (36 463)	16 600 (36 649)

[a]Includes MORL resized H_2 tank.
[b]Includes delta of resized H_2 tank compared to baseline H_2 tank.
[c]Does not include bosses, flanges, and fittings or line and valve plumbing weights.
[d]Includes pressurization gas and propellant for first 20 days of high thrust operation.

TABLE 27

CANDIDATE SYSTEM OPERATIONAL CHARACTERISTICS

	Storable bipropellant	Monopropellant	Cryogenic bipropellant
Propellant(s)	2 storable	1 storable	2 cryogenic
Ignition scheme	Hypergolic	Catalyst bed	Pilot catalyst bed
Thrustor materials	Refractory metals	Stainless steel	Nickel
Tankage	4 tanks (2 oxidizer, 2 fuel)	5 tanks	3 tanks (2 oxidizer, 1 H_2)
Propellant conditioning unit	---	---	Gas generator-heat exchanger system
Pressurization system	N_2 at 20 700 kN/m^2 (3000 psia)	N_2 at 20 700 kN/m^2 (3000 psia)	None required
Positive expulsion system	Metal bellows	Metal bellows	Not required (vapor fed)

The APS aboard the S-IVB can provide orbit injection. However, this system is both performance and life limited. Consequently, its reference payload capability is significantly reduced. An advanced APS unit utilizing the C-1 thrustor will provide longer life and better performance than the old APS unit as well as a 453-kg (1000-lbm) increase in payload capability. In both cases, four APS units must be mounted on the S-IVB, resulting in a chargeable weight and thus a decrease in reference payload.

The helium heater must utilize a spiral trajectory concept to provide orbit injection capabilities. Only an advanced version of the helium heater with extended life capabilities may be considered. Although mission losses do not preclude use of the helium heater spiral trajectory, a significant reduction in payload results from the high initial altitude required to maintain the 4.5-hour life limit.

The J-2S system could provide apogee circularization in the idle mode. Although its performance is reduced in idle-mode operation, the available residuals could be utilized at no expense to the system. The S-IVB weight may be reduced about 453 kg (1000 lbm) by utilizing a J-2S engine, which will allow an equal increase in payload capability. Although the J-2S would require high expenditures for its development, it does provide the highest reference payload capability of the considered orbit injection concepts.

A summary of the four candidate S-IVB orbit injection schemes is shown in table 28. Each of these concepts would carry the S-IVB into mission orbit by total or partial utilization of on-board S-IVB systems. The standard APS shows the lowest payload capability whereas the reference payload of the advanced APS and the helium heater shows comparable payload capabilities. The J-2S concept provides the maximum reference payload in orbit.

The H_2 high-thrust resistojet system is optimized by a tradeoff in Saturn IB direct-injection capabilities and propellant requirements for spiral transfer. The optimum H_2 system is established as four 1.11-N (0.25-lbf) thrustors providing a spiral transfer from a 168-km (91-nmi) circular orbit to the 304-km (164-nmi) circular mission orbit. Additional cryogenic tankage is required aboard the MORL to meet these requirements. The hydrogen concept provides a bout 1780-N (400-lbf) increased capability compared to the NH_3 concept and requires 2.7 less days of injection time.

The NH_3 high-thrust resistojet system is optimized near the maximum resistojet operating temperature limit. The optimum NH_3 system consists of four 0.67-N (0.15-lbf) aft-facing injection thrustors, providing a spiral transfer from a 180-km (97.5-nmi) circular orbit to the 304-km (164-nmi) circular mission orbit. An additional NH_3 tank is required aboard the MORL, but the NH_3 is stored at ambient temperatures. This precludes any requirements for complicated cryogenic storage. During emergency operation, the NH_3 thrustors suffer severe performance losses due to the NH_3 dissociation at the low chamber temperatures associated with the reduced emergency electrical power availability.

TABLE 28

S-IVB ORBIT-INJECTION-SYSTEMS

Description	APS	Advanced APS	Helium heater	J-2S
Thrust level, N (lbf)	4 at 320 (72) = 1360 (288)	4 at 445 (100) = 1780 (400)	71 (16)	26 700 (6000)
I_{sp}, sec	255	297	300	244
Impulse, N-sec (lb-sec)	768 000 (176 800)	1 430 000 (322 000)	1 155 000 (259 200)	1 400 000 (314 000)
ΔV, m/sec (fps)	25.6 (84)	46.4 (152)	37.2 (122)	44.5 (146)
Injection time	600 sec	805 sec	4.5 hours	69 sec
Propellant weight, kg (lbm)	307 (678)	490 (1080)	390 (860)	587 (1295)
Chargeable weight, kg (lbm)	844 (1858)	965 (2146)	0	-495 (-1091)
Reference payload, kg (lbm)	15 520 (34 222)	15 950 (35 224)	16 100 (35 360)	17 430 (38 461)

Attitude Control and Orbit Keeping

The attitude-control and orbit-keeping system is required to orient and stabilize the laboratory and to provide orbit keeping during both the operational and experiment activities of the mission. The performance requirements of the stabilization and control system associated with the operational events and the experimental program are listed in table 29. Fig. 69 shows a simplified picture of the configuration used in deriving the gravity-gradient torques and aerodynamic drag for the purpose of establishing the impulse requirements of the resistojet system. This configuration consists of the basic MORL with two Apollo command modules and a cargo module stowed on the conical forward section of the laboratory. The centerlines of the stowed vehicles are canted 0.296 rad (17^{o}) from a normal to the MORL centerline.

This section concerns the analytical work performed to evaluate the candidate CMG/resistojet control systems in conjunction with candidate operational control (high-thrust) systems. NH_3, H_2, and CO_2 biowaste resistojet thrustor systems were integrated and evaluated with the candidate higher thrust systems. The analytical data are presented in parametric form.

CMG/resistojet control systems. – Thrust levels and thrust schedules were derived for the resistojet systems to provide the impulse requirements

TABLE 29

STABILIZATION AND CONTROL PERFORMANCE REQUIREMENTS

Mission event or function	Orientation	Attitude accuracy (steady-state) rad (°)		Rate stabilization (steady-state) rad/sec	(°/sec)
Orbit injection	Belly-down	±0.0085	(±0.5)	0.00051	(0.03)
Orbit keeping	Belly-down	±0.0085	(±0.5)	0.00051	(0.03)
Long-term manned zero-g	Belly-down	±0.0085	(±0.5)	0.00051	(0.03)
Rendezvous and docking (manned)	Belly-down	±0.0085	(±0.5)	0.00051	(0.03)
Experiments					
Routine Earth experiments	Belly-down	±0.0085	(±0.5)	0.00017	(0.01)
Precession Earth experiments	Belly-down	±0.0017	(±0.1)	0.00017	(0.01)
Inertial or celestial oriented	Inertial (arbitrary)	±0.0017	(±0.1)	0.00017	(0.01)

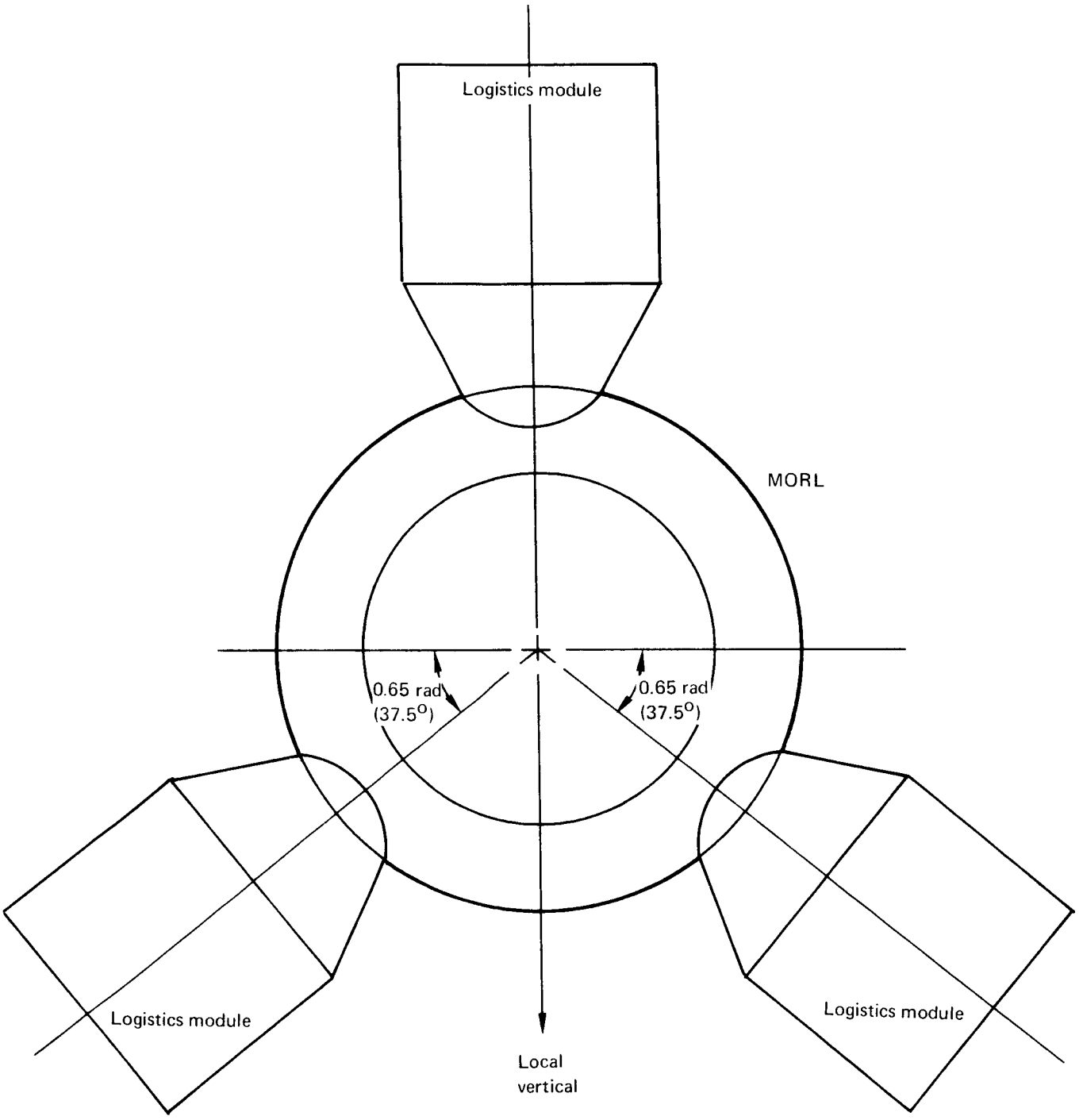

Figure 69. Disturbance Torque Model

shown in table 30. The thrustor locations which most nearly satisfy all the ground rules are shown in fig. 12 and were used in the derivation of all thrust schedules.

Impulse requirements and thrust schedules: Fig. 70 shows the thrust schedule for a worst-case inertial orientation. CMG desaturation is accomplished as indicated by the three pictorial diagrams. Orbit keeping, being deferred to the belly-down orientation, is not required.

The effect of thrust schedule on CMG size is best determined by a study of the angular impulse histories shown in fig. 71 which occur during a worst-case inertial orientation. The CMG storage requirement about pitch is the maximum difference between disturbance impulse and desaturation impulse--approximately 258 N-m-sec (190 ft-lbf-sec). The requirement about yaw is 177 N-m-sec (130 ft-lbf-sec), the maximum value of the cyclical disturbance. Roll requirements are established primarily by 1-g centrifuge operation and are therefore not shown. Another inertial orientation in which the pitch and yaw axes are interchanged must be considered to finalize a CMG size based only on environmental disturbance control. In this orientation, the pitch-disturbance impulse is cyclical, with a peak value of

TABLE 30

RESISTOJET P/RCS IMPULSE REQUIREMENTS

Orientation	Control function	Impulse per orbit	
		N-sec	(lb-sec)
Inertial	Orbit keeping[a]	640	(144)
	Pitch desaturation	721	(162)
	Yaw desaturation	71	(16)
	Roll desaturation	71	(16)
Belly-down	Deferred orbit keeping[b]	165	(37
	Normal orbit keeping	244	(55)
	Pitch desaturation	338	(76)
	Yaw desaturation	36	(8)
	Roll desaturation	36	(8)

[a]Deferred to belly-down orientation.

[b]Deferred orbit keeping evenly distributed over orbits spend in belly-down orientation.

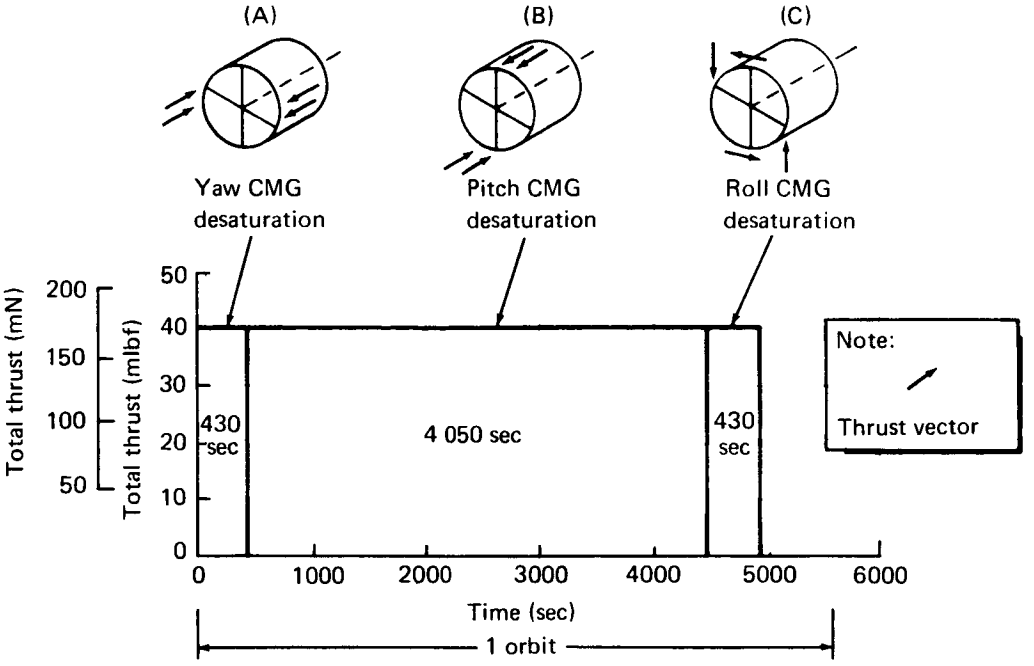

Figure 70. Inertial Orientation – Thrust Schedule

313 N-m-sec (230 ft-lbf-sec); the yaw disturbance impulse contains a linearaly increasing term, 1360 N-m-sec (1000 ft-lbf-sec) over 1 orbit and a cyclical term. CMG storage requirements are pitch--313 N-m-sec (230 ft-lbf-sec) and yaw, 122 N-m-sec (90 ft-lb-sec). A comparison of the CMG storage requirements of the two orientations shows that constant to near-constant desaturation thrust provides minimum CMG weight. That is, the CMG's are sized to just store the largest cyclical disturbance (which is the minimum acceptable size). Any variation in a near-constant thrust schedule for the inertial orientation can only result in increased CMG storage requirement.

Fig. 72 shows the thrust schedule and manner of thrust application for the belly-down orientation. That the CMG's as sized by inertial orientation requirements will fulfill belly-down requirements is established by a study of disturbance impulse histories during belly-down operation. A cross-product of inertia produces a constant gravity-gradient disturbance torque about the pitch axis. The angular impulse which results from the disturbance impulse and desaturation impulse of 190 N-m-sec (140 ft-lbf-sec) establishes pitch storage requirements for the CMG's. The maximum yaw-storage requirement is 109 N-m-sec (80 ft-lbf-sec) regardless of the thrust schedule. Both of the above requirements are less than inertial orientation requirements and therefore do not affect the CMG size.

Effect of launch date on mission requirements: The baseline initial launch date of 1972 and a 5-year mission places the entire mission within a period of near-minimum atmospheric density. An orbit-altitude optimization performed during the MORL Phase IIB study, based on maximizing logistics

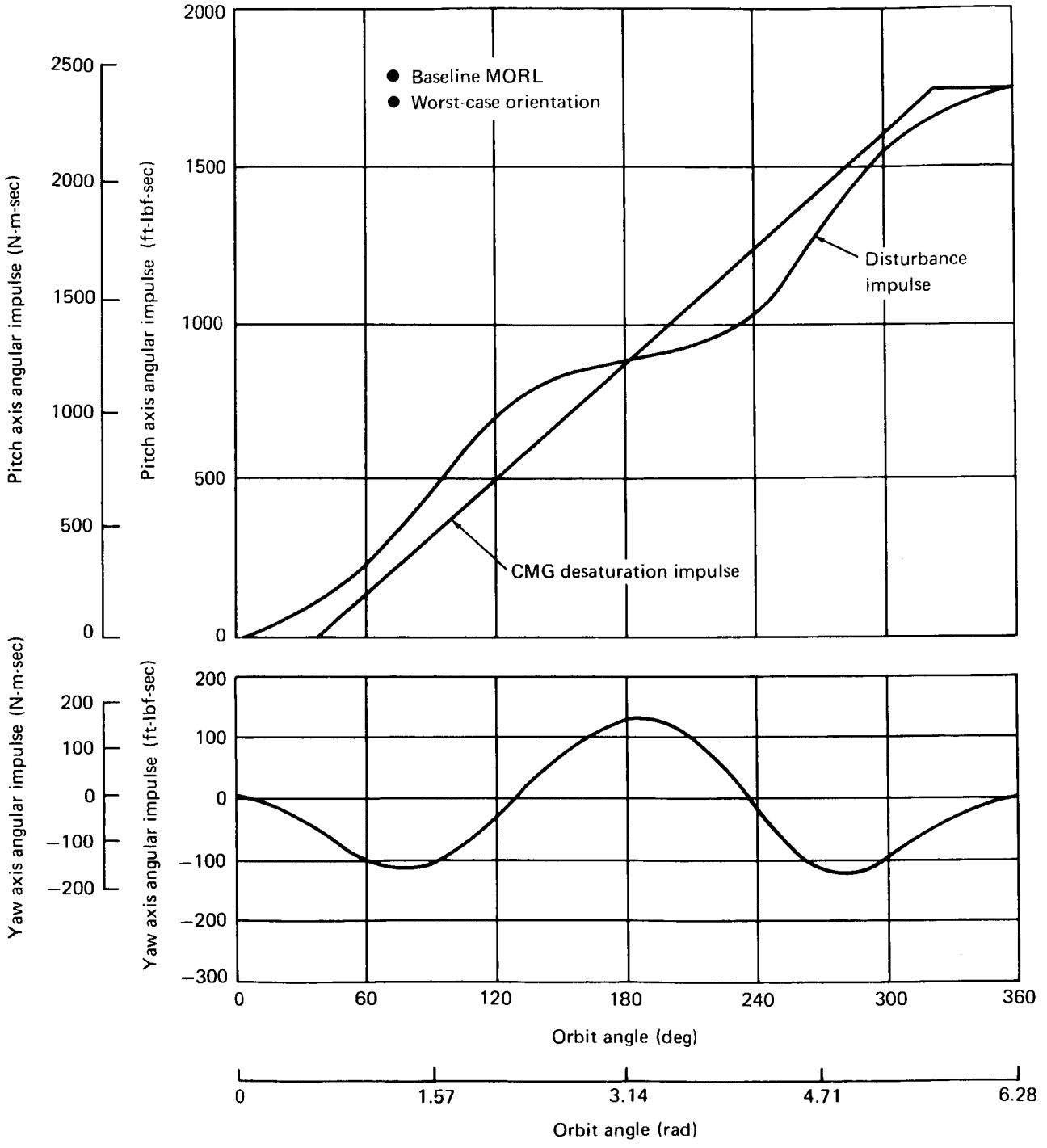

Figure 71. Angular Impulse Histories – Inertial Orientation

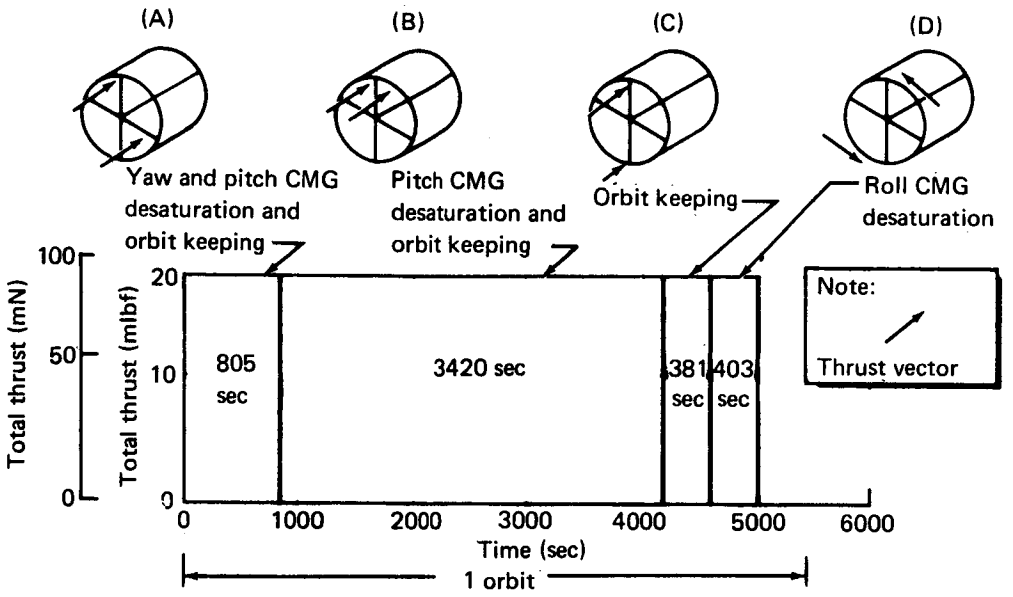

Figure 72. Belly-Down Orientation Thrust Schedule

resupply discretionary payload, established a baseline orbit altitude of 304 km (164 nmi). This altitude is not optimum but was selected for being subsynchronous at a slight payload loss. A delay in initial launch of 1 to 2 years places the latter portion of the mission in years of maximum-density atmosphere. This section deals with the effect of an initial launch delay upon logistics resupply, resistojet system sizing, and, in turn, electrical power requirements and weight. Launch-date delays may require increased orbit altitudes to stay within such constraints as electrical-power limitations. Further, an orbit-altitude variation can be employed to maximize logistics resupply discretionary payload.

High-altitude density variations are mainly the result of varying solar activity levels both long term (11-year cycle) and diurnal in nature. It has been generally accepted that measuring the solar flux at a 10.7-cm wavelength adequately correlates high-altitude variations. Fig. 73 shows the expected average solar activity of the 10.7-cm wavelength as a function of calendar year. Note that a 2-year initial launch delay will result in operation in a maximum-density atmosphere near the end of the mission. Fig. 74 shows the high-altitude density as a function of orbit altitude for various levels of solar activity.

Fig. 75 shows 90-day impulse requirements for the resistojet P/RCS as a function of year for various orbit altitudes. The subsynchronous altitudes are 304, 355, and 404 km (164, 192, and 218 nmi). The requirements are based on the resistojet P/RCS performing orbit keeping and CMG desaturation

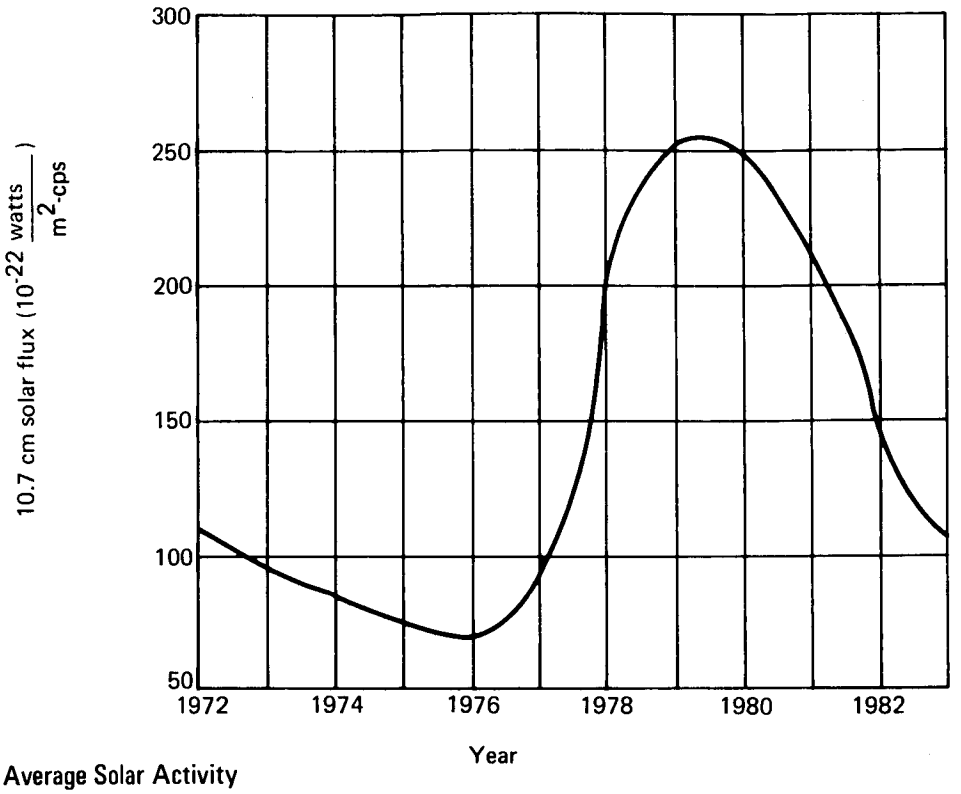

Figure 73. Average Solar Activity

and account for all but a small portion of the total impulse. Whenever possible, the two functions are combined to minimize impulse, which accounts for the flat portion of the curves between 1972 and 1977. In this period, orbit-keeping impulse, being less than belly-down pitch and yaw CMG desaturation impulse, is obtained as a by-product of CMG desaturation. Therefore, impulse requirements remain constant at a value required for CMG desaturation. The difference between the curves along the flat portion shows that CMG desaturation requirements change only slightly over the altitude range under consideration. Time spent in each orientation per day is 4.5 hours inertial and 19.5 hours belly-down. All orbit keeping is performed while in the belly-down orientation. The impulse accumulated in an inertial orientation is evenly distributed over the belly-down orbits. At about 1977, orbit-keeping requirements exceed belly-down CMG desaturation requirements. The total requirements then comprise orbit keeping, CMG desaturation during the inertial orientation, and roll CMG desaturation during the belly-down orientation.

Orbit-altitude optimizations can be based on a variety of ground rules. In this particular case, the optimization maximizes discretionary payload of the logistics resupply system over a 5-year mission. Such other vehicle resources as electrical power may also be considered in an optimization. The logistics-resupply system assumed for the optimizations is a Saturn IB/Apollo system. Resupplies are nominally 90 days apart for a total of 20 over 5 years.

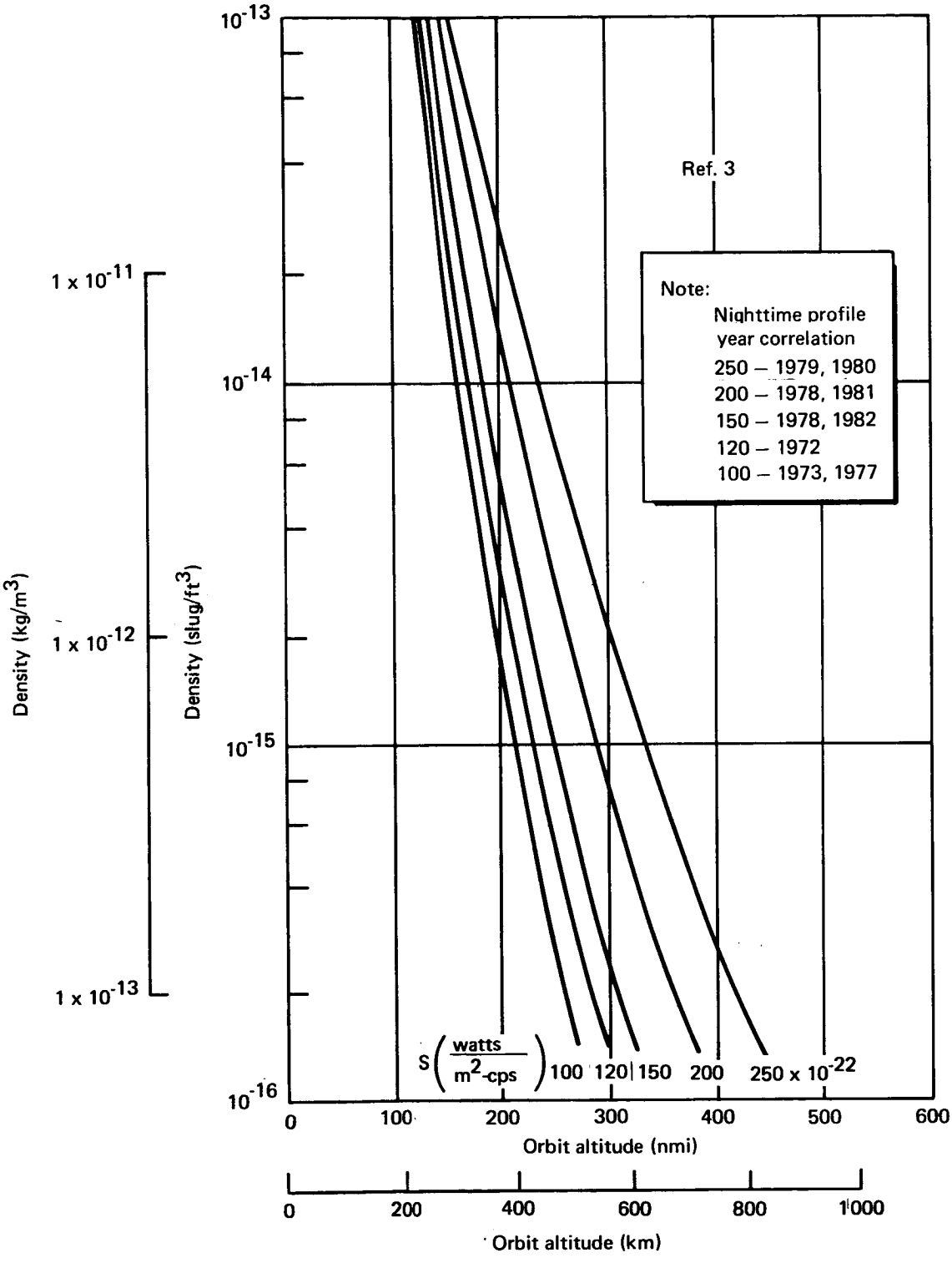

Figure 74. Average Density Profile

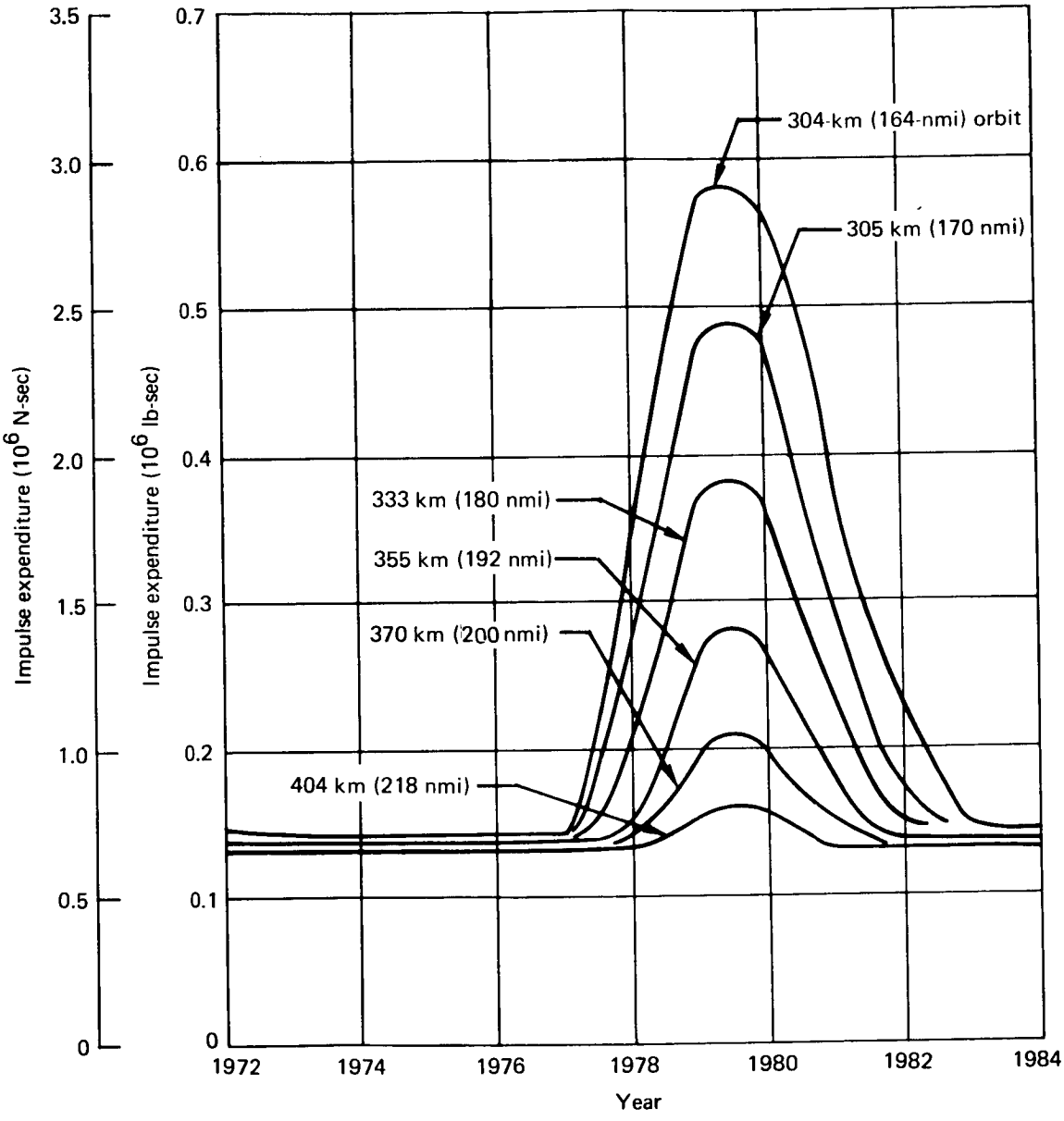

Figure 75. 90-Day Impulse Requirement as a Function of Year

Fig. 76 shows the results of an orbit-altitude optimization performed for the 1974 to 1979 period for three different P/RCS's and corresponding specific impulses (I_{sp}), as follows: (1) 270-sec I_{sp} corresponds to a bipropellant P/RCS, (2) 377-sec I_{sp} corresponds to a resistojet P/RCS utilizing NH_3 propellant and (3) 750-sec I_{sp} corresponds to a resistojet P/RCS utilizing H_2 propellant. The lower solid line shows the change in logistics-system payload capability as orbit altitude increases. The upper solid curves show the possible increase in discretionary payload through decreased propellant consumption as a function of orbit altitude. Net payload change, represented by the dotted lines, shows that discretionary payload decreases as orbit altitude increases for the I_{sp}'s considered.

Fig. 77 presents identical data for the 1976 to 1981 period. The effect of increased atmospheric density is beginning to show on certain of the curves. For an I_{sp} of 270 sec, discretionary payload can be increased 906 kg (2000 lbm) by raising the orbit altitude from 314 to 324 km (170 to 175 nmi). A slight payload increase is possible at an I_{sp} of 377 sec. At an I_{sp} of 750 sec, no increase is possible.

Impulse Requirements

Fig. 79 shows 90-day impulse requirements for the resistojet P/RCS as a function of year for various orbit altitudes. The subsynchronous altitudes are 304, 355, and 404 km (164, 192, and 218 nmi). The requirements are based on the resistojet P/RCS performing two functions, orbit keeping and CMG desaturation, and accounts for all but a small portion of the total impulse. Whenever possible, the two functions are combined to minimize impulse which accounts for the flat portion of the curves between 1972 and 1977. In this period, orbit-keeping impulse, being less than belly-down pitch and yaw CMG desaturation impulse, is obtained as a by-product of CMG desaturation. Therefore, impulse requirements remain constant at a value required for CMG desaturation. The difference between the curves along the flat portion shows that CMG desaturation requirements change only slightly over the altitude range under consideration. Time spent in each orientation per day is 4.5 hours inertial and 19.5 hours belly down. All orbit keeping is performed while in the belly-down orientation. The impulse accumulated in an inertial orientation is evenly distributed over the belly-down orbits. At about 1977, orbit-keeping requirements exceed belly-down CMG desaturation requirements. Therefore, the total requirement comprises orbit keeping, CMG desaturation during the inertial orientation and roll CMG desaturation during the belly-down orientation.

Fig. 78 concerns the 1978 to 1983 period, when average atmospheric density is near maximum. At an I_{sp} of 270 sec, a discretionary payload increase of 2260 kg (5000 lbm) can be realized by going to an orbit altitude of 324 km (175 nmi). At an I_{sp} of 377 sec, the discretionary payload increase is 453 kg (1000 lbm) at an orbit altitude of 316 km (171 nmi). An increase is not possible at an I_{sp} of 750 sec.

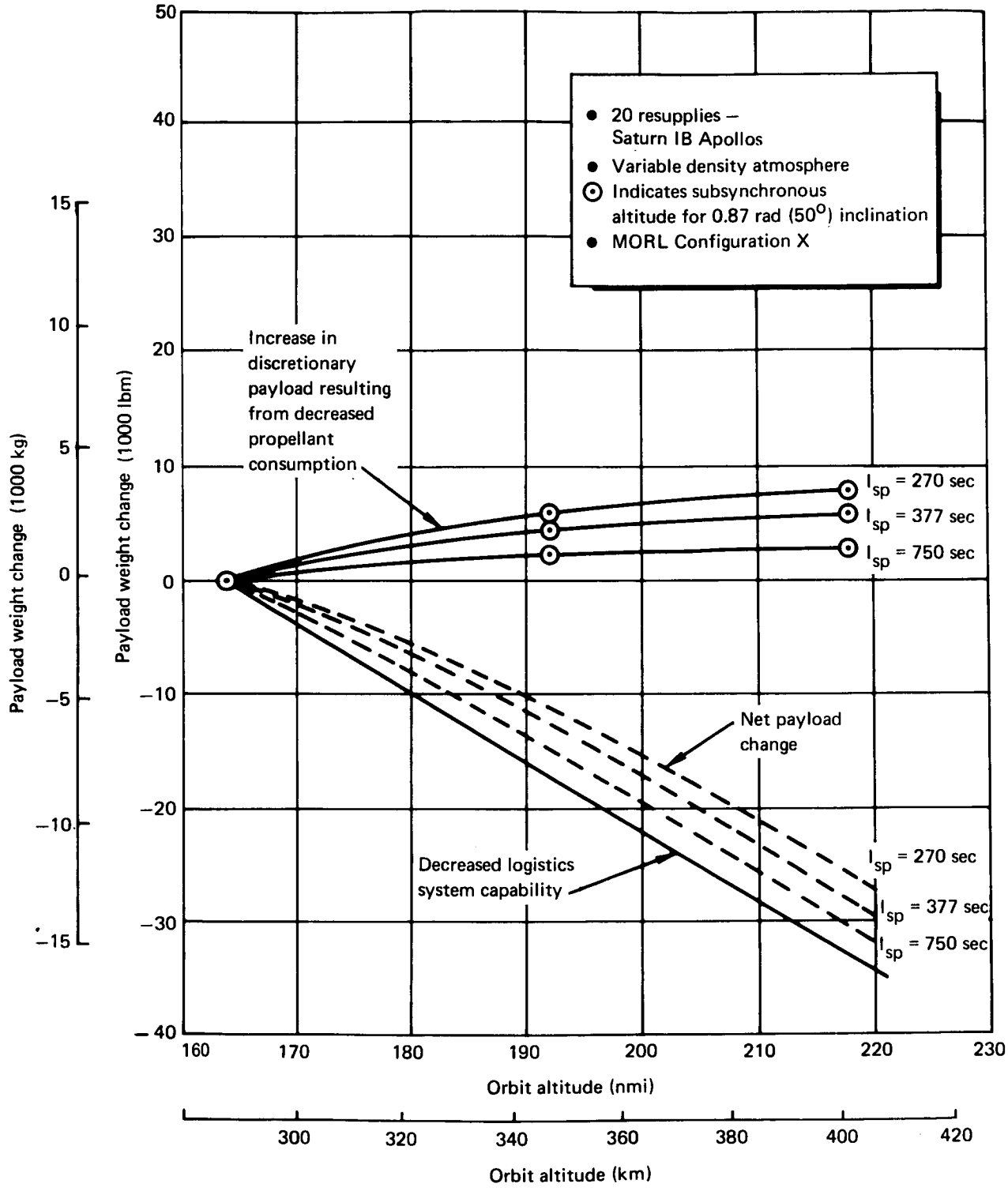

Figure 76. Orbit-Altitude Optimization – 1974 to 1979 Mission

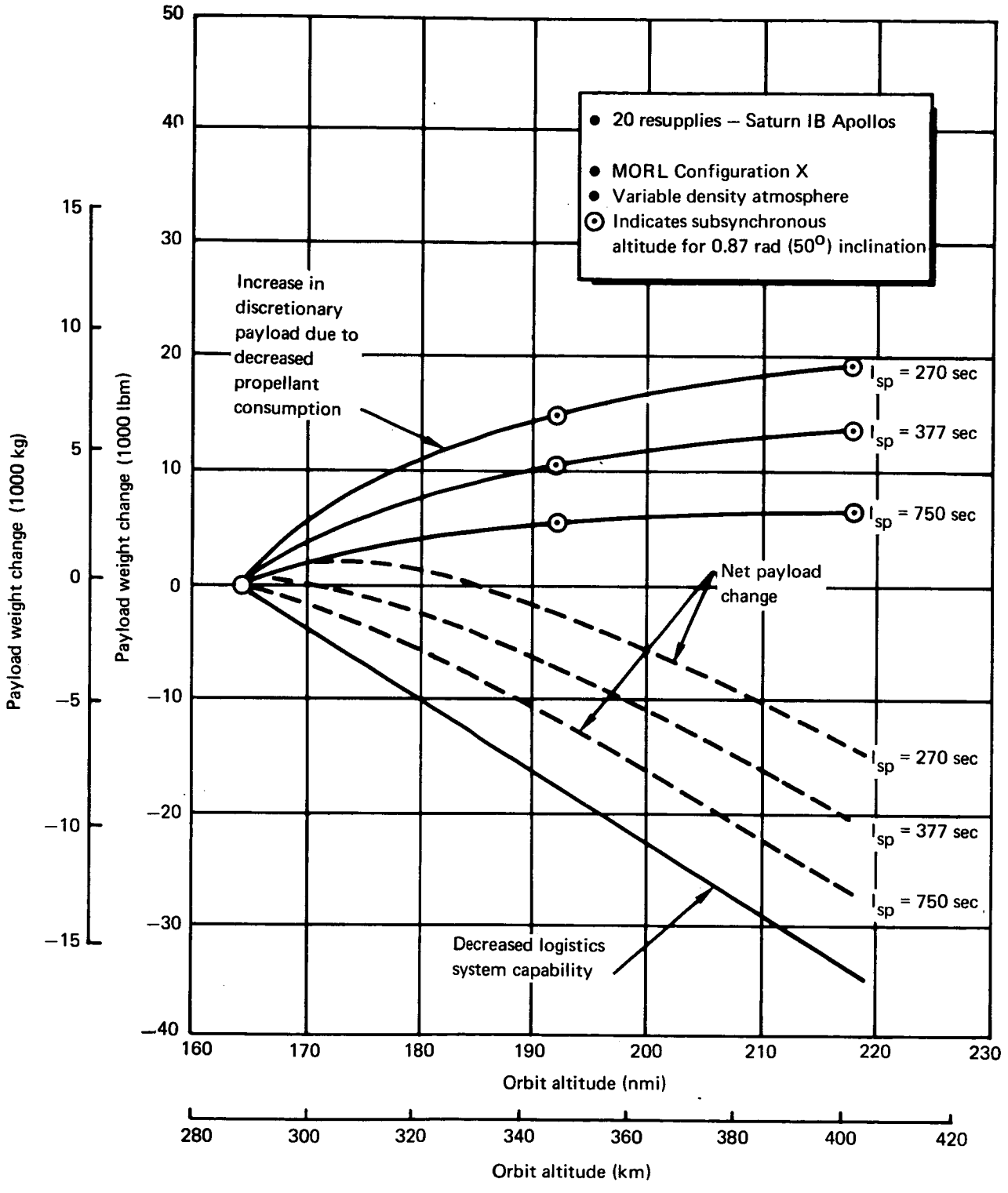

Figure 77. Orbit Altitude Optimization – 1976 to 1981 Mission

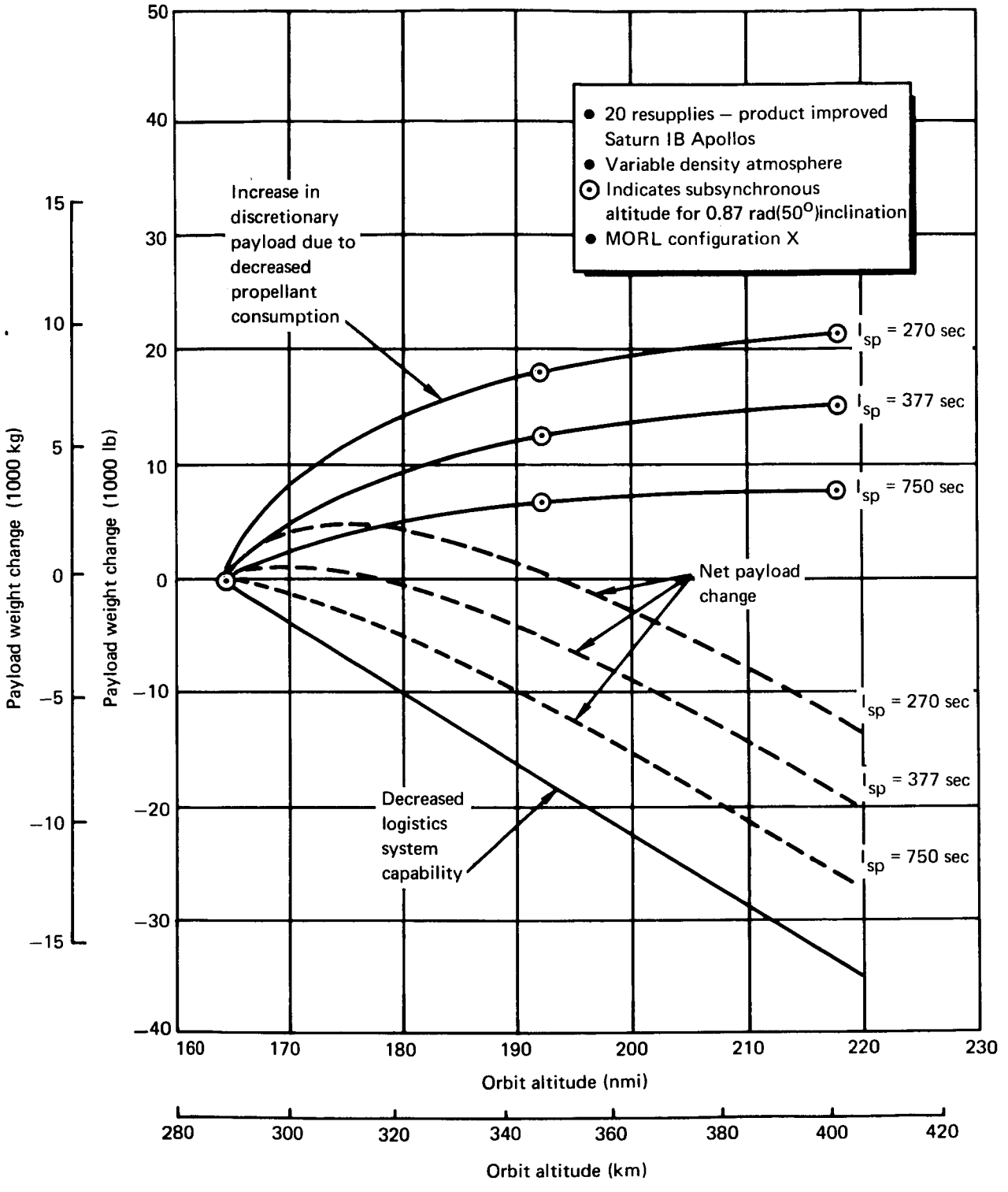

Figure 78. Orbit Altitude Optimization – 1978 to 1983 Mission

Care should be taken not to misinterpret the data presented in figs. 76 through 78. The upper curves represent incremental propellant weights about baseline system weights required for operation in a 304-km (164-nmi) orbit for each of the three P/RCS's. The baseline system weights will differ for each system. Hence, discretionary payload and launch weight also differ for each system. Absolute propellant weight for any 5-year mission and orbit altitude can be derived from the information in fig. 75. Variations in propellant requirements are accompanied by tank weight and tank-size variation on both the MORL and logistics spacecraft. These latter weight variations are not reflected in figs. 76 through 78.

Propellant consumption over a 5-year period is computed for a constant-orbit altitude, which implies an initial launch to that same altitude. The propellant-consumption decrease is the difference between the value at the altitude under consideration and the value at 304 km (164 nmi) (reference point). Another mission profile might be considered when atmospheric density is minimum at initial launch and maximum at mission end. The initial launch is into a 304-km (164-nmi) orbit. As atmospheric density increases, a slow spiral outward is initiated to maintain atmospheric density at some predetermined level. This method results in low launch-system penalties; however, extra propellant must be provided by the resupply system to increase the orbit altitude. The merits of this method versus constant-orbit altitude for 5 years have not been evaluated.

Although orbit-altitude optimizations, which maximize discretionary payload, show 304 km (164 nmi) to be optimum for the high Isp's, problems are encountered in other areas. The most important area is that of increased electrical-power demand by the resistojet P/RCS because of increased thrust levels, as illustrated by fig. 79. Minimum acceptable thrust (total) is shown as a function of year for two orbit altitudes. With the 356-km (192-nmi) orbit and using either NH_3 or H_2 propellant, the resistojet P/RCS electrical-power requirement remains within the present allotment of 1.1 kWe. At decreased orbit altitudes with H_2 propellant, the power allotment will be exceeded during maximum density years. The use of NH_3 propellant allows a decrease in altitude to approximately 33 km (180 nmi) before the power allotment is exceeded.

The effects of a maximum-density atmosphere (1979 to 1980) upon the resistojet P/RCS while operating in a 304-km (164-nmi) orbit are further illustrated by impulse requirements and associated thrust schedules. Table 31 lists the resistojet P/RCS impulse requirements. Maximum thrust levels and power requirements are established by the belly-down thrust schedule of fig. 80. A total thrust of 410 mN (92 mlbf) is maintained over the entire orbit for which electrical power is 2.56 kWe. The thrust level of each thrustor is 104 mN (23 mlbf). Fig. 81 shows the thrust schedule for the inertial orientation. A constant thrust of 208 mN (46 mlbf) applied over a portion of the orbit requires 1.23 kWe.

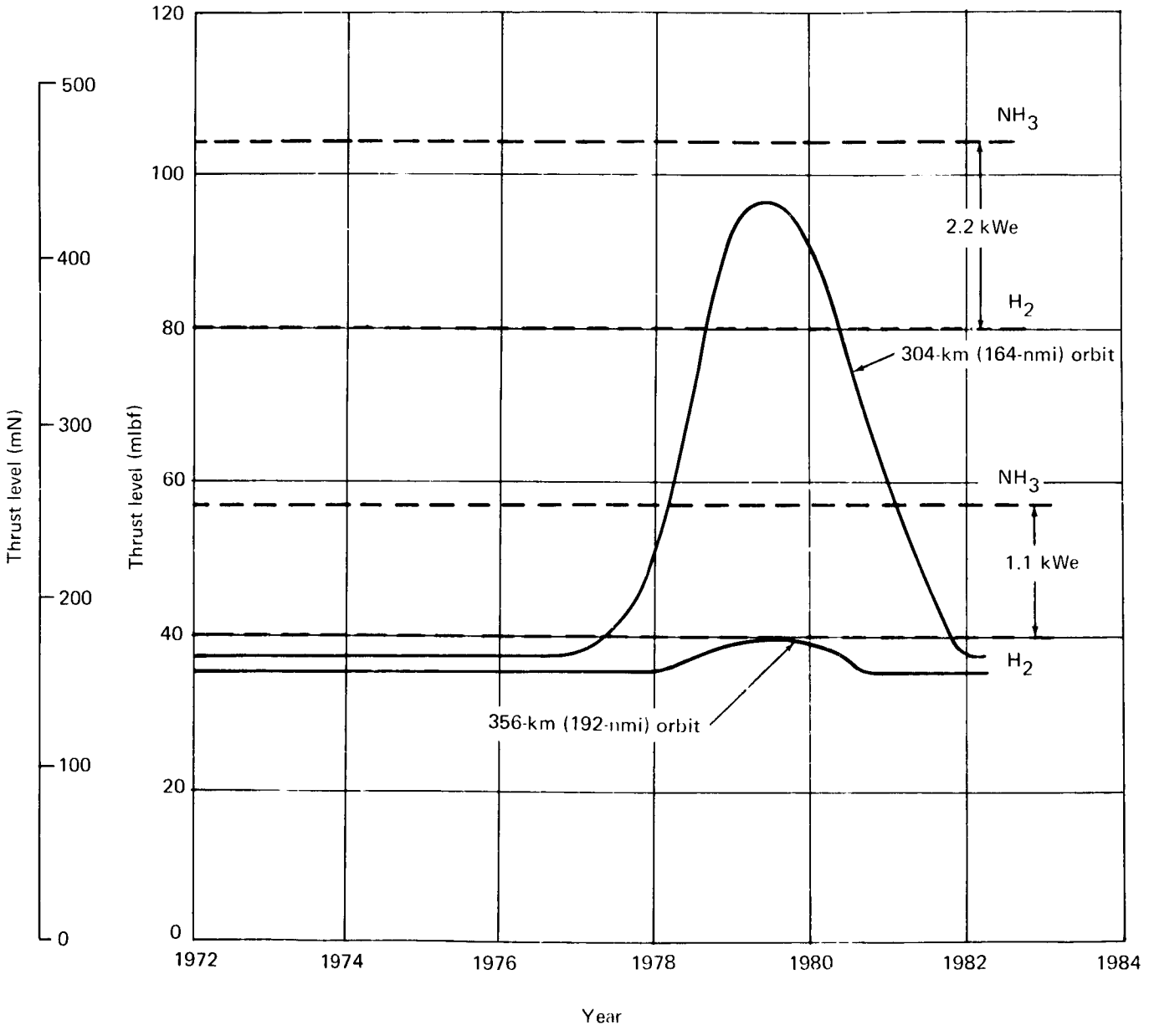

Figure 79. Minimum Acceptable Thrust

TABLE 31

RESISTOJET P/RCS IMPULSE REQUIREMENTS

Function	Requirement,[c] N-sec/orbit	(lb-sec/orbit)
Inertial orientation		
Drag (orbit-keeping)[a]	3560	(800)
Pitch CMG desaturation	800	(180)
Yaw CMG desaturation	80	(18)
Roll CMG desaturation	80	(18)
Belly-down orientation		
Deferred drag[b]	836	(186)
Normal drag	1360	(305)
Pitch CMG desaturation	338	(76)
Yaw CMG desaturation	35.6	(8)
Roll CMG desaturation	35.6	(8)

[a]Orbit-keeping deferred to belly-down operation.

[b]Deferred drag distributed evenly over orbits spent in belly-down orientation

[c]304-km (164-nmi) orbit, maximum-density atmosphere.

Resistojet system optimization. – The H_2 and NH_3 propellants were selected during Phase IIB of the MORL System Improvement Study (ref. 1) as being the two best candidates of those considered. The H_2 exhibits high specific impulse (700 to 800 sec), while the NH_3, although having lower specific impulse (300 to 400 sec), is considerably less complex. An evaluation of the N_2H_4 resistojet system was made for use together with an N_2H_4 monopropellant high-thrust system. Results of that analysis showed that, in spite of propellant commonality, the integrated N_2H_4 system is heavier and more complex than the NH_3 resistojet used together with the same high-thrust system. This is because of the disadvantages of decomposing the N_2H_4 before resistojet heating, and because anhydrous N_2H_4 is required to avoid severe performance degradation or oxidation problems. Because N_2H_4 is very hygroscopic, special processing and handling techniques are needed to keep the water level to less than 5 ppm. Moisture control throughout logistics and operational phases of the mission results in an additional cost penalty. For the foregoing reasons, N_2H_4 resistojets were eliminated from further consideration.

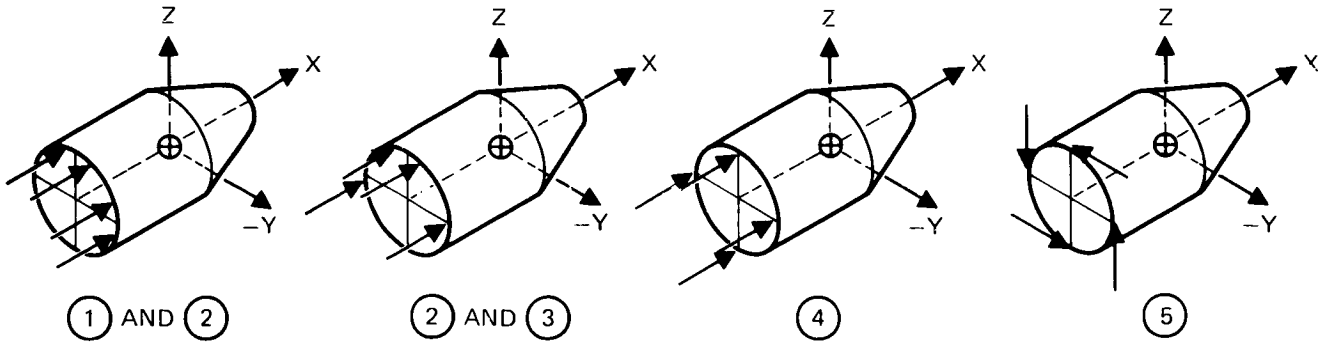

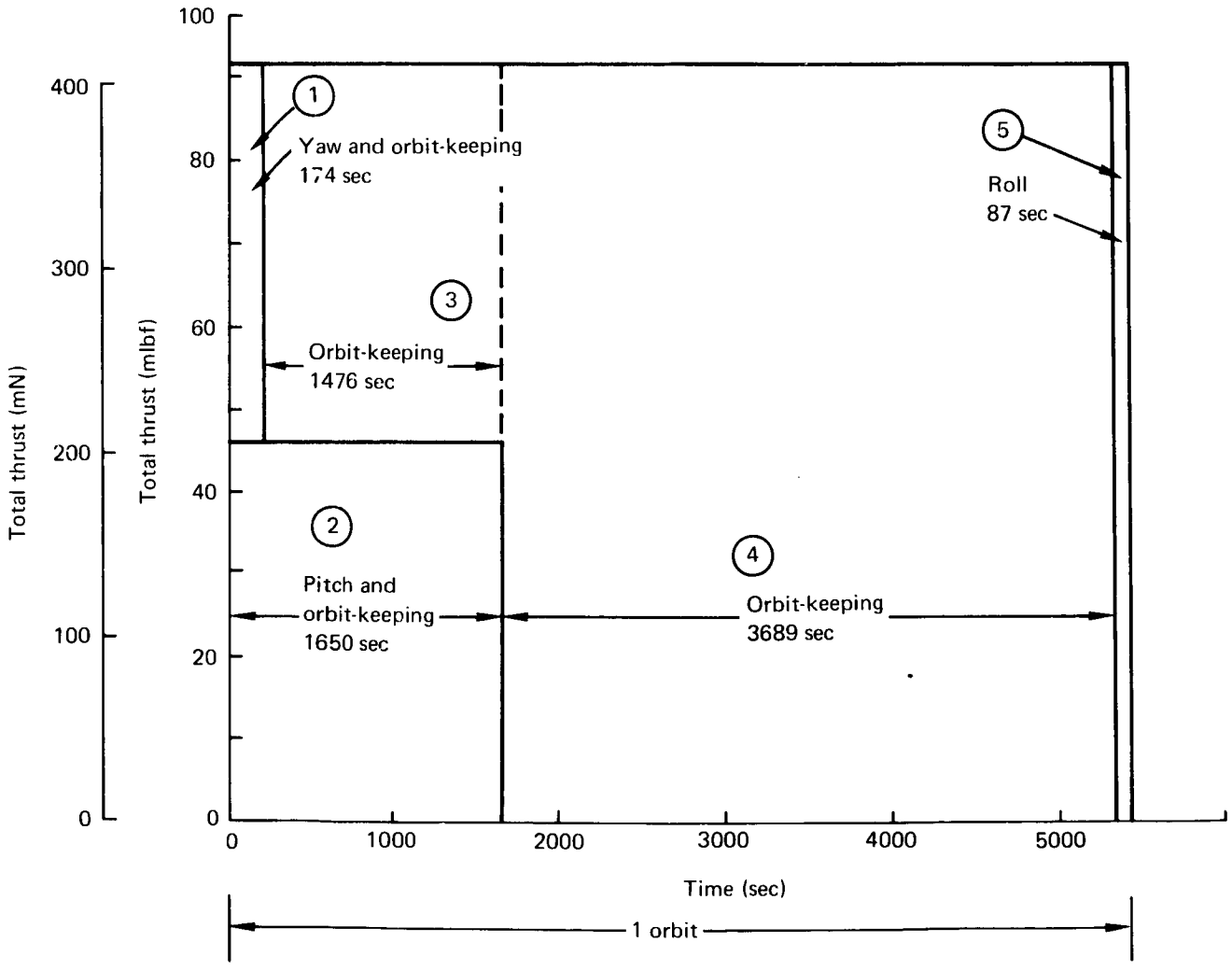

Figure 80. Belly-Down Thrust Schedule

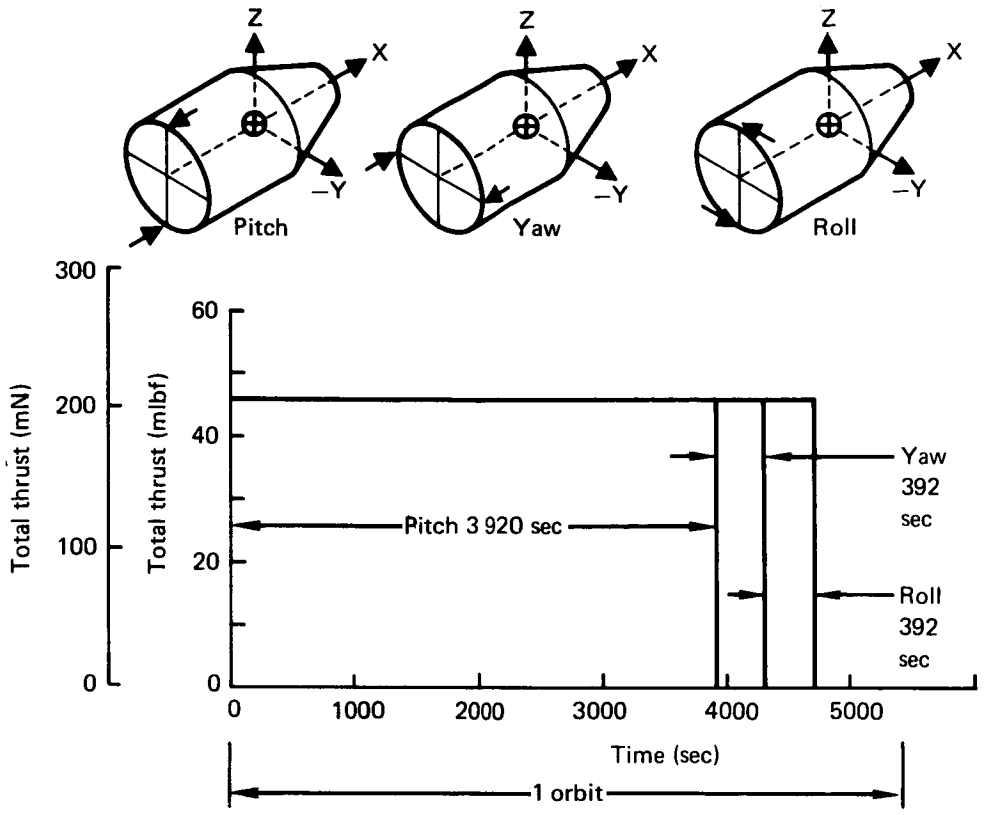

Figure 81. Inertial Orientation Thrust Schedule

A separate evaluation of the use of biowaste propellants led to the preliminary definition of two biowaste resistojet systems: one utilizes CO_2 only, the other uses both CO_2 and biowaste H_2. This evaluation is presented in Volume III of this report.

In the following paragraphs, the NH_3 and cryogenic H_2 thrustor system analyses are discussed.

H_2 and NH_3 resistojet systems: The H_2 resistojet thrustor is physically identical to the NH_3 evacuated concentric tube type described in detail in the selected system description section. The tank and feed systems for the two systems under consideration are described in subsequent paragraphs.

The optimization of a thrustor system typically includes a tradeoff of system weight and performance variations with thrust chamber operating pressure. Figs. 82 and 83 show the delivered specific impulse and the minimum required power variations with chamber pressure for both H_2 and NH_3 at the 0.0445-N (0.010-lbf) thrust level. A rapid decrease in specific impulse accompanied by increases in power requirements occurs below a chamber pressure of about 138 000 N/m^2 (20 psia). Fabrication and geometric considerations limit the maximum operating pressure to approximately 310 000 to 344 000 N/m^2 (45 to 50 psia). The NH_3 tank is uninsulated, and consequently, the tank pressure is the NH_3 vapor pressure at the MORL

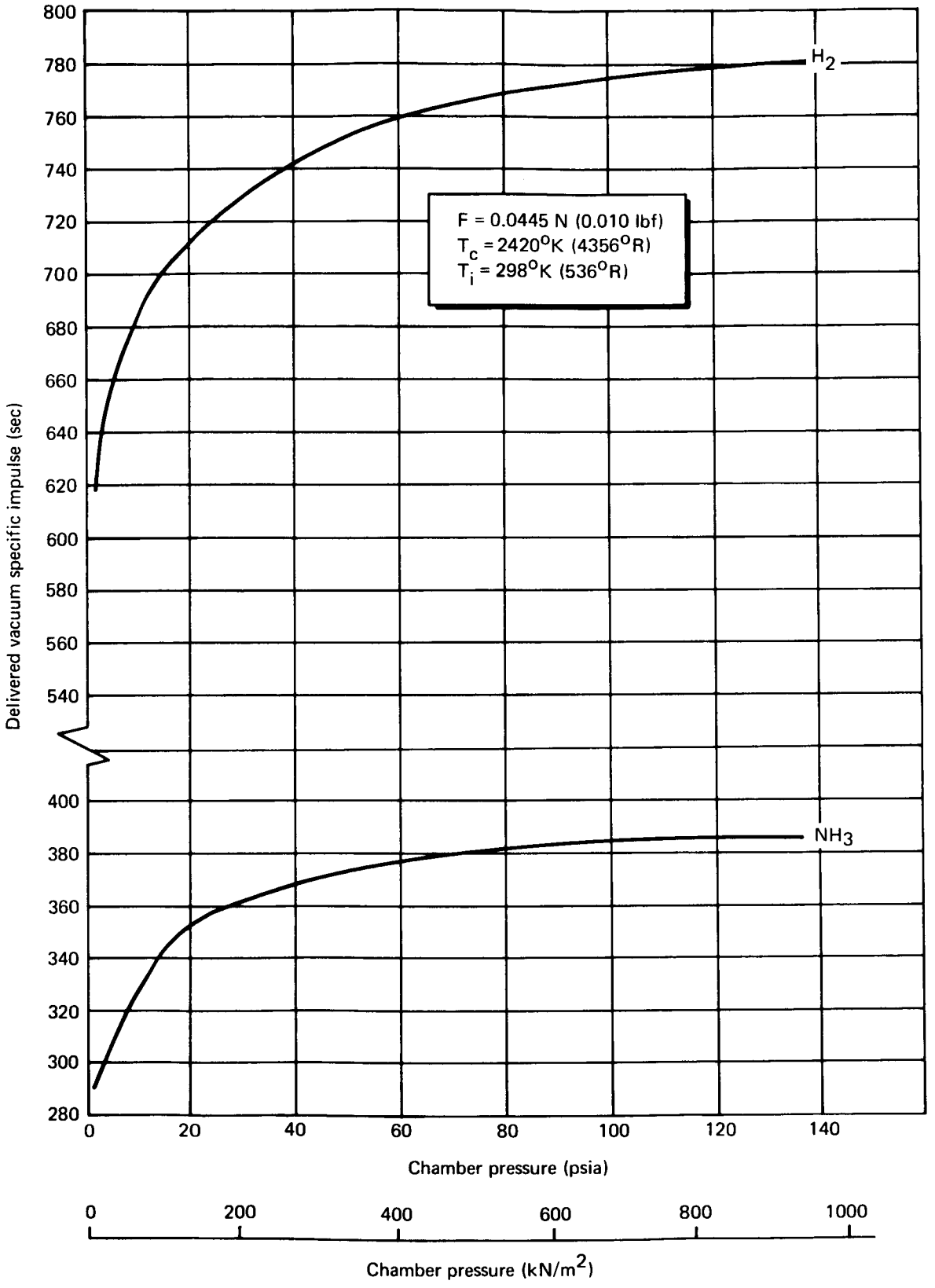

Figure 82. Chamber Pressure Effects on Resistojet Performance

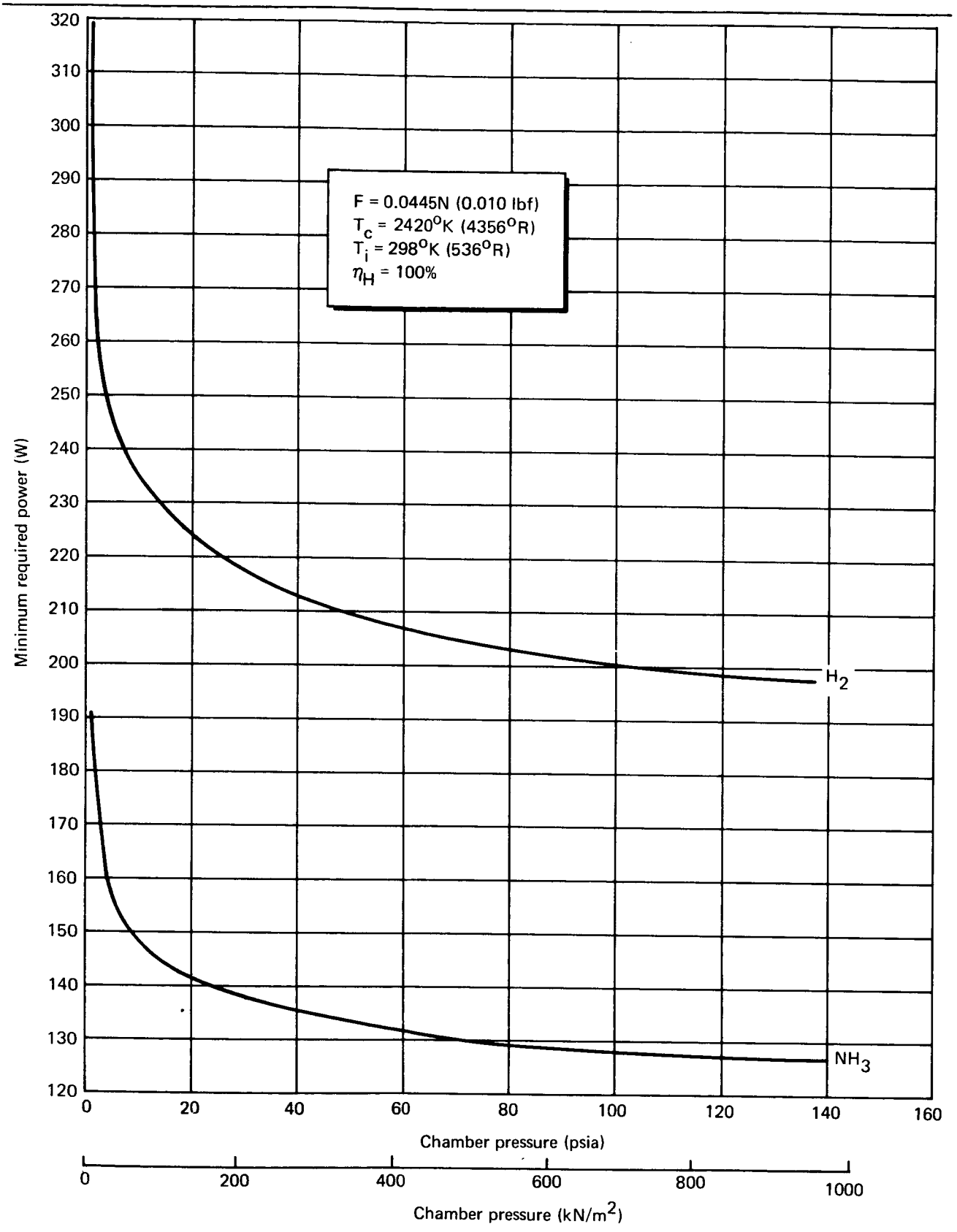

Figure 83. Chamber Pressure Effects on Resistojet Power Requirement

aft interstage ambient temperature of 324°K (585°R) 2 130 000 N/m^2 (310 psia). The small range of reasonable chamber pressures available [138 000 to 344 000 N/m^2 (20 to 50 psia)] has no effect on the tank conditions, because there will always be sufficient pressure drop in the feed system. The result is that the NH_3 system chamber pressure may be selected on the basis of delivered performance and power requirements with negligible effect on system weight. The H_2 system operates with a minimum pressure drop between the tank and thrust chamber, and, the selected chamber pressure directly affects the propellant-tank pressure requirement. Fig. 84 shows the results of the chamber-pressure tradeoff for the H_2 system. The tank weight increases at a higher rate than the rate of decrease in propellant weight with increasing chamber pressure, and consequently, the total system weight exhibits a slight increase. The weight assessment for electric-power consumption decreases with increasing pressure; therefore, the sum of these two weights becomes the criterion for chamber-pressure selection. The summation curve is essentially flat, yielding the same conclusion as for the NH_3 system, that is, chamber pressure has a negligible effect on the system weight. Figs. 82 and 83 indicate that the higher pressure should be selected to maximize performance and minimize the power requirement. These considerations led to the selection of 241 000 N/m^2 (35 psia) operating pressure for both systems to yield high performance, while still maintaining some conservatism regarding fabrication and geometric limits. The performance and power requirements for this chamber pressure are shown in table 32. The delivered specific impulse is based on a chamber temperature of 2420°K (4356°R), the maximum allowable temperature to obtain required operating life. The minimum required power is based on an initial propellant temperature of 298°K (536°R) and 100% heater efficiency.

Both the H_2 and NH_3 systems have their propellants resupplied from a logistics vehicle at the forward end of the MORL vehicle. The H_2 flow schematic from the fill line to the thrustors is shown in fig. 85, and the tank and feed system is shown in fig. 86. The H_2 flows from the fill line through a shutoff valve and check valves to the insulated storage tank, which has a relief and vent system to prevent overpressure. The H_2 tankage and feed system supplies H_2 vapor to the thrustors. The H_2 flows from the tank as liquid or vapor through a shutoff valve provided for possible tank isolation, then through a solenoid-actuated throttling valve and a regenerative coil attached to the storage tank between the tank wall and insulation. Electric heaters are provided in the tank to ensure sufficient heat to raise the vapor pressure in the tank if a prolonged demand for a high-flow rate causes undue lowering of tank pressure. From the regenerative coil, H_2 flows through a Brayton-cycle waste-heat exchanger to ensure complete vaporization of the H_2 and then into an accumulator at 310 kN/m^2 (45 psia). The flow then passes through a filter and three-way solenoid valve to a redundant pressure-regulator system to a 241-kN/m^2 (35-psia) accumulator. The three-way solenoid valve and redundant regulator system prevents thrustor outage from regulator failure, thus increasing the reliability of the feed system. From the 241-kN/m^2 (35-psia) accumulator, the H_2 flows through, and is heated by, another Brayton-cycle waste-heat exchanger, then to a manifold around the MORL vehicle perimeter, and finally to the thrustor modules. A shutoff valve and disconnect are provided at each thrustor module to allow removal and replacement.

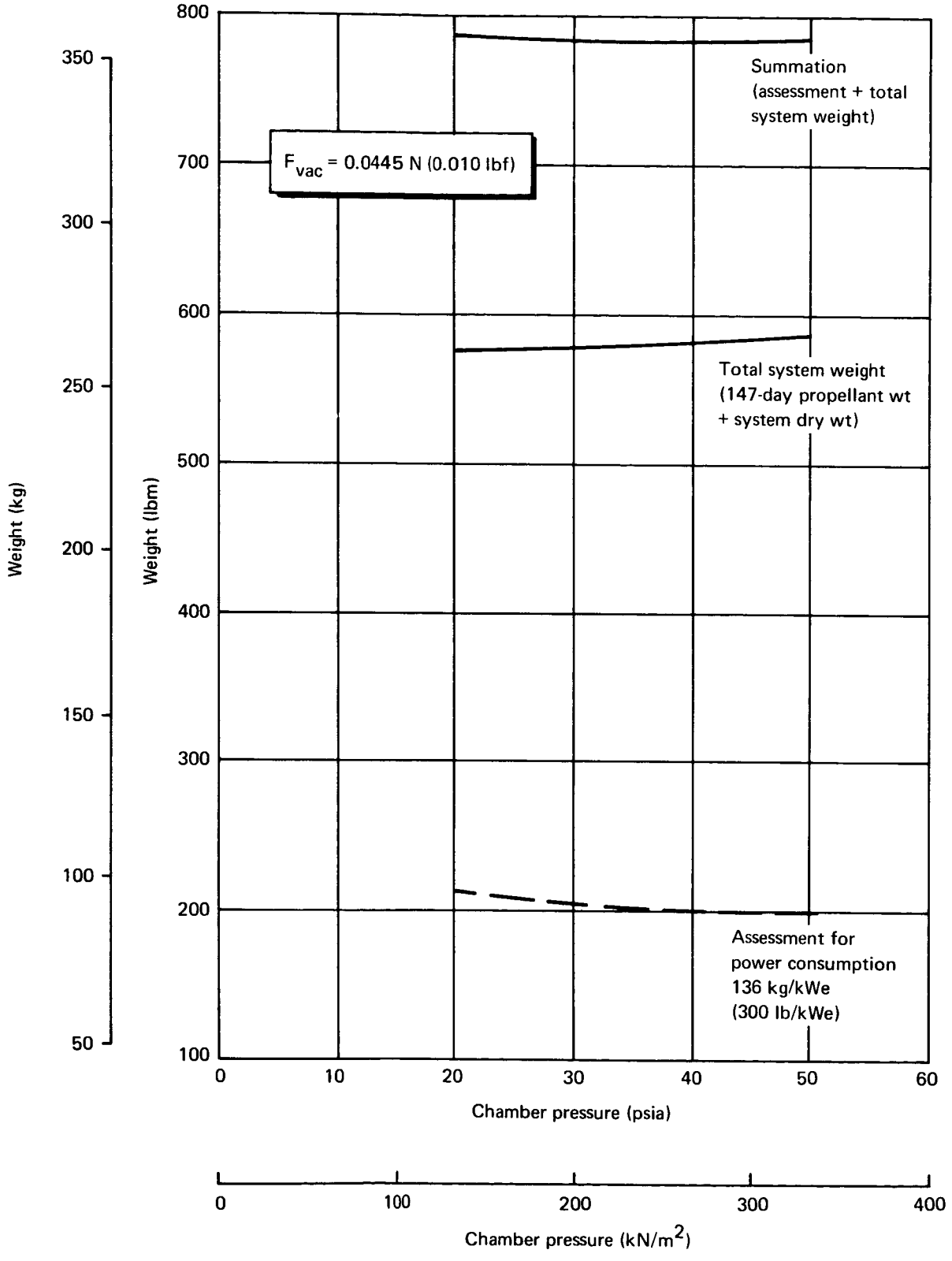

Figure 84. Chamber Pressure Effects on H_2 Resistojet System Weight

TABLE 32

H_2 AND NH_3 PERFORMANCE AND POWER REQUIREMENTS

Propellant	Thrust		Chamber pressure		Temperature		Delivered specific impulse, sec	Minimum power N_H = 100%, W	Heater efficiency, %	Required power,* W
	mN	mlbf	1000 N/m^2	psia	^oK	^oR				
H_2	44.5	10	241	35	2420	4356	735	215	0.918	234
NH_3	44.5	10	241	35	2420	4356	364	135	0.913	149

*Line-power losses not included.

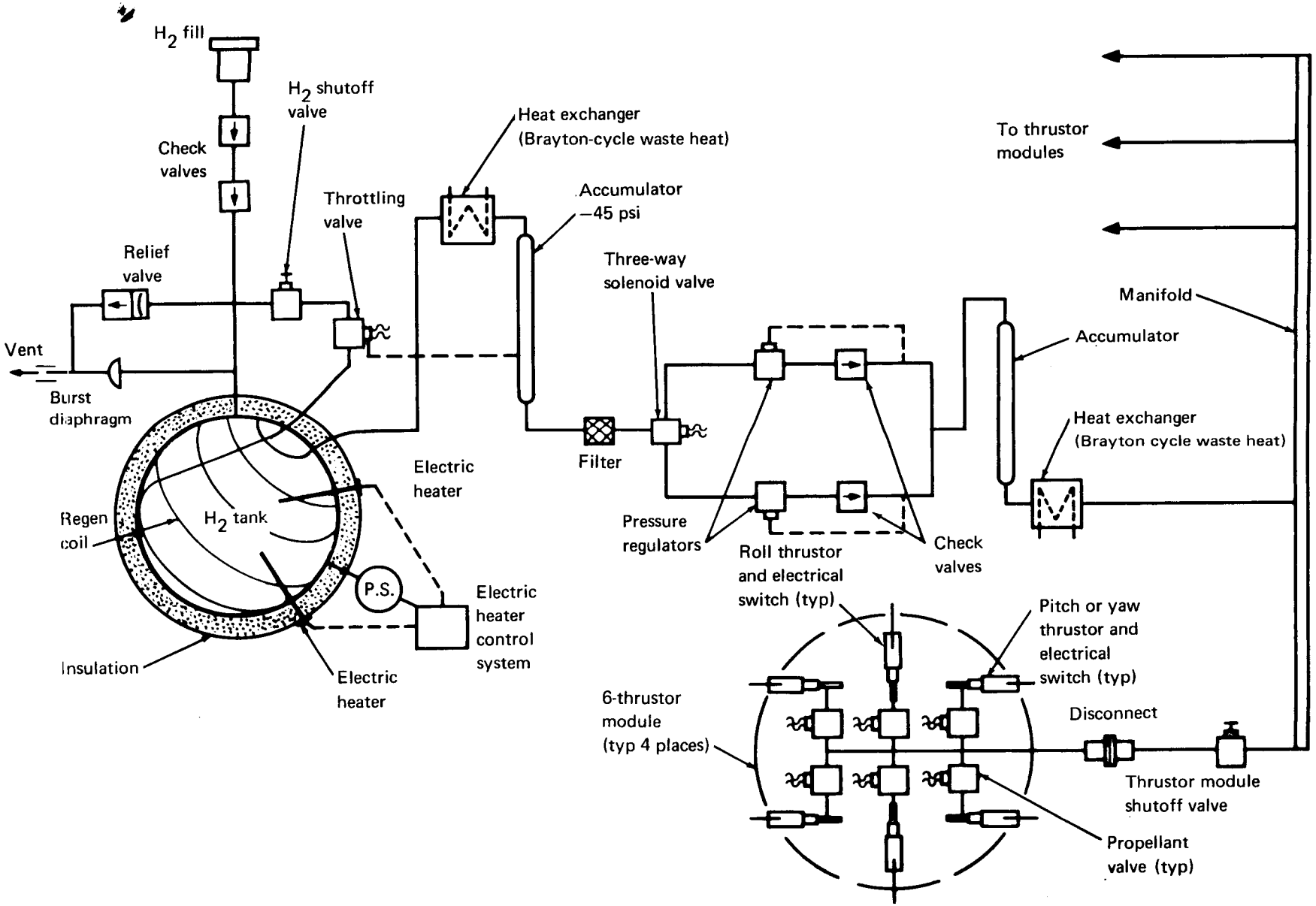

Figure 85. H_2 Resistojet System

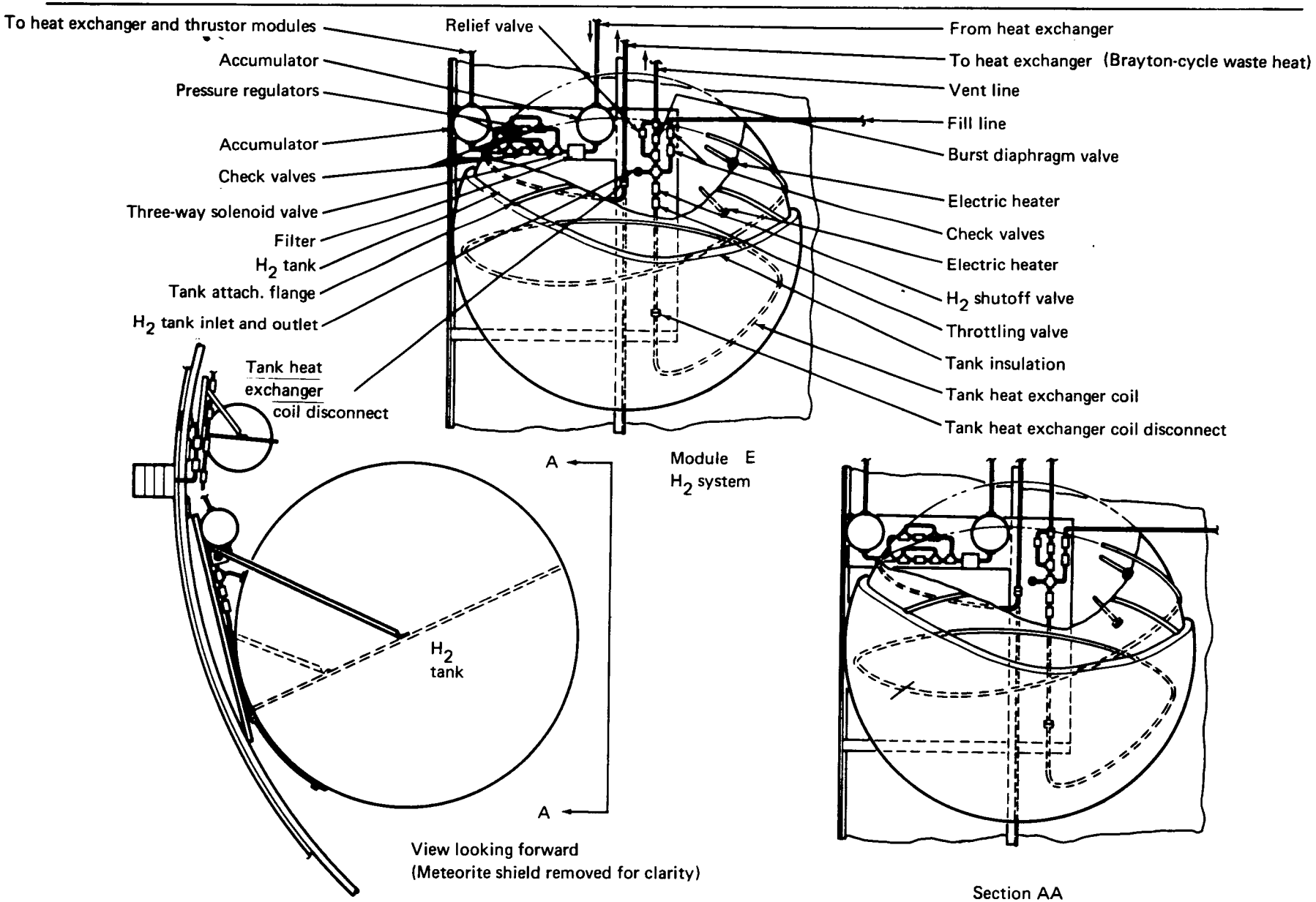

Figure 86. H_2 Resistojet Tank and Feed System

The LH_2 tank can be sufficiently insulated to maintain the tank pressure within design limits, if the required low mass outflow rate of 0.0123 g/sec (2.72×10^{-5} lbm/sec) is being withdrawn from the tank as vapor. However, in low-g operation either liquid or vapor may be present at the tank outlet. With liquid being withdrawn from the tank, the volumetric outflow rate is much less than with vapor, and the permissible heat leak would be correspondingly lower. More high-performance insulation (HPI) would be required to control the tank pressure than would be necessary with vapor outflow. Under the imposed operating conditions for this system, the insulation weight necessary to provide a sufficiently small heat leak for liquid outflow would be excessive. To reduce the insulation weight, the thermodynamic vapor-liquid separator concept is applied to the thermal control of the LH_2 tank.

The thermodynamic vapor-liquid separator uses the tank effluent as a heat sink to absorb part of the heat leak through the insulation. The fluid flow is throttled to a lower pressure and temperature and is passed through a heat exchanger in thermal contact with the tank and contents. When the effluent is vapor, the available heat sink is not significant and the separator acts only as a connecting line to the feed system. The tank insulation is sized for this condition. When the effluent is liquid, the latent heat of vaporization provides a large heat sink in the heat exchanger. This vaporization in the separator, rather than additional external insulation, is used to reduce the net heat leak to the tank contents to the lower value required for liquid outflow.

The conventional application for such a device is in low-gravity, cryogenic, vent systems in which the objective is to prevent liquid loss and to minimize the vent mass flow required to control the tank pressure. It is called a separator because only vapor leaves the system although either vapor or liquid may enter. The proposed MORL application is somewhat different. The tank pressure must be controlled, but propellant is continuously withdrawn at specified rates without any overboard venting. With variable operating conditions, the design point (complete vaporization of all liquid effluent) must be chosen as the worst case in terms of maximum total heat leak and minimum mass-outflow rate. Under other conditions, the required heat sink can be provided without complete vaporization, and the flow leaving the separator may be two-phase rather than all vapor. The flow is passed through a Brayton-cycle waste-heat exchanger to ensure that it is fully vaporized before reaching the pressure regulators.

Distributed internal, compact internal, and distributed external thermodynamic separators were considered for this system. The distributed-internal heat exchanger consists of a cooling tube coiled within the tank and spaced more or less evenly throughout the tank volume. The basis for its operation is that all fluid is within a short distance from the heat-exchanger surface, giving adequate thermal contact. It was found that this system exhibited the poorest performance of the three systems. It takes less tubing to provide the equivalent required heat transfer over the tank surface in the distributed-external system than throughout the volume in the distributed-internal system. The compact-internal system can also be achieved at significantly lower weight if a pump is used to circulate fluid through the exchanger. Therefore, the distributed-internal heat exchanger was eliminated.

The compact internal heat exchanger is currently receiving the most attention in vapro-liquid separator development, with parallel analytical and experimental programs being performed by several companies. This system exhibits the following advantages:

(1) Lower weight for large vehicle applications.

(2) Packaging in a single compact envelope and the same general configuration used for a variety of vehicle applications and heating rates.

(3) Heat transfer is forced-convection dominated because a mixer or pump is used to circulate the tank contents through the exchanger; therefore, operation is easily demonstrated at 1 g.

However, this development is oriented toward a standard vent-control system, and is not as desirable for continuous operation with very low flow rates.

With the distributed-external heat exchanger, the coolant (vent fluid) is circulated through a tube which is coiled around the exterior of the tank. The coil is in thermal contact with the wall at selected conductive attachment points, more or less evenly spaced. The tank wall acts as a fin for a finned-tube heat exchanger, with the attachment point being the fin root.

Heat leak through the insulation reaches the tank wall and is conducted through a temperature gradient to the attachment point of the cooling tube. The heat leak is intercepted before it reaches the tank contents, rather than being subsequently removed from the fluid as in internal exchangers. The cooling tube is in thermal contact with the tank wall only at discrete points, rather than throughout its length, to distribute the resulting heat transfer evenly over the tank surface. The proposed MORL application imposes the following restrictions which affect the system choice:

(1) The fluid removed from the tank is not dumped overboard as in a common vent control system, but must be supplied to the thrustor at a specified pressure. This places a practical limit on the pressure difference between the tank and the cooling tube.

(2) A continuous and controlled flow rate must be provided to the thrustors.

(3) A very long operating life is mandatory.

These factors make use of the compact-internal heat exchanger less advantageous. Continuous operation of the mixer for continuous venting is very inefficient and results in high electrical heat input to the tank contents. The operation of the mixer also poses reliability problems for the necessary long-duration use. The distributed-external heat exchanger appears to be the most suitable for the MORL application.

Because a system of the proposed type has not yet been operated in a space environment, conservative performance estimates were adopted. Insulation was sized to permit a maximum heat leak corresponding to the minimum flow rate. Positive control of the tank pressure can be maintained with an electrical heater.

The heat of vaporization of LH_2 at 378 kN/m^2 (55 psia) is 3.94 x 10^5 J/kg (170 Btu/lb) for a permissible total heat leak of 4.24 J/sec (14.45 Btu/hr) at the minimum H_2 flow rate. From previous detailed analyses on cryogenic storage systems, heat-leak values were estimated as follows:

Tank supports	0.146 J/sec	(0.5 Btu/hr)
Lines	0.146	(0.5)
Insulation attachments	0.292	(1.0)
Total	0.584 J/sec	(2.0 Btu/hr)

The remaining allowable heat leak through the insulation is 3.64 J/sec (12.45 Btu/hr) or 0.034 W/m^2 (0.1075 Btu/ft^2-hr). Fig. 87 is a plot of NRC-2 insulation performance for the specified environmental temperature of 325°K (585°R). This curve indicates 58 sheets of HPI; however, considerable uncertainty exists as to the actual performance of the installed insulation. For a standard safety factor of two, the HPI is sized for one-half the desired heat leak, which is 0.0169 W/m^2 (0.0537 Btu/ft^2-hr); therefore, 116 sheets of HPI suffice. To determine insulation weight, the following factors are assumed:

Basic weight per layer	0.0088 kg/m^2	(0.0018 lb/ft^2)
Installation weight of tank area	0.146 kg/m^2	(0.03 lb/ft^2)
Overlap factor	12%	

for a total installed HPI weight of 14.1 kg (31.0 lb).

Table 33 presents the requirements for H_2 based on the cryogenic H_2 tank-design criteria and storage conditions presented in table 34. Weight estimates for the control system components shown in fig. 85 are given in table 35. Allowances have been included for redundant components and manual valves for use in system repair and other maintenance tasks. Thrustor module weight is not included.

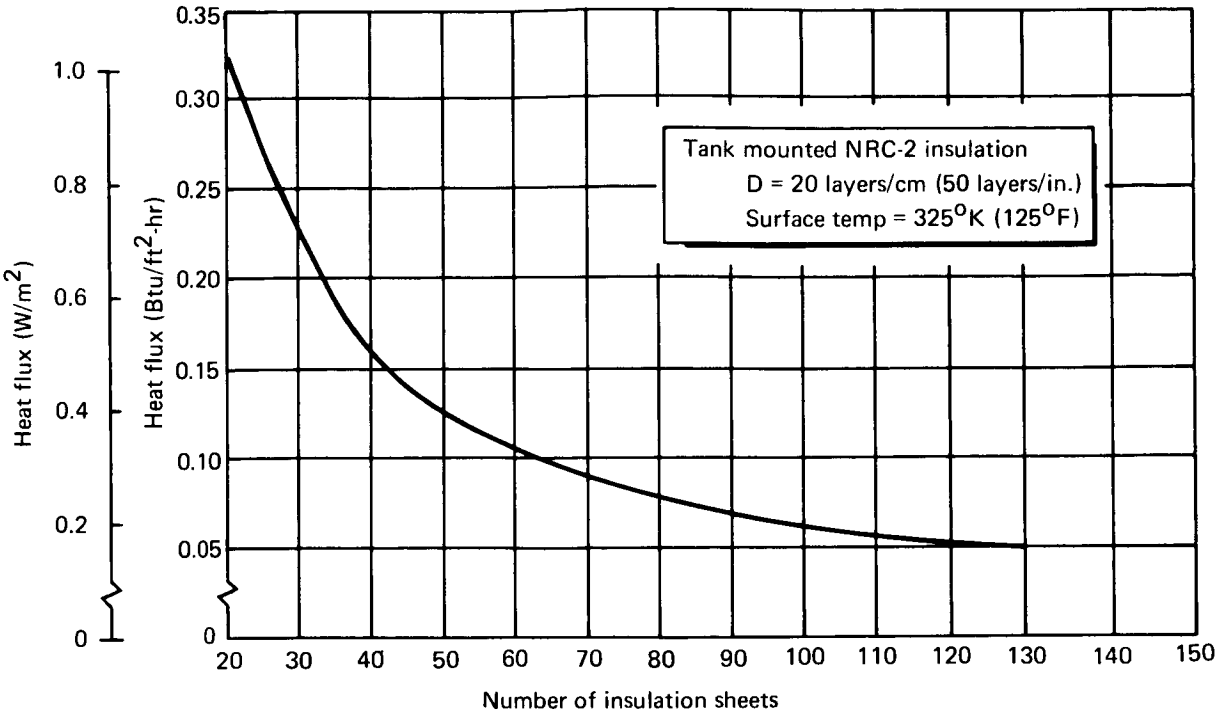

Figure 87. HPI Performance

TABLE 33

CRYOGENIC H_2 PROPELLANT AND PROPELLANT-TANK REQUIREMENTS[a]

Item	Requirement
Total impulse, N-sec (lb-sec) (147-day normal operation)	1.22×10^6 (2.75×10^5)
Specific impulse, sec[b]	735
Required propellant weight, kg (lbm)	170 (375)
Loaded propellant weight, kg (lbm)	191 (423)
Propellant volume, m^3 (ft^3)	3.34 (118)
Propellant tank diameter, cm (in.)	185 (73)
Propellant tank wall thickness, mm (in.)[c]	1.42 (0.056)
Propellant tank weight, kg (lbm)[d]	47 (104)
Insulation weight, kg (lbm)	14 (31.0)
Total loaded weight, kg (lbm)	251 (554)

[a]Based on initial ullage of 5%
[b]44.5 mN (10 mlb) thrustor.
[c]757 000 N/m^2 (110 psia) limit pressure.
[d]10% allowance for weld and wall-thickness tolerance included.

TABLE 34

CRYOGENIC TANK DESIGN CRITERIA AND STORAGE CONDITIONS

Item	Criterion or condition
Cryogenic H_2 tank design criteria	
Material	2014 - T6 Al
Ultimate tensile strength, N/m^2 (psia)	4.6×10^8 (67 000)
Density, g/cm^3 ($lb/in.^3$)	2.76 (0.101)
Safety factor on ultimate strength	1.4
Proof pressure	1.33 x limit pressure
Weld and thickness tolerance	10%
Minimum gage, mm (in.)	0.504 (0.020)
Cryogenic H_2 tank storage conditions	
Nominal pressure, N/m^2 (psia)	378 000 (55)
Nominal temperature, ^oK (^oR)	25.6 (46)
Maximum pressure, N/m^2 (psia)	551 000 (80)
Maximum temperature, ^oK (^oR)	27.8 (50)
Limit pressure, N/m^2 (psia)	757 000 (110)

TABLE 35

LH_2 CONTROL-SYSTEM WEIGHT ESTIMATES

Item	Weight kg (lbm)	
Throttling valve	0.91	(2.0)
Control valves	0.45	(1.0)
Regulator valves	1.36	(3.0)
Hand valves	1.59	(3.5)
Filters	0.18	(0.4)
Pressure sensors	0.36	(0.8)
Electrical heater	0.05	(0.1)
Accumulators	1.59	(3.5)
Heat exchangers	2.27	(5.0)
Total	8.75	(19.3)

A schematic drawing of the NH_3 propellant tank and feed system is shown in fig. 88. The NH_3 is stored at its vapor pressure at a nominal temperature of 325°K (585°R) in a tank fabricated from 6A1-4V-Ti. The nominal NH_3 storage is therefore 2 146 000 N/m^2 (310 psia) [at (585°R)] and has a maximum storage condition of 2 750 000 N/m^2 (400 psia) [at 333°K (600°R)]. The propellant tank contains no positive-expulsion system. The NH_3 is expelled by its own vapor pressure. Table 36 presents a summary of the NH_3 tank based on the storage conditions and the design criteria in table 37.

The NH_3 leaving the tank flows through the Brayton-cycle waste-heat loop to provide the heat necessary to ensure that the fluid is vaporized. A negligible pressure drop is assumed through the valves and the feed lines from both the propellant tank to the regulator and from the accumulator to the thrustors because of the extremely low flow rates. Weight estimates for the control system components shown in fig. 88 are given in table 38. Thrustor weights are not included.

Power control system analysis: The recommended power-control system achieves a ±1% power regulation at the resistojet thrustors. A 1% power regulation requires ±1/4% voltage regulation. This was achieved by utilizing the 260-Vdc link bus power source, with inverters and step-down transformers. The inverter is capable of ±1/4% voltage regulation; the remaining 1/4% tolerance is taken up in the distribution system.

An alternate system which uses a higher-efficiency ac source can provide an average power saving of 6.5%; however, voltage regulation is increased to ±5%, compared to ±1/4% with the inverter system. This results in a 5% increase in propellant consumption and propellant storage capacity (approximately 22.7 kg or 50 lb/90 days). The recommended power and alternate control systems are described in the following paragraphs.

The available power buses (based on the system described in ref. 4) for resistojet system operation are shown in table 39.

Table 40 shows the design parameters estimated for the various resistojet power-system analyses. The thrustors are in four modules located on the perimeter of the vehicle. In any module, two thrustors may be fired at any one time; in the entire system, a maximum of four may be fired simultaneously.

Because voltage reduction is needed to operate the system, a voltage-conversion step is necessary. Several alternate methods of voltage reduction were considered. One method would be to pulse-width modulate power from the 56-Vdc load bus to obtain a dc rms output of 4.8 V (for the NH_3 system). Table 39 shows that this method would result in utilizing the least efficient bus. Use of the 260-V link bus with dc pulse-width modulation is not practical

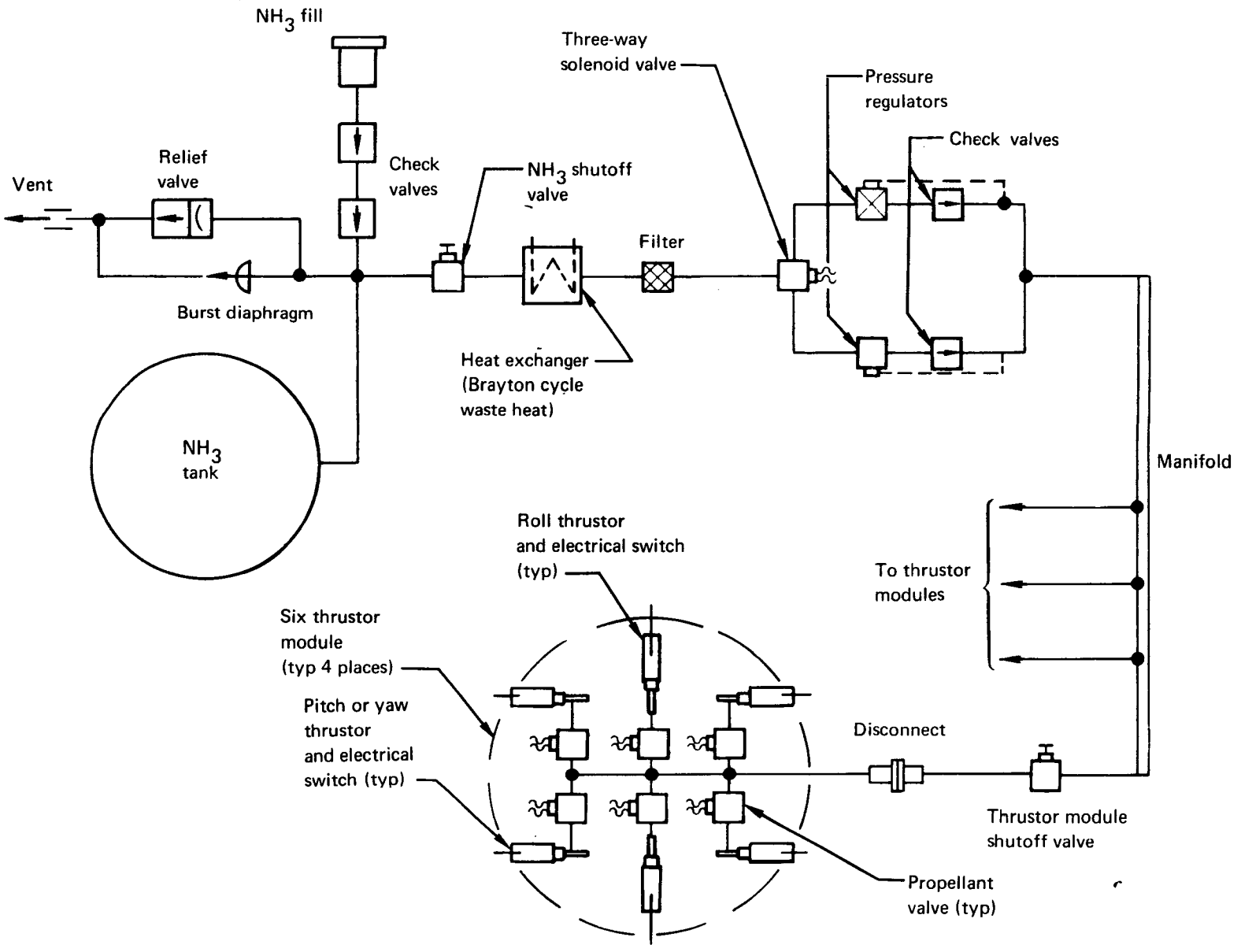

Figure 88. NH_3 Resistojet System

TABLE 36

NH_3 PROPELLANT AND PROPELLANT-TANK REQUIREMENTS[a]

Item	Requirements	
Total Impulse, N-sec (lb-sec) (147-day normal operation)	1.23×10^6	(2.75×10^5)
Specific impulse, sec[b]		364
Required propellant weight, kg (lbm)	342	(755)
Loaded propellant weight, kg (lbm)	352	(779)
Propellant volume, m^3 (ft^3)	0.068	(24.0)
Propellant tank diameter, cm (in.)	109	(43)
Propellant tank wall thickness, mm (in.)[c]	1.65	(0.065)
Propellant tank weight, kg (lbm)[d]	29.4	(65)
Total loaded weight, kg (lbm)	404	(894)

[a]Based on initial ullage of 5% and a maximum-pressure condition of 2 750 000 N/m^2 (400 psia).
[b]44.5 mN (10 mlb) thrustor.
[c]3 440 000 N/m^2
[d]10% allowance for weld and wall-thickness tolerance included.

TABLE 37

NH_3 TANK DESIGN CRITERIA AND STORAGE CONDITIONS

Item	Criterion or condition
NH_3 tank design criteria	
Material	6-Al-4V-Ti
Ultimate tensile strength, N/m^2 (psia)	1.07×10^9 (155 000)
Density, g/cm^3 ($lb/in.^3$)	4.32 (0.160)
Safety factor on ultimate strength	1.4
Proof pressure	1.33 x limit pressure
Weld and thickness tolerance	10%
Minimum gage, mm (in.)	0.504 (0.020)
NH_3 tank storage conditions	
Nominal pressure, N/m^2 (psia)	2 130 000 (310)
Nominal temperature, ^oK (^oR)	320 (585)
Maximum pressure, N/m^2 (psia)	2 760 000 (400)
Maximum temperature, ^oK (^oR)	334 (600)
Limit pressure, N/m^2 (psia)	3 440 000 (500)

TABLE 38

NH_3 CONTROL SYSTEM WEIGHT ESTIMATES

Item	Weight, kg (lbm)	
Control valves	0.45	(1.0)
Pressure regulators	3.18	(7.0)
Hand valves	1.59	(3.5)
Filters	0.18	(0.4)
Accumulators	1.36	(3.0)
Heat exchanger	1.36	(3.0)
Total	6.75	(14.9)

TABLE 39

POWER BUS AVAILABILITY

Bus	Efficiency, %
Alternator, 112/194 V, 3 1067 Hz	97.00
High-voltage dc link, 260 Vdc	95.00
DC load, ±28 V or 56 V	82.45
Motor (square wave), 115/200 V, 400 Hz	89.36
Experimental (sine wave), 115/200 V, 400 Hz	87.46

TABLE 40

THRUSTOR ELECTRICAL CHARACTERISTICS

Unit	Propellant		
	NH_3	H_2	CO_2
Voltage, volts	4.8	6	3
Current, amperes	34.0	40	17
Power, watts/thrustor	163.2	240	51

from a distribution standpoint because of the narrow pulses necessary to reduce the voltage to the proper level. The most efficient and reliable means of achieving the required voltage conversion would be to use a stepdown transformer connected to an ac source. However, direct connection to the stepdown transformer to any ac load bus is not desirable because of the wide voltage-regulation tolerances specified for these buses.

The electrical block diagram for the selected power system is shown in fig. 89. Electrical power is supplied from two 400-Hz single-phase, 200-V, square-wave inverters to be described later. The inverters are connected with one supplying the entire system; a second is on standby. Output voltage regulation is 1/4%. This inverter power comes from the 260-V dc link bus and the control power comes from the nonessential 28-V dc load bus.

In designing the inverter, several tradeoffs were considered. The alternatives considered in designing the output stage were a push-pull output or a bridge output. Also considered was the use of transistors or silicon control rectifiers (SCR's) as the power switches. The bridge output stage was selected because the voltage on the semiconductor would be equal only to the input voltage of 260 V, instead of twice that value in the push-pull output stage. The lower voltage in the bridge circuit would offset the small additional loss in the semiconductor by having two saturated devices on at the same time, rather than one as in the push-pull design.

Transistors should be used in the output stage rather than SCR's. Transistors, now available in 500-V ratings, will work well in this application. The small increase in efficiency gained in the SCR circuit because of the elimination of base drive requirements does not warrant the increase in circuit complexity resulting from the commutation components needed to turn off the SCR's. Although the output transistors do not have the surge capability of the SCR, the transistors will be protected from overloads on the output by an SCR "crowbar" circuit.

The drive-stage frequency will vary directly as a function of input voltage. Therefore, frequency of the output will vary from 375 to 425 Hz, with a 25.5 to 28.5 input voltage range. The output transformers were designed around a 1.2 T (12 000 G) flux density at 400 Hz. At the low frequency, this would raise the flux density to 1.28 T (12 800 G) and the core loss would increase 1.1 W/kg (0.5 W/lbm). This increase would raise the transformer dissipation 0.25 W/transformer. The saving of 2 W in the entire system does not warrant the increased circuit complexity of regulating the input voltage to the driver stage.

Output regulation is accomplished by pulse-width modulating the drive waveform to the output transistors. This modulation is accomplished by a magnetic amplifier control as described above in response to feedback from the output voltage. Pulse-width modulation was chosen for regulation because of its low losses. Table 41 shows a breakdown of the dissipation and efficiency of the inverter.

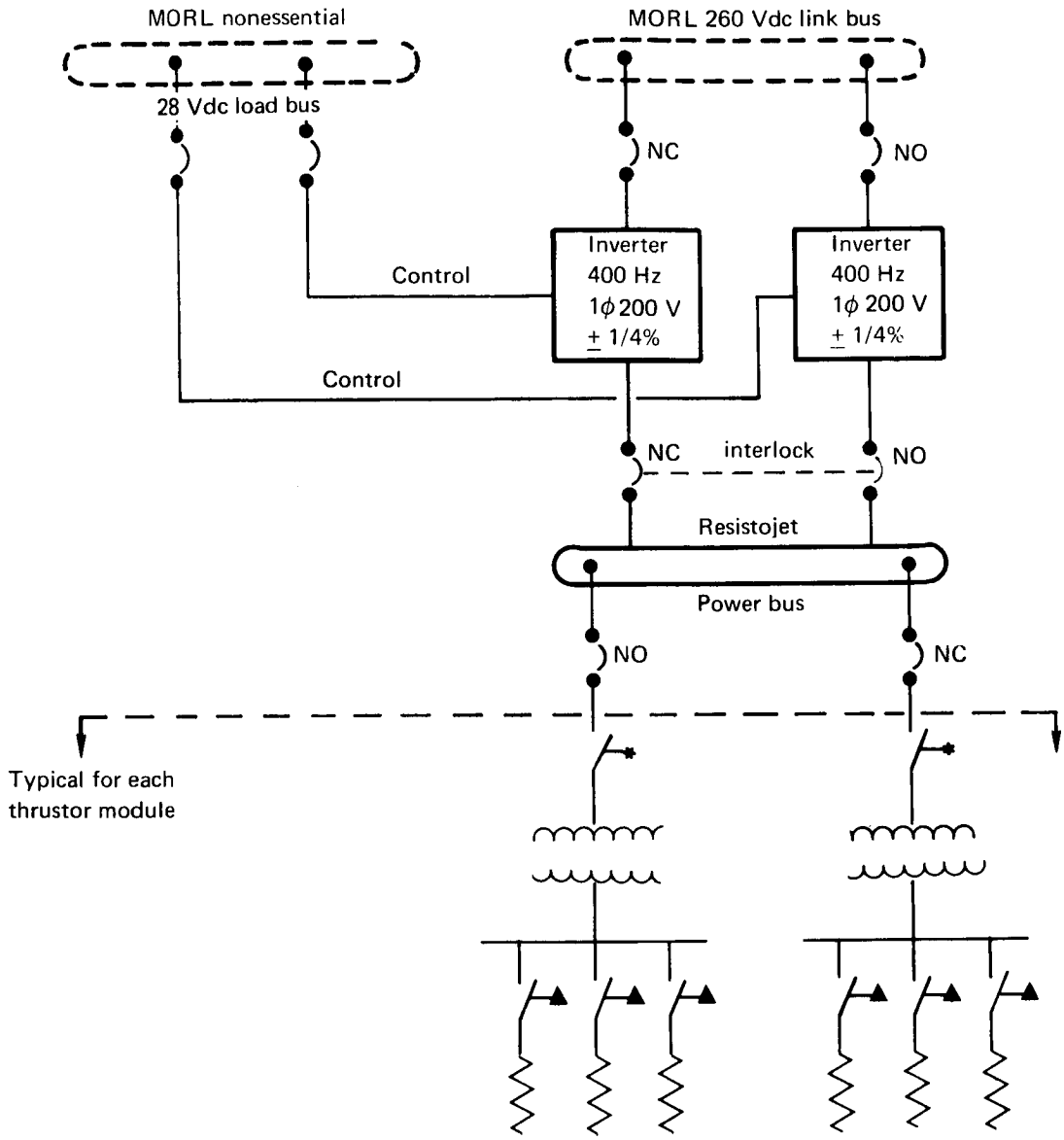

Figure 89. Resistojet Power System Block Diagram

TABLE 41

INVERTER POWER DISSIPATION*

Description	Power (W)
Output transistors	2.0
Base resistors	0.8
Driver transformer	0.5
Crowbar	0.25
Magnetic amplifier	0.25
Miscellaneous	2.20
	6.0

*Power output: 600 W
Efficiency: 99%

The efficiency tabulated in table 41 is higher than is generally experienced for inverters. The high efficiency is largely the result of the following design factors:

(1) The power-handling elements operate at high voltage and low current.

(2) Transistors operate in the highly efficient switching mode. No output transformer is required in the inverter. The control circuit operates at low voltage, but handles only a small percentage of the output power. This factor also improves the reliability of control elements.

A three-phase inverter of similar design now in service on the Saturn S-IVB exhibits an efficiency of 97% when supplied with 56-V power. This includes the loss of a low-voltage regulator and over-driving timer, both of which are not of high efficiency.

Fig. 90 shows a block diagram of the MORL resistojet inverter. Input power from 28-V and 260-V dc sources supplies the inverter which has a pulse-width-modulated, ac, square-wave output as shown in fig. 91. This waveform is modulated to 200 V rms with ±1/4% voltage regulation when the 260-Vdc input is held to the ±1% regulation specified for the dc link bus.

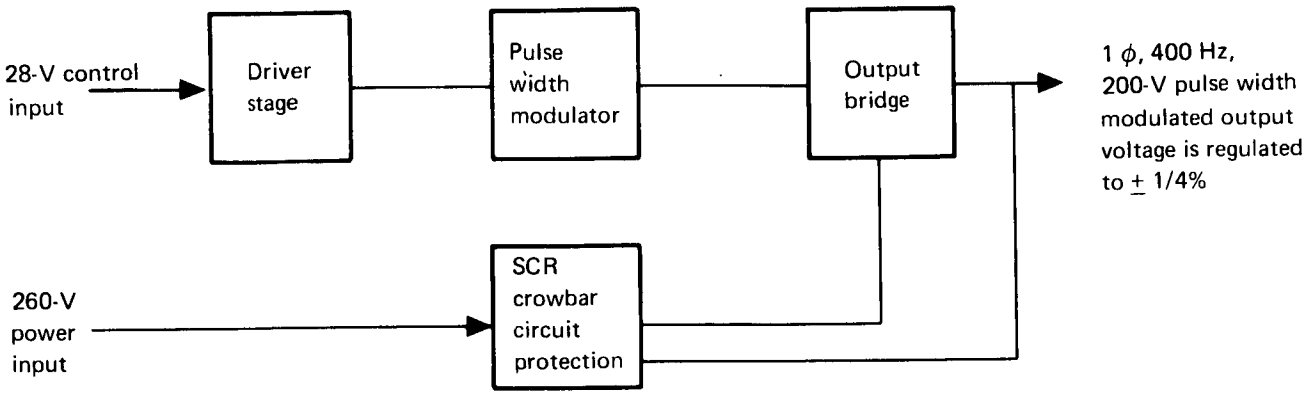

Figure 90. Inverter Design

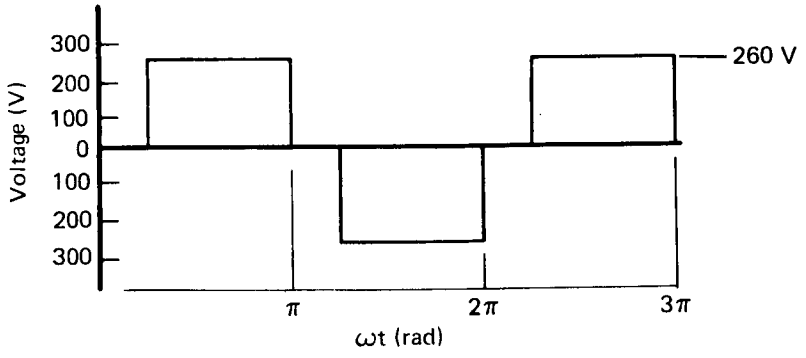

Figure 91. Inverter Output

The inverter schematic is shown in fig. 92. The output stage is protected from external shorts by an SCR crowbar circuit that opens the 260-V input circuit breaker, should the output voltage fall below a specified level. The output stage is driven by a magnetic-coupled multivibrator which is supplied directly from the 28-Vdc load bus. The driver output is pulse-width-modulated by a magnetic amplifier whose gate windings are connected in series with the base of one of the two conducting series output transistors. Two of the bridge-connected transistors are therefore allowed to conduct for a controlled period in each half-cycle. Current for the control windings will be supplied from a feedback control circuit that senses the output voltage. By variation of this control current, the width of the zero dwell of the output waveform will be adjusted to hold the rms voltage value to within the 1/4% tolerance required.

In designing the power-control system, the main variables to be determined were the number of stepdown transformers to be used and their location on the vehicle. These factors affected weight and efficiency of the system more than any other design criteria.

In selecting the transformer design, a study was made to determine whether a single-phase or a three-phase design would be used. Design showed that the single-phase unit was lighter and more efficient than the three-phase design, because the three-phase transformer could be required to operate with only one phase loaded.

Table 42 shows the transformer combinations considered, and the resultant weights and efficiencies are presented in fig. 93 for H_2 and NH_3.

The lower total efficiency and higher weight in fig. 93 of the 1-k VA transformer over the two 500-VA units (Hz system) resulted because of a change from a C-core in the 500-VA design to an E-core design in the 1000 VA. No C-cores were available in the 1-k VA range.

The transformers used to supply power to the resistojet were designed to meet, in order of importance: (1) efficiency, (2) reliability, and (3) weight requirements.

Four-mil grain-oriented silicon steel C- and E-cores were selected for core material. These cores were selected over a toroidal core because of the large strap wire needed to carry the high secondary currents; 1.2 T (12 000 G) was selected as the flux density of the magnetic material.

Table 43 shows the circuit lengths assumed in the power distribution systems for the optional transformer configurations considered.

Fig. 94 (a) and (b) shows power-distribution weight as a function of design efficiencies, including the weight of mounting hardware for the electrical cables and transformers. The total power system weight and efficiency for H_2 and NH_3 are shown in fig. 95 (a) and (b). Fig. 95 (a) shows that the lightest, most efficient system for H_2 propellant is one that uses eight 250-W transformers, two for each thrustor module. Fig. 95 (b) for NH_3 propellant shows that the eight-transformer design has a slight advantage until a system

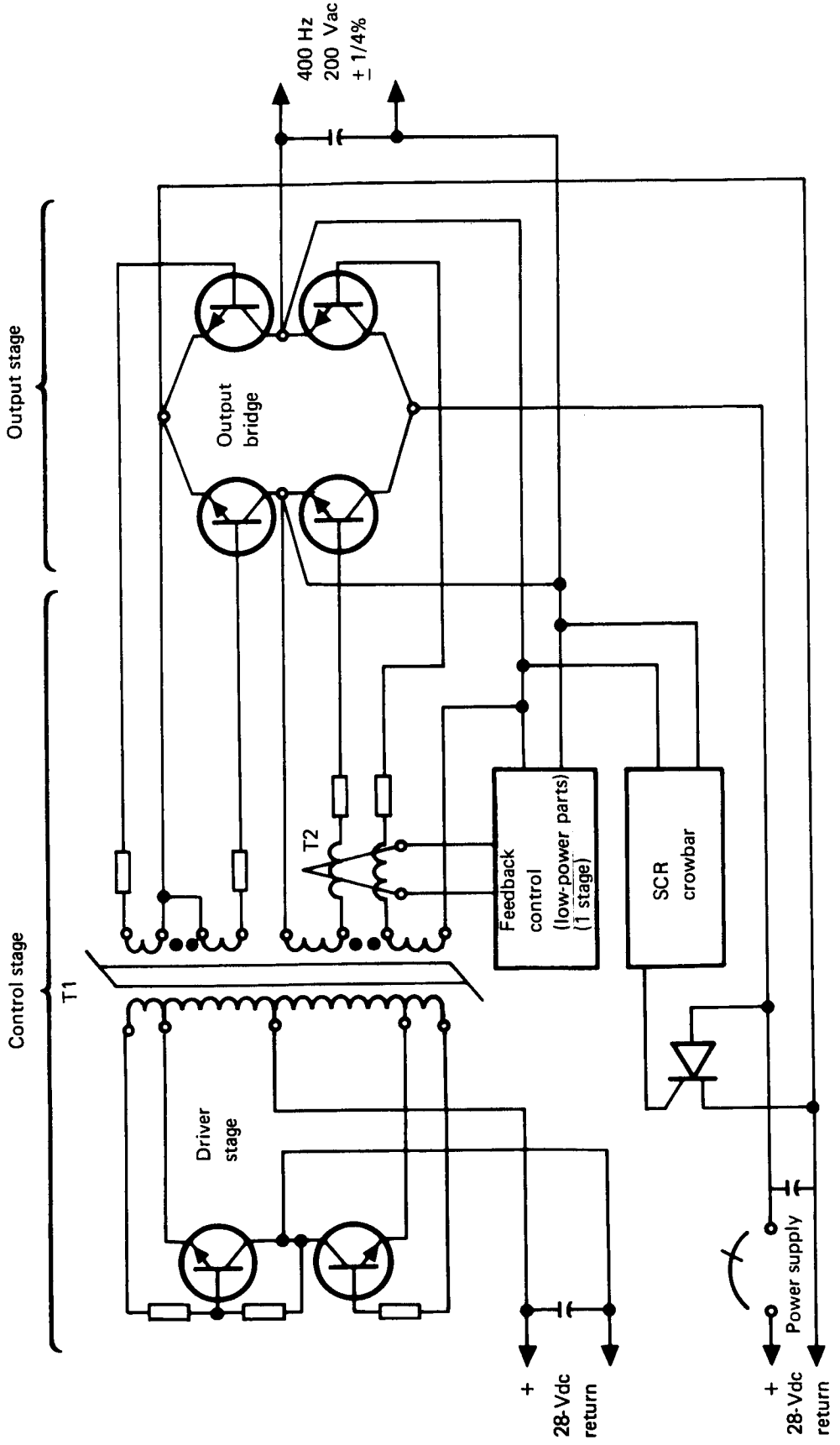

Figure 92. MORL Resistojet Power Inverter

TABLE 42

TRANSFORMER COMBINATION

Number of transformers	Transformer rating (VA)		Number of thrustors supplied by each transformer
	H_2	NH_3	
1	1000	650	All
2	500	326	Three thrustors in four modules.
4	500	326	Three thrustors in two modules
8	250	163	Three thrustors in one module.
12	250	163	Two thrustors in one module.

efficiency of about 95% is approached. Future system changes which may not permit use of the vehicle structure because of electric currents would not affect the eight-unit system, but would significantly degrade all the other system concepts.

Based on the foregoing analysis, the eight-transformer system is the system chosen for both resistojet systems.

Fig. 96 (a) and (b) show the results of an optimization of the eight-transformer systems for the NH_3 and H_2 systems. The effect of system efficiency on the power system weight, as well as the weight assessment for power consumption, is indicated. Because both these weights must be charged to the resistojet system, the summation curve shown in the figures becomes the important criterion insofar as weight is concerned. Thus, for the NH_3 resistojet system, a power control system weighing 16.3 kg (36 lbm) and yielding an efficiency of 94% was selected while for the H_2 system, the power control system weighs 16.7 kg (37 lbm) and also has an efficiency of 94%. Similar tradeoffs for the CO_2 system yield a 15.8 kg (35 lbm) power-control system at an efficiency of 94%.

To evaluate the possibility of using sources that have a higher electrical efficiency without additional regulation of their voltage output, an alternate power control system was defined. As shown in table 39, on the basis of efficiency, the alternator bus appears the best choice. Selection of the alternator bus is enhanced by its present capability of supplying thrustor loads, whereas both the motor bus inverter and the experimental bus inverter would require redesign for higher power. The introduction of loads directly upon the alternator buses, however, would represent a violation of the following ground rules applied to the MORL power system study: (1) all vehicle loads shall be shared between the alternators and (2) no vehicle loads shall be supplied from within the zone of protection established by the current differential protection subsystem.

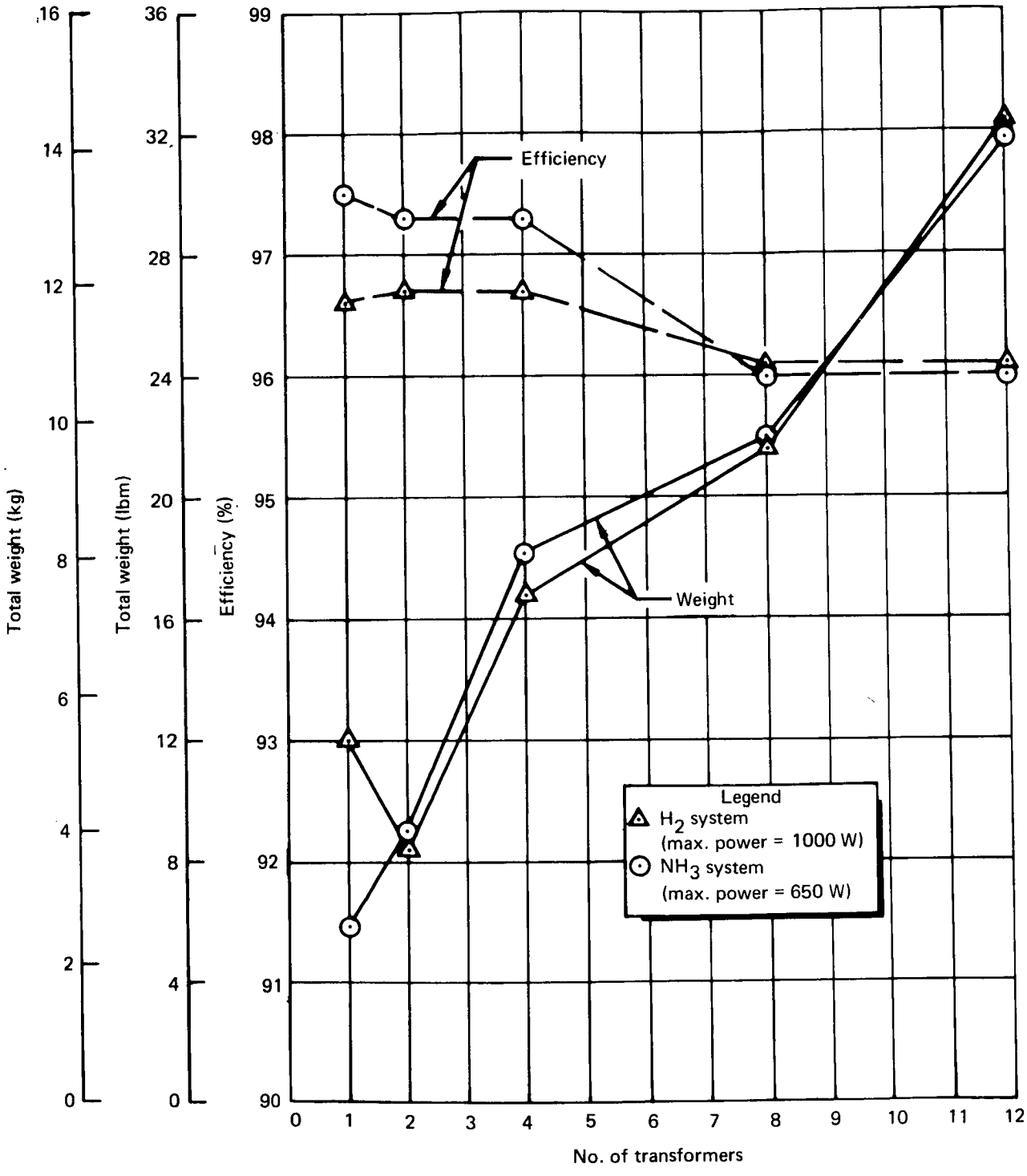

Figure 93. Total Transformer Weight and Efficiency for H_2 and NH_3

TABLE 43

POWER-DISTRIBUTION SYSTEMS

System	Number of transformers	Transformer size, W	Circuit length, m	Circuit length, (ft)	Circuit voltage, (V)
1	1	1000	17.3	(056.6)	4.8
2	2	500	37.6	(123.2)	4.8
3	4	500	21.0	(068.8)	4.8
4	8	250	17.3 4.9	(056.6) (016.0)	200.0 4.8
5	12	250	19.7 7.3	(064.6) (024.0)	200.0 4.8

Fig. 97 shows the portion of the MORL electrical power system which would be involved in an alternator bus supply scheme. Possible points of connection for the resistojet power bus are identified as Points A or B. The current differential protection-zone boundary is defined by the current transformers (CT's). It is possible to avoid this load exclusion zone by connection at Point B rather than A. The load-balancing circuit, however, is located in the output regulations section of each high-voltage rectifier. A degree of load balancing can be obtained by connecting the resistojet bus and loads as shown in fig. 97 and by operating them on a controlled schedule to equalize the alternator loading. This operating mode would increase the complexity of the thrustor control logic, however, and a random equalization may be preferable for the small thrustor power demand. Future growth of the system would require a change in the control logic and load circuits. The three-way interlock circuit ensures that the alternators can never be inadvertently connected in parallel. It also permits all resistojet thrustors to be energized if either alternator is removed from service. In this event, it is also possible to operate the thrustors without electrical power. The thrustors can be supplied from the three-phase source bus as shown in fig. 98. There are eight groups of thrustors in four locations. Only one thrustor of each group (such as a, b, or c) is operative at a time. The groups are assigned to electrical power phases A, B, and C as shown with 3, 3, and 2 groups, respectively.

The above evaluation shows that the resistojet power-control system can be supplied directly from the 1067-Hz alternator. The imbalances of the alternator load and of electrical phase loads are tolerable but are restrictive should power demands increase.

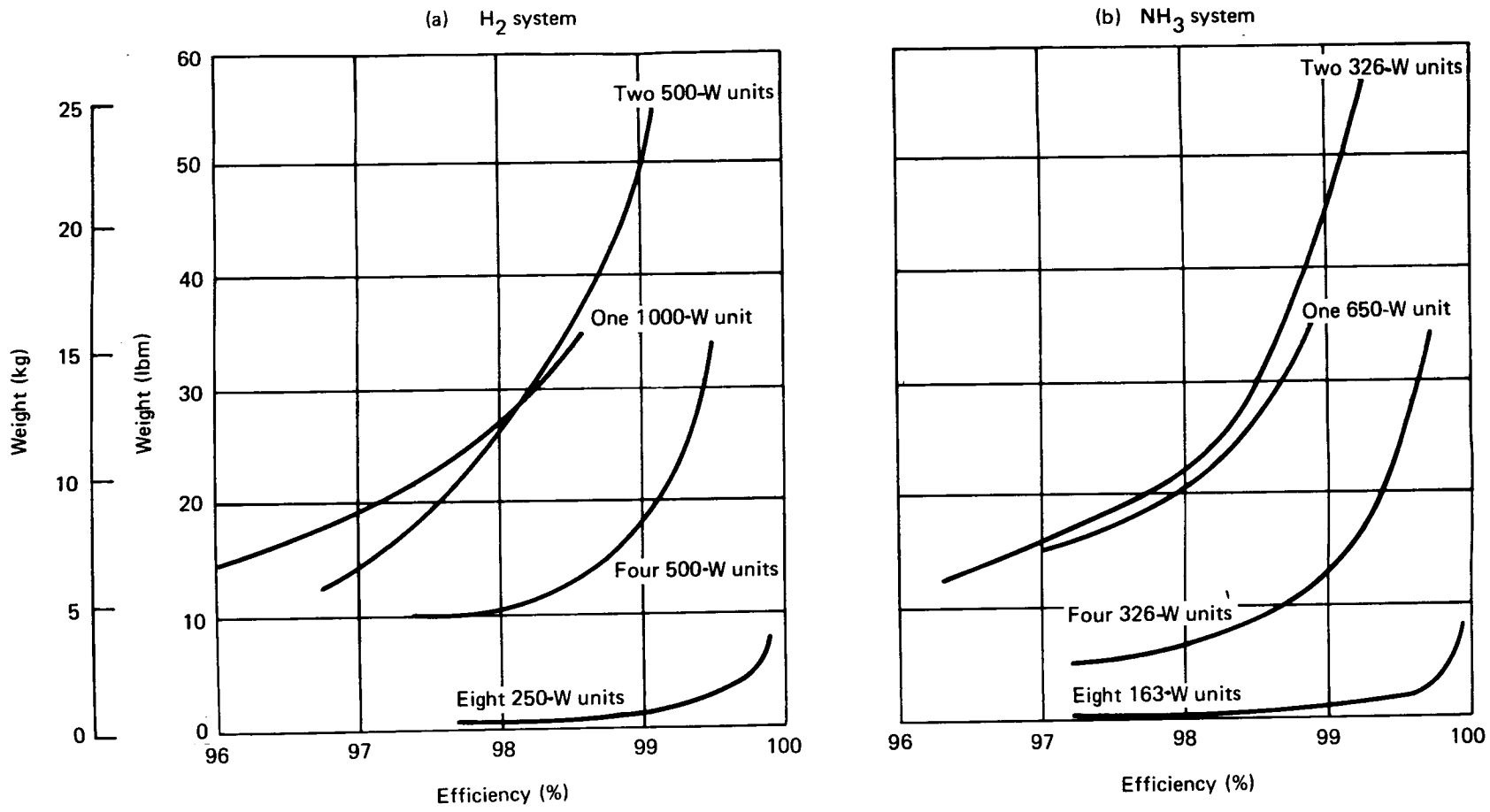

Figure 94. Resistojet Power Distribution System

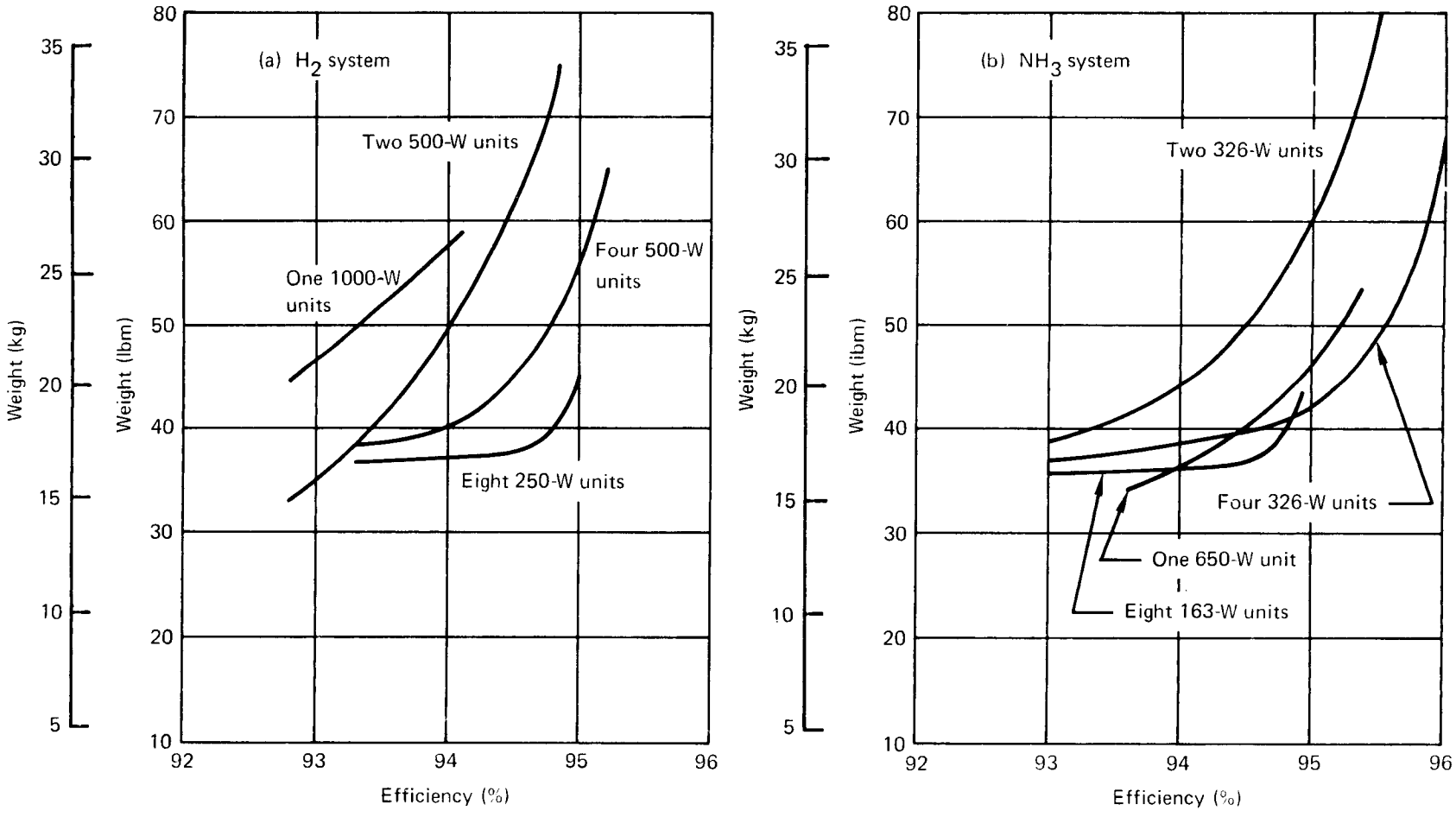

Figure 95. Resistojet Power Control System

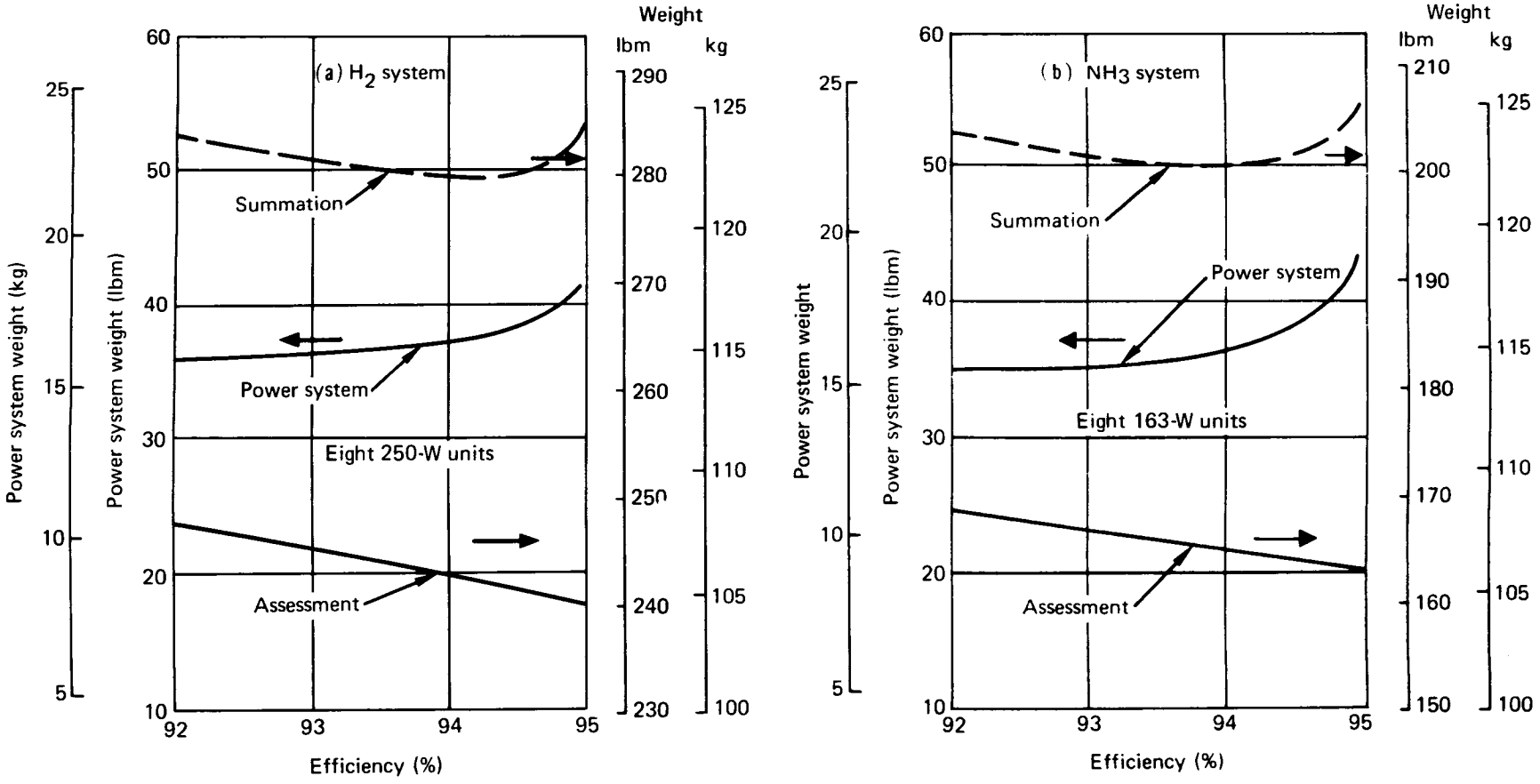

Figure 96. Resistojet Power Control System Optimization

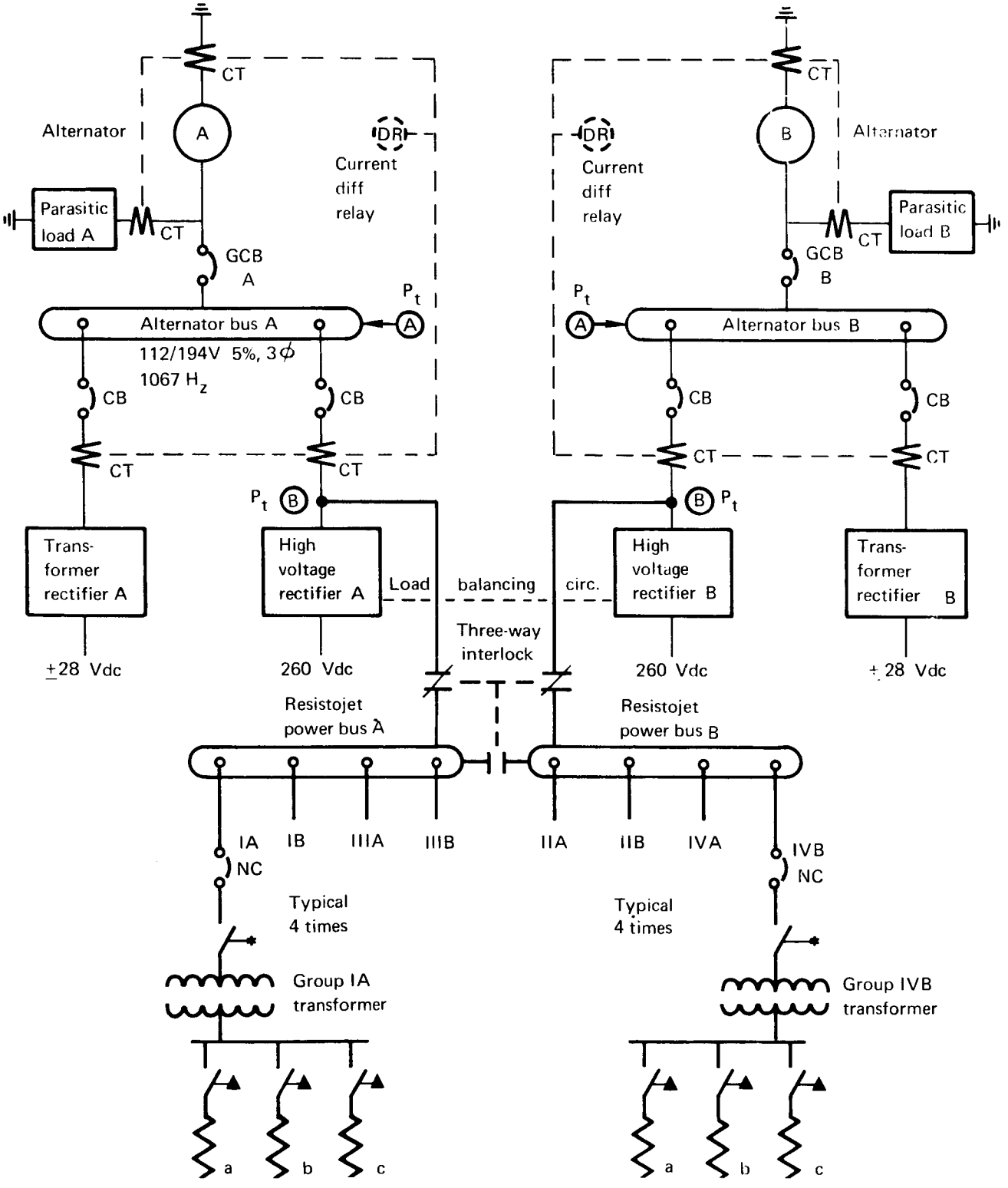

▲ Individual thrustor control switch

* Master thrustor control switch

Figure 97. Alternate AC Power Supply for Resistojet System

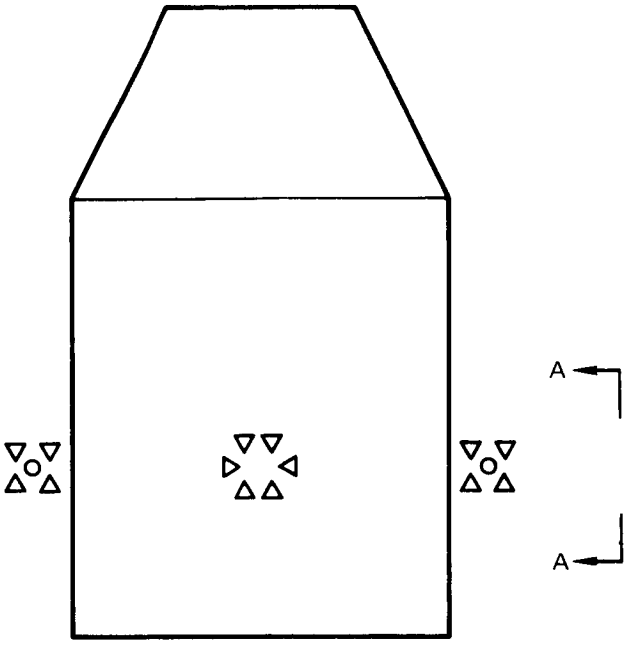

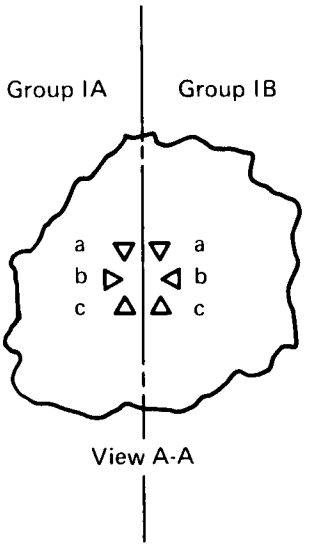

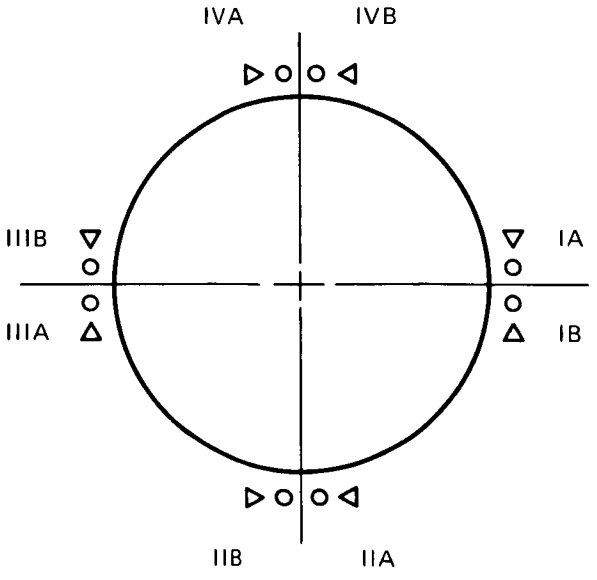

Electrical source and phase assignment

Group	Source	Phase
IA	Alt. A	A
IB	Alt. A	B
IIA	Alt. B	B
IIB	Alt. B	C
IIIA	Alt. A	C
IIIB	Alt. A	A
IVA	Alt. B	B
IVB	Alt. B	A

Figure 98. Thrustor Group Power Supply

The alternate system without inverters increases the power-control system efficiency by 4% and therefore reduces the average power demand by 6 W per thrustor. Reliability of the power-control system is not appreciably changed, because loss of inverter voltage-regulator control in the recommended system is comparable to loss of the alternator-field voltage-regulator control in the alternate system shown in fig. 101. Elimination of the inverters, which are connected in series with the resistojet thrustors, would increase the reliability of thrustor power supply. However, power-supply continuity is necessary only for maximum performance and is not essential for thrustor operation during an emergency or power loss.

The resistojet performance variation for both the ±1/4% inverter system and the ±5% alternate system is shown in table 44. For either system, the propellant supply is 276 kN/m^2 ±7 kN/m^2 (40 psia ± 1 psia). This pressure-supply variation results in a resistojet thrust variation ranging from (0.0434 to 0.0457 N) (9.75 to 10.25 mlbf), regardless of the power-control system. The power-control system affects the resistojet power and, therefore, the inner-heating-element temperature, thus controlling the unit performance (specific impulse). Table 44 was established by setting the maximum operating voltage for the NH_3 resistojet (4.8 V) in conformance with the requirement to eliminate or minimize degradation for extended operating life.

For the ±1/4% system, the voltage variation is negligible; therefore, maximum, nominal, and minimum voltage were considered identical. The performance variation shown is the result of propellant-supply pressure and results in a total variation of 4 sec of specific impulse (1.3%) and 3 W of thrustor power (2%).

For the ±5% system, the maximum voltage had to be set at 4.8 V to minimize degradation. This resulted in thrustor voltages of 4159 V and 4.36 V for nominal and minimum operating design points. At each voltage, the performance and power variation from propellant-supply pressure are identical to that of the ±1/4% system. At a fixed supply pressure, however, the effect of voltage results in a variation of 30 sec of specific impulse (10%) and 20 W of power (14%). Maximum variation is determined as the difference between resistojet operation at maximum voltage with minimum propellant supply pressure and minimum voltage with maximum propellant supply pressure. This maximum variation is 34 sec of specific impulse (11%) and 23 W of power (16%).

If the baseline ±1/4% system is compared with the alternate ±5% system, it should be noted that the system must be designed around the nominal design point (table 44). Because of the difference in performance, the alternate system requires a 5% increase in propellant resupply and the associated larger capacity and weight of propellant tankage [approximately 22.7 kg (50 lbm)] per resupply. The alternate system, however, requires 6.5% less power and provides less severe thrustor operating conditions (lower nominal inner-heating-element temperature). The performance variation with the ±5% system may require a more complicated logic control for thrustor operation, because performance becomes a primary variable.

TABLE 44

RESISTOJET PERFORMANCE VARIATION

Measurement	Supply pressure, N/m^2 (psia)	Thrust, mN (mlbf)	±1/4% Baseline system			±5% Alternate system		
			Max.	Nominal	Min.	Max.	Nominal	Min.
P, W	26.8 (39)	43.4 (9.75)	4.812	155.5	4.788	155.5	145.5	135.5
V, V				4.8		4.8	4.585	4.358
R, ohms				0.153		0.153	--	--
I, A				31.9		31.9	--	--
I_{sp}, sec				310		310	295	280
P, W	27.5 (40)	44.5 (10.0)	4.812	154	4.788	154	144	134
V, V				4.8		4.8	4.585	4.358
R, ohms				0.15		0.15	0.146	0.142
I, A				32.0		32.0	31.45	30.7
I_{sp}, sec				308		308	293	278
P, W	28.2 (41)	45.6 (10.25)	4.812	152.5	4.788	152.5	142.5	132.5
V, V				4.8		4.8	4.585	4.358
R, ohms				0.147		0.147	--	--
I, A				32.25		32.25	--	--
I_{sp}, sec				306		306	291	276

= nominal design points

Evaluation and selection: By use of the guidelines set forth in the Statement of Work, it is possible to establish the significant criteria upon which an evaluation of the several candidate resistojet thrustor systems can be made. These criteria include performance, power requirements, launch weight, resupply weight, growth potential, development risk, maintainability, reliability, and crew time.

The selection of the recommended system can be influenced to some degree, depending on the importance assigned to each of the various criteria. For the presently defined mission, the thrustor system which best satisfies most of the criteria is the NH_3 resistojet. In the following paragraphs the ability of each of the three candidate resistojet thrustor systems to satisfy the established criteria is discussed. Table 45 presents a summary of the H_2, NH_3, and CO_2 biowaste resistojet systems.

Table 45 shows that the NH_3 resistojet requires about 35% less power than the H_2 engine. The 1667°K (3000°R) biowaste thrustor exhibits the lowest power requirement of the three. The H_2 system can achieve the highest specific impulse of the candidate thrusors and consequently requires less propellant per day. However, because the biowaste system does not require propellant resupply, specific impulse is not a critical parameter so long as sufficient daily impulse is available. Thus, the fact that the CO_2 system I_{sp} is lower than either H_2 or NH_3 is not a significant criterion for evaluation of the biowaste system.

The H_2-system chargeable launch weight is higher than the NH_3 system, in spite of its higher specific impulse and lower propellant-weight requirement. This is basically caused by the very low density of the H_2 and the resultant large propellant-tank volume required. The volume of the H_2 tank is about five times that of the NH_3 tank. In addition, the propellant tanks contain only a 20-day supply at launch; consequently, the difference in propellant weight between the H_2 and NH_3 systems represents only a small percentage of the launch-weight penalty.

The biowaste system has the lightest launch-weight penalty because no propellant is onboard. Furthermore, the propellant tank (accumulator) is small, because it stores only a 1-day supply of CO_2, as opposed to the H_2 and NH_3 tanks which must be sized to store a 147-day propellant supply.

In terms of resupply weight, the impact of the high specific impulse of the H_2 system is evident. Even though it has a higher system dry weight than the NH_3 resupply system, its loaded propellant weight is only about half the weight of NH_3 required. This results in a lower total chargeable 90-day resupply weight for the H_2 system. The biowaste CO_2 has no chargeable resupply weight.

Both the H_2 and NH_3 resistojet systems exhibit total-impulse growth potential that is limited by the maximum tank volume allowed and the maximum power available. The H_2 tank required to provide total impulse of the baseline MORL is about 1.98 m (6.5 ft) in diameter, while the NH_3 tank is approximately 1.07 m (3.5 ft) in diameter. In terms of available volume for

TABLE 45

RESISTOJET SYSTEMS SUMMARY

Parameter	H_2	NH_3	CO_2
Chamber temperature	2420°K (4356°R)	2420°K (4356°R)	1667°K (3000°R)
Delivered specific impulse	735 sec	364 sec	177 sec
Required power	249 W	159 W	102 W
Propellant tank volume	3.34 m^3 (118 ft^3)	0.68 m^3 (24 ft^3)	0.25 m^3 (8.8 ft^3)
Power-control system weight	16.8 kg (37 lbm)	16.3 kg (36 lbm)	15.9 kg (35 lbm)
Total dry weight	113.0 kg (248 lbm)	79.3 kg (174 lbm)	49.5 kg (109 lbm)
Weight assessment for electric power	107.0 kg (236 lbm)	68.6 kg (151 lbm)	44.0 kg (97 lbm)
20-day loaded propellant weight	27.0 kg (59 lbm)	48.1 kg (106 lbm)	4.5 kg (10 lbm)
Total chargeable launch weight	247.0 kg (543 lbm)	196.0 kg (431 lbm)	98.0 kg (216 lbm)
147-day loaded propellant weight	192 kg (423 lbm)	354 kg (779 lbm)	4.8 kg (10.5 lbm)
Logistics vehicle chargeable dry weight	109 kg (241 lbm)	60 kg (134 lbm)	---
Logistics vehicle pressurant weight	13 kg (28 lbm)	20 kg (44 lbm)	---
Logistics vehicle loaded propellant weight	116 kg (256 lbm)	216 kg (475 lbm)	---
Total chargeable resupply weight per 90 days	238 kg (525 lbm)	296 kg (653 lbm)	---

Notes: 1. Thrust = 0.045 N (10 mlbf).

2. Chamber pressure 241 kN/m^2 (35 psia).

packaging the propellant tank in the MORL aft interstage, the NH_3 system has the greater growth potential. The weight of the tank hardware will increase with the increasing total-impulse requirement and, in terms of a fixed, maximum launch weight, the NH_3 system again demonstrates the greater growth potential.

If it is assumed that fixed, maximum power is available, the biowaste system exhibits the largest growth potential in terms of increasing power requirements. For early application, a biowaste CO_2 system operating at 1111°K (2000°R) can meet the baseline daily impulse requirements if all the available CO_2 is used. However, it offers no growth potential until high-temperature oxidation-resistant materials are sufficiently defined to permit higher operating temperatures and increased specific impulse. The system shown in table 45 at 1667°K (3000°R) chamber temperature has the capability of a 35% increase in total impulse (over the baseline requirement) by increasing the accumulator size to accommodate all the CO_2 available. Growth beyond this point would require either a further increase in operating temperature or the use of the combined CO_2/H_2 biowaste thrustor system.

The cryogenic H_2 system and the biowaste system represent higher development risks than the NH_3 system. One of these risk areas is the design of the cryogenic H_2 tank and insulation. It must be sized so that the maximum heat leak into the LH_2 just provides sufficient boiloff to maintain the minimum flow rate required. In addition, the electric heater must be capable of raising the boiloff to the maximum flow rate required without allowing excess boiloff after the heater is turned off. This entire tank and feed system must operate and be tested in a zero-g environment. The thermal vapor-liquid separator also requires testing in a zero-g environment.

The biowaste thrustors present a materials development risk in that they must survive for an extended period of time in an oxidizing environment at elevated temperatures. These materials have not yet been identified, although some work along these lines is being pursued in the industry. A biowaste CO_2 thrustor operating at 1111°K (2000°R) can be fabricated from stainless steel, but at temperatures above this, an advance in the materials technology is required.

The NH_3 and H_2 resistojet systems will require approximately the same crew time in system monitoring and propellant resupply operations. The biowaste system represents a significant reduction in crew time required to maintain the resistojet/CMG control system. Because no propellant resupply is required, the crew activity needed for manual operations during propellant transfer is eliminated.

For comparison, gross reliability predictions were made for the three resistojet reaction-control systems. These systems differ only with respect to type of propellant and a few associated items unique to each propellant. Reliability was expressed as both (1) the probability of no system shutdown, and (2) the probability of no system loss from a single failure, assuming that the system can be shutdown to effect repair.

Probabilities (1) and (2) vary inversely with each other and, therefore, could not be simultaneously maximized but, rather, had to be traded off to optimize the total RCS. Alternate feed-system configurations were considered in maximizing (1) and (2) for each propellant. Of the configurations considered for attaining the highest probability of no system shutdown, the NH_3 system ranked first, while all the configurations analyzed for attaining the highest probability of no system loss achieved a probability value very close to unity. Table 46 presents the results of the comparative reliability for the configurations yielding maximum probability of no system shutdown.

The failure rates used in this analysis were obtained from the S-IVB Program or the Apollo Extension System (AES) or they were estimated. All probabilities were assumed time-dependent where time equalled the calendar time in space. This assumption yields only a small error in the results because the RCS is normally continually on with very little cycling. This implies that the expected failures caused by cycling are extremely small. The thrustor module was not considered in this comparative analysis because it is common to all systems and configurations.

A resistojet system presents fewer potentially hazardous situations than conventional chemical-thrustor systems. No combustion is required, eliminating prime sources of danger: hypergolicity or ignition system malfunctions. Other potential hazards can be eliminated by careful design. For example, all propellant lines and storage tanks are located in unpressurized sections of the vehicle, completely isolated from the habitable areas. In case of propellant leakage, the vapors are quickly dissipated to space, and (in the absence of O_2) H_2 leakage will not present a hazardous situation. In this respect, NH_3 and CO_2 are potentially safer propellants. The toxicity of NH_3 will not affect crew safety during thrustor-system maintenance, because pressure suits are required for maintenance operations.

If the power supply to the resistojet heat-exchanger element fails, or the element itself fails, the resistojet can still operate at the required thrust level with an increase in propellant flow. This will permit stabilization of the vehicle until it is convenient to curtail the experiment program to make corrective repairs. In any event, the high-disturbance control system (N_2H_4 monopropellant) can be used as a backup for control.

TABLE 46

COMPARATIVE RELIABILITY PREDICTIONS

System	Probability 1	Probability 2
NH_3	0.871	0.983
H_2	0.816	0.967
CO_2	0.839	~1

The foregoing comparison has led to the selection of the NH_3 resistojet system for use on the MORL baseline. It yields a lower launch weight, lower power requirement, greater growth potential, and less development risk than the cryogenic H_2 system. The NH_3 system is also simpler and more reliable: no cryogenic system is required, no chilldown operations are necessary, and a prolonged countdown hold will not affect the system.

The biowaste CO_2 resistojet remains an attractive candidate system but requires basic materials research to identify a performance thrustor. The level of performance required as a function of the impulse required per day.

Operational disturbance control. — This following discussion concerns the operational disturbances from docking impact, logistics vehicle stowage, and 9-g centrifuge operation. The disturbances are defined and their effect on vehicle attitude and rate is derived. Typical crew-motion disturbances are treated in the same manner as operational disturbances. A thrustor system capable of meeting the baseline stabilization and control system (SCS) performance requirements is defined. The requirements are then reviewed to determine their applicability to the operational disturbances. Wherever possible, SCS requirements (thrust level and/or CMG momentum storage capacity) are reaffirmed or applicable requirements are established for the operational disturbance and other events requiring high thrust.

Definition of disturbances: — The disturbance imparted to the MORL by the docking of a logistics vehicle was previously defined as a body rate of 0.004 rad/sec (0.25°/sec). A combination of errors which will produce this rate are a misalignment of 0.0875 rad (5°), a docking velocity of 0.3 m/sec (1/fps), and a lateral offset of 0.15 m (0.5 ft) (fig. 24).

Gemini docking requirements are as follows:

(1) 0.15 m/sec (0.5 fps) lateral rate.

(2) 0.3 m/sec (1.0 fps) axial rate.

(3) 0.3 m/sec (1.0°/sec) pitch and yaw rate.

(4) 0.3 m/sec (1.0°/sec) roll rate.

(5) 0.3 m (1.0 ft) lateral offset.

(6) 0.175 rad (10.0°) attitude error.

A comparison of the Gemini requirements with the selected values indicates that a tumble rate of 0.004 rad/sec (0.25°/sec) is reasonable.

A typical stowage cycle (considered to be minimum time) consists of performing the two rotations of fig. 99 utilizing a constant 222.5 N-m (50 ft-lbf) moment. The exact attitude history of the MORL during stowage of a logistics vehicle with no control actuation would be very difficult to determine because of varying configuration and mass. However, a reasonable

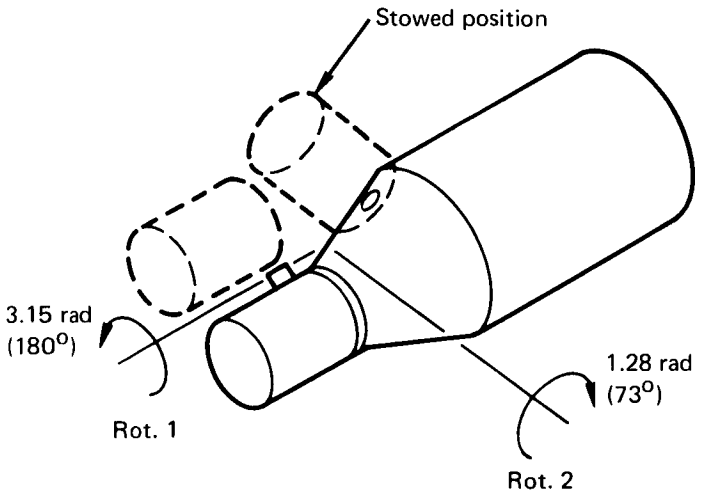

Figure 99. Stowage Disturbance

approximation can be obtained by ignoring the above effects. Angular displacements imparted to the MORL (Configuration X) by stowage are as follows:

(1) Rotation 1

(A) Roll = 0.67 rad (38°).

(B) Pitch = 0°.

(C) Yaw = 0°.

(2) Rotation 2

(A) Roll = 0.058 rad (3.3°).

(B) Pitch = 0.11 rad (6.5°).

(C) Yaw = 0.14 rad (8.0°).

Rotation 1 requires 144 sec and Rotation 2 requires 99 sec.

The above displacements are for a stowage port with a centerline canted 0.30 rad (17°) to the plane formed by the pitch and yaw axes and inclined 0.79 rad (45°) to the same axes. Note that the stowage cycle cited is typical of those experienced during the MORL mission. Parameter variation, such as configuration changes of the MORL and logistics vehicle and stowage port location would affect the displacement angle.

The belly-down orientation can be maintained during stowage with the baseline CMG's, provided that the stowage cycle is properly regulated. Assume application of a 67.8 N-m (50 ft-lbf) moment until a 1355 N-m-sec (1000 ft-lbf-sec) of angular momentum about pitch and/or yaw or 3387 N-m-sec (2500 ft-lbf-sec) about roll has been generated. The logistics vehicle then rotates at a constant rate, maintaining constant momentum. At an appropriate stowing angle, a 67.8 N-m (50 ft-lbf) decelerating moment will be applied to stop the logistics vehicle. During deceleration, the angular momentum generated during acceleration will be removed. Stowing times are increased to 160 sec for Rotation 1, 3.15 rad (180°) and 138 sec for Rotation 2, 1.28 rad (73°).

The centrifuge onboard the MORL provides 1-g acceleration for occupants undergoing normal crew conditioning. Past studies have shown that a weight saving is realized by sizing the roll CMG's to store the angular momentum generated by 1-g operation. A 9-g centrifuge operation (re-entry simulation) determines the fitness of crew members to withstand the gravity forces during re-entry.

A 9-g centrifuge operation is initiated on the 11th day after beginning the fitness program; every 18 days thereafter, a re-entry simulation will be conducted for each crew member. For the MORL Resistojet Control System Study, the first re-entry simulation is assumed to occur 18 days after initial manning. Because two crew members ride the centrifuge at the same time, three separate re-entry simulations are required every 18th day for a total of 15 over a 90-day period and 24 over a 147-day period.

The re-entry simulation alternately accelerates and decelerates the occupants at realistic on-set rates to produce an approximation of the gravity forces experienced during re-entry which are shown on fig. 100 for a worst-case (minimum range) Apollo re-entry from a 370-km (200-nmi) orbit. Each centrifuge run will last about 20 min, including a 1-g hold for 15 min after the re-entry run, to more closely simulate an actual re-entry. The peak angular momentum and disturbance torque generated by a 9-g re-entry simulation will be 11 924 N-m-sec (8800 ft-lbf-sec) and 81.3 N-m (60 ft-lbf), respectively.

During uncontrolled centrifuge operation, there is a momentum exchange between centrifuge and spacecraft. In the absence of external torque, the total momentum of the spacecraft remains constant. Therefore, centrifuge operation has a negligible effect upon the spacecraft cone angle and precession rate (cone rate). It can be shown analytically that cone angle and precession rate are unaffected by centrifuge operation, provided that certain conditions are fulfilled. The conditions are (1) the centrifuge has mass properties of a flat disk and (2) the spacecraft has equal moments-of-inertia (MOI) about

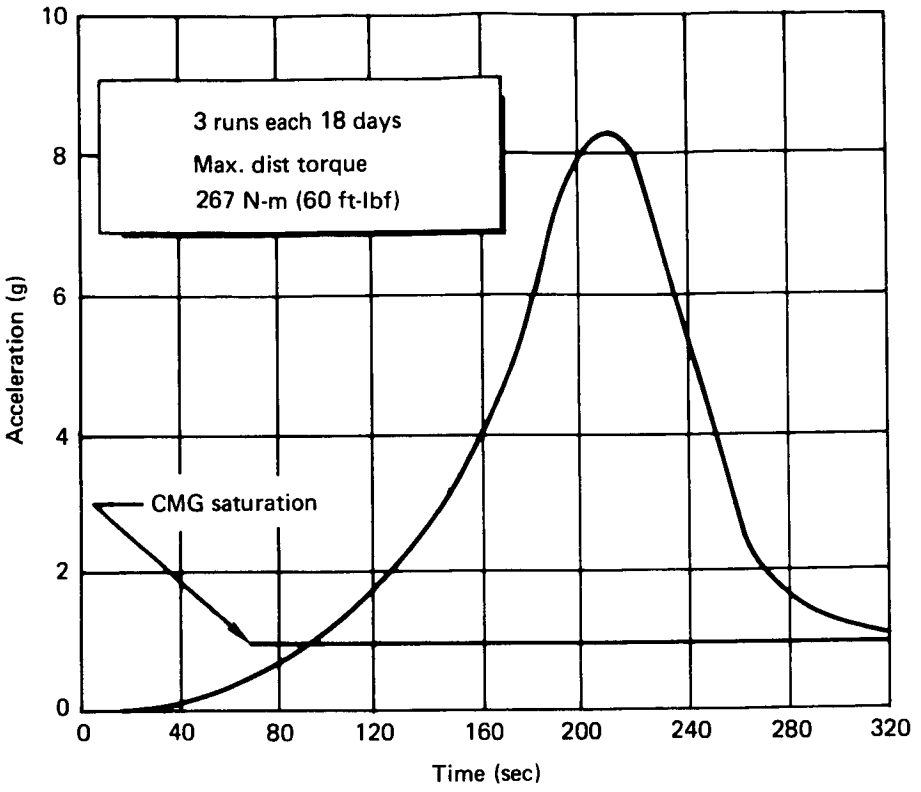

Figure 100. Centrifuge Simulated Re-entry Profile

pitch and yaw. A typical cone angle and precession rate are illustrated by the following example. Assume a vehicle with 0.678×10^6 kg-m^2 (0.5×10^6 slug ft^2) roll MOI and 0.95×10^6 kg-m^2 (0.7×10^6 slug ft^2) pitch and yaw MOI; the initial angular body rates are 0.0009 rad/sec (0.05°/sec) about all three axes. The cone angle and precession rate which result are 1.1 rad (63°) and 0.005 rad/sec (0.278°/sec), respectively (fig. 101). It has been established by a computer simulation that coning motion for the MORL drag configuration of interest is quite similar to the example above.

Centrifuge operation does not have a significant effect upon vehicle roll rate and roll attitude. For example, 9-g centrifuge operation onboard the MORL produces a maximum roll rate of 0.012 rad/sec (0.7°/sec). At the end of the operation, the roll attitude error would be 1.2 rad (68°). Pitch and yaw attitude errors are considerably smaller (approximately 0.175 rad [10°]) because a 9-g run extends over only a small portion of the total precession period. After a run, the CMG's manuever the spacecraft to a belly-down orientation.

During experimentation, the crew is normally restrained to the extent necessary to meet attitude-hold and rate-stabilization requirements. However, during high disturbances the crew may be required to perform functions which produce large crew-motion disturbances. In a recent Douglas Study (Contract No. NAS1-5937--Experimental Study of Dynamic Effects of Crew Motion in a Manned Orbital Research Laboratory-MORL), crew-motion effects were determined experimentally.

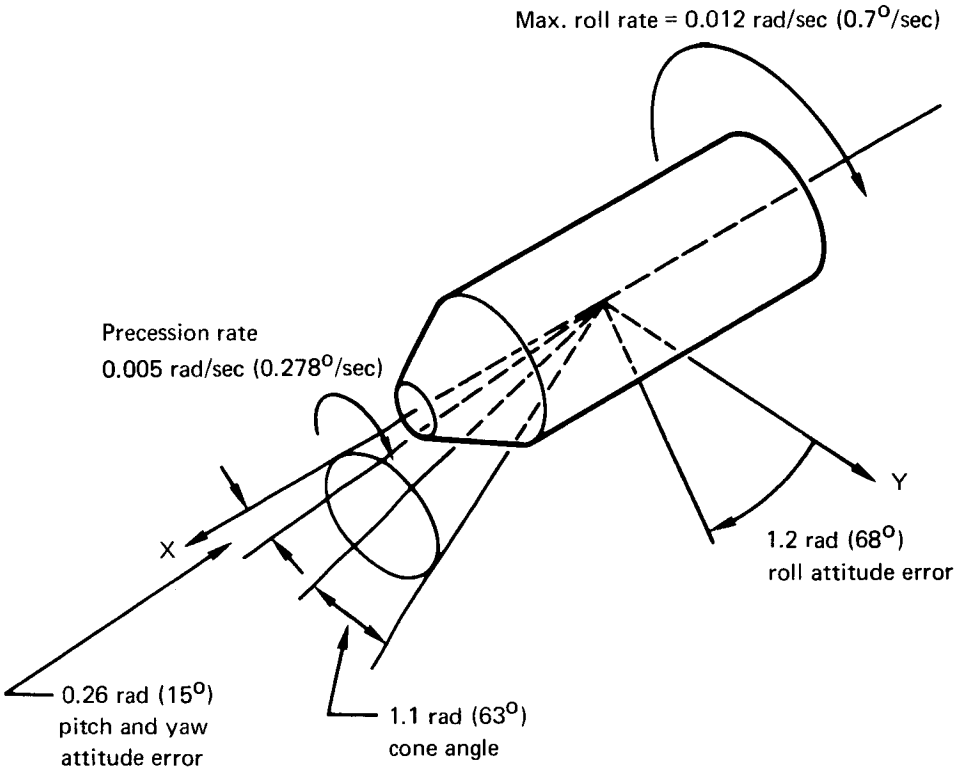

Figure 101. Centrifuge Disturbance Effects

Table 47 shows the effect of basic crew motions (1 man) upon attitude-hold and rate stabilization errors of a MORL spacecraft. The MORL is assumed to be uncontrolled because these disturbances, which are sinusoidal, exhibit a much higher frequency than the baseline MORL control system. Disturbance frequencies are in the range of 1 to 2 cps, whereas the MORL control-system (CMG's) response is 0.03 cps for roll and 0.0067 cps for pitch and yaw. The MORL attitude error resulting from the astronaut's soaring free for a distance of 6.1 m (20 ft), with either a nominal or maximum effort, is twice as large as the 0.002 rad (0.13°) assumed in the MORL Phase IIB stabilization and control system study. The maximum effort of free soaring, in which a velocity of 34.3 N/sec (7.7 ft/sec) was attained, could be injurious to the astronaut when terminating his motion. Note the small difference in attitude error for nominal and maximum free soaring.

Requirements analysis and thrust-level selection: In supporting the experimental program, the laboratory acts as an experiment-mounting platform and provides various degrees of attitude accuracy and rate stabilization. Attitude-hold and rate-stabilization requirements as established by the experimental program were determined primarily from an examination of the MORL data bank. In the study, 700 experiment descriptions were categorized into 9 general classes and grouped into 163 different experiments. A total of 102 of the 163 experiments have some attitude-orientation requirements.

Pointing-accuracy and rate-stabilization requirements for the experimental program are summarized in figs. 102 and 103, respectively. The pointing requirements of fig. 102 are expressed in two categories: (1) those

TABLE 47

MORL RATE AND ATTITUDE ERRORS RESULTING FROM CREW-MOTION DISTURBANCES

Motion	Max. force, N (lbf)	Max. rate error, rad/sec (degrees/sec)	Max. attitude error, rad (degrees)	Comments
Single pendulum arm motion	14.2 (3.2)	0.03×10^{-3} (1.7×10^{-3})	0.016×10^{-3} (0.9×10^{-3})	
Leg motion	33.8 (7.6)	0.08×10^{-3} (4.7×10^{-3})	0.047×10^{-3} (2.7×10^{-3})	
Bending at waist	40.1 (9.0)	0.16×10^{-3} (9.0×10^{-3})	0.148×10^{-3} (8.5×10^{-3})	
Free soaring				
Nominal	409 (92)	0.63×10^{-3} (96×10^{-3})	0.0045 (0.26)	Distance traveled 6.1 m (20 ft)
Maximum	1557.5 (350)	1.68×10^{-3} (96×10^{-3})	0.0049 (0.28)	

Constants:

78.1 kg (172 lb) subject.
Motion: 6.1 m (20 ft) from spacecraft center of mass
Spacecraft MOI: 73×10^5 kg m^2 (500 000 slug ft^2)(MORL)

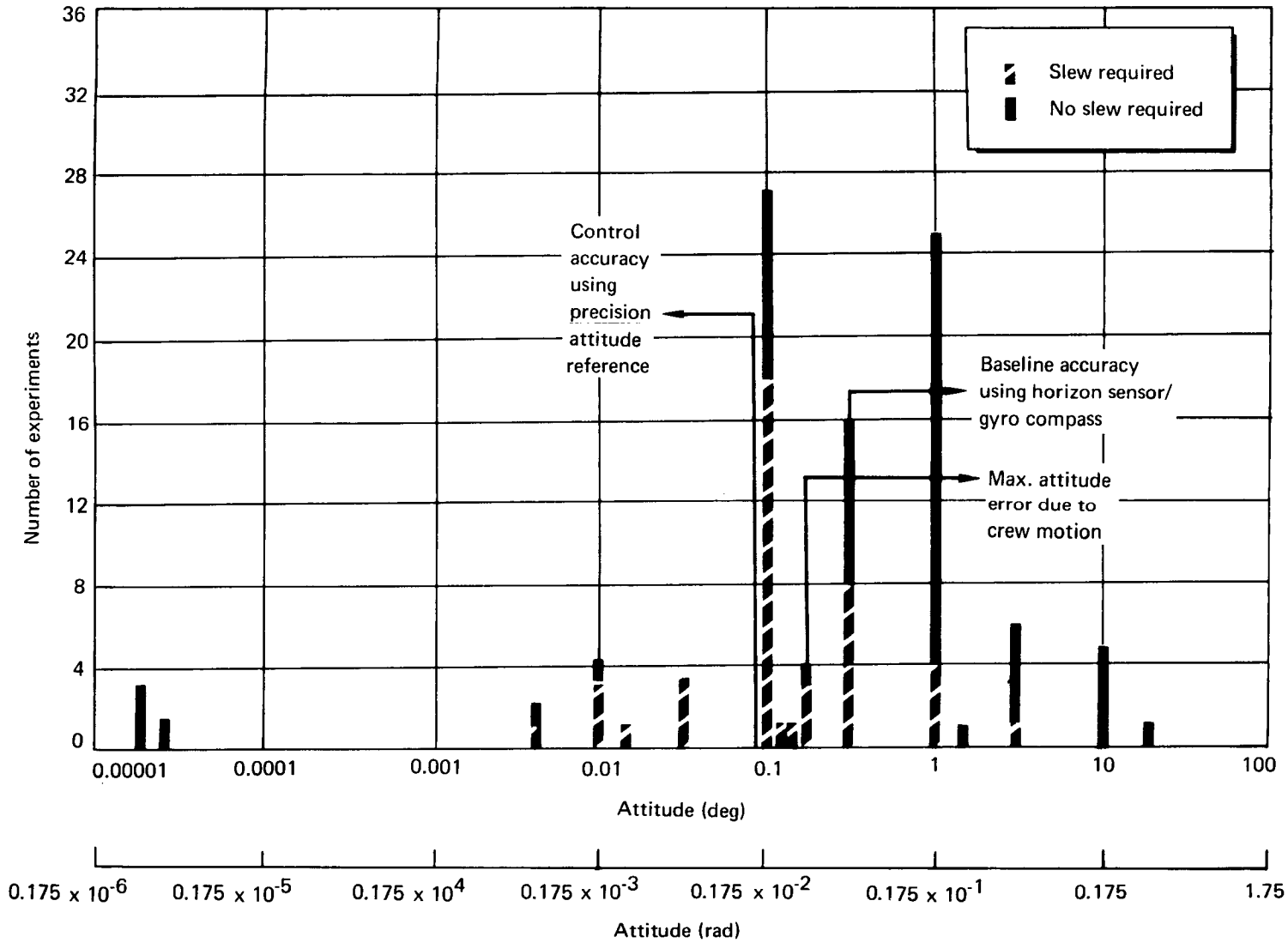

Figure 102. MORL Experiment Requirements – Attitude

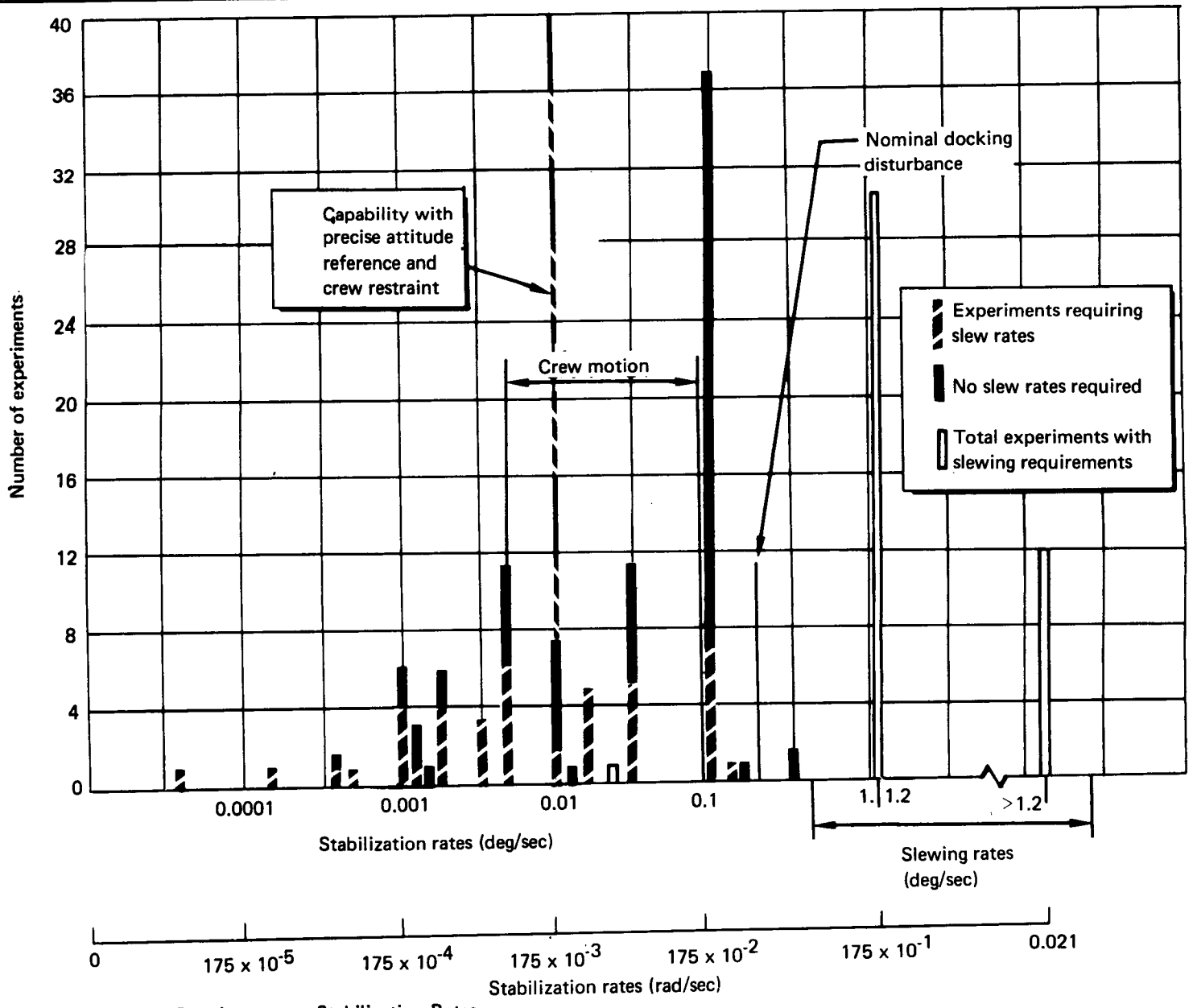

Figure 103. MORL Experiment Requirements – Stabilization Rates

in which the experiment is fixed relative to the laboratory orientation (belly-down or inertial) and (2) those in which the experiment axes must be slewed or rotated relative to the laboratory. The latter category is typified by an Earth-surface-tracking experiment or a satellite-tracking experiment.

In the presence of nominal disturbances, control accuracy is 0.00175 rad (0.1°) using the precision attitude reference. This accuracy will accommodate approximately 94% of the experiments shown; the remainding experiments provide their own attitude-error sensing and control.

Fig. 103 shows the rate-stabilization requirements derived from the list of 163 experiments. There are 101 individual experiments that have some form of rate specification. For experiments that do not involve slewing or tracking, the specification applies to the allowable instantaneous vehicle rate. Many experiments require control of the instantaneous rate relative to a slewing rate [for example, 0.021 rad/sec $\pm 0.175 \times 10^{-2}$ rad/sec (1.2°/sec ±0.1°/sec); where 0.021 rad/sec (1.2°/sec) is the slewing rate and 0.175×10^{-2} rad/sec (±0.1°/sec) is the stabilization rate or allowable rate error]. Fig. 103 indicates that 31 experiments have a peak slewing rate of approximately 0.021 rad/sec (1.2°/sec), which is the peak value associated with ground tracking. Twelve experiments require slewing rates greater than this amount. Fig. 103 also shows the effects of crew-motion disturbances and the nominal docking disturbance.

The utilization of a P/RCS for primary control actuation will allow the attitude error caused by crew motion to be maintained within close tolerance, 0.175×10^{-2} rad (±0.1°). However, rate errors caused by crew motion cannot be controlled to the baseline requirements.

A typical docking disturbance of 0.004 rad/sec (0.25°/sec) is sufficient in magnitude to halt nearly all experiments which have a rate-stabilization requirement (fig. 103). Therefore, a tight attitude-hold requirement after docking does not appear necessary. Fig. 104 shows minimum acceptable thrust level as a function of allowable attitude error for the above docking disturbance. The times shown in fig. 104 indicate the time required to null the docking rate. Reorientation can be accomplished by the baseline CMG's at a maneuver rate of 0.175×10^{-2} rad/sec (0.1°/sec). As a typical example, assume a thrust level of 26.7 N (6 lbf). The rate is nulled in 55 sec, at which time an attitude error of 0.149 rad (8.5°) exists. Reorientation with the CMG's requires 85 sec. Hence, the total time to stabilize after docking would be 140 sec. Thrust levels for attitude errors greater than 0.0875 rad (5°) are quite nominal; for errors less than 0.0875 rad (5°), thrust requirements increase rapidly. Because no clear-cut requirements exist for tight attitude control, a total thrust level of greater than 44.5 N (10 lbf) does not appear necessary.

The use of CMG's for controlling docking and centrifuge disturbance was investigated. Resizing the CMG's to handle the nominal docking disturbance results in a 544.8-kg (120-lbm) weight penalty and doubling of the momentum storage capability. The attitude error which results when CMG's provide control is primarily a function of control system gains and gimbal torquer capability. Determination of the actual attitude is beyond the scope of this study.

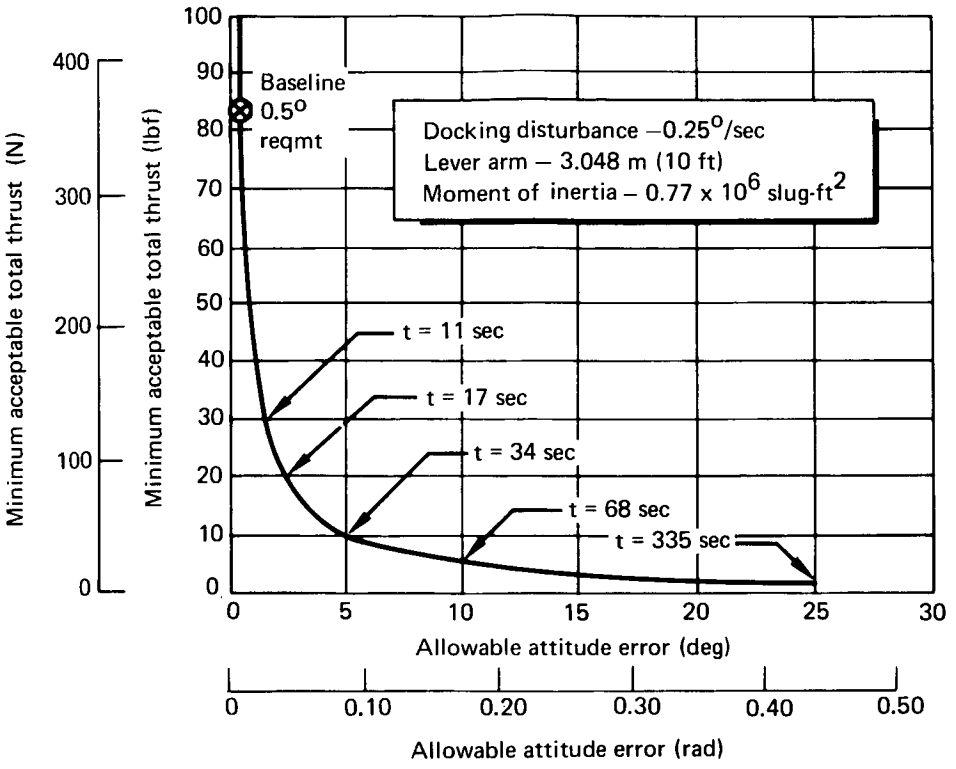

Figure 104. Thrust Requirement for Docking Disturbance

Attitude-hold and rate-stabilization requirements during stowage are no more stringent than those for docking because crew-motion disturbances preclude most experiments which have stabilization requirements. The baseline CMG's will provide control actuation during stowage. To allow this, the stowing cycle (moment) must be regulated. The only penalty incurred will be a small increase in stowing time.

A roll thrust level of 89 N (20 lbf) has been established for a P/RCS which must provide control during 9-g centrifuge operation. Use of the baseline CMG's as primary controllers, with the P/RCS providing CMG desaturation during the 9-g centrifuge operation will allow a roll thrust of 26.7 N (6 lbf). The reduction is possible because the P/RCS now provides CMG desaturation rather than primary control. Hence, the control thrust need not be greater in magnitude than the disturbance.

Control to the baseline SCS requirements will not be possible during centrifuge operation because of crew motion and the disturbance of the centrifuge. A further consideration is the requirement for an inertial orientation during 9-g centrifuge operation. Use of the belly-down orientation causes large disturbance torques because of cross-coupling between the orbital body rate and the centrifuge angular momentum. Operation in a belly-down orientation would require 2.72-kg (6-lbm) propellant/event. In view of these considerations, an unorientated mode during 9-g centrifuge operation appears desirable. The main benefit derived is a savings of 626.5 N-sec (1380 lbf-sec) of impulse per run. Over a 90-day period, the total saving would be 9398 N-sec (20 700 lbf-sec). After each run, the vehicle could be maneuvered to a desired orientation with the CMG's.

Resizing the roll CMG or ganging CMG's to provide control during 9-g centrifuge operation does not appear desirable. A 127-kg (280-lbm) weight penalty would be incurred with resizing. In addition, large CMG's would have to be developed: 7140 N-m-sec (5250 ft-lbf-sec) each if two (SG CMG's)* were utilized. The 127-kg weight penalty would not be prohibitive. However, the cost of developing larger CMG's is considered excessive. Ganging of CMG's results in a 272.4-kg (600-lbm) weight penalty plus added complexity and volume. This concept is also considered to be unfeasible.

Deorbit, if required, would necessitate a velocity increment of approximately 76.3 m/sec (250 fps). If it is assumed that the minimum thrust-to-weight ratio for deorbit is 0.01 and that the vehicle weight at deorbit is 18 160 kg (40 000 lbm), the required deorbit thrust would be 1780 N (400 lbf). A few additional pounds would be required for roll control. Pitch and yaw control moments would be generated by thrust modulating the deorbit thrustors.

A solid system could be utilized for deorbit. However, a high-thrust system would be required to provide attitude control. Thrust requirements for the system are defined in fig. 105 for the assumptions shown.

The baseline CMG's are sized to perform maneuvers. Therefore, a thrust requirement cannot be established on the basis of maneuvers. A minimum-thrust level for backup attitude hold is established on the basis of ability to maneuver into a belly-down oreintation. In effect, the thrust level is sized to provide control moments greater in magnitude than the maximum gravity-gradient disturbance. The minimum thrust level established was 0.445 N (100 mlbf) per axis. However, higher thrust levels would be desirable and the 26.7 N (6 lbf) requirement for centrifuge operation is entirely adequate.

A thrust level of 26.7 N per axis is adequate to control the nominal high disturbance to the following accuracies:

(1) Docking--0.149 rad (8.5°).

(2) Stowing--0.00875 rad (0.5°).

(3) 9-g centrifuge--0.00875 rad (0.5°).

Rate-stabilization accuracy during stowing and 9-g centrifuge is determined primarily by crew motion and control system gains. Estimated accuracy is 0.00175 rad/sec (0.1°/sec).

Operational disturbance control systems. — Six reaction-control systems were initially considered to provide attitude control during the scheduled operational disturbances affecting the MORL. Three of these systems are conventional chemical-propulsion concepts: (1) an O_2/H_2 cryogenic bipropellant system, (2) an N_2O_4/MMH storable bipropellant system, and (3) an N_2H_4 monopropellant system. The other three systems are referred to as heated-gas systems: (4) a cryogenic H_2 system, (5) an NH_3 system, and (6) a GN_2 system.

*Single-gimbal CMG's

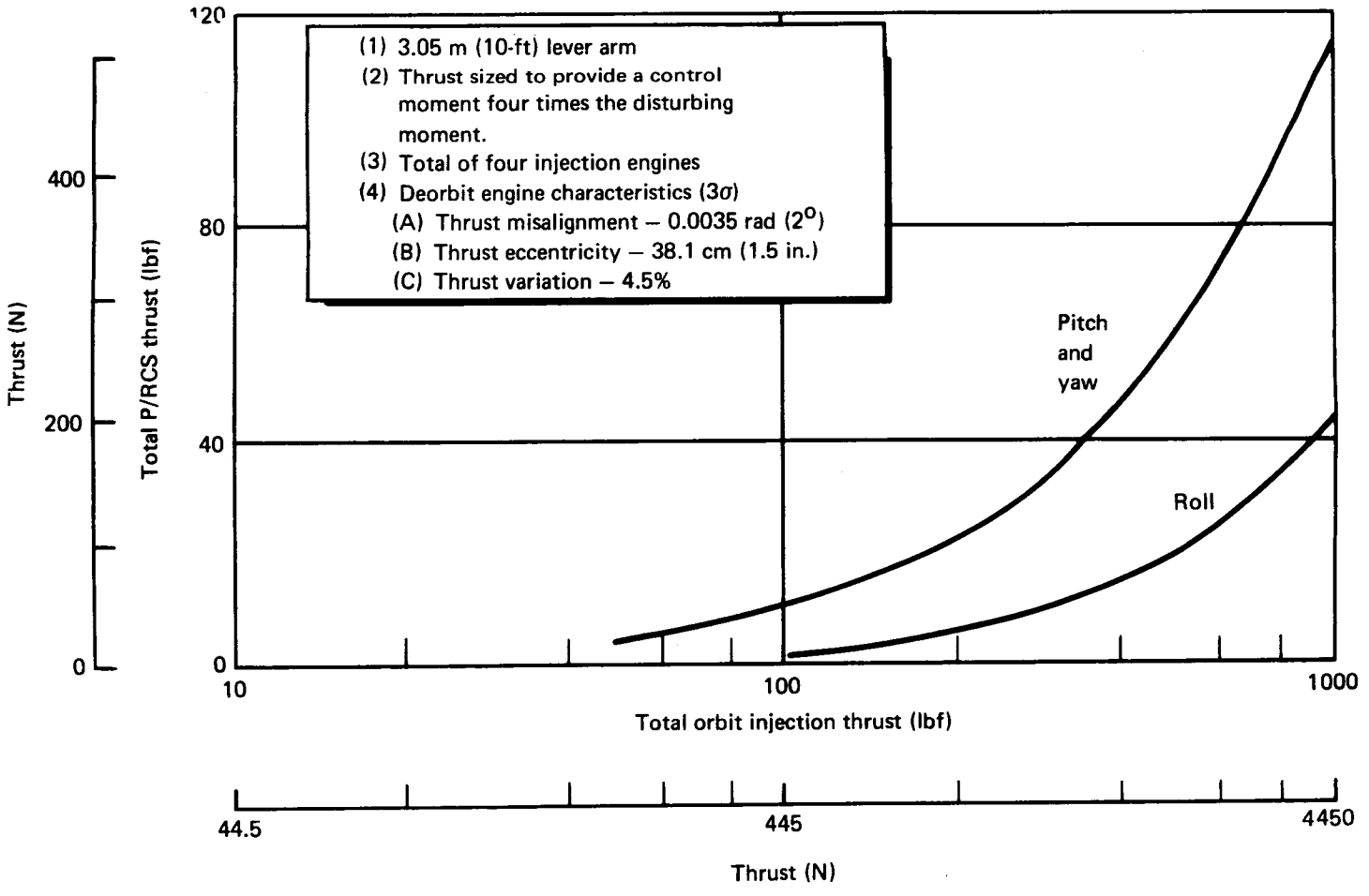

Figure 105. Effect of Deorbit Thrust Level on P/RCS Thrust

Chemical thrustor systems: Because the system weights of the more conventional systems are essentially independent of the thrust level required, a roll thrust of 89 N (20 lbf) was selected for sizing these systems. This thrust is sufficient to allow use of the P/RCS as the primary controller during 9-g centrifuge operation. The thrust is provided by 44.5-N (10-lbf) thrustors in each case. An 89 N-thrust level in each axis is obtained by means of grouping the thrustors in four modules, each containing three engines (one roll and two pitch or yaw).

The cryogenic bipropellant system was considered for use with the H_2 resistojet system because of propellant commonality. The H_2 for both systems is stored in the same tank to avoid having a vent when the bipropellant system is not in use. Heat transfer into the H_2 tank, even with a sophisticated thermal insulation system, is at a rate equivalent to 0.454-kg (1-lbm) boiloff/day. A loss of this magnitude would more than double the amount of H_2 required for control of the scheduled operational disturbances as well as create venting disturbances. The insulation for the common H_2 tank is sized so that all the boiloff is usefully consumed in the resistojet system. To avoid venting, O_2 is stored in a supercritical state at 206.7×10^5 N/m^2 (3000 psia) and at the ambient temperature of 324.8°K (585°R).

The O_2/H_2 system is shown schematically in fig. 106. The feed system consists of a pressure regulator/follower, a gas-generator/heat-exchanger propellant conditioner, and accumulators. These keep the propellants at constant thermodynamic conditions to assure delivery of GO_2 and GH_2 to the thrustors at a predictable mixture ratio. The accumulator pressures are controlled by a pressure regulator on the H_2 line and by a pressure follower on the O_2 line. The regulator senses the H_2 accumulator pressure and maintains it at a nominal pressure of 117 kN/m^2 (17 psia). The pressure follower senses the pressure differential between the O_2 and H_2 accumulators and operates so that the O_2 accumulator pressure follows that of the H_2. This concept maintains any variations in accumulator pressure in close phase, thus limiting the potential mixture-ratio variation and enhancing system stability. The temperature of the accumulators is maintained at 111°K (200°R) by the propellant-conditioning system. The gas generators receive O_2 and H_2 from the accumulators at a mixture ratio of 1.33, which provides an exhaust gas of about 1388°K (2500°R) to be used in the heat exchangers through which the propellants pass. The gas generators operate only when the thrustors are firing and propellant is flowing. If the temperature of the propellant in the accumulators decreases, the gas-generator valves are signalled to open. Electric heating elements located in the accumulators provide temperature control when the thrustors are inoperative and no propellant is flowing. The accumulators are made of aluminum and serve as pneumatic capacitors as well as propellant manifolds.

The propellants are delivered to the thrustors at a mixture ratio of 1.0, which results in a chamber temperature of about 833°K (1500°R). This relatively low temperature allows both the combustion chamber and nozzle to be fabricated of electrodeposited nickel for extended operational life without the need for special cooling techniques. Each thrustor consists of a mechanically linked bipropellant valve, injector, pilot catalyst ignition bed, combustor, and converging-diverging nozzle. Only a small portion of the total flow (2 to 5%) passes through the catalyst bed so that good pulse repeatability

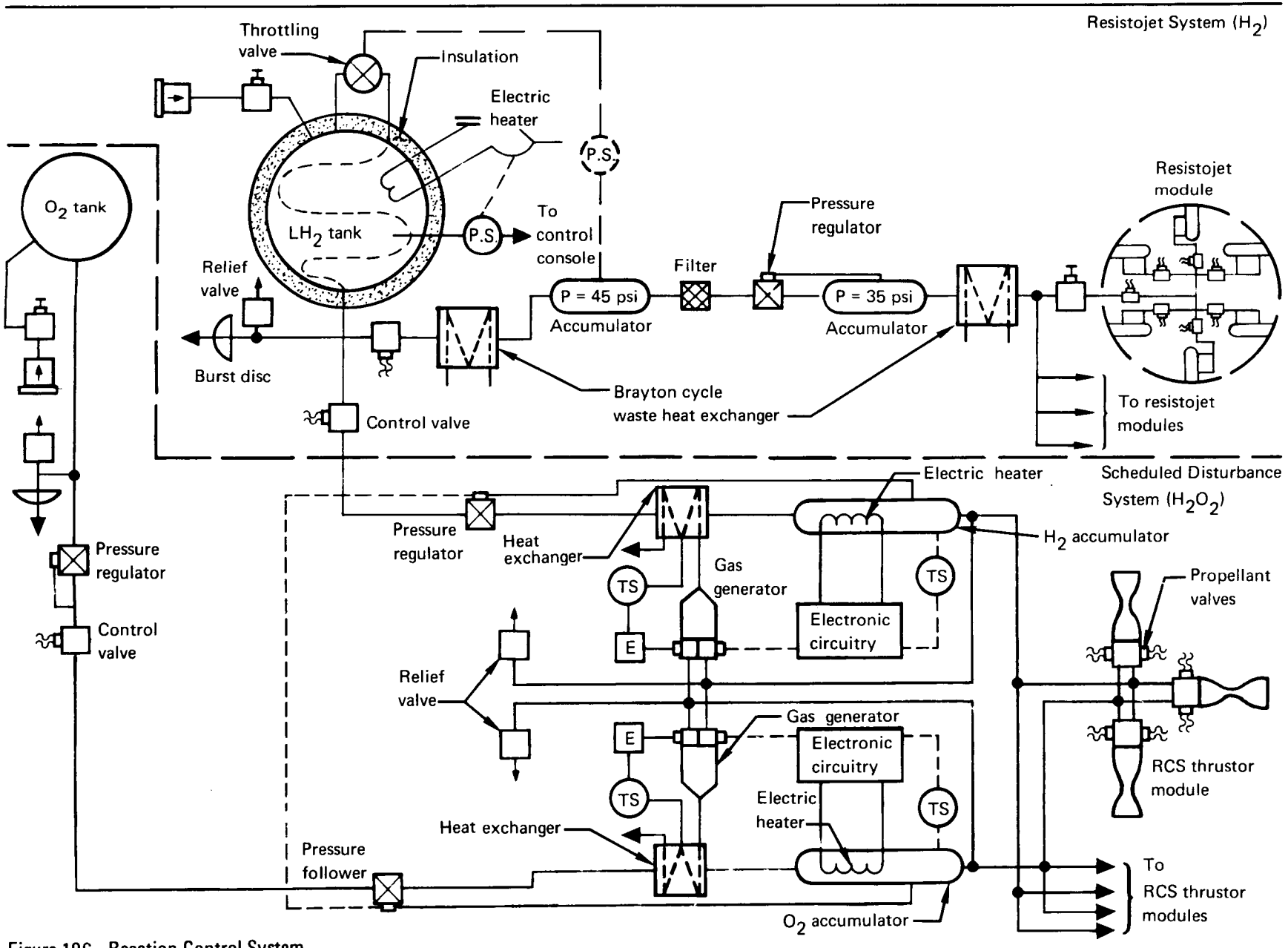

Figure 106. Reaction Control System

can be maintained. The balance of the flow enters the combustion chamber downstream of the pilot bed and is ignited by the hot gases. The initial temperature of the bed is maintained near operating temperature by an electric heater. Table 48 presents a weight breakdown for the cryogenic O_2/H_2 RCS, while table 49 gives a performance summary.

The candidate storable bipropellant system shown in fig. 107 utilizes radiation-cooled thrustors burning the hypergolic propellants, N_2O_4 and MMH, at a nominal mixture ratio of 1.6:1. The propellant tanks are fabricated of minimum-gage AM-350 stainless steel and store the propellants at a pressure of 1722.5×10^3 N/m^2 (250 psia). The tanks are pressurized by a 206.7×10^5 N/m^2 (3000 psia) N_2 bottle which is allowed to blow down to a minimum pressure of 20.67×10^5 N/m^2 (300 psia) at the end of 147 days. This ensures that 1722.5×10^3 N/m^2 propellant-tank pressure will be maintained. The propellants are expelled by a metal-bellows positive-expulsion system. The metal bellows are compatible with the stored propellants over the 5-year mission and can be recycled to allow for propellant resupply from the logistics vehicle. A weight breakdown for the N_2O_4/MMH system is shown in table 50, and table 51 gives a performance summary.

The candidate monopropellant reaction control system is presented in fig. 108. This system uses N_2H_4 propellant which is exothermally decomposed by means of passing it over a Shell 405 catalyst bed in the thrustor reaction chamber. The propellant is stored in a single tank at a pressure of

TABLE 48

O_2/H_2 RCS—WEIGHT BREAKDOWN

Item	Weight	
	kg	(lbm)
Propellant tanks[a]	38.6	(85)
Tank insulation[b]	1.36	(3)
Valves, regulators	5.9	(13)
Quantity gauge system	0.9	(2)
Umbilical panel	0.45	(14)
Thrustor modules (4)	9.08	(20)
Pressure regulator/follower	12.7	(28)
Heat exchangers	13.6	(30)
Gas generators	10.0	(22)
Accumulators	4.5	(10)
Total chargeable dry weight	103.5	(228)
Loaded propellant at launch	10.4	(23)
Total chargeable launch weight	113.9	(251)
147-day loaded propellant weight	59.0	(130)
Total chargeable wet weight in orbit	162.5	(358)

[a] Includes O_2-tank weight and incremental weight for resized resistojet-system H_2 tanks.

[b] Incremental weight for resized resistojet-system H_2 tank.

TABLE 49

O_2/H_2 RCS—PERFORMANCE SUMMARY

Item	Performance
Thrust/engine (12 engines)	44.5 N (10 lbf)
90-day total impulse	102 795 N-sec (23 100 lbf-sec)
Mission specific impulse	308 sec
90-day propellant weight	34.05 kg (75 lbm)
Chamber pressure (psia)	68.9×10^3 N/m^2 (10 psia)
Expansion ratio	40
Chamber temperature	1089°K (1960°R)
Delivered specific impulse	
Steady state	318 sec
Pulsed (limit-cycle operation)	298 sec
O_2 tank pressure	206.7×10^5 N/m^2 (3000 psia)
O_2 tank temperature	325°K (585°R)
H_2 tank pressure	379×10^3 N/m^2 (55 psia)
H_2 tank temperature	25.5°K (46°R)
Mixture ratio	1.0

1722.5×10^3 N/m^2 (250 psia) and an ambient temperature of 324.8°K (585°R). A positive-expulsion metal bellows system is used to ensure compatibility with the stored propellant over the 5-year mission. This bellows system may be recycled to allow for propellant resupply from the logistics vehicle. Pressurization of the propellant tank is provided by a 206.7×10^5 N/m^2 (3000 psia) N_2 bottle which is allowed to blow down to a minimum of 20.67×10^5 N/m^2 (300 psia) over the 147-day period, thereby ensuring that a propellant tank pressure of 1722.5×10^3 N/m^2 can be maintained at all times. Table 52 gives a weight breakdown for the N_2H_4 RCS, and table 53 gives the performance summary.

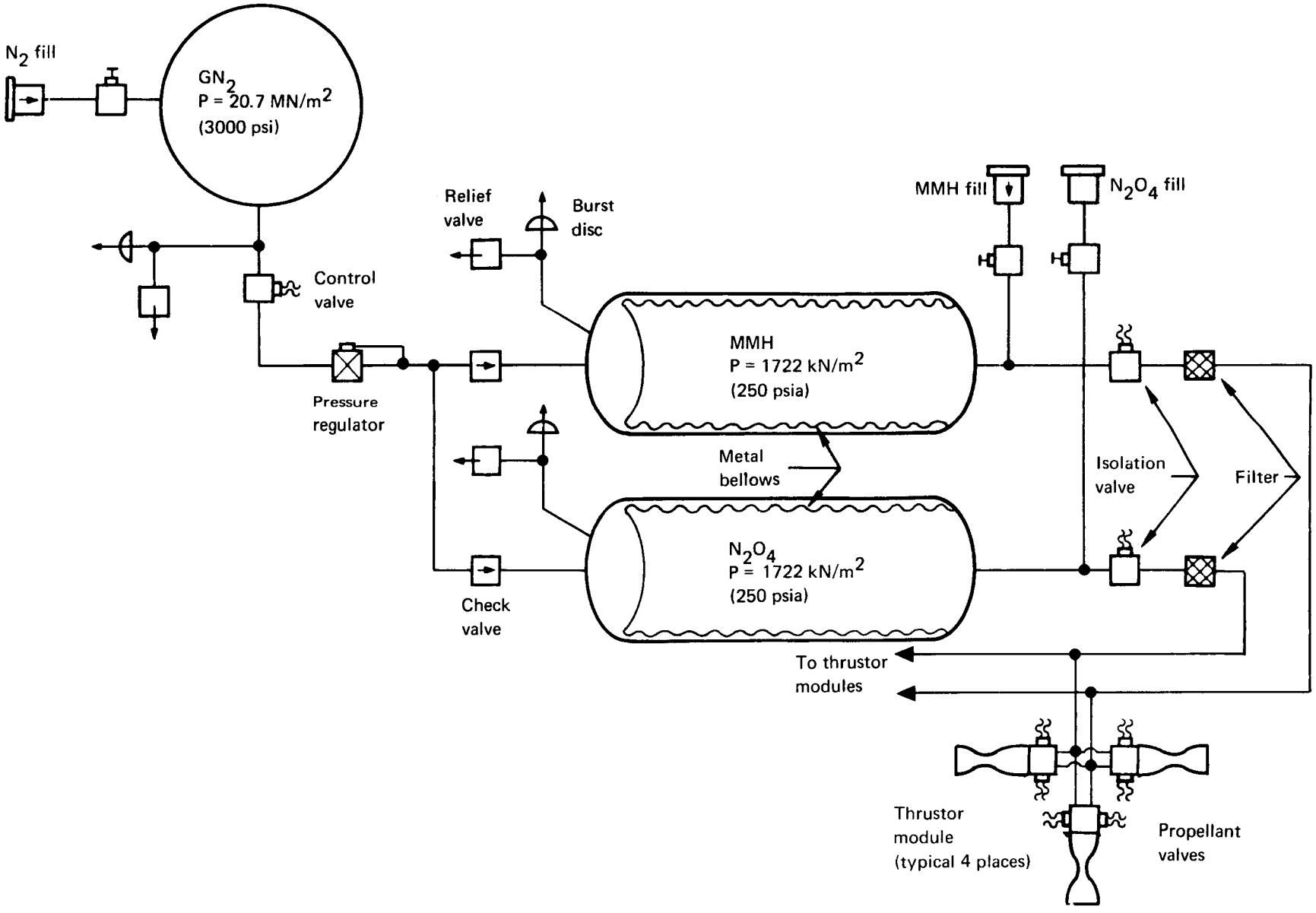

Figure 107. Scheduled Disturbance Reaction Control System (N_2O_4/MMH)

TABLE 50

N_2O_4/MMH RCS—WEIGHT BREAKDOWN

Item	Weight	
	kg	(lbm)
Propellant tanks	11.35	(25)
Metal bellows	18.16	(40)
Valves, regulators	4.99	(11)
Quantity gauge system	4.99	(11)
Umbilical panel	1.36	(3)
Lines, fittings, etc.	6.36	(14)
Thrustor modules (4)	16.35	(36)
Pressurant bottle	3.18	(7)
Total chargeable dry weight	66.73	(147)
Pressurant gas	3.63	(8)
Loaded propellant at launch	9.53	(21)
Total chargeable launch weight	79.89	(176)
147-day loaded propellant weight	62.20	(137)
Total chargeable wet weight in orbit	132.57	(292)

TABLE 51

N_2O_4/MMH RCS PERFORMANCE SUMMARY

Item	Performance
Thrust per engine (12 engines)	44.5 N (10 lbf)
90-day total impulse	102 795 N-sec (23 100 lbf-sec)
Mission specific impulse	282 sec
90-day propellant weight	37.23 kg (82 lbm)
Chamber pressure	689×10^3 N/m^2 (100 psia)
Expansion ratio	40
Chamber temperature	1500°K (2500°R)
Delivered specific impulse	
Steady state	290 sec
Pulse (limit-cycle operation)	272 sec
Propellant tank pressure	1730×10^3 N/m^2 (250 psia)
Propellant tank temperature	325°K (585°R)
Initial N_2 bottle pressure	206.7×10^5 N/m^2 (3000 psia)

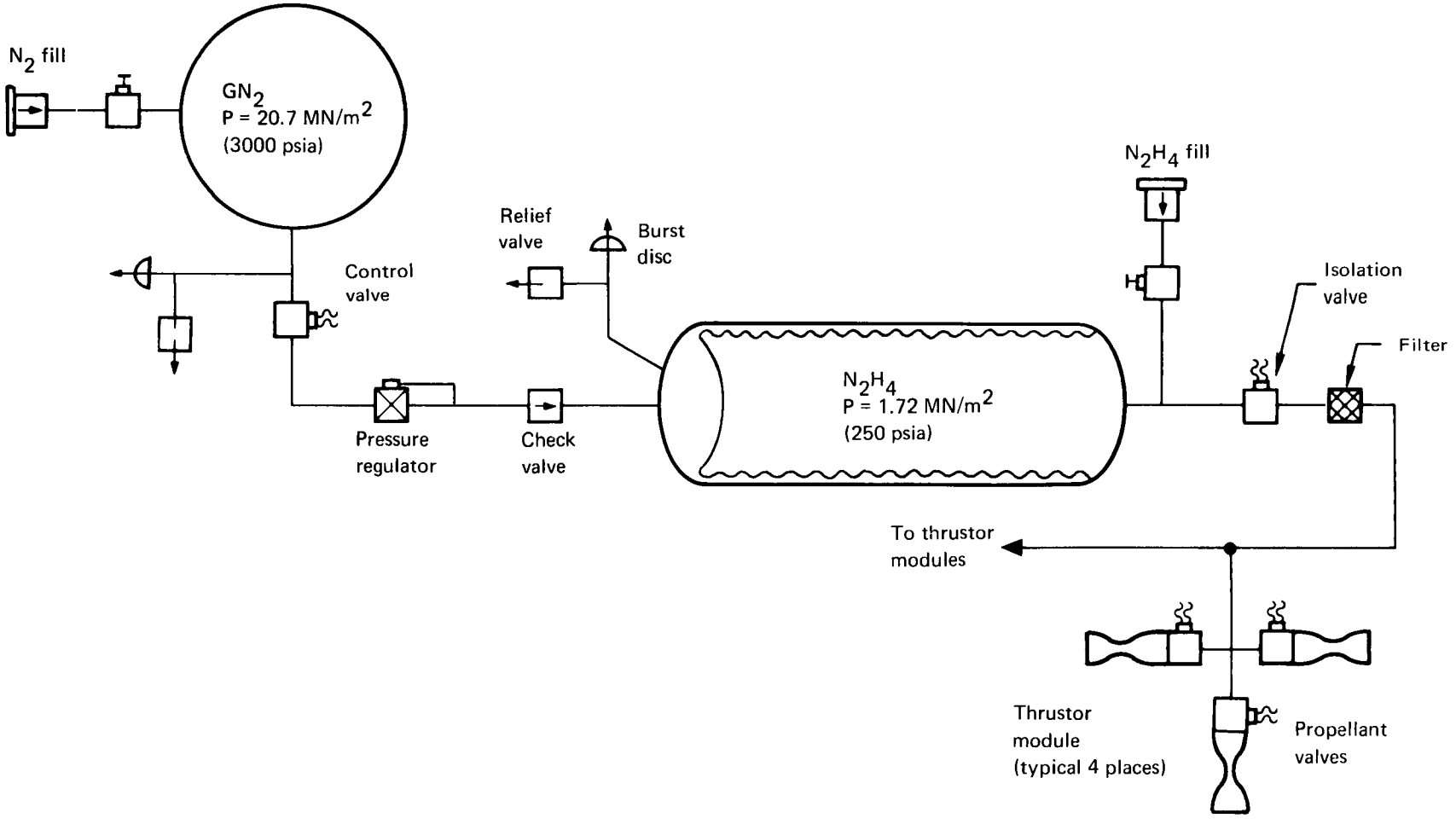

Figure 108. Scheduled Disturbance Reaction Control System (N_2H_4)

TABLE 52

N_2H_4 RCS WEIGHT BREAKDOWN

Item	Weight	
	kg	lbm
Propellant tank	11.35	25
Metal bellows	23.15	51
Valves, regulators	3.63	8
Quantity gauge system	3.63	8
Umbilical panel	0.9	2
Lines, fittings, etc.	4.08	9
Thrustor modules (4)	13.6	30
Pressurant bottle	4.08	9
Total chargeable dry weight	64.42	142
Pressurant gas	4.54	10
Propellant loaded at launch	14.07	31
Total chargeable launch weight	83.03	183
147-day propellant weight	92.62	204
Total chargeable wet weight in orbit	161.62	356

TABLE 53

N_2H_4 RCS PERFORMANCE SUMMARY

Item	Performance
Thrust per engine (12 engines)	4.5 N (10 lbf)
90-day total impulse	102 795 N-sec (23 100 lbf-sec)
Mission specific impulse	188 sec
90-day propellant weight	55.8 kg (123 lbm)
Chamber pressure	689×10^3 N/m^2 (100 psia)
Expansion ratio	50
Chamber temperature	1255°K (2260°R)
Delivered specific impulse	
steady state	235 sec
pulsed (limit cycle operation)	120 sec
Propellant tank pressure	1730×10^3 N/m^2 (250 psia)
Propellant tank temperature	69°K (125°R)
Initial N_2 bottle pressure	206.7×10^5 N/m^2 (3000 psia)

Heated gas systems: The system weights of the heated-gas systems increase with the increasing thrust level, primarily because of the increased propellant weight resulting from the lowered specific impulse as the propellant-flow rate through the heat exchangers is increased. (Gas output temperature decreases with increasing propellant flow rate.) Sizing data for these systems are therefore presented parametrically and primarily as a function of propellant-flow rate or thrust level.

The parametric model for the heated H_2 RCS is shown in fig. 109. This system is considered for use with the H_2 resistojet system because of propellant commonality and because the propellant for both systems is stored in the same tank to avoid having to vent the tank when the higher-thrust system is not in use. An electric heater is placed in the H_2 tank to increase the boiloff rate during the periods of higher flow-rate requirements. This heater is connected to a 260-Vdc bus which can supply up to 5.57 kWe of power. An overall heater system efficiency of 90% was assumed, resulting in a maximum power level of 5 kWe available for increasing the mass flow rate of H_2 out of the tank. At the storage temperature of 27.7°K (50°R), the heat of vaporization of LH_2 is 406 J/kg (175 Btu/lbm); thus, the maximum boiloff rate at 5 kWe is 0.0123 kg/sec (0.0272 lbm/sec). A mechanical vapor-liquid separator is used to prevent liquid from entering the propellant-feed system.

Waste heat from the Brayton-cycle power-system radiator is used to heat the flowing H_2 gas to obtain higher specific impulse. The radiator fluid is FC-75 flowing at 12.53 kg/min (27.6 lbm/min) and has a maximum temperature of 399.8°K (720°R). The maximum heat load available is assumed to be that which is normally dumped overboard, 26 106 W (89 000 Btu/hr). Fig. 110 shows the H_2 flow-rate influence on achievable output temperature using counterflow heat exchangers of various effectiveness ratios. All of the temperature curves exhibit a sharp break at a flow rate of 0.0154 kg/sec (0.034 lbm/sec). At flow rates below this value, all of the heat available cannot be absorbed and the H_2 output temperature is a function only of heat-exchanger effectiveness ratio. As the H_2 flow rate is increased, the amount of heat absorbed increases to achieve the same output temperature until, at the breakpoint, all of the available heat is being absorbed by the cold fluid (H_2). At flow rates above this point, more heat than is available from the hot fluid is required to achieve the same temperature and, consequently, the H_2 output temperature must decrease. The effect of limited heating rate is to impose a boundary on the achievable output temperature as shown by the solid curves (fig. 110) for three heating-rate limits. A further constraint on the system is imposed by the maximum power available to increase the flow rate out of the H_2 tank, 0.0123 kg/sec ($\dot{m}_{max.}$ = 0.0272 lbm/sec).

The effect of H_2 flow rate on the estimated heat-exchanger weight is shown in fig. 111 for an effectiveness ratio of 0.80 and maximum heat loads constrained to 26 100 W (89 000 Btu/hr), 11 740 W (40 000 Btu/hr), and 5870 W (20 000 Btu/hr). The variation in specific impulse with H_2 temperature is presented in fig. 112. The thrustors for this system are all designed to produce the same thrust level and, at a given total thrust level, six thrustors are firing so that each one uses one-sixth of the total flow rate. Consequently, the specific impulse with two thrustors firing will be higher than with four thrustors firing, and the propellant consumption is a function

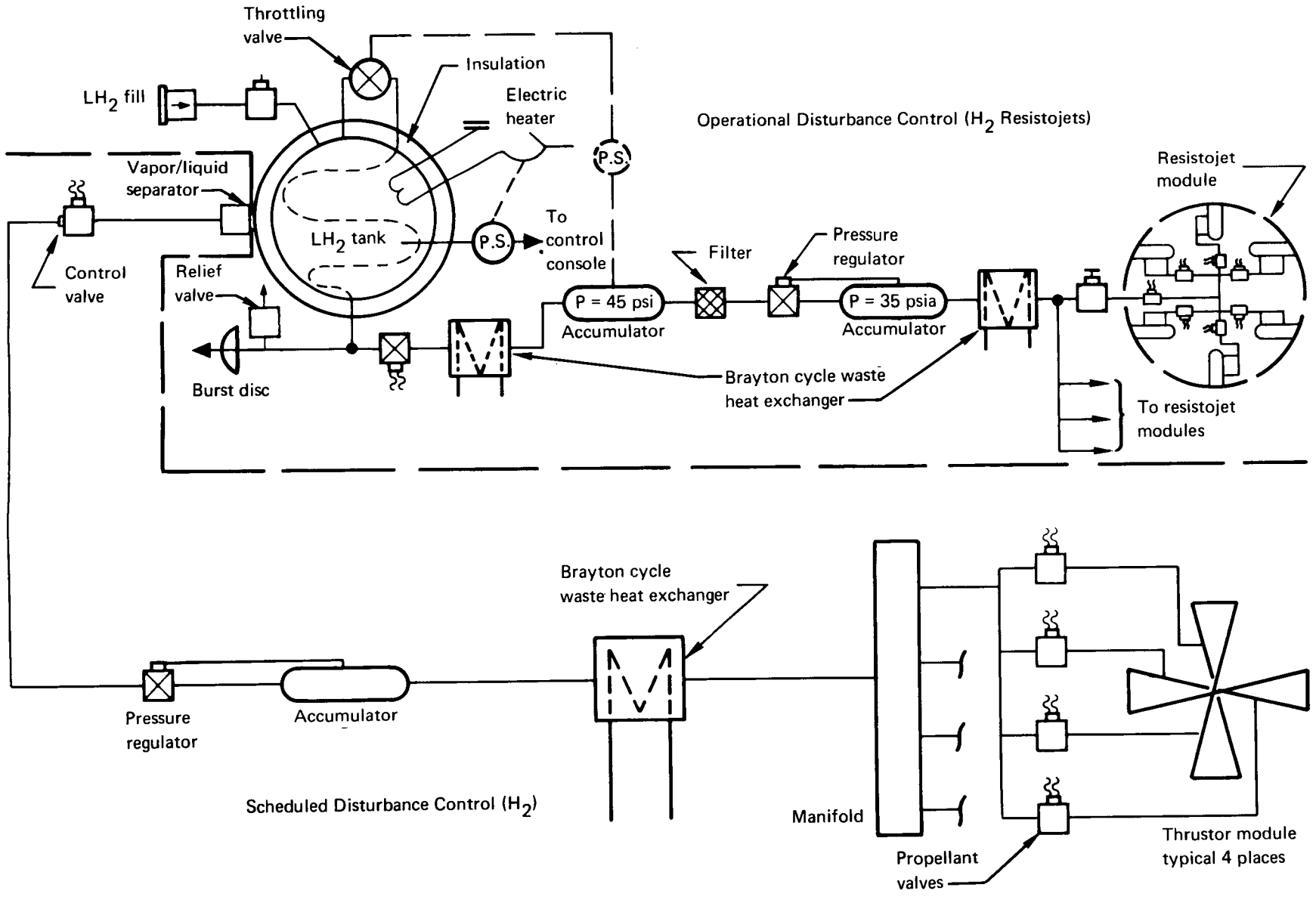

Figure 109. Reaction Control System

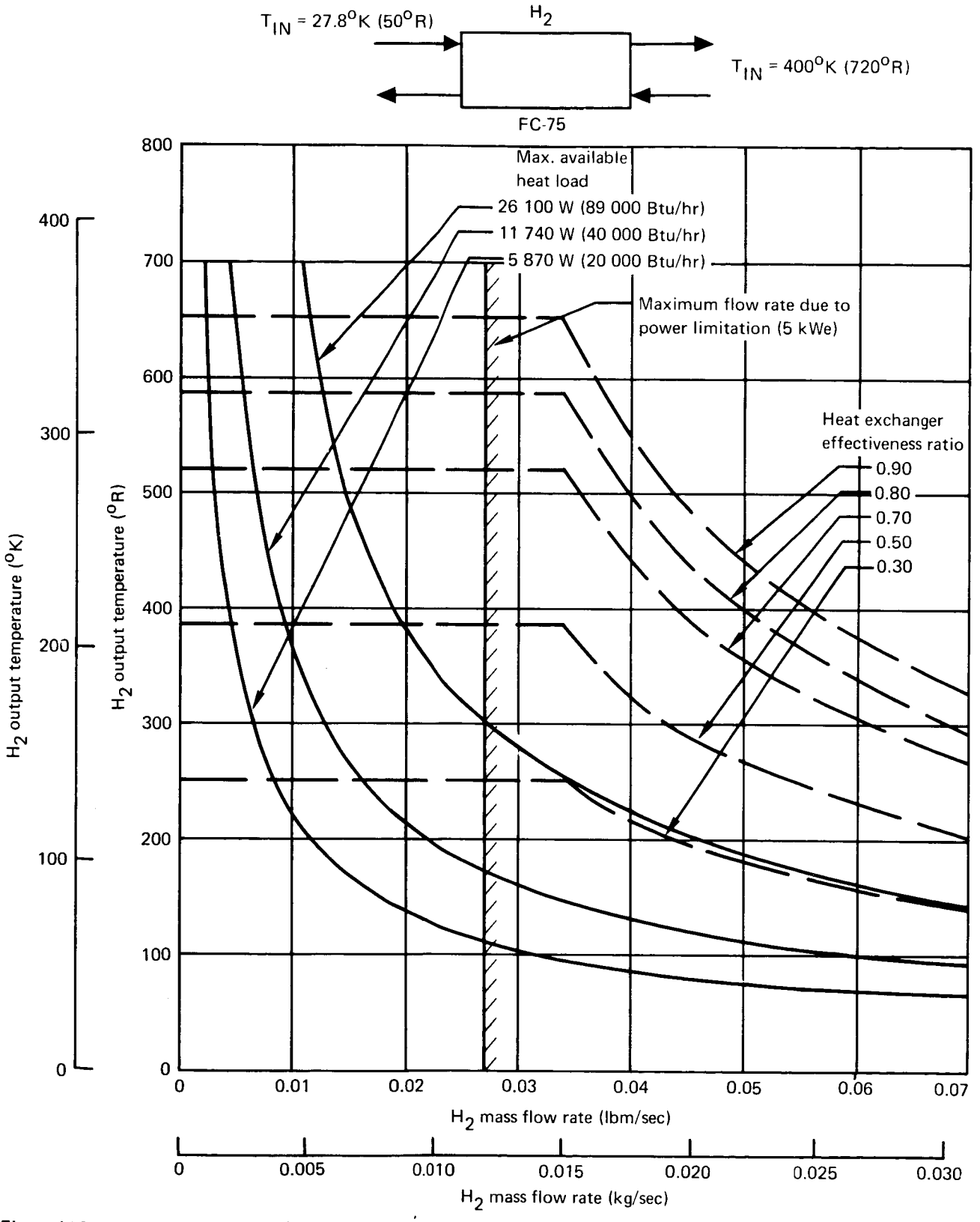

Figure 110. H_2/FC-75 Heat Exchanger Characteristics

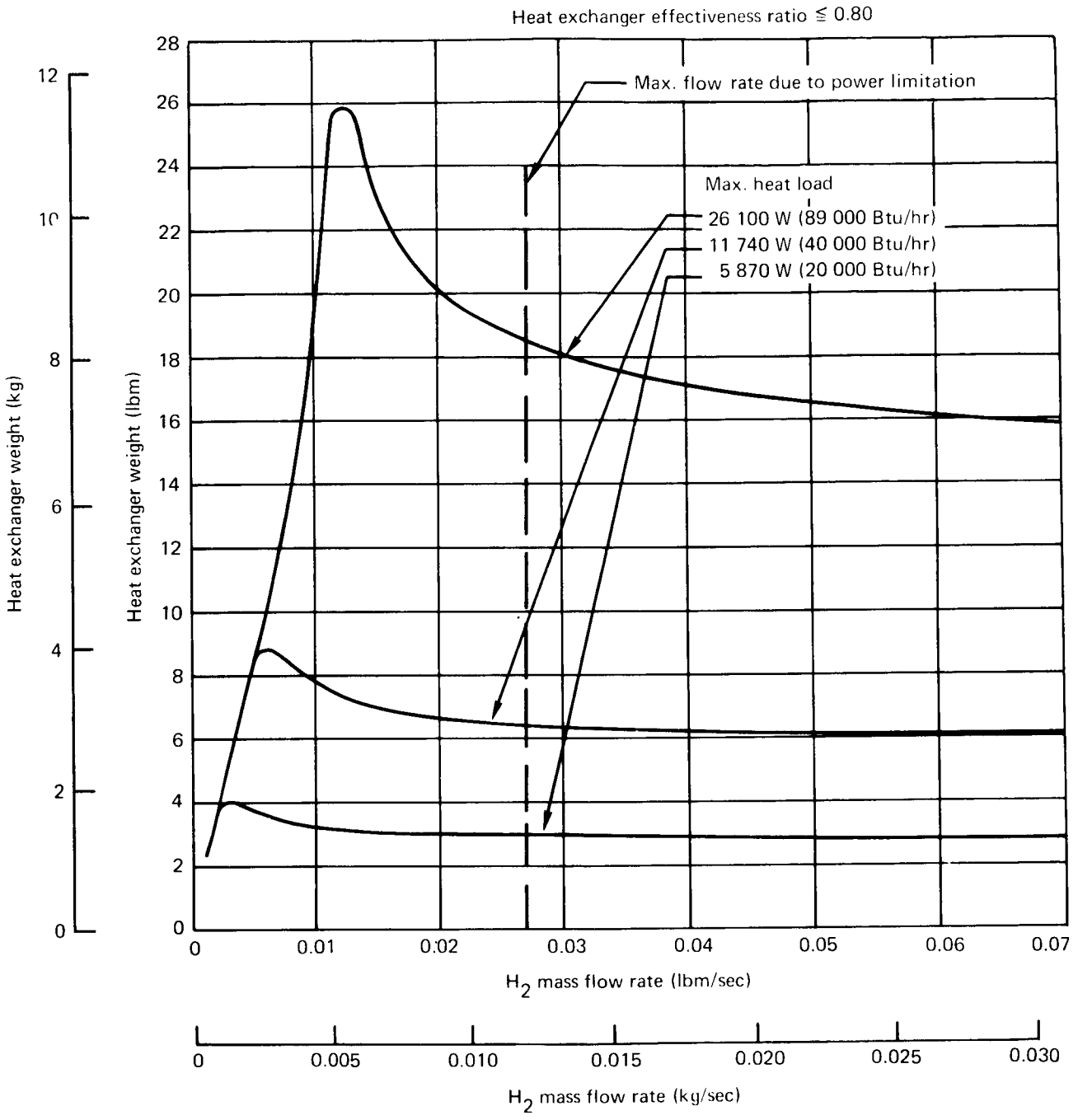

Figure 111. H_2/FC-75 Heat Exchanger Weight

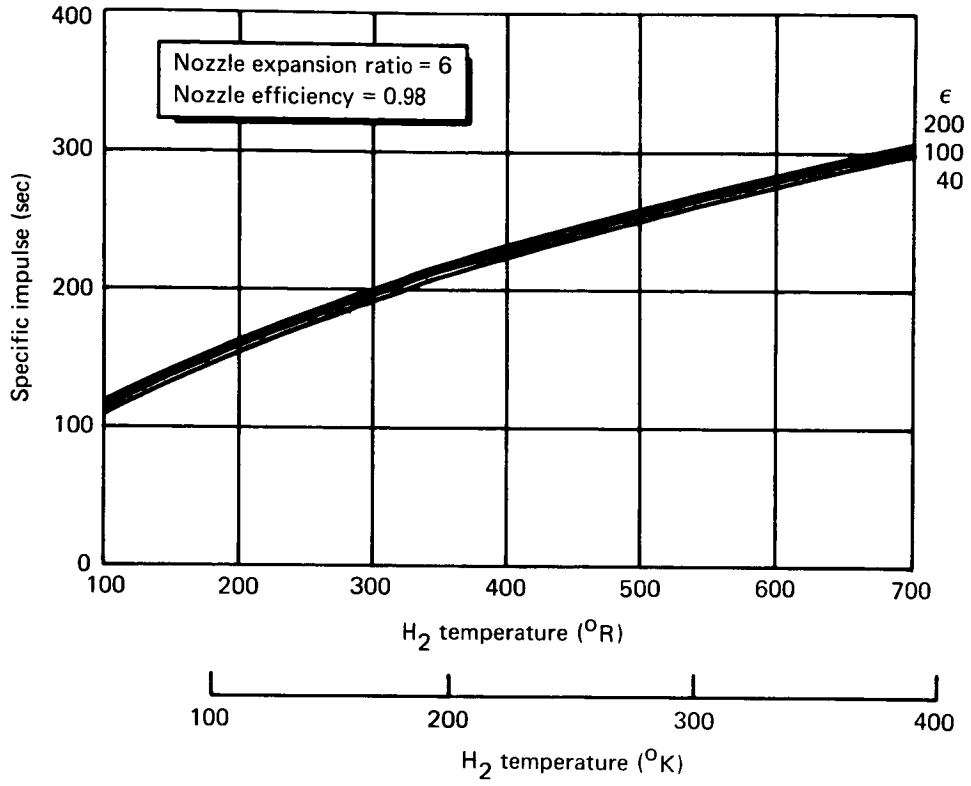

Figure 112. Specific Impulse Versus Temperature

not only of total impulse but also the impulse required in each operating mode. The equation expressing this is

$$W_p = \frac{I_{T1}}{I_{s_1}} + \frac{I_{T2}}{I_{s_2}} + \cdots\cdots + \frac{I_{Tn}}{I_{s_n}}$$

where

W_p = propellant weight

I_t = total impulse

I_s = specific impulse

(Subscripts refer to number of thrustors operating.)

The impulse requirements breakdown shown in table 54 was used to calculate the propellant weights shown in fig. 113 as a function of H_2 flow rate. Because the LH_2 is to be stored in a common tank with resistojet H_2, only that increase in tank and insulation weight caused by the increase in

TABLE 54

IMPULSE REQUIREMENT BREAKDOWN

Control requirement	IMPULSE REQUIREMENT, N-sec (lbf-sec)		
	Number of thrustors operating		
	2	4	6
Roll control		150 410 (33 800)	
Docking		2181 (490)	1068 (240)
Backup attitude control	10 903 (2450)	2937 (660)	712 (160)
Subtotal	10 903 (2450)	155 528 (34 950)	1780 (400)
Total impulse	168 211 (36 800)		

required tank volume is charged to the higher thrust system. These weight increments are shown in fig. 114, and system wet weight is given in fig. 115 as functions of achievable thrust.

A preliminary investigation of the NH_3 system has revealed that although this system has the advantage of being completely storable at MORL temperatures, it has the disadvantage of a poor specific-impulse/temperature relationship (compared to H_2) because of a comparatively high molecular weight. Use of the storable NH_3 system requires that the heat of vaporization be supplied to the liquid during operation to convert it to the gaseous state before it is consumed in the thrustors. Additional heating is desired, if possible, to obtain higher specific impulse and, consequently, to reduce the propellant weight requirement. NH_3 has a relatively high heat of vaporization and is therefore, for a fixed heating load, limited to relatively low thrust levels. The following three heating loads were considered to be available to the NH_3 RCS:

(1) A 4111-W (3.9-Btu/sec) heat load from the EC/LS heat transport fluid.

(2) A 5007-W (4.75-Btu/sec) heat load from the electrical power system.

(3) A 26 034-W (24.7 Btu/sec) heat load from the Brayton-cycle waste heat.

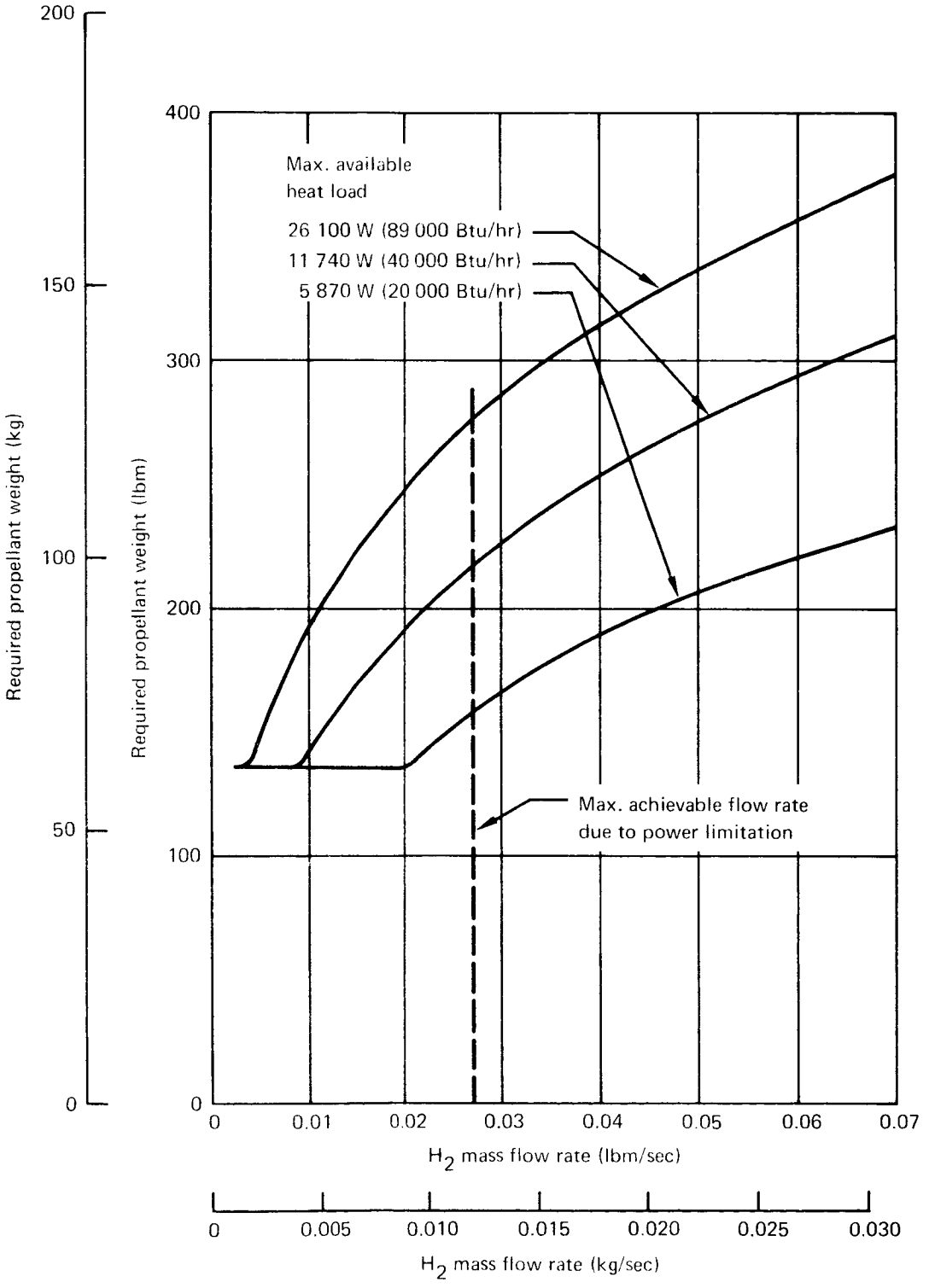

Figure 113. H_2 Heated-Gas System Propellant Weight Requirements

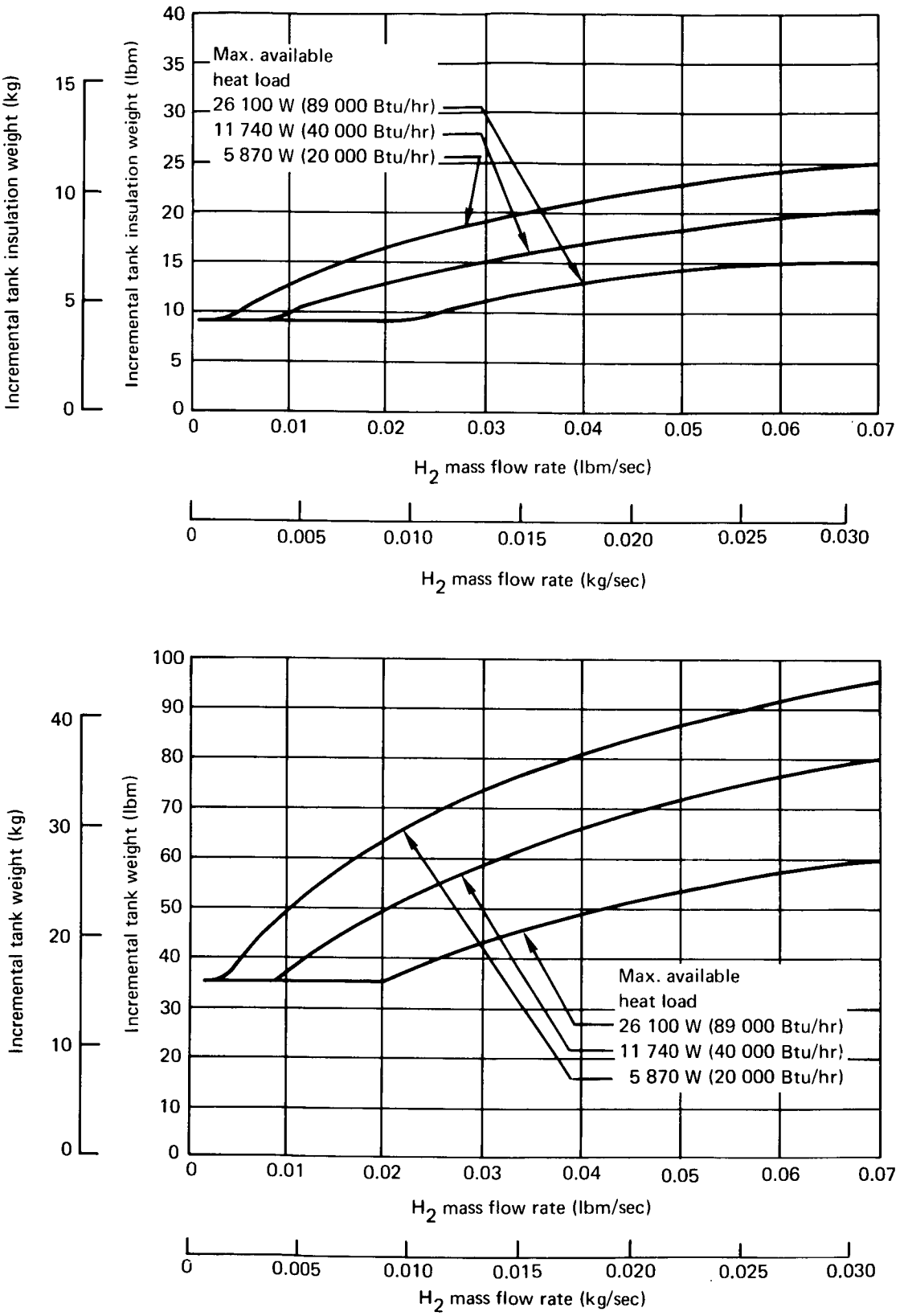

Figure 114. H_2 Tank and Insulation Weights Chargeable to the Heated Gas System

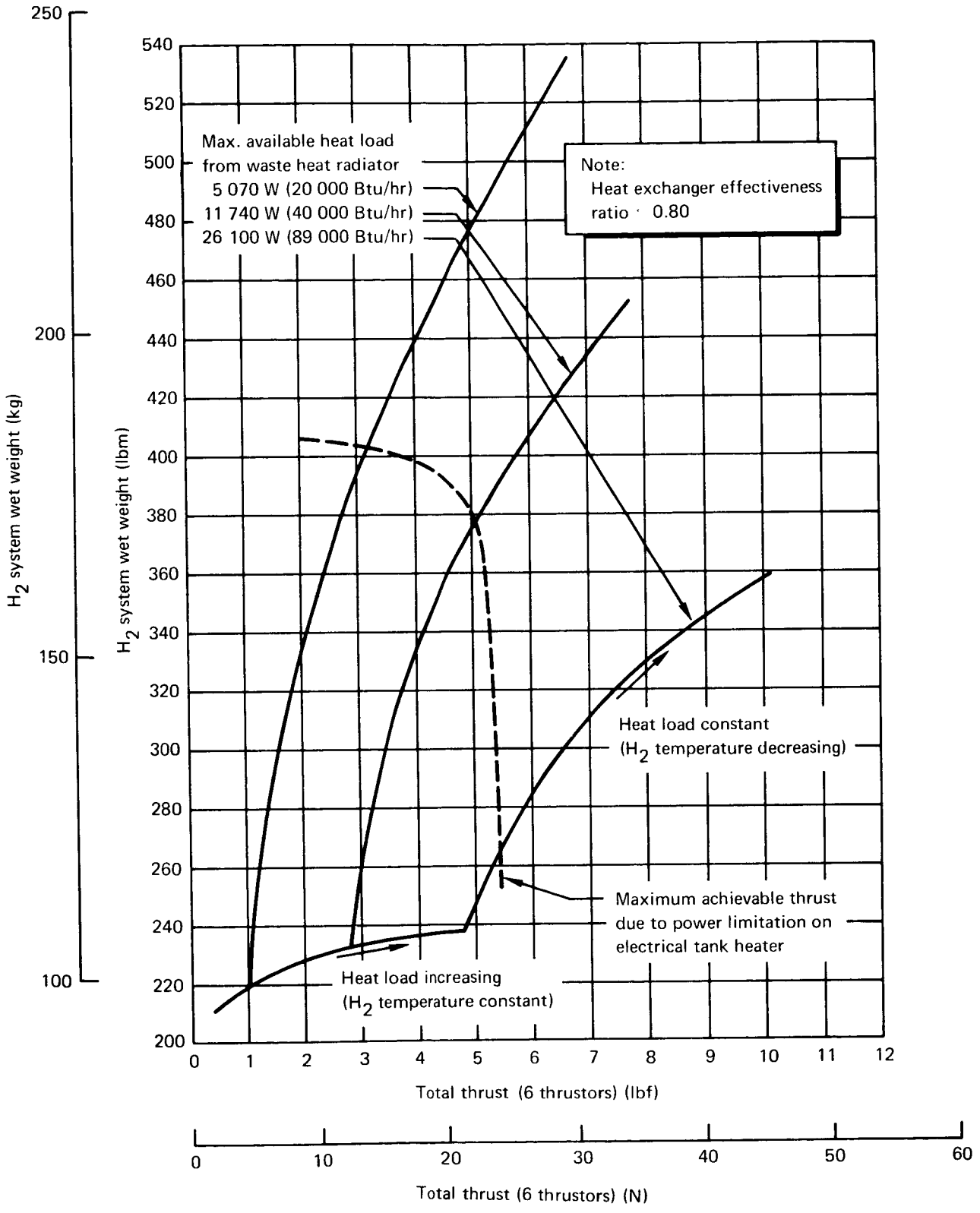

Figure 115. H_2 Heated-Gas System Weights

Fig. 116 shows propellant weight as a function of total thrust for each of the heat sources. The NH_3 system has two temperature limits: one occurs at the point at which the heat added is just sufficient to boil off the required amount of propellant (the minimum temperature extreme and the maximum weight point shown for each of the curves in (fig. 116); the other occurs at the maximum temperature extreme. In the case of heat loads (1) and (3), the maximum temperature is limited by the temperature of the heat-transfer medium. These limits are 456°K (820°R) and 400°K (720°R), respectively. Therefore, the horizontal portion of curves (1) and (3) are lines of constant NH_3 temperature. At the break in the curve, all of the available heat is utilized, while at lower thrust levels, only a part of the available heat is transferred to the NH_3. The electrical heat load curve(2) is not temperature-limited and, in this case, a maximum temperature had to be assumed. The temperature selected for structural reasons, for heat loads (2) and (4) is 1167°K (2100°R). Thus, in each case, the horizontal part of the curves represents an NH_3 temperature of 1167°K. The rapid rise in all of the curves, which occurs above the break, reflects the effects of rate of temperature change with flow rate at constant heat load. Curve (4) exhibits the highest achievable thrust, and the system shown in fig. 117 is representative of such a concept. All the heat input at this point is being used to vaporize the liquid and, consequently, no improvement in specific impulse is realized above the cold flow value.

The parametric model for the heated GN_2 system is shown in fig. 118. GN_2 is stored at an initial pressure 206.7×10^5 N/m^2 (3000 psia) and is allowed to decay to a minimum of 6.89×10^5 N/m^2 (100 psia) as it is consumed over 147 days. During periods when control for scheduled operational disturbances is required, it is permissible to divert the EC/LS system heating loop and use it to heat the GN_2 as it flows to the thrustors. The parametric heat-exchanger characteristics shown in fig. 119 were derived for counter flow heat exchangers using the EC/LS heat-transport fluid H_2O at an input temperature of 445°K (800°R) and a mass flow rate 34.5 kg/hr (76 lbm/hr). Fig. 120 demonstrates the output temperatures and estimated heat-exchanger weight as a function of GN_2 flow rate for exchangers exhibiting an effectiveness of 80%. The variation of specific impulse as well as required N_2 weight and tank weight variation with GN_2 temperature is shown in fig. 121. The total RCS weight as a function of thrust level is shown in fig. 122.

Evaluation and selection: The six previously discussed RCS's were compared and evaluated on the basis of performance, weight, and complexity. The N_2H_4 monopropellant system was selected for the MORL to provide attitude control during the schedule operational disturbance.

To minimize system weight, the heated-gas systems were sized at the minimum required thrust level 26.7 N (6 lbf) of roll thrust. Neither the H_2 nor the NH_3 heated-gas systems were capable of achieving the minimum required thrust and, hence, both were eliminated.

Table 55 presents a weight breakdown of the four remaining systems. The N_2 heated-gas system is from two to four times heavier than the other systems and was dropped from further consideration. The 90-day resupply

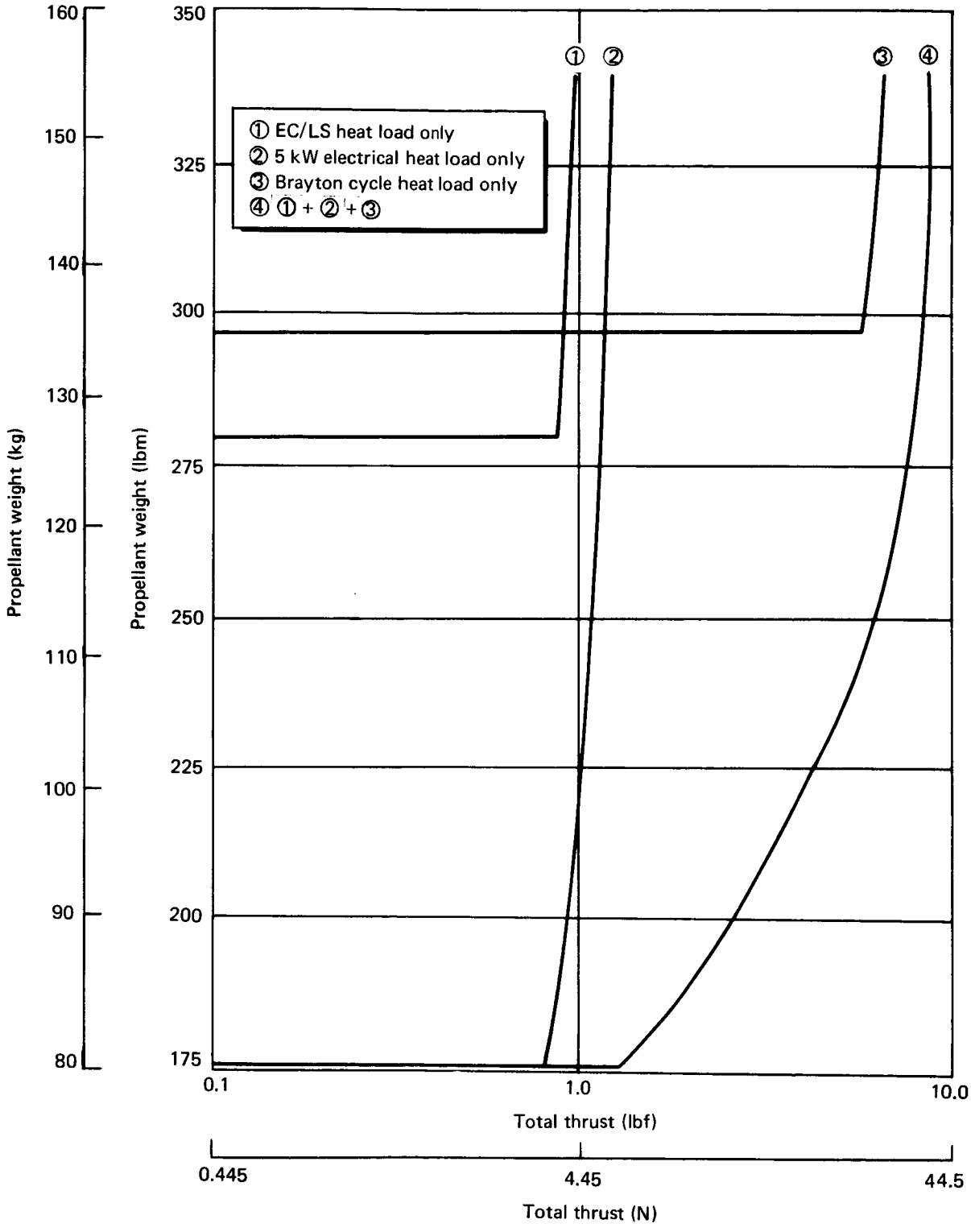

Figure 116. NH_3 Heated Gas RCS Propellant Weight

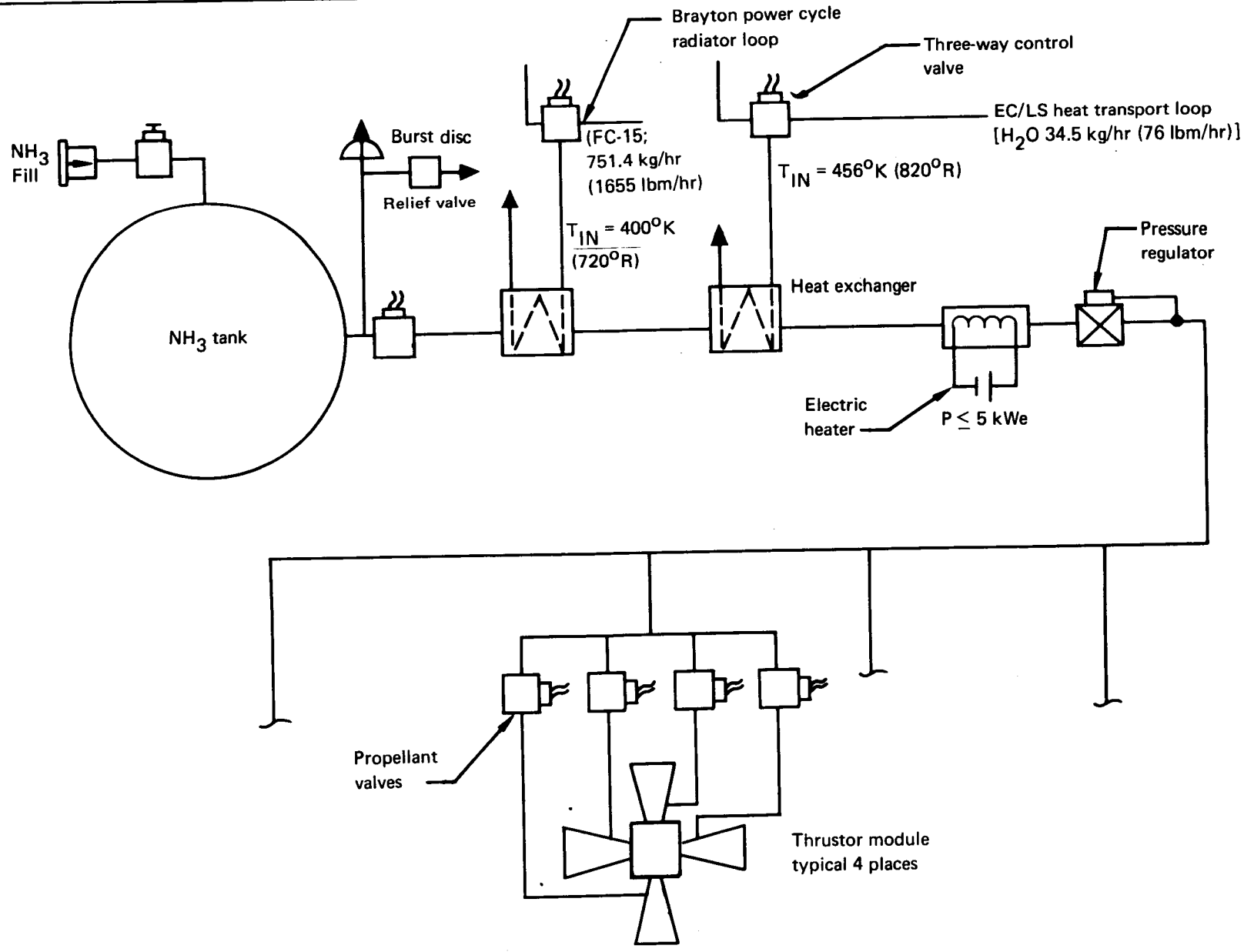

Figure 117. Scheduled Disturbance Reaction Control System (NH_3)

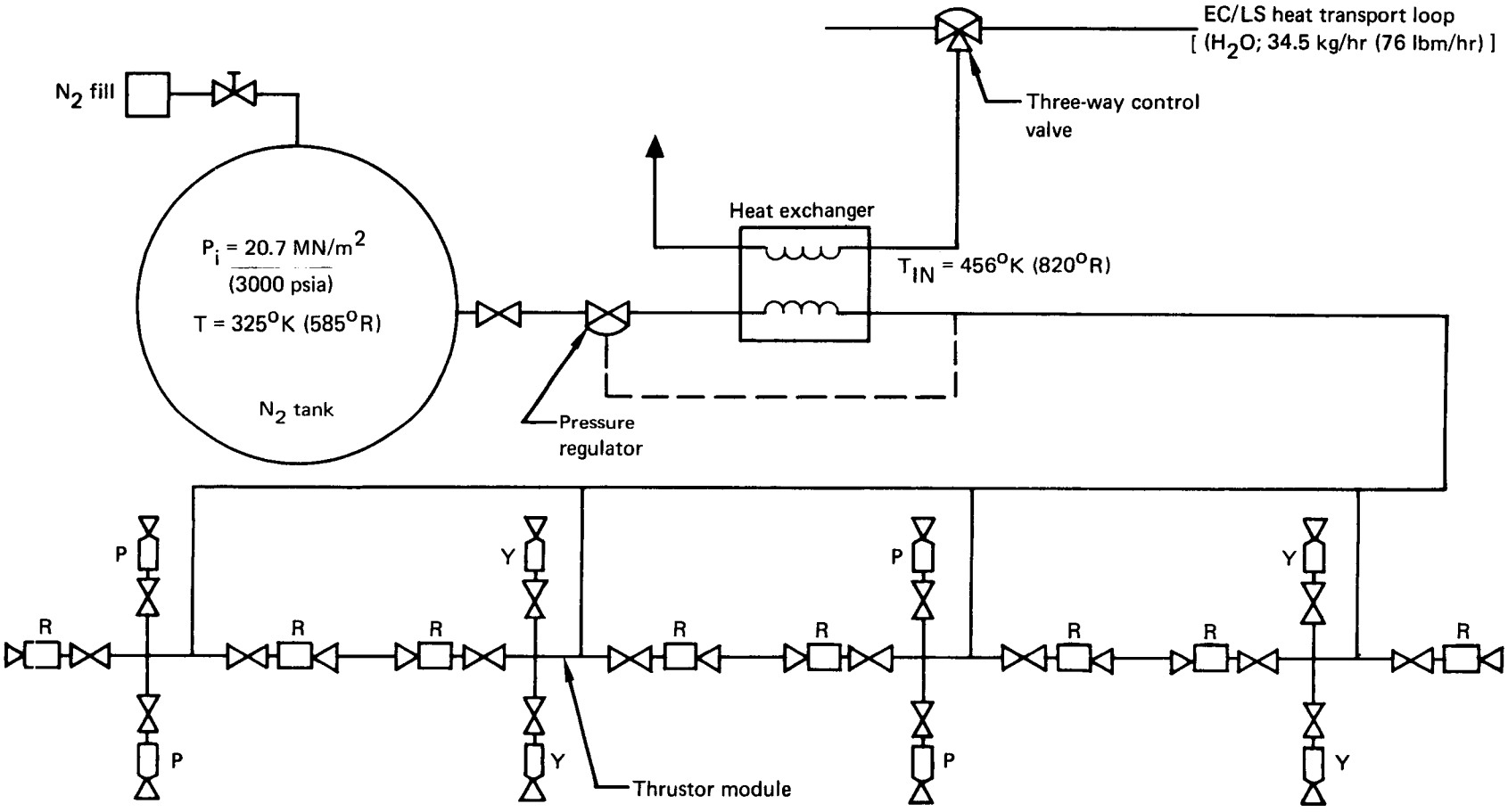

Figure 118. GN_2 Reaction Control System Parametric Model

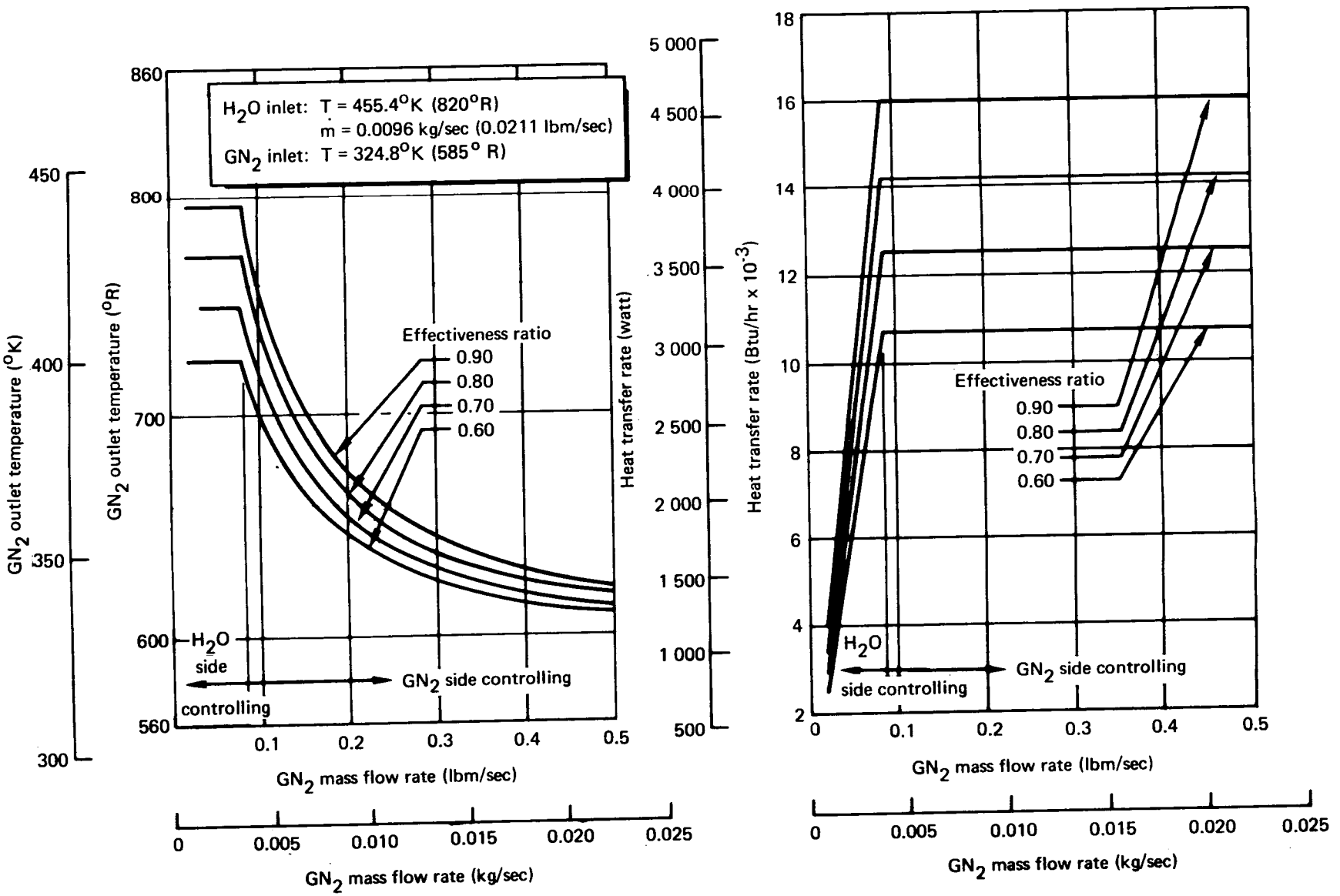

Figure 119. H_2O/GN_2 Heat Exchanger Characteristics

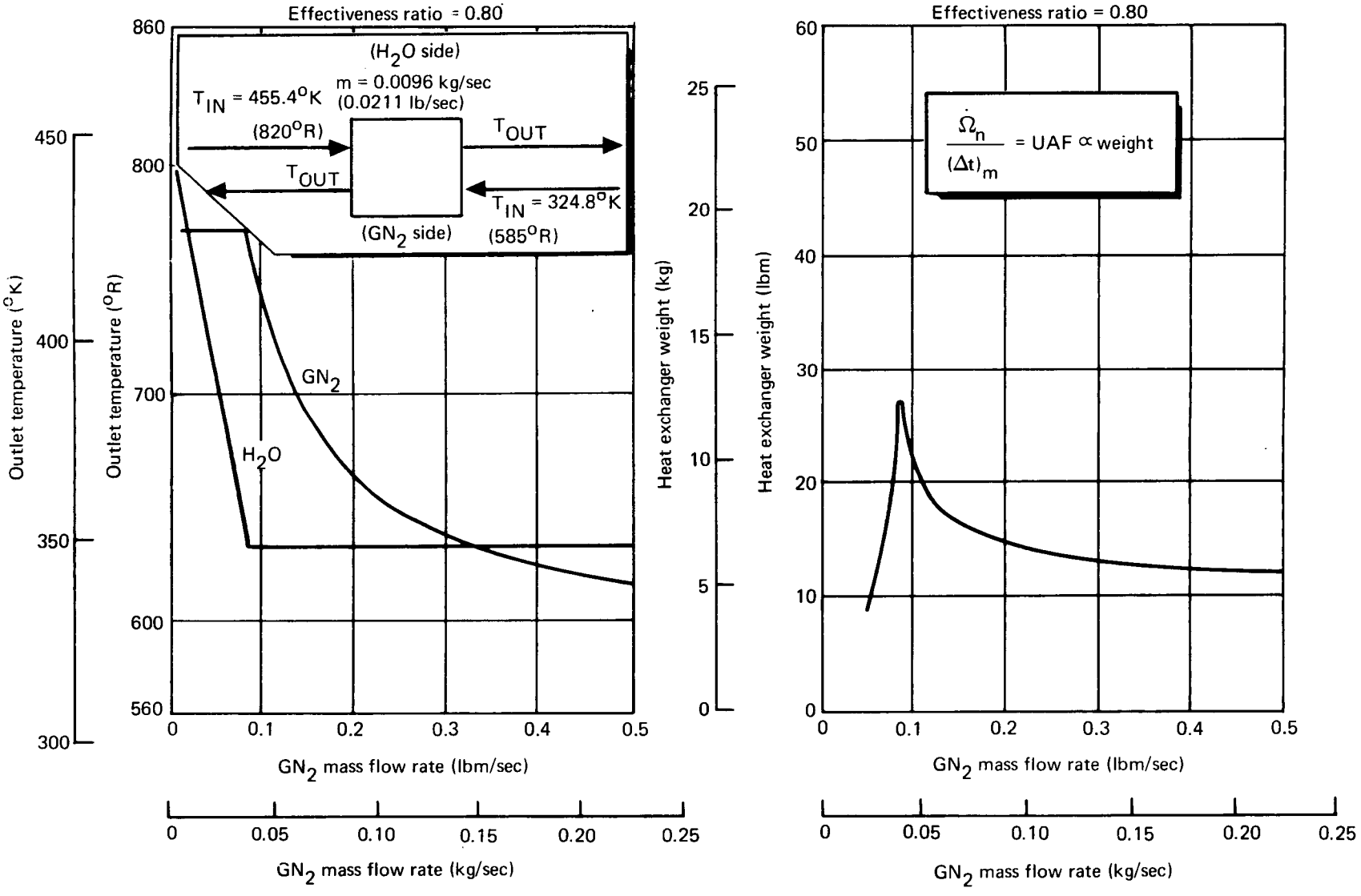

Figure 120. H_2O/GN_2 Heat Exchanger Characteristics Variation with Effectiveness Ratio

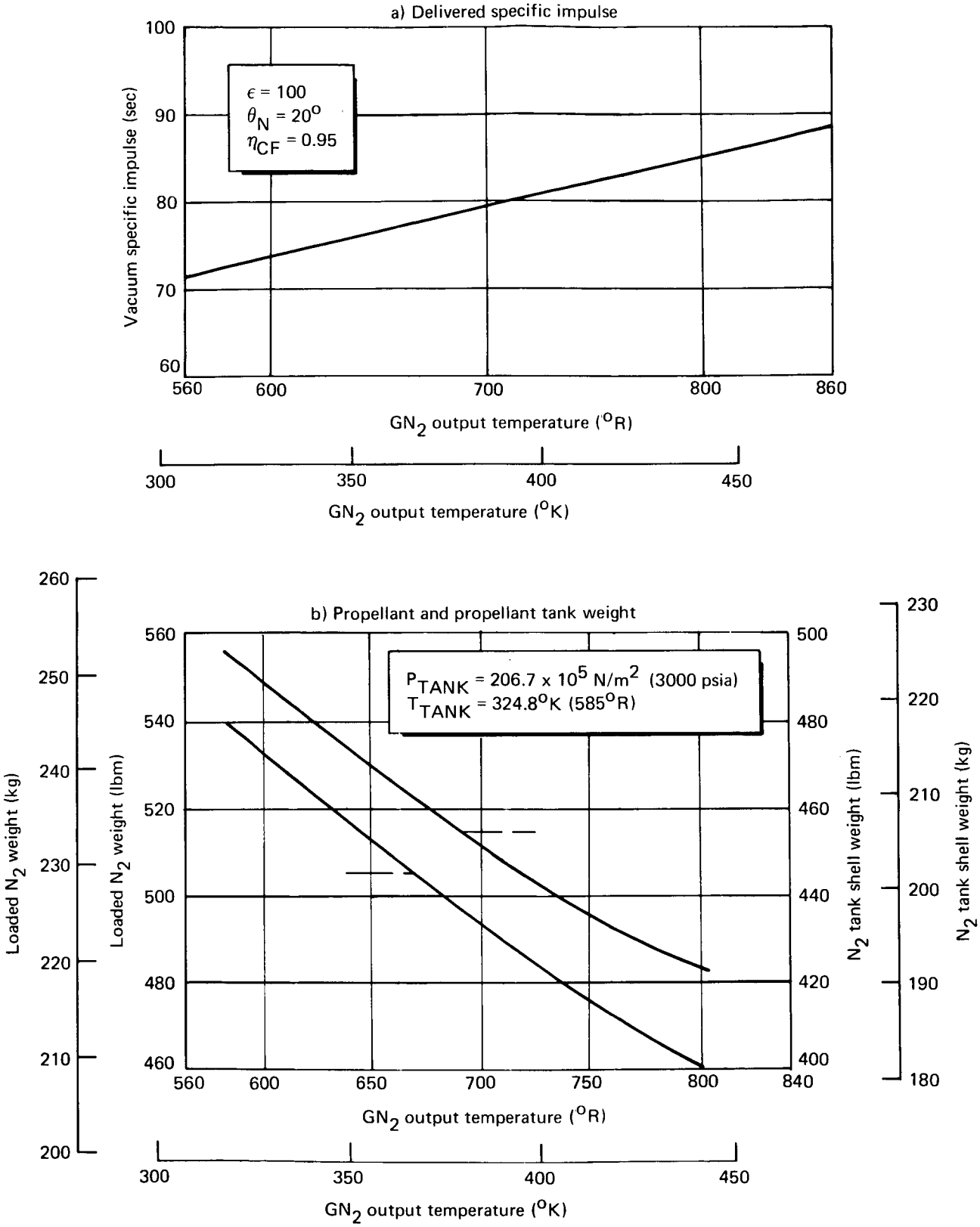

Figure 121. GN_2 Reaction Control System Characteristics

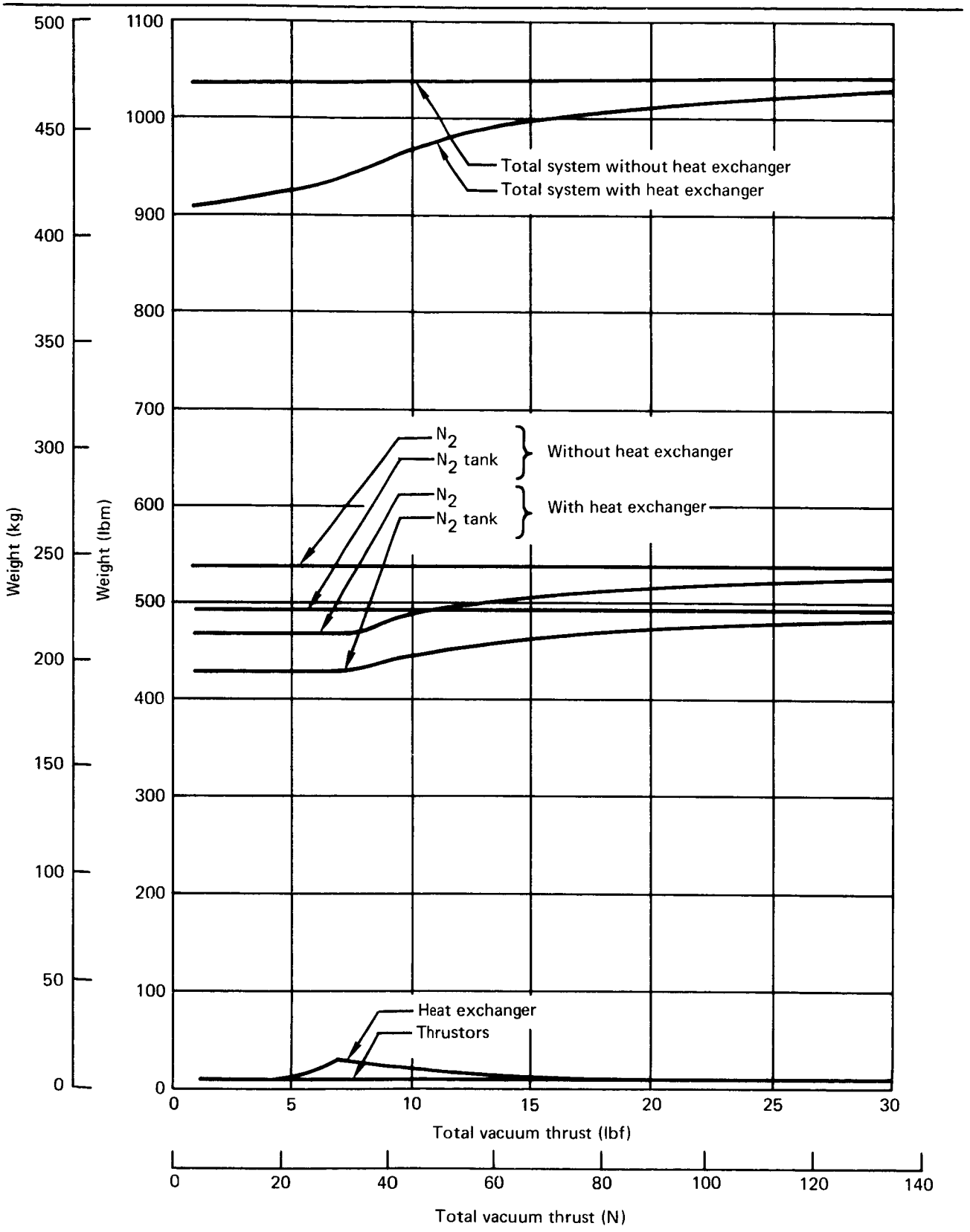

Figure 122. GN_2 Reaction Control System Weights

TABLE 55

SCHEDULED OPERATIONAL-DISTURBANCE RCS WEIGHT SUMMARY

System	N_2H_4 kg (lbm)	N_2O_4/MMH kg (lbm)	O_2H_2 kg (lbm)	GN_2 kg (lbm)
Propellant tanks	11.35 (25)	11.35 (25)	38.59 ([a]85)	200.21 (441)
Tank insulation	---	---	1.36 ([b]3)	---
Metal bellows	23.15 (51)	18.16 (40)	---	---
Valves, regulators	3.63 (8)	4.99 (11)	5.90 (13)	4.54 (10)
Quantity gauge system	3.63 (8)	4.99 (11)	0.91 (2)	0.91 (2)
Umbilical panel	0.91 (2)	1.36 (3)	0.45 (1)	0.45 (1)
Lines, fittings, etc.	4.09 (9)	6.36 (14)	6.36 (14)	8.17 (18)
Thrustor modules (4)	13.62 (30)	16.34 (36)	9.08 (20)	4.09 (9)
Pressurant bottle	4.09 (9)	3.18 (7)	---	---
Pressure regulator/follower	---	---	12.71 (28)	---
Heat exchangers	---	---	13.62 (30)	9.08 (20)
Gas generators	---	---	9.99 (22)	---
Mechanical vapor/liquid separator	---	---	---	---
Accumulators	---	---	4.54 (10)	---
Total chargeable dry weight	64.47 (142)	66.73 (147)	103.51 (228)	227.45 (501)
Pressurant gas weight	4.54 (10)	3.63 (8)	---	---
Propellant loaded at launch	14.07 (31)	9.53 (21)	10.44 (23)	29.51 (65)
Total chargeable launch weight	83.08 (183)	79.89 (176)	113.95 (251)	256.96 (566)
147-day propellant weight	92.62 (204)	62.20 (137)	59.02 (130)	217.92 (480)
Total chargeable wet weight in orbit	161.62 (356)	132.57 (292)	162.53 (358)	445.37 (981)
Logistics vehicle chargeable propulsion dry weight	19.98 (44)	24.97 (55)	33.60 (74)	---
Loaded consumables	62.65 (138)	43.13 (95)	36.32 (80)	---
Total logistics vehicle chargeable launch weight	82.63 (182)	68.10 (150)	69.92 (154)	---

[a]Includes O_2 tank and incremental weight for resized resistojet system H_2 tank.

[b]Incremental weight for resized resistojet system H_2 tank.

propellant weight of the cryogenic bipropellant system is lower than the storable bipropellant or monopropellant systems because of its somewhat higher specific impulse. The O_2H_4 system dry weight, however, is higher because of the complex propellant-conditioning system required. This system was eliminated because it could not offer a significant performance advantage over the storable bipropellant system and because it is highly complex.

Table 55 shows that the dry weights of the storable bipropellant and monopropellant systems are about the same. The N_2O_4/MMH system has the advantage of a somewhat higher specific impulse, which results in about a 19.5 kg (43 lbm) reduction in resupply consumables required every 90 days. It is more complex than the N_2H_4 system, and two propellants must be resupplied as opposed to one. This has the net effect of reducing the total chargeable logistics weight advantage of the bipropellant RCS to 14.5 kg (32 lbm). The monopropellant system, because of its relative simplicity, will exhibit a higher reliability and is a safer system. The N_2H_4 RCS will also have a lower development cost. These factors led to the selection of the monopropellant scheduled-distrubance RCS in preference to the N_2O_4/MMH system, even though the latter exhibits a slight resupply weight advantage.

Backup attitude control. – Present ground rules for the MORL mission require that the SCS has backup attitude-hold capability which would be utilized when the CMG's were inoperative for either scheduled or unscheduled maintenance.

The SCS performance requirements for the backup mode have only been loosely defined. Therefore, the requirements for normal operation are assumed to hold. If these requirements are made less stringent at a later date, certain systems now excluded may be considered further.

This section presents a preliminary investigation of the feasibility of various systems for providing backup attitude control for the MORL. System candidates are the high-thrust bipropellant P/RCS, the resistojet orbit-injection system with certain modifications and the resistojet P/RCS used for orbit-keeping and CMG desaturation. Advantages and disadvantages of the various systems are presented.

Bipropellant P/RCS: The bipropellant P/RCS considered for backup attitude hold is defined in the scheduled-disturbance control systems section. This system will satisfy all the baseline SCS requirements during backup attitude hold, but only at the considerable propellant expenditure of 2.13 kg/hour (4.7 lbm/hour). The addition of a minimum-impulse mode to provide 25 m/sec pulses would reduce propellant consumption to 0.19 kg/hour (0.42 lbm/hour) in a belly-down orientation and 0.41 kg/hour (0.9 lbm/hr) in an inertial orientation. A further requirement of 0.45 kg/day (1 lbm/day) provides for maneuvers. Therefore, total propellant consumed per day would be 5.99 kg (13.2 lbm) assuming a minimum-impulse mode of operation. The minimum-impulse mode would be implemented by a feedback loop around the switching amplifier which contains a passive lag network. The loop would be opened during control of large dynamic disturbance to prevent unwanted pulsing.

Resistojet orbit-injection system: The capability of a modified resistojet orbit-injection system to provide precise attitude hold may be marginal. However, for the present, such capability is assumed, and the feasibility of utilizing the system for backup attitude hold is investigated from other aspects.

The modification of the resistojet orbit-injection system consists of adding four 0.34 N (0.25-lbf) forward-facing thrustors, one to each module. Two benefits are derived from the modification. Control capability is increased and control moments can be applied as couples. Pitch and yaw control moment capability is increased to 7.45 N-m (5.5 ft-lbf) and roll capability remains unchanged at 0.60 N/m (0.44 ft-lbf).

The primary problem associated with using the resistojet orbit-injection system for providing backup attitude hold is limited moment capability at an I_{sp} only slightly higher than that of a bipropellant P/RCS. I_{sp} levels are directly attributed to limited electrical power. For example, during experimentation, approximately 1.1 kWe is available for the propulsion system. This power level will allow normal operation of the 0.0045-kg (10-mlbm) roll thrustors (750 I_{sp}). Power available for the 0.11-kg (0.25-lbm) pitch and yaw thrustors in the form of waste heat will provide an I_{sp} of 275 sec. Propellant consumption rates for the above I_{sp}'s are 0.41 kg/hour (0.9 lbm/hour) for the inertial orientation and 0.23 kg/hour (0.5 lbm/hour) for the belly-down orientation. These values are based on control logic which provides a 2.5-sec pulse width for the 0.011-kg (0.25-mlbm) thrustors and a 30-sec pulse width for the 0.0045-kg (10-mlbm) thrustors. Impulse consumption with the above pulse widths is the same as that of the bipropellant system. Propellant consumption per day would be 5.99 kg (13.2 lbm), which includes maneuvering.

An additional mode of operation could be considered which alters the experimental program to provide an additional 2 kWe to the propulsion system. The extra power would be allotted to the 0.11-kg (0.25-lbm) thrustors to provide an operating I_{sp} of 325 sec. Propellant consumption rates for this mode of operation are 0.27 kg/hour (0.6 lbm/hour) for the inertial orientation and 0.14 kg/hour (0.30 lbm/hour) for the belly-down orientation. Propellant consumption per day would be 4.09 kg (9.0 lbm). This may not be significant in selecting a mode of operation because operating time for backup control is small.

Resistojet orbit operation system: The resistojet system used for orbit operations (CMG desaturation and orbit keeping) has only limited backup attitude-control capability. The MORL could be stabilized in a belly-down orientation with the system. However, the capability of the system to provide precise attitude control is marginal. The system is unable to perform maneuvers or maintain an inertial orientation because of disturbance torques exceeding available control torque over a wide range of orientations.

Operational I_{sp}'s are 750-sec roll and 275-sec pitch and yaw for a power level of 1.1 kWe, and 750 sec for all thrustors for a 3-kWe power level. Propellant consumption rates are 4.99 kg/day (11 lbm/day) and 2.72 kg/day (6 lbm/day) respectively, for the two power levels.

Conclusions: The capability of the various systems to provide backup attitude control is presented in table 56. At present, the bipropellant system will most adequately provide backup attitude control. However, if requirements are made less stringent, the resistojet orbit-injection system becomes more suitable for providing backup attitude control. The most obvious relaxing of requirements would be cessation of experiments requiring precise attitude hold and/or an inertial orientation. In that event, the resistojet orbit-injection system becomes a close second to the bipropellant system.

TABLE 56

SYSTEM CAPABILITY

Function	Bipropellant system	Resistojet orbit operation system	Resistojet orbit injection system
Maintain belly-down orientation	Yes Propellant consumption rate high unless minimum-impulse mode of operation is provided	Yes • Capability to provide precise attitude hold very marginal • Power limitation may result in I_{sp}'s equivalent to those of bipropellant P/RCS	Yes • Capability to provide precise attitude hold marginal • Power limitation may result in I_{sp}'s equivalent to those of bipropellant P/RCS
Perform Maneuvers	Yes	No Disturbance torques exceed control torques over wide range of orientations	No More costly in terms of time and propellant than bipropellant system
Maintain inertial orientation	Same as belly-down orientation	No Disturbance torques exceed control torques over wide range of orientations	Same as belly-down orientation

Logistics Resupply

Previous studies have shown the advantages of utilizing a propellant-transfer mode for resupplying propellant from the logistics vehicle to the propellant tanks in the aft interstage of MORL. Tank replacement was shown to be undesirable because of MORL access problems and crew-safety requirements. These problems are further complicated by the momentum problem involved with the large, unwieldy propellant tanks and their handling in a very restrictive space. Both the H_2 and the NH_3 resistojet systems are designed to be resupplied every 90 days. The thermodynamic problems in transferring a cryogen in zero-g are considered in detail. Logistics resupply systems are also defined for the three candidate high-thrust systems.

Cryogenic H_2.— LH_2 will be transferred from the logistics vehicle to the MORL supply tank at a very low level of liquid acceleration relative to the vehicle. An operation of this type is distinguished from ground-transfer operations by the need to provide for positioning of the liquid over the drain. The methods can be accelerating the liquid toward the drain by either applying axial thrust or rotating the vehicle, the use of capillary devices, and the positive displacement. Both methods of accelerating the liquid are undesirable for the MORL mission because they would interfere with experiments and would place severe requirements on the attitude-control system. The use of capillary devices for liquid positioning shows promise for applications of this type, but the technology was considered primitive, particularly in the use of cryogenics where venting is required.

The Air Force has been conducting a program for the construction and testing of reversing stainless-steel bladders. The work has been carried out by Arde, Inc. A 58.4-cm (23-in.)-diam bladder has been constructed and tested successfully with H_2O and LH_2. Arde is presently building a 1.83-m (6-ft)-diam bladder. Although some problems in fabrication have arisen, they expect to have it completed and ready for testing by the end of this year. The bladder is a reversing stainless steel hemisphere with circular reinforcements (see fig. 123). The estimated weight of such a system including tank and bladder is 1.32 kg (0.6 lbm) of hardware per pound of LH_2.

Thermodynamic analysis: Transfer procedures and systems requirements have been identified based on the following considerations:

(1) No venting will occur during transfer.

(2) Withdrawal of hydrogen for the resistojets will not be interrupted.

(3) Compatibility of tank conditions with the resistojet feed system will be maintained.

(4) MORL hardware weight should be minimized.

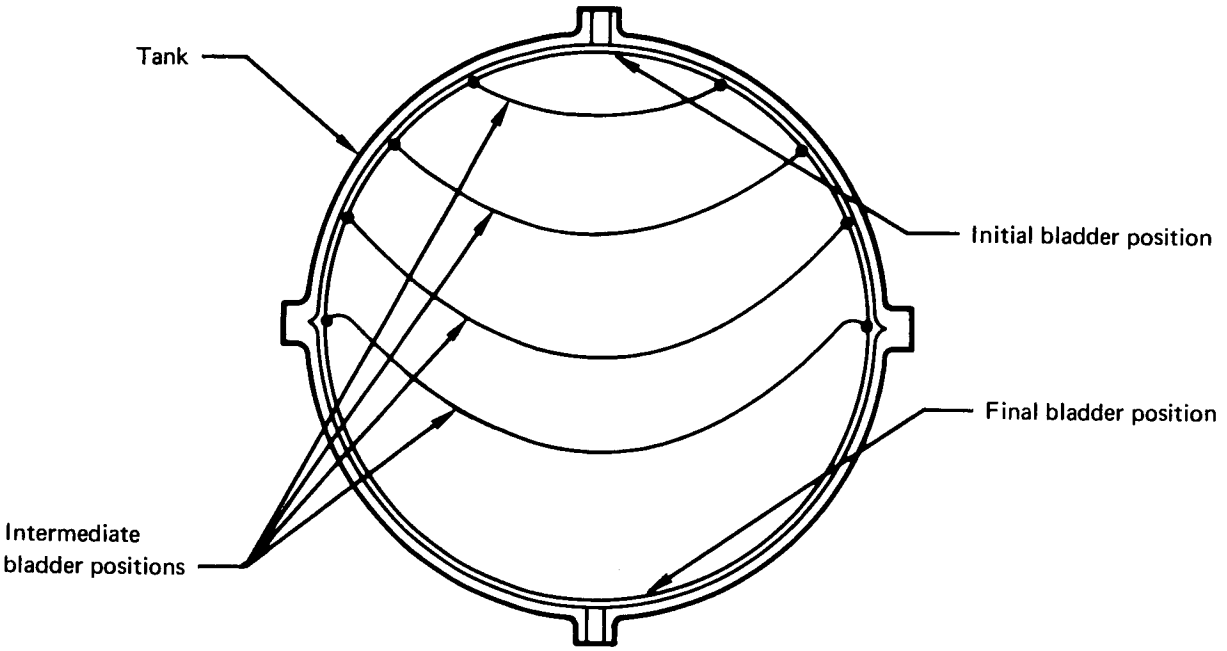

Figure 123. Bladder Configuration

Venting should be avoided for two reasons. First, venting under low-gravity conditions involves the possibility of large losses of liquid overboard. No procedures are available to provide quantitative estimates of such losses, and, although many schemes have been advanced to minimize such losses, none has been verified to date, nor shows great promise for applications of the type considered here. Second, venting during transfer could easily result in intolerable vehicle disturbances. Even if a nonpropulsive vent is used, the unbalanced impulse resulting from vent nozzle misalignment and plume impingement could be of the order of 445 N-sec (100 lbf-sec).

Because shutdown of the resistojets is not desirable for more than a few seconds at a time, conditions must be maintained in the supply tank which are compatible with the resistojet feed system throughout the transfer operation. An alternative to this would be to have two supply tanks loaded one after the other; however, the analysis discussed below indicates that, over the entire range of expected tank conditions before resupply, the feed system criteria can be met throughout the resupply operations. The initial conditions in the MORL tank will include a pressure between $310 \times 10^3 N/m^2$ (45 psia) and $0.448 \times 10^3 N/m^2$ (65 psia) and a quantity of liquid between 0 and a 57-day supply (since the interval between resupplies will range from 90 to 147 days). Analysis of the resistojet feed system has shown that a minimum tank pressure of $310 \times 10^3 N/m^2$ (45 psia) is needed for proper operation but that it will be permissible to load to pressures above the

normal operating maximum of 448 x 10^3 N/m^2 (65 psia). The upper limit on loading pressure is governed by the desire to hold the tank relief pressure to 552 x 10^3 to 620 x 10^3 N/m^2 (80 to 90 psia) to minimize hardware weight.

The basic problem of predicting pressure transients during cryogenic propellant transfer is extremely difficult and is currently being investigated in detail by NASA and others. Existing analytical procedures were evaluated but none was judged sufficiently accurate to provide assurance that the above criteria could be met. Analyses of limiting cases indicated a wide range of possible pressure profiles, depending on the degree of thermal mixing in the tank during transfer. Because liquid inlet velocities will be large, it is felt that a good degree of mixing will be obtained and that the tank conditions will approach the limiting case of thermal equilibrium. On the other hand, small differences in temperature between the liquid and the ullage could result in significant pressure deviations from the equilibrium case. Because predictable tank conditions must be provided it was decided to use a mechanical mixer in the tank to ensure a close approach to thermal equilibrium. The mixer would be completely submerged in the tank and would have to be capable of handling both liquid and vapor. Such a device is believed to be well within present technology.

Use of the mixer will also provide for a relatively simple transfer procedure. Once transfer is initiated, the operation can be controlled by a pressure switch that senses MORL tank pressure. When the pressure reaches an upper limit, the switch will close the transfer valve and turn on the mixer. When the pressure switch drops out, transfer flow can be resumed. The analysis below indicates that at the point when further mixing does not produce a sufficient decrease in pressure to drop out the pressure switch, the required mass of hydrogen will be on board the MORL. Calculations have shown that a 50-W mixer could thoroughly mix the fluid in a 1.83-m (6-ft)-diam tank in about 5 min (see fig. 124). This duration is acceptable for the transfer procedure described here and probably will never be completely needed because the liquid will be partially mixed by the inflow effects.

The tank pressure at the end of resupply was based on the assumption that thermodynamic equilibrium was parameterized in terms of initial pressure and mass of H_2 in the tank, inlet temperature of the transferred liquid, and tank volume. The results are plotted in fig. 125. The figures indicate that a tank which has 5% ullage volume at the maximum loading will have acceptable equilibrium pressures between 310 x 10^3 and 5.52 x 10^3 N/m^2 (45 and 80 psia) for the entire range of initial tank conditions as long as the saturation pressure of the incoming fluid is held between 2.02 x 10^5 and 3.53 x 10^5 N/m^2 (2 and 3.5 atm). Slightly wider ranges of inlet conditions could be provided for if a larger tank were to be used; but, because hardware weight on the MORL vehicle is one of the prime considerations, it will be desirable to keep the tank as small as possible. The following discussions of the sources of uncertainty for the liquid inlet temperature indicate that there should be no problem in providing liquid within the 1.51 x 10^5 N/m^2 (1.5 atm) band.

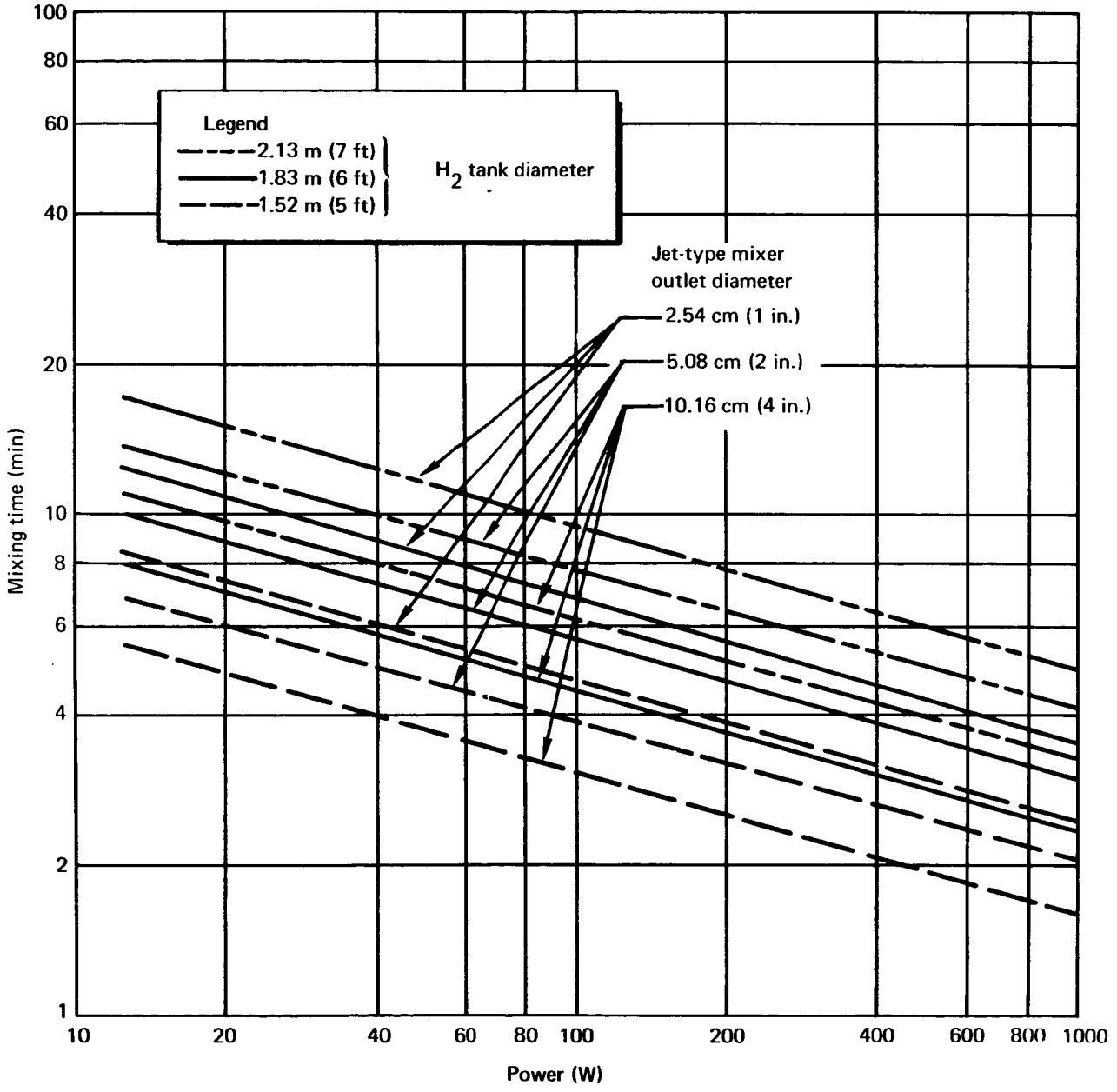

Figure 124. H_2 Tank Mixer Power Requirements

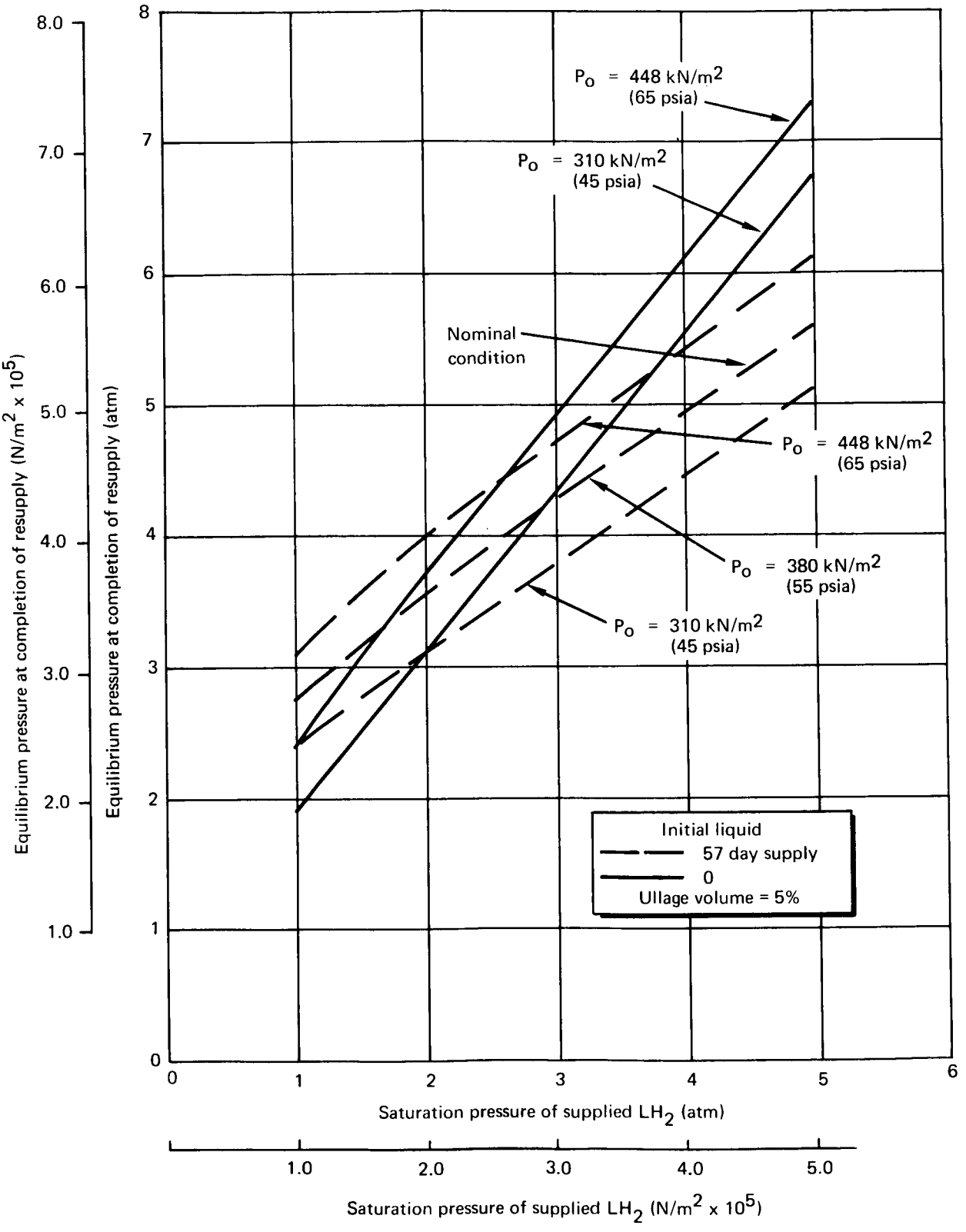

Figure 125. Resupply Pressure Calculations

The factors affecting delivery temperature of the H_2 supply to the MORL tank are heating of the propellant in the logistics vehicle before transfer, heat transfer from the pressurant during transfer, and sensible heat of the transfer hardware which is absorbed by the fluid. The last of these was found to be insignificant. Based on a conservative estimate of the transfer hardware weight, it was found that the saturation pressure of the transferred liquid would be raised less than 6.9×10^3 N/m^2 (1 psi). On the other hand, the first two factors will be of great importance in the transfer operation. Fig. 126 shows the predicted liquid temperature history for the logistics vehicle.

In analyzing heating of the hydrogen of the logistic vehicle, it was assumed that the tank would be insulated with a large thickness of high performance insulation (HPI). Current methods were used to predict heat fluxes through the HPI and evaluation transients. It is assumed that the transfer tank can remain vented to the atmosphere, with boiloff continually replenished until 1 min before liftoff. During this minute, the saturation pressure of the H_2 will rise approximately 20.7×10^3 N/m^2 (3 psi). It is expected to take approximately 10 hr after orbital insertion for complete evacuation of the HPI. During this period, the heat flux is relatively high. It is estimated that if the tank is not vented, the saturation pressure will rise 172×10^3 N/m^2 (25 psi) during this 10-hour period. Once the insulation is evacuated, it is expected that a heat flux as low as 0.226×10^4 J/m^2 (0.2 Btu/ft^2) can be achieved. This corresponds to a 9-psi rise during a 62-hr period before the propellant transfer. Thus, if the supply tank on the logistics vehicle is not vented, the liquid temperature will be too high before transfer is begun. It is recommended that the transfer tank be vented to a low level sometime after the first 10 hrs of flight. The AS-203 experiment demonstrated that saturated blowdowns can be accomplished at low gravity while maintaining control of propellant if moderate blowdown rates are used. About 9.1 kg (20 lbm) of H_2 must be vented to reduce the temperature to an acceptable level. The level should be such that subsequent heating before the start of transfer will not cause any hardship. Sequencing of this blowdown will have to be coordinated with the logistics vehicle mission profile. It should be as late as possible to minimize the uncertainty in delivered temperature. A typical blowdown procedure is shown in fig. 126.

An analysis of convective heat transfer between the pressurant and the LH_2 on the logistics vehicle indicates that such heat transfer could be a significant problem if the pressurant is much warmer than the H_2. The overall heat-transfer coefficient was estimated to be 0.14 J/m^2 sec $^\circ$K (0.25 Btu/hr ft^2 $^\circ$R.)

A temperature difference of 55.5°K (100°R) yields a saturation pressure rise of about 1 atm/hr. This will require a transfer operation to be completed in about 1 hr to ensure that venting is avoided. The rate at which transfer can be accomplished in the recommended procedure is fixed by the power level available for mixing (currently about 200 W maximum). Because several mixing cycles may be required, it is felt that a 1-hr transfer time is about the best that can be hoped for, and therefore, cold pressurant must be used. Use of the cold pressurant will also be advantageous in regard to

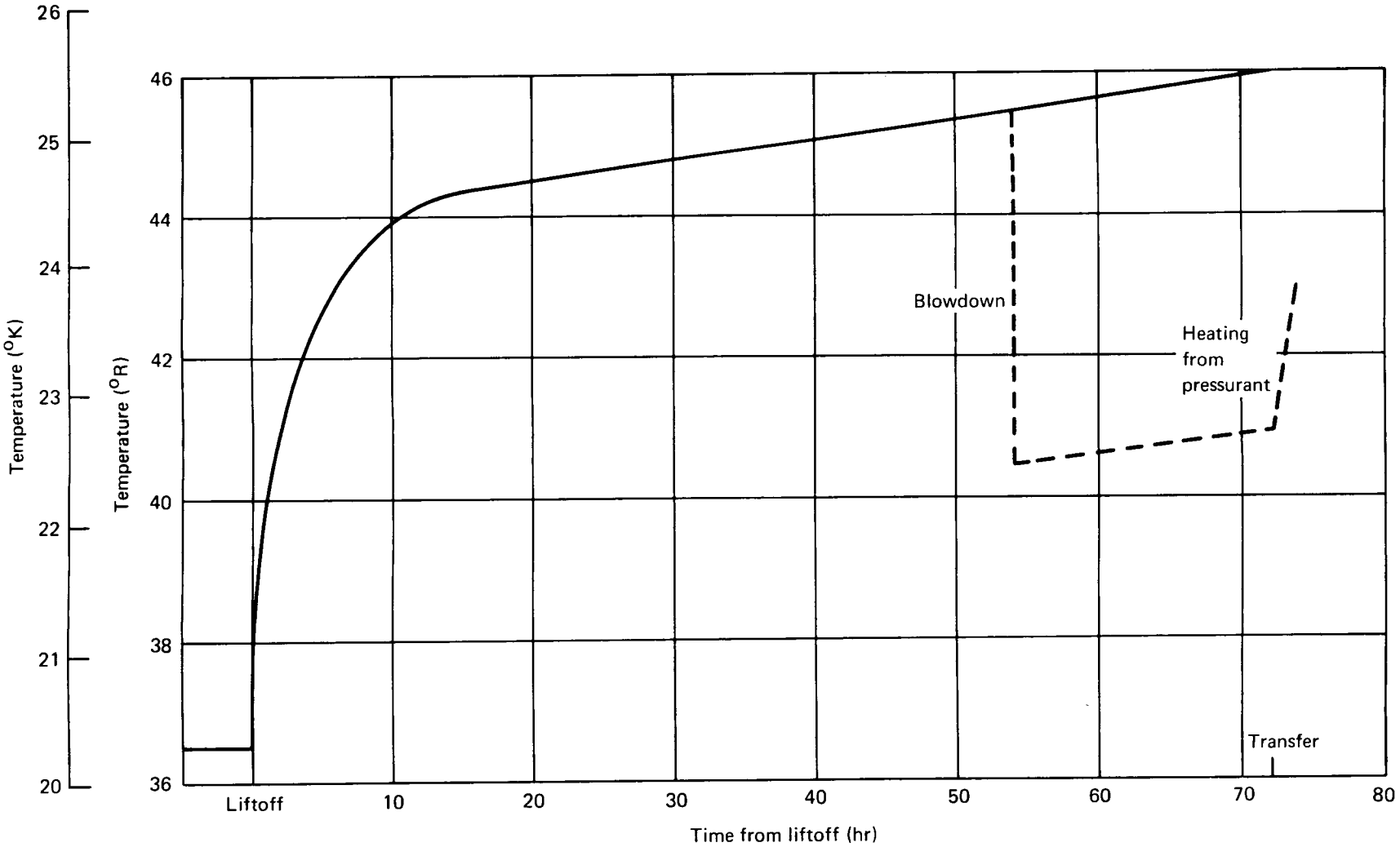

Figure 126. Logistics Vehicle LH_2 Temperature

bladder structural considerations. Preliminary analysis indicates that use of HPI on pressurant storage tanks will provide for helium temperatures below 55.5°K (100°R) after 3 days in orbit. Coordination must be maintained between the pressurant temperature and the blowdown level to ensure that propellant at the proper condition is supplied to the MORL tank.

The temperature-entropy diagram presented in fig. 127 illustrates the thermodynamic conditions of the MORL H_2 tank and the logistics vehicle tank during the transfer process. The path shown for the MORL tank was selected for nominal tank conditions [initial tank pressure of 379k N/m^2 (55 psia), final tank pressure of 552k N/m^2 (80 psia) and 5% ullage, and transfer of a 90-day supply of propellant]. The following procedure was followed to determine the required logistics tank conditions. The initial MORL tank pressure of 379k N/m^2 (55 psia) and final pressure of 552 kN/m^2 (80 psia) are found in fig. 125. The resultant saturation pressure of the supplied LH_2 is 462k N/m^2 (67 psia), assuming a minimum pressure drop between tanks of 69k N/m^2 (10 psia), and yields a requirement for 621k N/m^2 (90 psia) in the resupply tank. Thus, the initial logistics-tank state point (fig. 128) is on the 621k N/m^2 isobar at the temperature 26.80°K (48.3°R) corresponding to a saturation pressure of 462k N/m^2 (67 psia). The 1° temperature rise shown for the resupply H_2 is taken from fig. 126, assuming a 1-hour propellant transfer duration.

In summary, the following recommendations are made for the resupply system:

(1) The MORL tank should have a volume corresponding to 105% of the design mass based on the density at 552k N/m^2 (80 psia).

(2) The tank relief pressure should be set at 586k N/m^2 (85 psia).

(3) A mechanical mixing device submerged in the tank should be used to ensure that resupply criteria will be met. The power requirement for the mixer will be 50 to 100 W.

(4) The transfer operation should be controlled by pressure switches in the receiver tank with monitoring of tank pressures by the crew for backup.

(5) The propellant on the logistics vehicle should be conditioned by tank blowdown at sometime after liftoff plus 10 hours.

(6) The temperature of the bladder pressurant should be as close as possible to liquid hydrogen temperature and should, in any case, be less than 83°K (150°R).

(7) An experimental investigation of the degree of thermal mixing during inflow should be initiated to determine whether the mechanical mixer can be eliminated or reduced in size.

System design: The logistics resupply system for cryogenic H_2 is designed by utilizing the results of the thermodynamic analysis. A flow

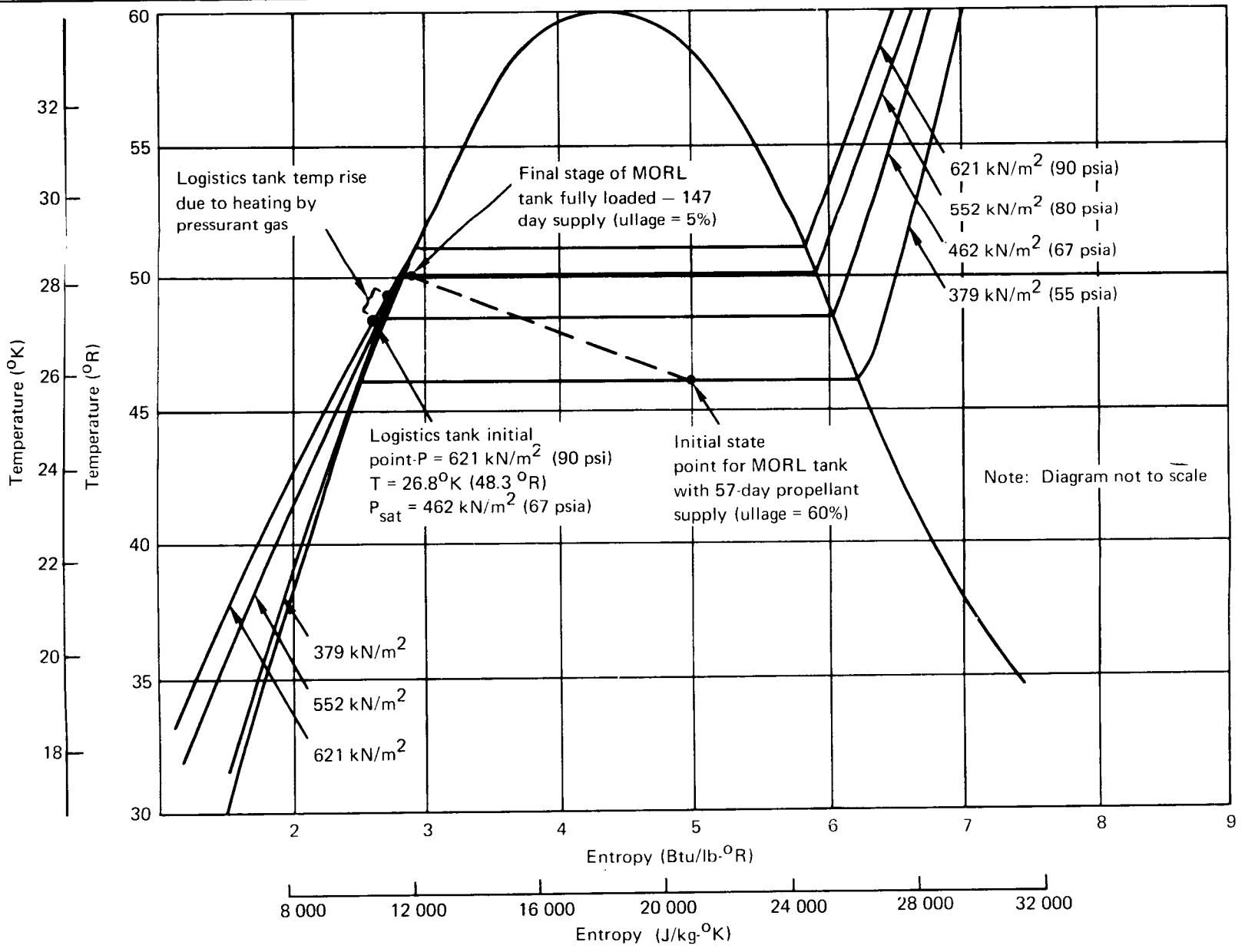

Figure 127. Propellant Transfer Process (Thermodynamic Equilibrium)

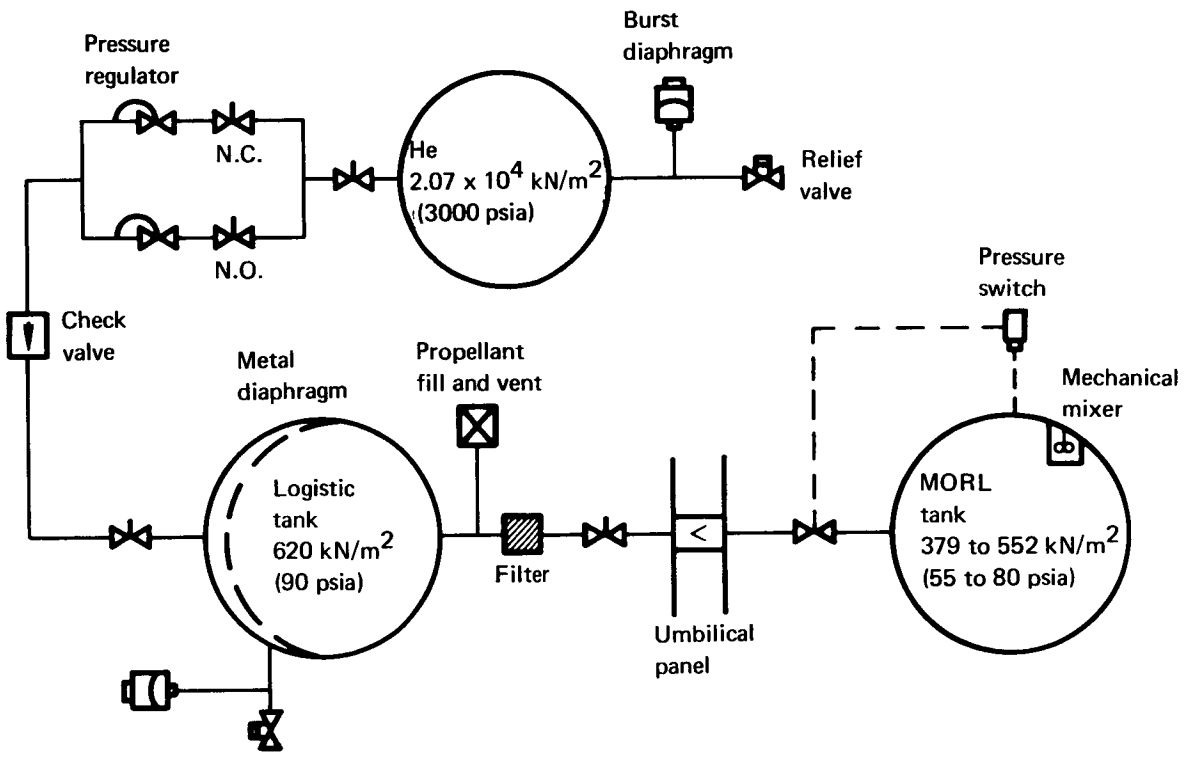

Figure 128. H_2 Resupply System

schematic of the H_2 resupply system is shown in fig. 128. The H_2 is stored in a spherical tank with a stainless-steel reversing hemisphere for positive expulsion. GHe is used as the pressurant for transferring the H_2 to the MORL tank. This He is stored at 20 700 kN/m^2 (3000 psia) at a cryogenic temperature of 83.2°K (150°R). The reduced temperature of the He is necessary to reduce heat transfer through the metal diaphragm to the subcooled H_2 in the logistics tank. Thermal insulation surrounds the He sphere to keep the He at this reduced temperature. The H_2 is loaded in a subcooled state at about 1-atm pressure on the logistics launch pad. The HPI is saturated with He gas before liftoff to prevent cryopumping of the ambient atmosphere during launch (that is, to prevent air from condensing to its liquid and solid state between the sheets of HPI). During the first 10 hours after boost, the He-saturated HPI will slowly outgas to the ambient vacuum environment. Heat transfer through the HPI is excessively high before the HPI is fully outgassed. This requires about 9.07 kg (20 lbm) of H_2 to be vented sometime after 10 hours from logistics launch but before logistics transfer. Just before the transfer process, the He will pressurize the logistics H_2 to 621 kN/m^2 (90 psia). The H_2 to be transferred will be in a subcooled state at 26.8°K (48.3°R). This will ensure that the ullage vapors in the MORL tank will be condensed after completion of the transfer. The H_2 in the MORL tank is initially under the vapor dome at 379×10^3 N/m^2 (55 psia). As H_2 is transferred to the MORL tank, this pressure increases to 552×10^3 N/m^2 (80 psia) at which time a pressure switch stops the flow of H_2. A mechanical mixer onboard the MORL tank will then mix the H_2 in

the MORL tank until an equilibrium condition is reached, in which subcooled H_2 from the logistics vehicle will have condensed the H_2 vapor in the MORL ullage. After this ullage vapor has condensed, the pressure in the MORL tank will drop to a value which will cause the pressure switch to reinitiate the flow of H_2 from the logistics tank. This procedure is repeated as required until all the H_2 from the logistics vehicle is transferred to the MORL tank.

A weight breakdwon of the logistics H_2 system is summarized in table 57. A total of 104 kg (230 lbm) of H_2 must be resupplied. However, 9.07 kg (20 lbm) must be vented overboard before the transfer operation, and 2.7 kg (6 lbm) must remain trapped in the tank and lines after completion of the transfer operation. This requires a loaded-propellant weight of 116 kg (256 lbm) of H_2. The propellant tank will then weigh 69.8 kg (154 lbm), and includes the basic tank, structures, the metal reversing diaphragm, and the thermal insulation.

The logistics H_2 transfer system is charged 9.5 kg (21 lbm) for lines and valves. The total chargeable launch weight of the system is then determined to be 238 kg (525 lbm).

NH_3. – The NH_3 resistojet system requires 209.6 kg (462 lbm) of NH_3 to be resupplied every 90 days. This requirement is satisfied by propellant transfer of the required NH_3 from the logistics vehicle to the MORL tank. NH_3 is stored onboard the MORL at its vapor pressure of 2242×10^3 N/m^2 (325 psia) at the ambient temperature of 325°K (585°R). The resupply system will provide NH_3 at these conditions until the MORL tank is filled to its 5% ullage value. At this point, the MORL tank will be filled with 147-day supply of LNH_3. A schematic of the logistics NH_3 transfer system is shown in fig. 32. The NH_3 is stored in a 92.8-cm (36.5-in.) spherical tank with a positive-expulsion bladder for zero-g transfer. The transfer of the NH_3 is accomplished by a N_2 pressurization system. The N_2 bottle stores 19.9 kg (44 lbm) of N_2 at 20 700 kN/m^2 (3000 psia) in a 55.8-cm (22-in.)-diam bottle weighing 24 kg (53 lbm).

Table 58 summarizes the weight of the logistics NH_3 transfer system. A total of 5.9 kg (13 lbm) of NH_3 remains trapped in the system after the transfer process. The total launch weight chargeable to the NH_3 logistics system is seen to be 296 kg (653 lbm) as compared to 238 kg (525 lbm) for the H_2 resistojet concept. The H_2 shows a lower logistics chargeable weight because of its reduced propellant requirements, even though the system dry weight is less for NH_3.

High-thrust systems. – The design philosophy utilized for the logistics resupply system for both the monopropellant and the storable bipropellant systems is similar. A flow schematic of the monopropellant system is shown in fig. 33, and a schematic of the storable bipropellant is shown in fig. 129. A discussion of the monopropellant transfer procedure will suffice for a description of both systems, the essential difference being that the bipropellant system must provide provisions for transferring two fluid components rather than the monopropellant's one fluid component. The N_2H_4 onboard the logistics vehicle is stored in a spherical tank with a positive-explusion bladder. Transfer is effected by an N_2 pressurization system. The tank pressure is

TABLE 57

H_2-RESUPPLY SYSTEM WEIGHTS

Item	Weight kg (lbm)
Propellant	
Usable	104 (230)
Trapped	2.7 (6)
Vented	9.07 (20)
Loaded	116 (256)
Helium	12.7 (28)
Propellant tank[a]	69.8 (154)
Lines and valves	9.5 (21)
Pressurant bottle[a]	29.9 (66)
Total weight at launch	238 (525)

[a]Includes thermal insulation.

TABLE 58

NH_3-RESUPPLY SYSTEM WEIGHTS

Item	Weight kg (lbm)
Propellant	
Usable	209.6 (462)
Trapped	5.9 (13)
Loaded	215.5 (475)
N_2	19.9 (44)
Propellant tank	27.2 (60)
Lines and valves	9.5 (21)
Pressurant bottle	24 (53)
Total weight at launch	296 (653)

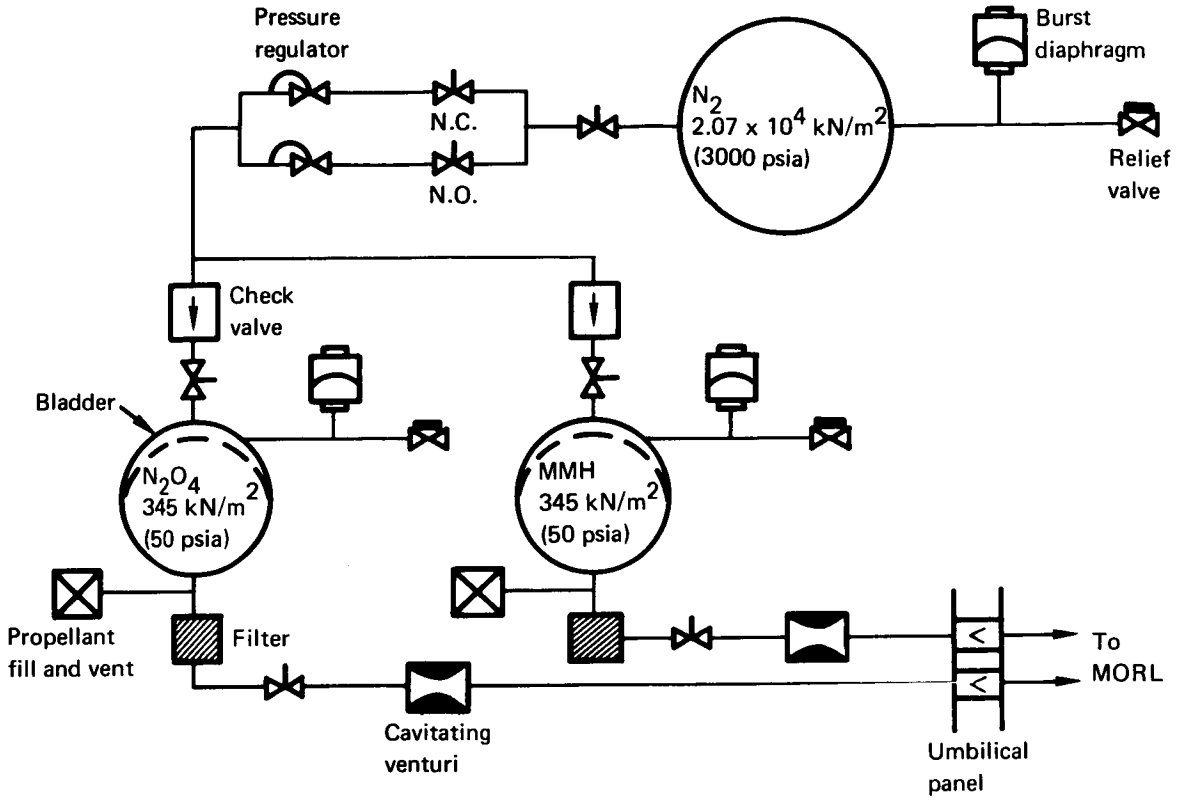

Figure 129. Bipropellant Resupply System

maintained at 345k N/m^2 (50 psia) during the transfer process. This will require venting of the 1725 k N/m^2 (250-psia) ullage of the MORL tanks. Flow control of the liquid propellant is accomplished by a cavitating venturi during the transfer process. After the transfer process, the MORL tank is repressurized to its operating pressure of 1725k N/m^2 (250 psia). N_2 is resupplied by bottle transfer of the stored N_2 gas. This is necessary because both an isentropic N_2 transfer and a pneumatic pumping scheme are excessively heavy. To transfer 3.63 kg (8 lbm) of N_2, an analysis indicated that about 14.5 kg (32 lbm) would be required because of the temperature drop during an isentropic transfer.

The O_2/H_2 system must supply both the O_2 and H_2 propellants. The H_2 requirement is met by the baseline H_2 resupply scheme. This requirement is satisfied by means of resizing the logistics H_2 tank from the baseline value of 156 cm (61.5 in.) to the resized value of 162 cm (64.1 in.). O_2 resupply is accomplished by tank transfer of a 90-day O_2 tank. This concept was determined to be optimum after consideration of various methods of transferring the O_2 in its supercritical state. The 57-day reserve requirements are provided by a reserve O_2 tank kept onboard MORL.

Table 59 presents a weight summary of the defined systems. The monopropellant dry weight is less than the bipropellant because only one component is transferred. However, the logistics chargeable launch weight is greater for the monopropellant system than for the bipropellant system

TABLE 59

LOGISTICS RESUPPLY OF HIGH-THRUST SYSTEM

Item	Propellants resupplied		
	Monopropellant (N_2H_4, N_2)	Bipropellant (NTO, MMH, N_2)	Cryogenic (O_2, H_2)
	kg (lbm)	kg (lbm)	kg (lbm)
90-day propellant weight[a]	60.3 (133)	40.8 (90)	34.5 (76)
System dry weight[b]	22.2 (49)	27.2 (60)	35.4 (78)
Weight chargeable to logistics launch	82.5 (182)	73 (150)	69.8 (154)

[a] Includes pressurant resupplied to MORL.

[b] Includes pressurant gas required for propellant transfer and trapped propellants.

because of the lower performance of the monopropellant system with its subsequent higher propellant requirements. The logistics chargeable weight is comparable for the bipropellant system and the cryogenic system. The reasons the cryogenic system shows weights comparable to the bipropellant system are because of the reduced propellant requirements and propellant commonality. This propellant commonality establishes that the chargeable weight for H_2 resupply includes only the delta weights between the baseline and the resized H_2 tanks.

REFERENCES

1. Report on the Development of the Manned Orbital Research Laboratory (MORL) System Utilization Potential, Task Area IV MORL System Improvement Study, Contract No. NAS1-3612. Douglas Report No. SM-48817, December 1965.

2. Integrated Mission Development Plan, Contract No. NAS1-3612. Douglas Report No. SM-48810, December 1965.

3. Harris, I. and Priester, W.: Theoretical Models for the Solar-Cycle Variation of the Upper Atmosphere. NASA TND-1444, August 1962.

4. Preliminary Design of a Pu-238 Isotope Brayton-Cycle Power System for MORL. Douglas Report No. SM-48832, September 1965.

APPENDIX
OPTIMIZED RESISTOJET PERFORMANCE PREDICTIONS

A general performance method is presented that can be used to calculate the actual specific impulse and power requirements of optimum resistojet thrustors for a number of propellants while considering chamber temperature, chamber pressure, and thrust as independent variables. The method is based on a Reynolds number correlation of nozzle performance that yields a closed-form solution to the resistojet performance equations.

Curves are given of predicted specific impulse and electric power for thrust levels from 5×10^{-3} to 1N (~1.0 to 250 mlbf), chamber temperatures from 1400 to 2400°K, and chamber pressures from 0.1 to 10 atm. Curves are presented for the following propellants and mixtures:

(1) H_2.

(2) NH_3.

(3) Water vapor.

(4) CO_2.

(5) N_2H_4.

(6) Mixtures.

(A) $0.9\ CO_2 + 0.1\ H_2$.

(B) $0.815\ CO_2 + 0.092\ H_2 + 0.093\ H_2O$.

The minimum electrical power requirements without thermal losses are also given. Preliminary thermal-loss estimates are shown for preliminary design. Specific loss figures are mission-dependent and must be evaluated for each case.

Nozzle Performance Analysis

An accurate prediction of the propellant utilization (thrust per unit of mass flow rate) of a resistojet requires an accurate prediction of the conversion efficiency of potential to effective kinetic energy in the thrustor exit

nozzle. This efficiency, η_N, is the square of the ratio of the delivered specific impulse to the ideal specific impulse of the thrustor

$$\eta_N = \left(\frac{I_{sp_{F,\ E,\ D,\ V}}}{I_{sp_{ideal,\ equilibrium}}} \right)^2 \tag{1}$$

The subscripts are used to indicate that the specific impulse includes losses from frozen flow, F; from incomplete expansion, E; from divergence of the flow leaving the nozzle, D; and from viscous effects, V. The nozzle efficiency then, is the product of the efficiencies that account for these four effects

$$\eta_N = \eta_F \, \eta_E \, \eta_D \, \eta_V \tag{2}$$

The product $\eta_E \, \eta_D \, \eta_V$ can be optimized for given thrustor sizes and operating conditions (pressure and temperature). Optimum values of this product can be correlated with Reynolds number.

The frozen-flow efficiency is given by

$$\eta_F = \left(\frac{I_{sp_{ideal,\ frozen}}}{I_{sp_{ideal,\ equilibrium}}} \right)^2 \tag{3}$$

Combining eqs. 1, 2, and 3, the Reynolds-number-dependent product is found to be

$$\eta_E \, \eta_D \, \eta_V = \frac{\eta_N}{\eta_F} = \left(\frac{I_{sp_{F,\ E,\ D,\ V}}}{I_{sp_{ideal,\ frozen}}} \right)^2 \tag{4}$$

$I_{sp_{F,\ E,\ D,\ V}}$ is the specific impulse with all losses considered; therefore it is the actual delivered specific impulse of the thrustors in space and is given by

$$I_{sp_{F,\ E,\ D,\ V}} = \sqrt{\eta_E \, \eta_D \, \eta_V} \, I_{sp_{ideal,\ frozen}} \tag{5}$$

The ideal frozen-flow specific impulse, which, in the subscript notation is simply I_{sp_F}, is accurately determined from a digital computer program. The program calculates one-dimensional rocket performance that assumes a thermally perfect and calorically imperfect gas, including the effects of dissociation and reassociation and the possibility of condensed species in the exhaust products.

An extensive survey and a correlation of experimental data for pure gas rockets were conducted and compared with analytical nozzle performance models to arrive at the Reynolds-number-dependent product

$$\sqrt{\eta_E \, \eta_D \, \eta_V} = f\,(Re_D^*) \tag{6}$$

For throat-diameter Reynolds numbers above about 200, this correlation appears to be independent of the propellant composition, while at lower Reynolds numbers, it is dependent on composition.

From these data, the optimum value of the efficiency product in eq. 6 was established.

The analytical models used are described in refs. A-1 and A-2. Fig. A-1 shows the results. Considerable experimental data (refs. A-3 through A-13) for hot and cold gas laminar flow rockets have become available to aid in a prediction of the resistojet nozzle efficiency. The data includes heated gases through nozzles of various shapes, divergence angles, and expansion area ratios. Table A-1 indicates the range of the variables considered from refs. A-3 through A-13.

Although most of these data correspond to nonoptimum performance, the optimum performance curve can be estimated with a reasonably high degree of confidence.

The approach described above relies primarily on experimental data to define the optimum overall nozzle efficiency (eq. 2). It does result, therefore, in a more realistic evaluation of the nozzle performance. The usual methods involve a separate evaluation of the expansion, divergence, and viscous efficiencies. It is difficult to establish each of these values accurately, let alone the optimum product, $\eta_E \, \eta_D \, \eta_V$.

Generalized Performance

The following performance calculation method was developed in this study to give a direct closed-form solution. This was used to calculate the values of the delivered specific impulse of the resistojets used in the study. The

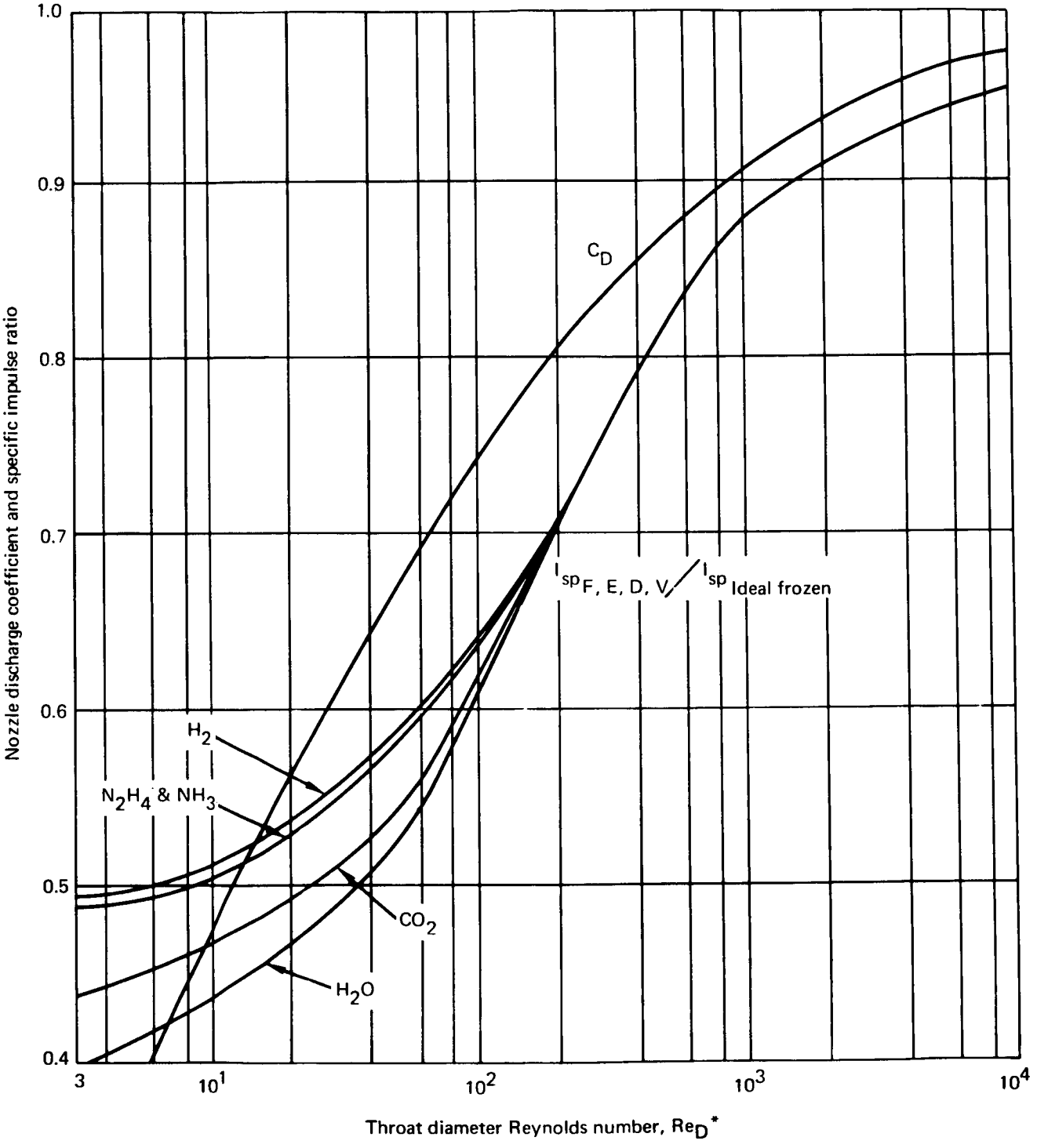

Figure A-1 Predicted Resistojet Nozzle Performance

TABLE A-1

PERTINENT CONDITIONS OF EXPERIMENTAL DATA USED IN THE NOZZLE PERFORMANCE CORRELATION

Element	Condition
Propellants	H_2, N_2, NH_3, H_2O, and subliming solids
Reynolds number range	2 to 50 000
Chamber pressure range	0.05 to 10 atm
Area ratio range	1 to 600
Divergence half-angle range	10 to 45°
Thrust range	0.445 mN to 383 N (0.1 to 860 mlbf)
I_{sp} range	60 to 860 sec

generalized performance method follows from substitution of the following simple definitions and identities, eqs. 7 through 10, into eq. 6.

$$C_D \frac{D^{*2}_{geom}}{4} = A^*_{eff} \tag{7}$$

$$I_{sp_{F,\ E,\ D,\ V}} = \frac{F}{\dot{m}} \tag{8}$$

$$R_{e_{D^*}} = \frac{(\rho\mu)^*\ D^*_{geom}}{\mu^*} \tag{9}$$

$$(\rho\mu)^* = \frac{\dot{m}}{A^*_{eff}} \tag{10}$$

It follows:

$$\frac{Re_D^* \ (\eta_E \ \eta_D \ \eta_V)^{1/4}}{C_D^{1/2}} = K \frac{F^{1/2} \ (m/A^*_{eff})^{1/2}}{\mu^* \ (I_{sp_F})^{1/2}} \tag{11}$$

Because the efficiency product and nozzle discharge coefficient are functions of Reynolds number, the following is defined

$$\left[f \ (Re_D^*)\right]^{1/2} = \frac{Re_D^* \ (\eta_E \ \eta_D \ \eta_V)^{1/4}}{C_D^{1/2}} \tag{12}$$

Substitution into eq. 11, squaring, and multiplying both sides by the chamber pressure P_t gives

$$\frac{f \ (Re_D^*)}{F \ P_t} = k^2 \frac{m/A^*_{eff}}{P_t \ \mu^* \ I_{sp_F}} \tag{13}$$

It is this equation that forms the basis for the generalized performance curves.

The function of Reynolds number, $f \ (Re_D^*)$, divided by the thrust in lbf, F, and divided by the chamber pressure in atmospheres, P_t, referred to as the resistojet performance parameter, is presented in fig. A-2 for the propellants of interest. This parameter is independent of pressure for chamber temperatures below about 2200°K; dissociation causes a slight variation in the parameter with chamber pressure. Thus, given a chamber temperature, chamber pressure, and thrust, the Reynolds number function, $f \ (Re_D^*)$, can be found from fig. A-2 for any of the propellants or mixtures indicated.

The actual-to-ideal frozen specific-impulse ratio is presented in fig. A-3 as a function of the Reynolds number function, $f \ (Re_D^*)$. Finally, from fig. A-4, the ideal-frozen specific impulse is found as a function of the chamber conditions. The actual specific impulse follows from the tautology

$$I_{sp_{F, E, D, V}} = I_{sp_F} \left(\frac{I_{sp_{F, E, D, V}}}{I_{sp_F}} \right) \tag{14}$$

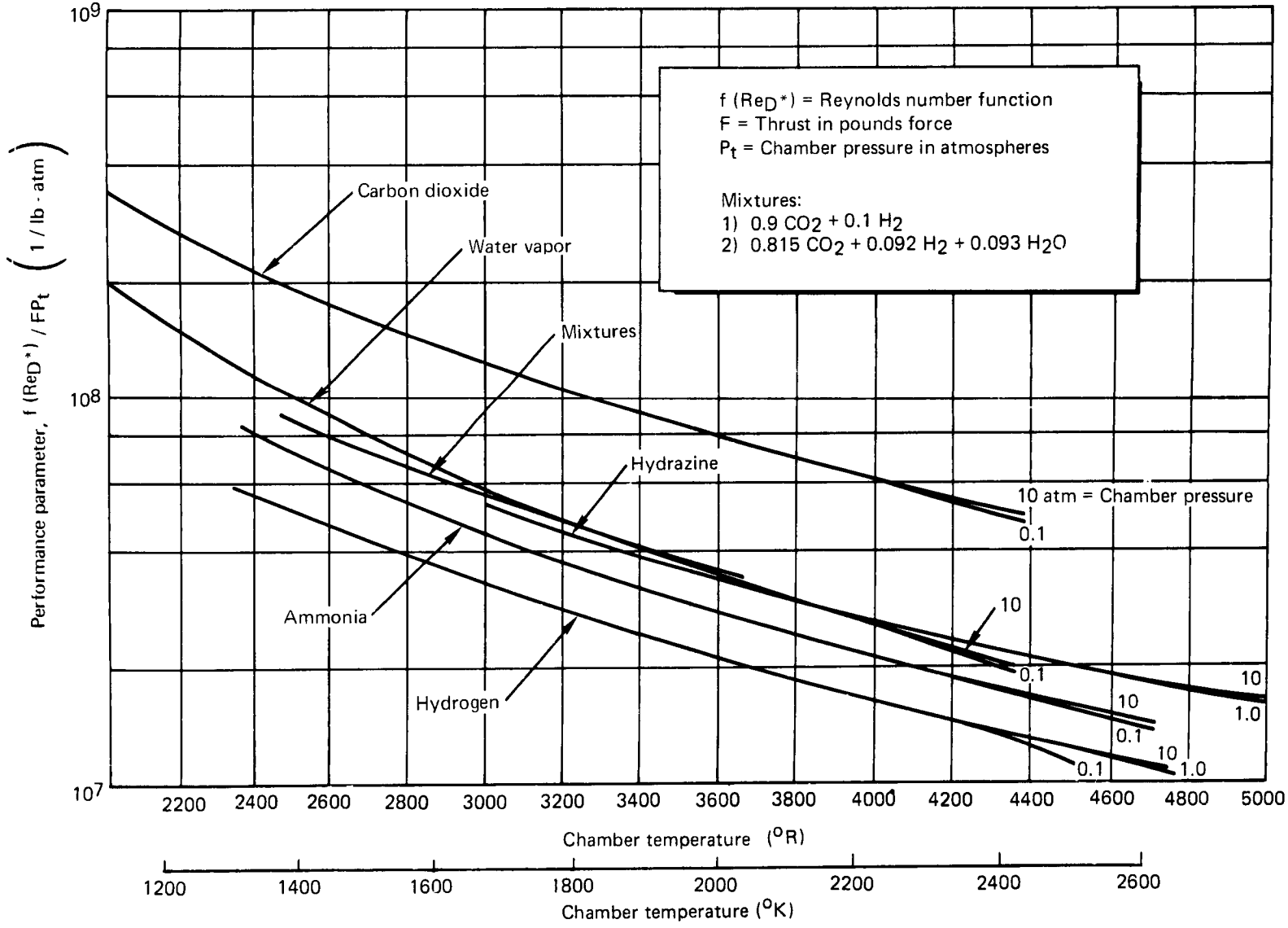

Figure A-2 Resistojet Performance Parameter

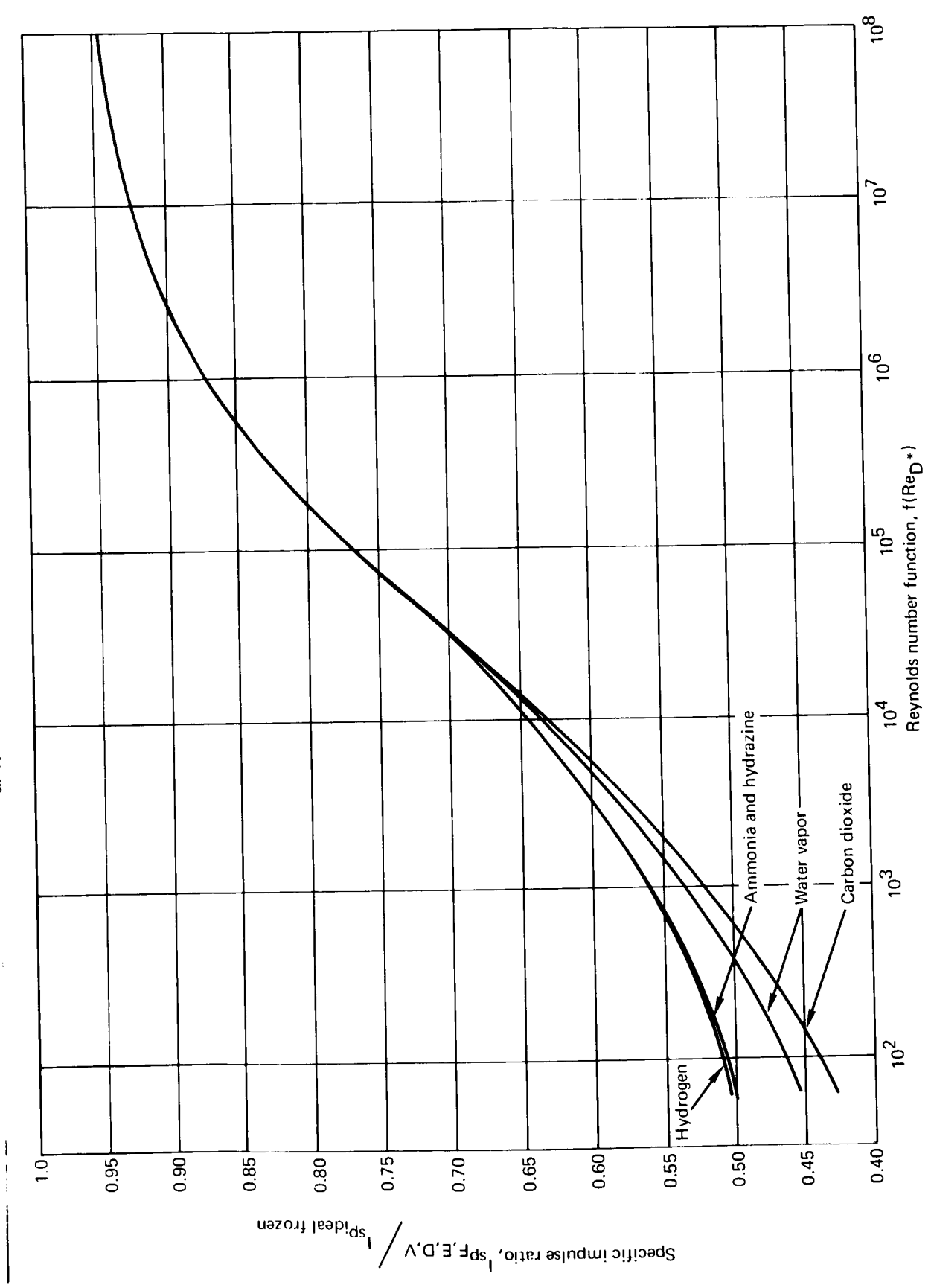

Figure A-3 Resistojet Nozzle Performance Correlation

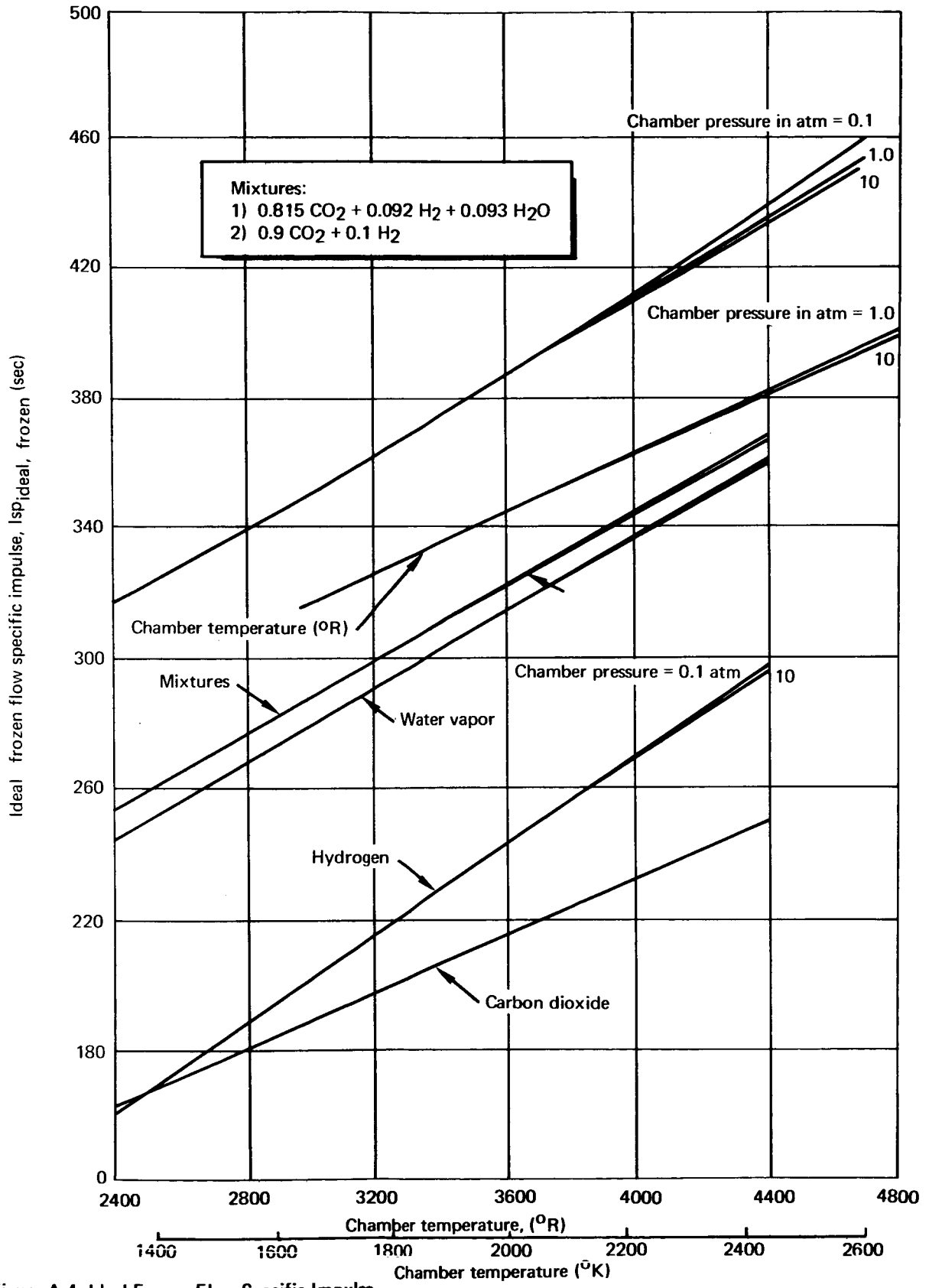

Figure A-4 Ideal Frozen Flow Specific Impulse

The generalized performance method permits the calculation of actual specific impulse with chamber temperature, chamber pressure, and thrust as independent variables. The curves presented (figs. A-2 through A-4) cover a chamber temperature range of 1390° to 2420°K (2500° to 4300°R) and chamber pressures of 0.1 to 10 atm. The performance calculated corresponds to the optimum resistojet for each set of conditions. With the actual specific impulse known, the required mass flow rate of the thrustor follows from the specific impulse definition.

$$\dot{m} = \frac{F}{I_{sp_{F,\ E,\ D,\ V}}} \tag{15}$$

The resistojet nozzle performance correlation has not been presented (fig. A-2) for the mixtures (0.9 CO_2 + 0.1 H_2) and (0.815 CO_2 + 0.092 H_2 + 0.093 H_2O). This presents a problem in performance interpretation for values of the Reynolds number function less than 10^5. It is suggested that the water-vapor curve in fig. A-3 be used at this time as representative of the mixtures being considered

Electric Power Requirements

The electric power that must be supplied to the resistojet thrustor depends on the power initially in the propellant, the power required in the propellant, and the thermal efficiency of the heater. The heater efficiency η_H is defined as the ratio of the power in the gas leaving the nozzle, P_{gas}, to the total input power. The total input power is the sum of the electric power, P_{elec}, and power initially in the propellant, P_{prop}. Thus

$$\eta_H = \frac{P_{gas}}{P_{elec} + P_{prop}} \tag{16}$$

Solving eq. 16 for the electric power required gives

$$P_{elec} = \frac{P_{gas}}{\eta_H} - P_{prop} \tag{17}$$

Heater efficiency will be installation-dependent. It is appropriate then to present, first, the power required for the hypothetical case corresponding to a heater efficiency of 100%. In effect, the power calculated with eq. 17 and a perfect heater will be a minimum required power. The preliminary design values given later in the section permit ready calculation of actual electric power requirements.

If eq. 17 is considered in more detail, the power in the gas, and initially in the propellant, can be expressed as a product of propellant mass flow rate and corresponding enthalpy changes

$$P_{gas} = m\ (h_2 - h_o) \tag{18}$$

$$P_{prop.} = m\ (h_1 - h_o) \tag{19}$$

The mass flow rate may be readily computed from specific impulse definition eq. 15 in each case. In eqs. 18 and 19, h is the enthalpy of the propellant. Subscript o refers to a reference enthalpy compatible with the evaluation of heater efficiency. Subscript 1 refers to the initial (as supplied) propellant condition, while subscript 2 refers to the final chamber condition of the gas. To avoid having to evaluate initial power in the gas for preliminary design, the η_H values supplied here are based upon h_1 taken equal to h_o at $T_o = 298^oK$ (536^oR). This is obvious in eq. 17 where $P_{prop.}$ would not be zero and would otherwise have to be separately evaluated to obtain the actual power required. For cases where h_1 is equal to h_o, then

$$P_{elec} = \frac{P_{gas}}{\eta_H} \tag{20}$$

P_{elec} is the actual required power, and η_H is the particular installation heater efficiency.

P_{gas} is referred to as the minimum required power and is also noted as $P_{min.}$ For both NH_3 and water, the initial state is considered as a vapor. The full equation (eq. 17) must be solved for cases where the propellant is supplied at the other than the assumed ambient condition.

The minimum required power, P_{gas}, is given by the product of propellant mass flow rate, m, and enthalpy rise within the resistojet.

$$P_{gas} = P_{min.} = \dot{m}\ (h_2 - h_o) \tag{21}$$

If one solves the enthalpy rise and substitutes the specific impulse definition for mass flow rate

$$(h_2 - h_o) = \frac{P_{min.} \times I_{sp}}{F} \tag{22}$$

This enthalpy difference, referred to as the minimum required power parameter, is presented in figs. A-5 through A-10 for the following propellants and mixtures:

(1) H_2.

(2) NH_3.

(3) N_2H_4.

(4) Water vapor.

(5) CO_2.

(6) Mixtures:

(A) $0.9\ CO_2 + 0.1\ H_2$.

(B) $0.815\ CO_2 + 0.092\ H_2 + 0.093\ H_2O$.

These curves span chamber temperatures from ambient to 2650°K (4770°R) for H_2 and NH_3, and from 1100°K (1960°R) for the other propellants and mixtures.

Example of General Procedure

The following example is illustrative of the method used. The case chosen [150-mlbf H_2 thrustor with chamber conditions of 2420°K (4360°K) and 3.0 atm] is actually the same as an experimental resistojet thrustor (ref. A-5). The results are in close agreement.

$$\frac{f\,(Re_D^*)}{F\,P_t} = 1.33 \times 10^7\ \frac{1}{\text{lbf - atm}} \tag{23}$$

$$f\,(Re_D^*) = (1.33 \times 10^7)\,(10.150)\,(3.0)$$

$$= 5.985 \times 10^6 \tag{24}$$

$$\frac{I_{sp_{F,\,E,\,D,\,V}}}{I_{sp_F}} = 0.916 \tag{25}$$

$$I_{sp_F} = 886\ \text{sec} \tag{26}$$

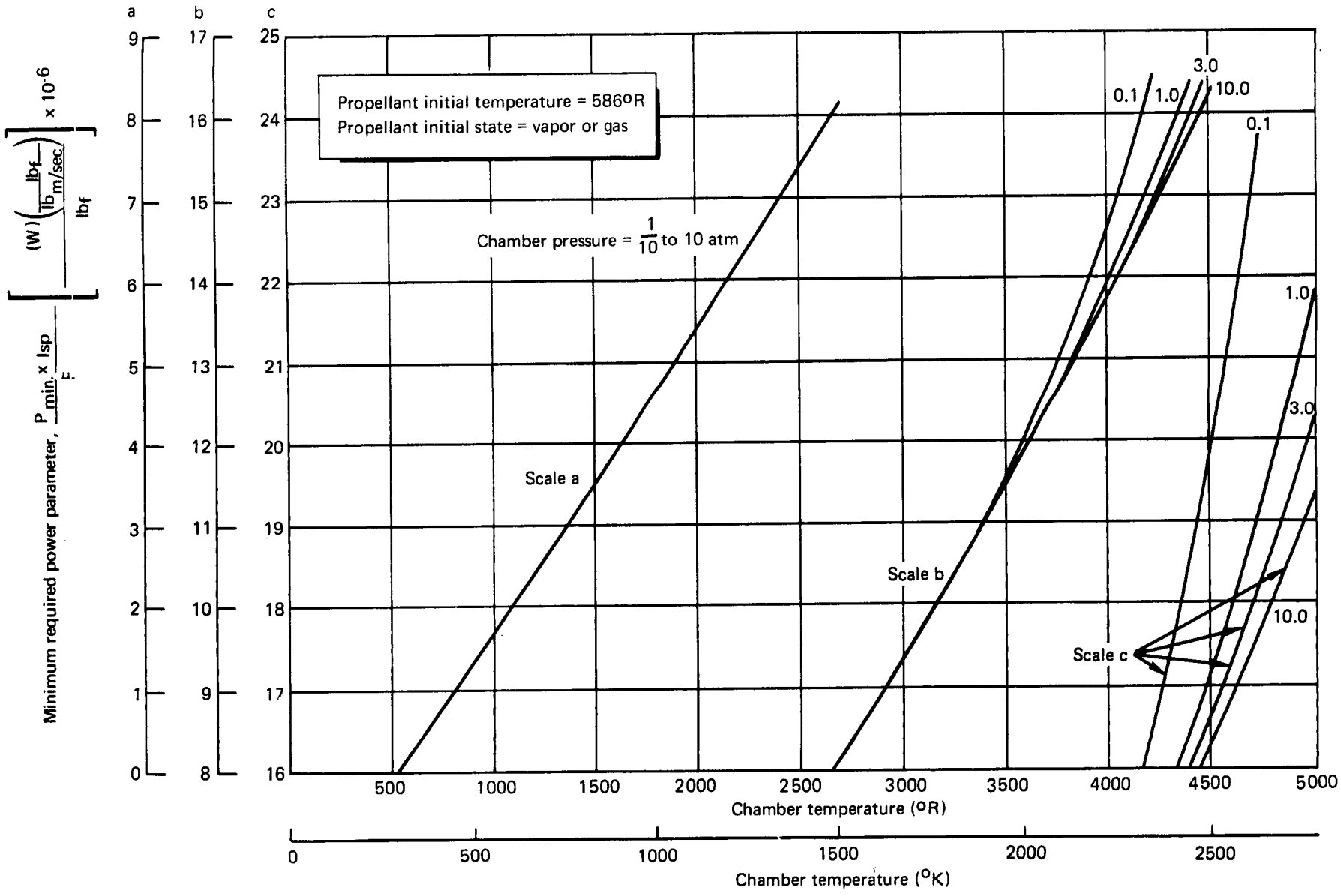

Figure A-5 Resistojet Minimum Required Power – H_2

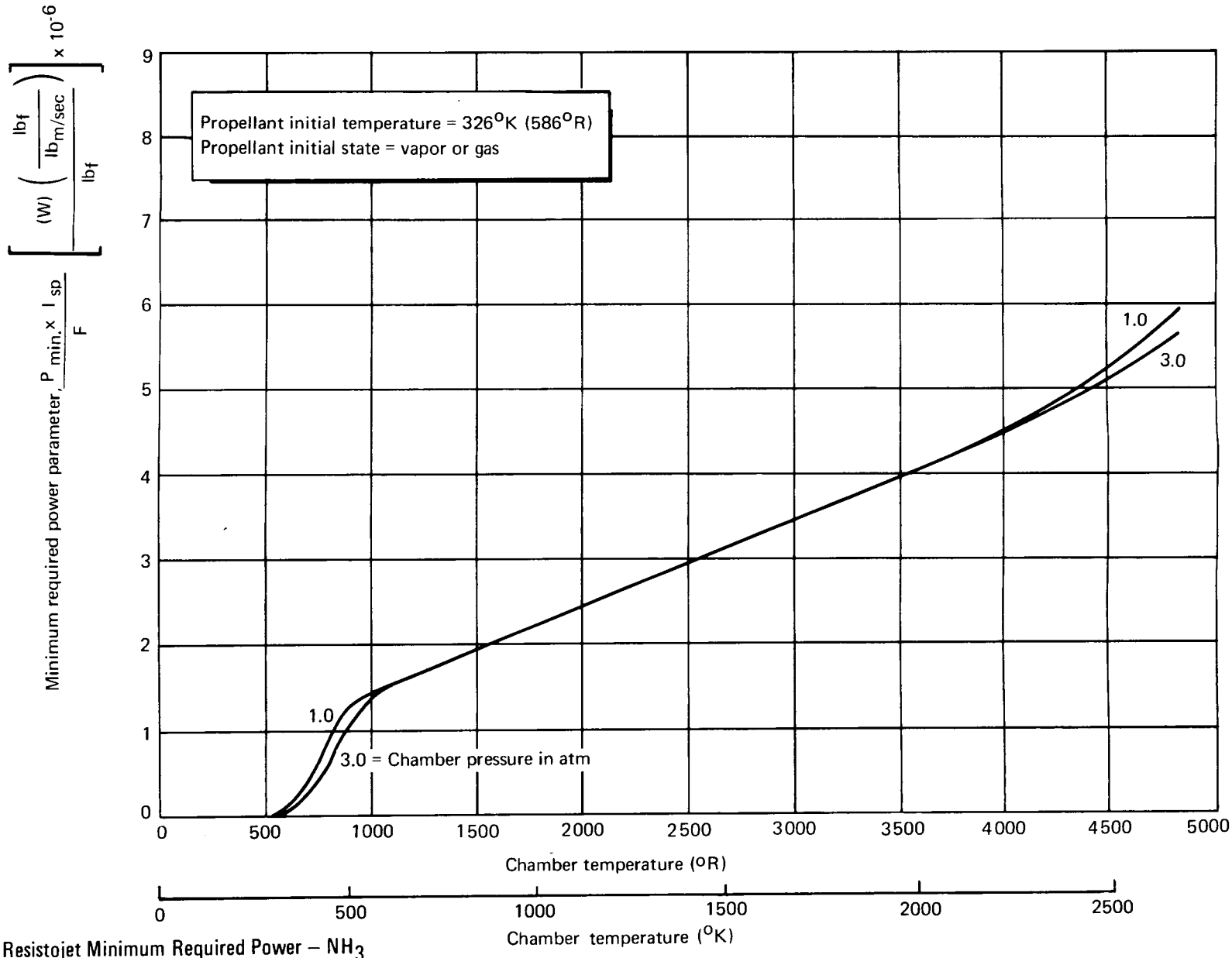

Figure A-6. Resistojet Minimum Required Power – NH_3

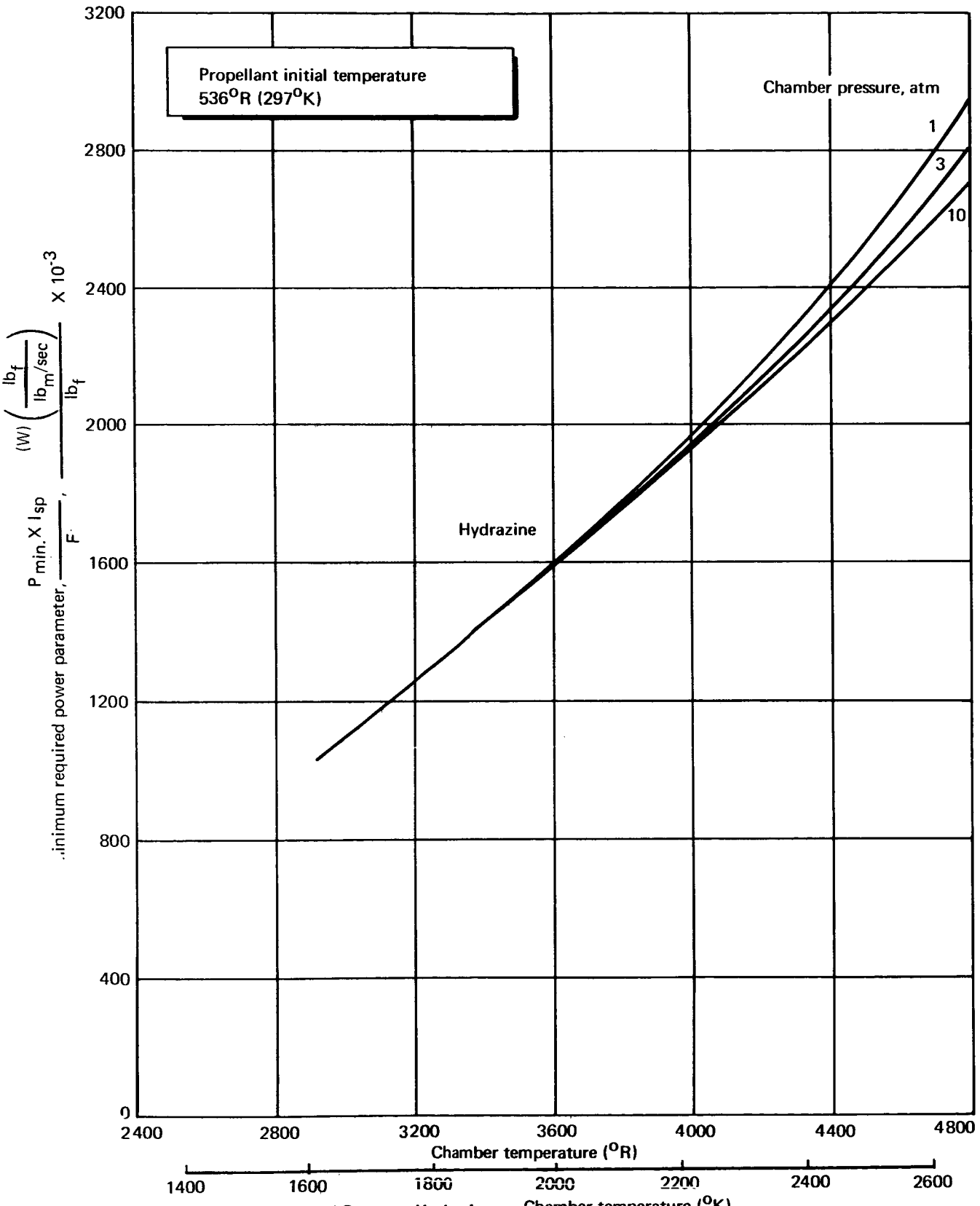

Figure A-7 Resistojet Minimum Required Power — Hydrazine

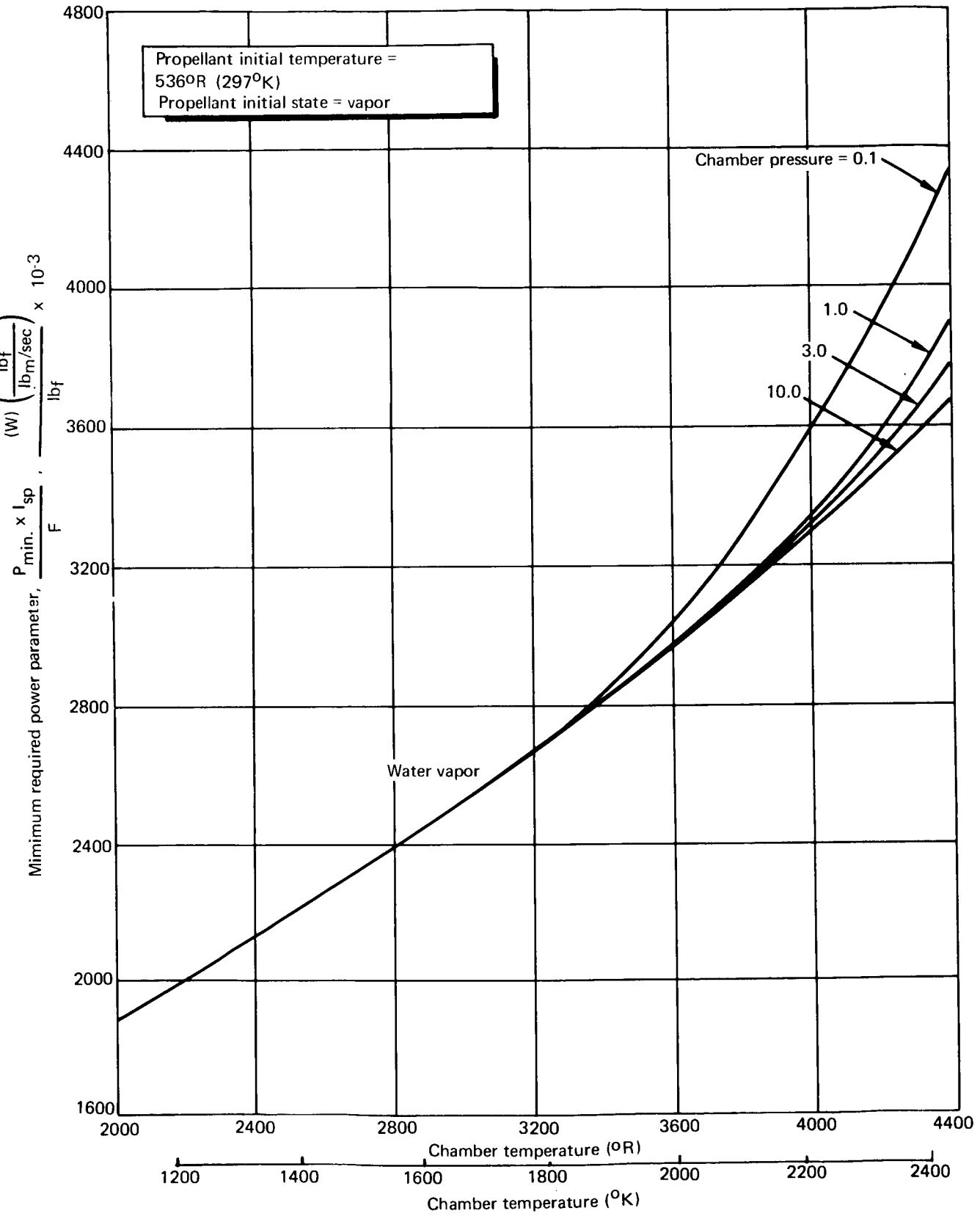

Figure A-8 Resistojet Minimum Required Power — Water Vapor

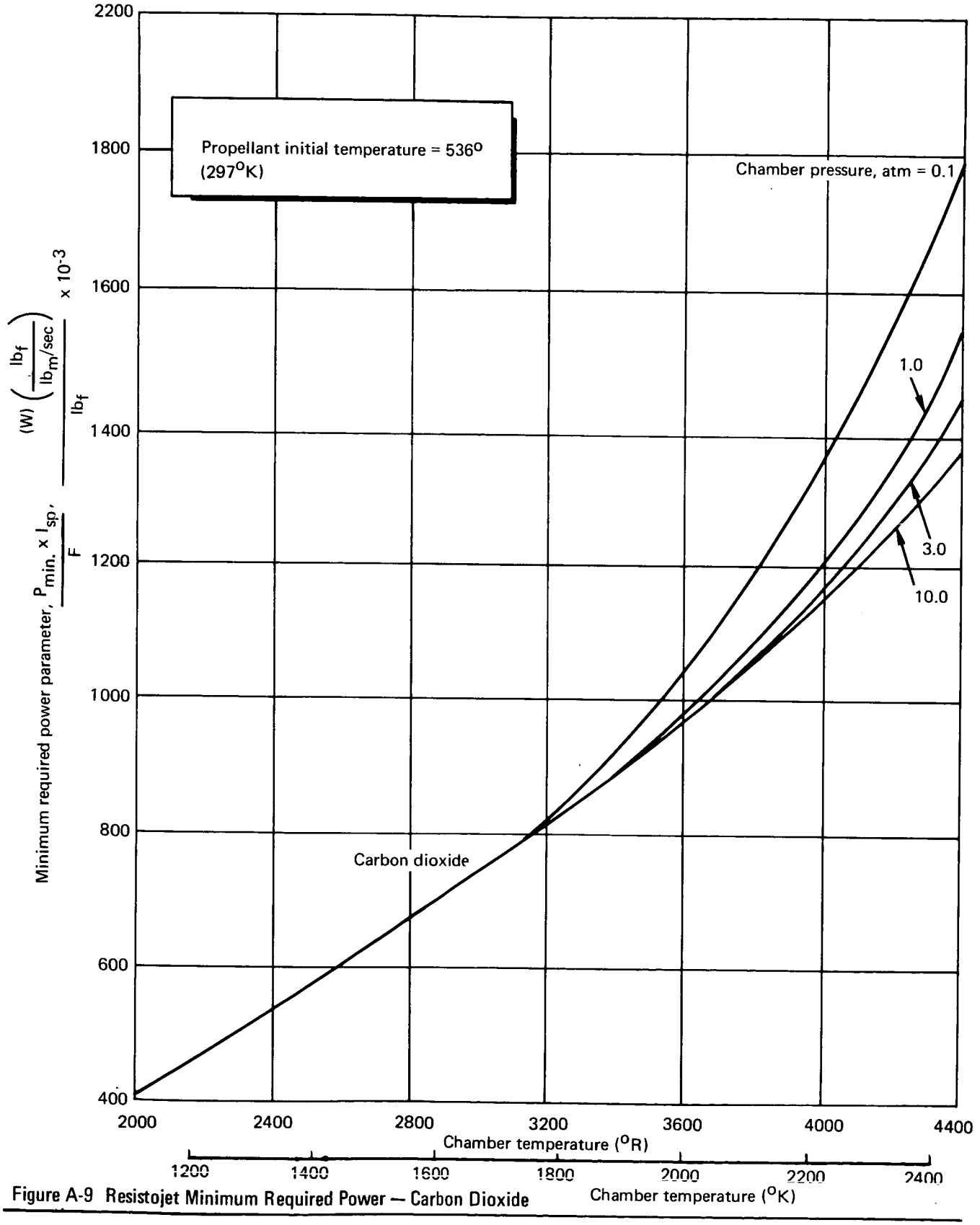

Figure A-9 Resistojet Minimum Required Power — Carbon Dioxide

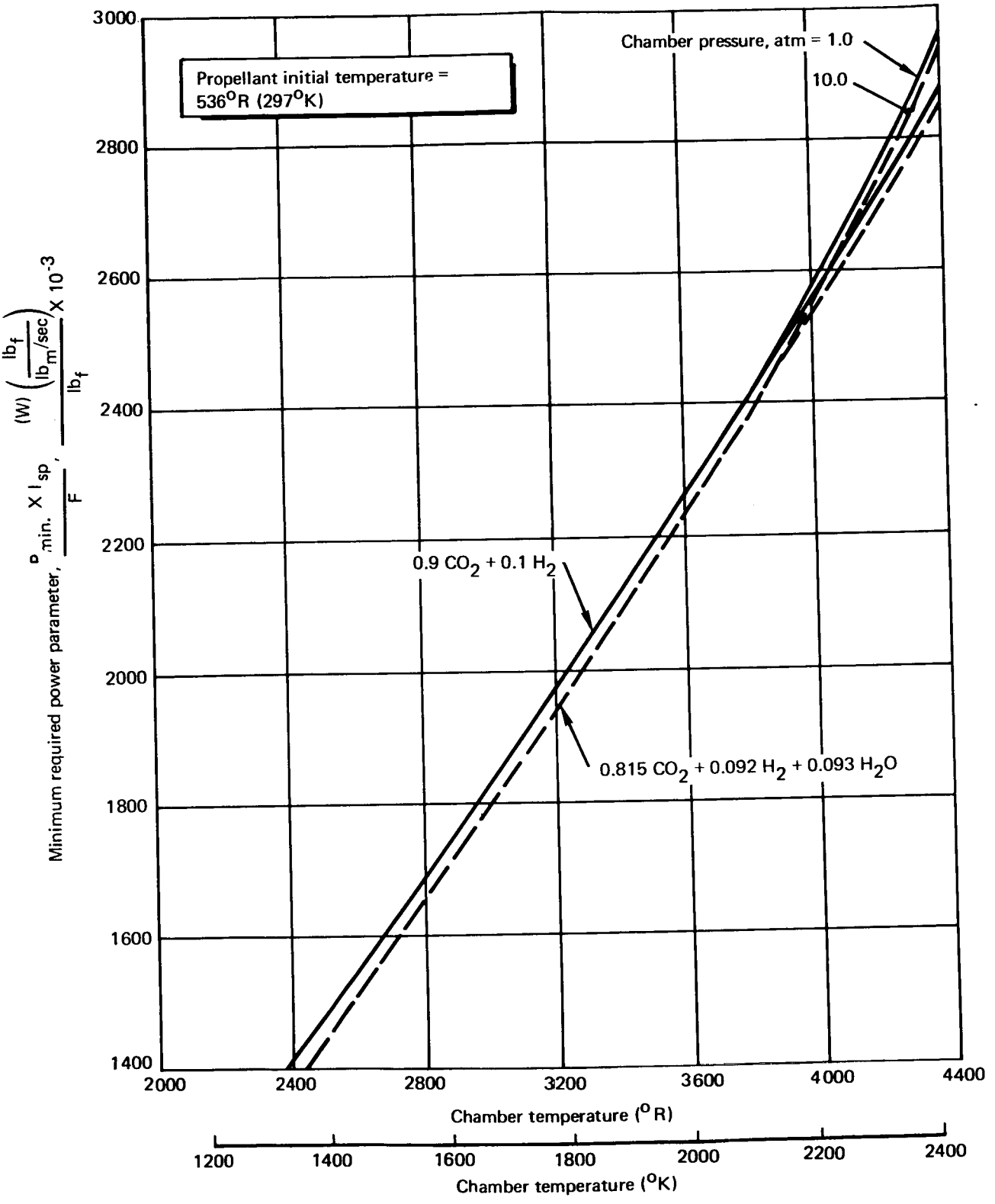

Figure A-10 Resistojet Minimum Required Power — Mixtures

$$I_{sp_{F,\ E,\ D,\ V}} = (886)\ (0.916)$$

$$= 812 \text{ sec} \qquad (27)$$

From fig. A-5, the minimum required power parameter is found to have a value of 15.77×10^6; therefore, P_{min} becomes

$$P_{min.} = \frac{0.150}{812}\ (15.77 \times 10^6) \qquad (28)$$

$$= 2910 \text{ W}$$

Preliminary design values of heater efficiency are given in fig. A-11 and can be used with eq. 20 to find the required electric power, P_{elec}. In this case, η_H is 0.93 and P_{elec} becomes 3130 W.

Performance of Mixtures of Propellants by Superimposition

During this study, the method of superimposing the specific impulses of constituents by weight proportions to arrive at mixture performance was examined. It is concluded that mixtures that contain H_2 affect the chemistry significantly for temperatures considered here, and this method does not yield even approximate results. On the other hand, mixtures of H_2O and CO_2 do behave on the basis of the constituents superimposed so that accurate estimates of specific impulse are possible by weight-proportioning constituent performance.

For the mixtures considered here (0.90 CO_2 + 0.10 H_2 and 0.815 CO_2 + 0.92 H_2 + 0.093 H_2O), the respective specific impulses at a given chamber temperature differ less than 1/2%. It would appear that these data may be used as a good estimate for mixtures with about 10% H_2 and CO_2 ranging from 80% to 90%, with H_2O ranging from 10% to 0%, respectively.

Recommended Operating Temperatures

On the basis of studies conducted to evaluate the corrosion rates of many candidate heater materials in air, a maximum chamber temperature of 1600°K (~2900°R) is recommended for the biowaste thrustors. Propellants which do not contain O_2, such as pure H_2, can be heated above 2400°K (~4300°R). However, the biowaste H_2 is likely to be contaminated with small amounts of O_2 and all the other biowaste propellant [do contain O_2]. The upper limit of 1600°K is compatible with thrustor lifetimes of thousands of hours.

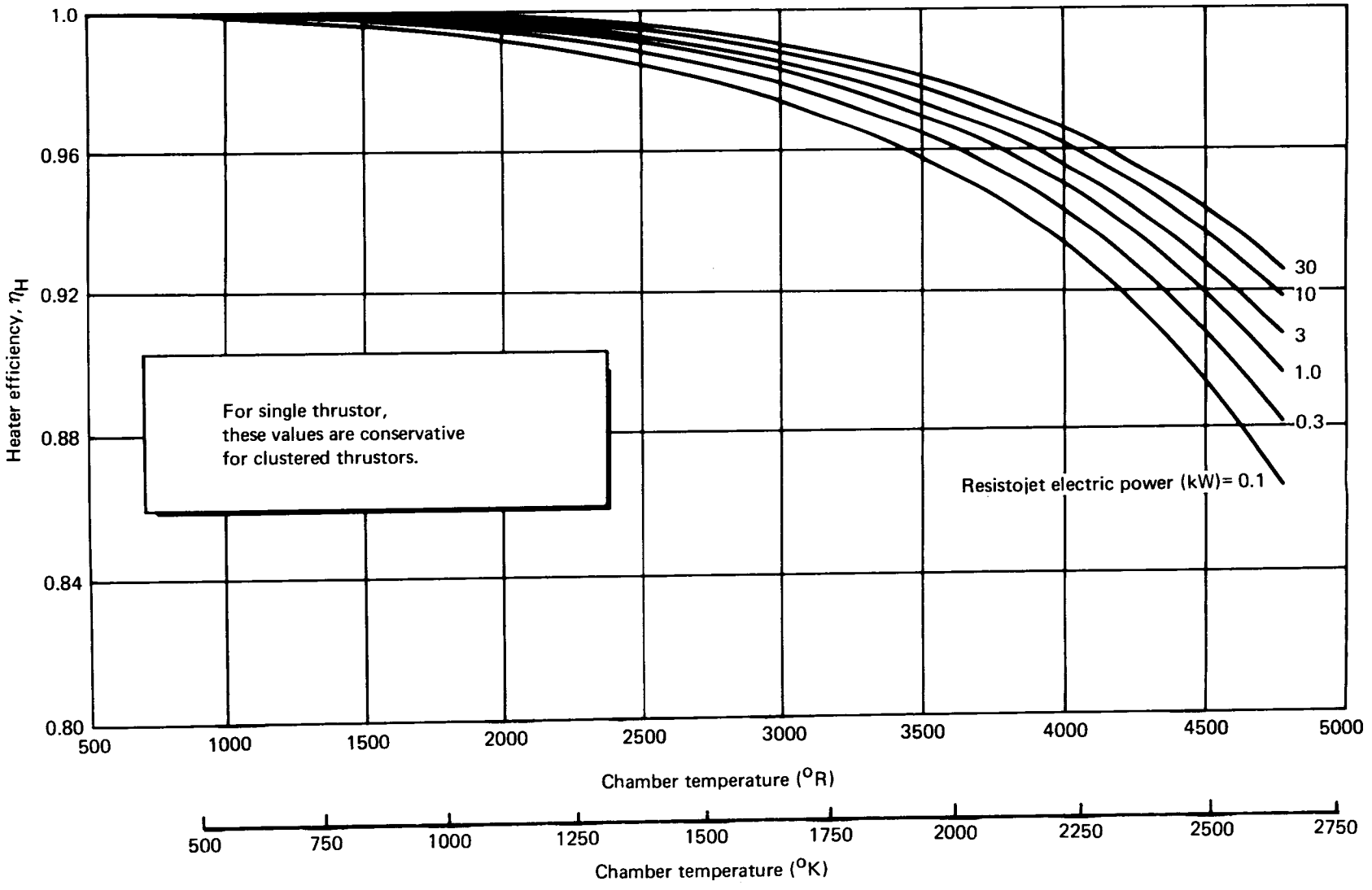

Figure A-11 Preliminary Resistojet Heater Efficiencies

REFERENCES FOR THE APPENDIX

A-1. Cohen, C. B. and Reshotko, E.: The Compressible Laminar Boundary Layer with Heat Transfer and Arbitrary Pressure Gradient, NACA Report 1294, 1956.

A-2. Cohen, C. B. and Reshotko, E.: Similar Solutions for the Compressible Laminar Boundary Layer with Heat Transfer and Pressure Gradient. NACA Report 1293, 1956.

A-3. Page, R. J. and Halbach, C. R.: Resistojet Engine Performance – A Comparison of Experiment with Theory. Paper presented at 4th AIAA Electric Propulsion Conference, Philadelphia, Pennsylvania, August 31, 1966.

A-4. Page, R. J., Halbach, C. R., and Short, R. A.: 3-KW Concentric Tubular Resistojet Performance. AIAA J. Spacecraft, 1966, Pages 1667-1674.

A-5. Electrothermal Engine Research and Development. NASA CR-64104, Avco Corp., Research & Advanced Development Division, RAD TR-64-32, July 20, 1964.

A-6. John, R. R. and Bennett, S.: Resistojet Research and Development – Phase II. First Quarterly Progress Report, NASA CR-54155. Avco Corporation, RAD SR 64-290, November 25, 1964.

A-7. John, R. R. and Morgan, D.: Resistojet Research and Development – Phase II. Second Quarterly Progress Report, NASA CR-54333. Avco Corporation, RAD SR-65-44, January 20, 1965.

A-8. John, R. R.: Resistojet Research and Development – Phase II. Final Report, NASA CR-54688, December 1966.

A-9. Spisz, E. W., Brinich, P. F., and Jack, J. R.: Thrust Coefficients of Low-Thrust Nozzles. NASA TN D-3056, October 1965.

A-10. Kanning, Gerd.: Measured Performance of Water Vapor Jets for Space Vehicle Attitude Control Systems. NASA TN D-3561, August 1966.

A-11. Sutherland, G. S. and Maes, M. E.: A Review of Microrocket Technology: 10^{-6} to 1 lbf Thrust. Journal of Spacecraft and Rockets, Vol. 3, No. 8, August 1966, pages 1153-1165.

A-12. Jonath, A. D.: Gasdynamic Problems in Low Pressure Microthrust Engines. Preprint 65-616, AIAA Propulsion Joint Specialist Conference, June 1965.

A-13. Murch, C. K. et al.: Low Thrust Nozzle Performance.: Preprint 67-91, AIAA 6th Aerospace Science Meeting, January 1968.